Structure, Specificity and Inhibition of Human Caspase-3 and -8

Dissertation

zur

Erlangung der naturwissenschaftlichen Doktorwürde
(Dr. sc. nat.)

vorgelegt der

Mathematisch-naturwissenschaftlichen Fakultät

der

Universität Zürich

von

Rajkumar Ganesan

aus Indien

Promotionskomitee

Prof. Dr. Markus Grütter (Vorsitz)

Prof. Dr. Raimund Dutzler

Zürich 2006

To my beloved parents

Mr. Ganesan and Mrs. Pappa

CONTENTS IN BRIEF

Contents in detail

Appendices

Research summary

Caspases constitute a family of cysteine proteases and are the key effector molecules of the programmed cell death/apoptosis. Apoptosis plays an important role in animal development and tissue homeostasis. Agents modulating the caspase activity are of great interest for the treatment of a wide variety of diseases, including cancer, AIDS, stroke and many neurodegenerative disorders. Several irreversible broad-spectrum caspase inhibitors have been identified and their *in vivo* and *in vitro* efficacy has been reported, in a variety of acute disease models. The design of specific caspase inhibitors with desirable therapeutic benefit remains a challenge, mostly due to the overlapping substrate specificity demonstrated among the caspase family members. Comprehensive structural information with respect to the substrate binding sites is a prerequisite for the design of inhibitors with desirable selectivity for a particular caspase. Caspase-3 is the primary executioner caspase which leads the cellular autodestruction process. This thesis work has its emphasis on the characterization of the structure, specificity and inhibition of caspase-3 using peptidic, peptidomimetic and small molecule inhibitors.

The introduction to caspases and apoptosis are discussed in Chapter 1. In Chapter 2, the architecture of caspase-3 active site is discussed in detail. The crystal structure of caspase-3 in complex with a peptidic inhibitor Z-DEVD-cmk resolved at 1.06Å led to the identification of the role of the N-terminal loop and the residues encompassing this loop in the recognition of the substrates. Additionally the study led to the identification of a tetrahedral reaction intermediate which might be formed during the course of the catalytic reaction.

Chapters 3 and 4 provide structural insights into the azapeptide epoxide and Michael acceptor inhibitors, two new classes of irreversible and highly specific inhibitors for caspases. The commonly used warheads (electrophilic groups) in the design of inhibitors for caspase include aldehydes and halogen methylketones. The unspecific nature of these warheads to inhibit other related proteases is the reason to search for caspase specific electrophilic groups. A comprehensive structural investigation of these inhibitors in complex with caspase-3 and 8 were performed. The studies reveal the mechanism of inhibition and the mode of binding especially in the prime site of caspases for these inhibitors.

Understanding the interaction between small molecules and caspases at the atomic level is imperative for the development of novel drugs. An *in silico* screening followed by an *in vitro* functional assay coupled to the determination of the structures of the protein ligand complexes was used to identify and optimize lead compounds that bind either in the active site or in an allosteric site (Chapter 5). New non-peptidic inhibitors were identified and the crystal structures of three caspase: small molecule inhibitor complexes were determined. The work performed on procaspase-3, caspase-5 and the S_4 subsite mutants of caspase-8 are presented in the appendices.

Zusammenfassung

Caspasen stellen eine Familie von Cystein-Proteasen dar und sind die hauptsächlichen Effektor-Moleküle beim programmierten Zelltod (Apoptose). Die Apotose spielt eine wichtige Rolle bei der geordneten Elimination von Zellen in der normalen Entwicklung und bei der Zellhomeostase. Wirkstoffe zur Modulierung der Caspase Aktivität sind von grossem Interesse für die Therapie verschiedener wichtiger Krankheiten wie AIDS, Schlaganfall und vieler neurodegenerativer Erkrankungen. Mehrere irreversibel wirkende Breitspektrum-Caspase-Inhibitoren sind bekannt und deren Wirksamkeit, *in-vivo* und *in-vitro,* ist für eine Reihe von Krankheits-Modellen beschrieben worden. Die Entwicklung von spezifischen Caspase-Inhibitoren mit der gewünschten therapeutischen Wirkung stelltjedoch immer noch eine grosse Herausforderung dar. Ein wichtiger Grund dafür sind die sich teilweise überschneidenden Substratspezifitäten der verschiedenen Enzyme der Caspase-Familie. Detaillierte strukturelle Informationen über die Substratbindungsstellen Sind eine wichtige Voraussetzung für das gezielte Design von Inhibitoren, mit der gewüschten Spezifität für eine bestimmte Caspase. Caspase-3 ist ein zentrales Enzym in der signaltransduktion der Apoptose und spielt daher eine wichtige Rolle beim Programmierten Zelltod. Das primäre Ziel der vorliegenden Doktorarbeit war die strukturelle Untersuchung und Charakterisierung der Caspase-3, im Hinblick auf ihre Spezifität und Inhibition durch peptidische, peptidomimetische und nicht-peptidische Inhibitoren.

Kapitel 1 gibt eine kurze Einleitung über die Apoptose und die Caspasen. Im zweiten Kapitel wird der Aufbau des aktiven Zentrums von Caspase-3 detailliert beschrieben. Durch die Bestimmung der Kristallstruktur von Caspase-3 im Komplex mit dem peptidischen Inhibitor Z-DEVD-cmk bei einer maximalen Auflösung von 1.06Å konnte gezeigt werden, dass der N-terminale loop von β-Untereinheit des Enzyms bei der Substrat-Erkennung eine Rolle spielt. Ausserdem führte dise strukturelle Untersuchung zur Identifikation eines tetraedrischen Zwischenprodukts, welches eventuell während der katalytischen Reaktion gebildet wird.

Die Kapitel 3 und 4 geben einen strukturellen Einblick in Aza-Peptide und Michael-Akzeptoren als eine neue Klasse von irreversiblen und hochspezifischen Caspase-Inhibitoren. Aldehyde und Halogen-Methylketone sind elektrophile Gruppen, die häufig als sogenannte „warheads„ beim Design von Caspase-Inhibitoren verwendet werden. Die unspezifische Natur dieser „warheads“ im Hinblick auf die Inhibition von auch anderen, verwandten Proteasen, war ein Grund für die Suche nach Caspase-spezifischen elektrophilen Gruppen. Die in der

vorliegenden Arbeit durchgeführten detaillierten strukturellen Untersuchungen dieser Inhibitoren im Komplex mit Caspase-3 und -8 führten zur Aufklärung des struktur-basierten Inhibitions-Mechanismus, des Bindungsmodus und der Spezifität in der "prime site" der Substratbindungstasche.

Das Verstehen der Wechselwirkungen zwischen den als Inhibitoren wirkenden kleinen Molekülen und Caspasen auf atomarer Basis, bildet eine wichtige Grundlage für die Entwicklung neuer Wirkstoffe. *In-silico* Screening, *in-vitro* Aktivitätstests und die Strukturbestimmung von Protein:Liganden-Komplexen wurden zur Identifikation und der sich daraus ergebenden möglichen Optimierung der gefundenen Substanzen, die entweder an das aktive Zentrum oder an eine allosterische Bindungsstelle binden, eingesetzt. Zusätzlich zur Identifikation von neuen, nicht-peptidischen Inhibitoren, konnten die Kristallstrukturen der Komplexe von Caspase-3 mit drei dieser nicht-peptidischen Inhibitoren aufgeklärt warden.

Die durchgeführten Versuche zur Strukturaufklärung einer Procaspase-3, der Caspase-5 und der S_4 subsite-Mutanten von Caspase-8 sind im Anhang beschrieben.

Chapter 1 Introduction

1.1 Apoptosis and caspases

Programmed cell death, or apoptosis, is a physiological process of cellular autodestruction (*1*). Apoptosis plays critical roles in development, maintenance of homeostasis and host defense in multicellular organisms. Dysregulation of this process is implicated in various diseases ranging from cancer and autoimmune disorders to neurodegenerative diseases and ischemic injuries (*2*). Diverse cell types can be triggered to undergo apoptosis by various signals derived from either the extracellular or intracellular milieu. Cells undergoing apoptosis exhibit a series of characteristic morphological changes, including plasma membrane blebbing, cell body shrinkage and formation of membrane-bound apoptotic bodies, which *in vivo* are quickly engulfed by macrophages (*3*). Thus, during apoptosis, intracellular contents are not released and potentially harmful inflammatory responses are prevented. The mammalian caspases have evolved additional roles in inflammatory responses apart from apoptosis.

The principal molecular engines that execute apoptosis are the caspase proteases (*4*). The term caspase denotes two key characteristics of these proteases: (i) they are cysteine proteases and use **C**ysteine as the nucleophilic group for substrate cleavage and (ii) they are **aspases** and cleave the peptide bond C-terminal to aspartic acid residues (*5*). Synthesized as latent precursors or procaspases, caspases are converted to active proteases during apoptosis through an intricately regulated proteolytic process (*6*). The proteolytic processing occurs at critical aspartic acid residues. Consequently, caspases often function in cascades. In such a caspase cascade, upstream caspases (initiator caspases) are activated by interactions with caspase adapters (*4, 6*). This activation represents a key regulatory step in apoptosis and is controlled by both pro- and anti-apoptotic proteins (*7-14*). Once activated, the initiator caspase processes and activates one or more downstream caspases (effector or executioner caspases). The activated effector caspases then cleave various cellular proteins, leading to apoptotic cell death.

1.2 Caspase structure, specificity and activation

1.2.1 Structure of procaspases

Caspases were implicated in apoptosis with the discovery that CED-3, the product of a gene required for cell death in the nematode *Caenorhabditis elegans*, is related to mammalian interleukin-1β-converting enzyme (ICE or caspase-1) (*15, 16*). Since then, at least 14 mammalian caspases and five *Drosophila* caspases have been cloned. Structurally, all procaspases contain a highly homologous protease domain, the signature motif of this family of proteases (Fig. 1). This domain can be further divided into two subunits, a large subunit of approximately 20 kDa (p17) and a small subunit of approximately 10 kDa (p12). In some procaspases, there is a short linker (about 10 amino acids) between the large and small subunits. Based on the sequence similarity among the protease domains, caspases can be divided into three groups (*17*). The first group consists of inflammatory caspases: caspase-1, -4, -5, -11, -12, -13 and -14, the second group contains initiator caspase-2, -8 and -9 and the third group consists of executioner caspase-3, -6 and -7. Each procaspase also contains a prodomain or NH_2-terminal peptide of variable length. Initiator apoptotic caspases and inflammatory caspases contain prodomains of over 100 amino acids, while the prodomains in effector caspases are usually less than 30 amino acids long. The long prodomains contain distinct motifs, notably the death effector domain (DED) and the caspase recruitment domain (CARD). A novel motif termed the death-inducing domain (DID) was recently identified (*18*). Procaspase-8 and -10 each contain two tandem copies of DEDs (*19-21*) whereas a single CARD domain is found in caspases-1, -2, -4, -5 and -9 as well as in CED-3 (*22*). These domains mediate homophilic interaction between procaspases and their adapters and play important roles in procaspase activation. In contrast, the short prodomains of executioner caspases are unlikely to mediate protein-protein interactions. Rather, prodomains seem to inhibit the activation rate *in vivo* (*23*). They regulate nuclear transport in caspase-7 (*24*) and retain caspase-3 in an inactive state (*25*).

The three-dimensional structure of procaspase-7 has been determined (*26, 27*). The structures of caspase prodomains, particularly those of the DED and the CARD domains, have also been solved (*28-30*). DED, CARD and a related domain, DD (death domain, present in cell death adaptor proteins), all consist of six alpha-helices and have similar overall folds. Nonetheless, there are some major differences among them. While charge-charge interactions

govern CARD-CARD (*30*) and DD-DD association (*31*), hydrophobic interactions govern DED-DED interaction (*32*).

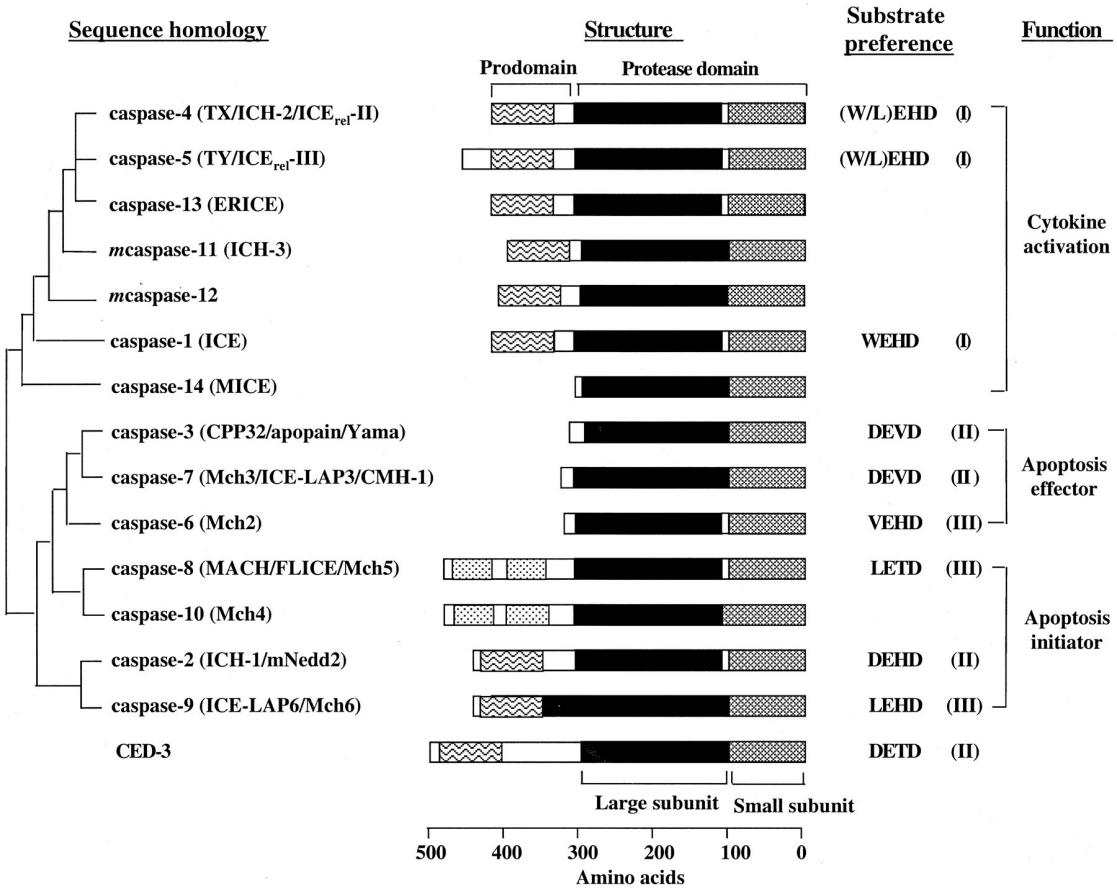

Figure 1. Mammalian caspase family and *C. elegans* caspase CED-3. All mammalian caspases listed are of human origin except for murine caspase-11 and -12, for which no human counterparts have been identified yet. Phylogenetic relationships are based on sequence similarity among the protease domains. Alternative names are listed in parentheses after each caspase. Dotted box - DED domains; wavy box - CARD domain. Substrate preferences at the P_1 to P_4 positions are indicated. Figure adapted from (*33*).

1.2.2 Structures of active caspases

The three-dimensional structures of caspase-1, -2, -3, -7 and -8 each complexed with peptide inhibitors, have been determined (*15, 34-42*). These structures reveal that a mature caspase is a tetramer (homodimer of the p17-p12 heterodimers with a twofold symmetry), with the two adjacent small subunits (p12) surrounded by two large subunits (p17) (Fig. 2). Each p17-p12 heterodimer forms a single globular domain and the core of the globular domain is a six-

stranded beta--sheet flanked on either side by alpha-helices. These two heterodimers associate with each other primarily through the interaction between the p12 subunits.

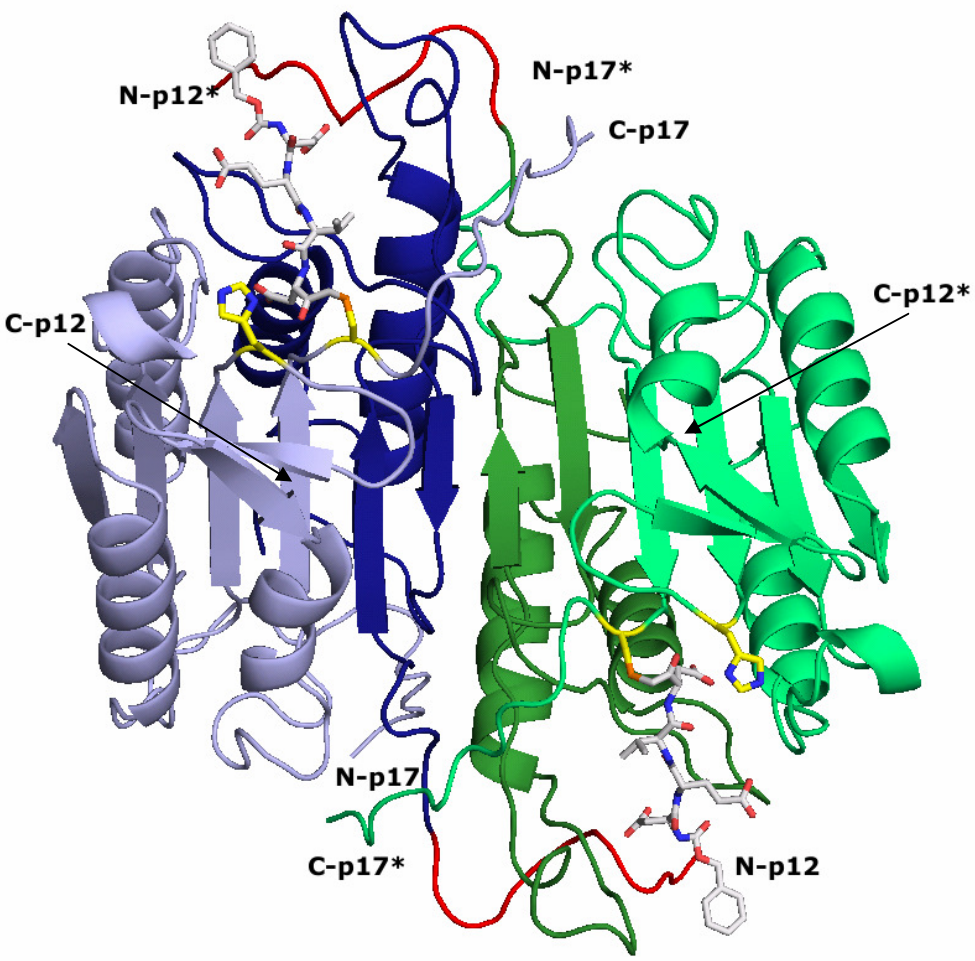

Figure 2. Structure of the caspase-3 tetramer in complex with Z-DEVD-cmk. The p17 and p12 chains are shown in light and dark colors. The p12 N-terminal tail is which was disordered in previous structures (*36, 37*) is given in red. The catalytic cysteine and histidine residues (yellow) and the inhibitor (grey) are given in stick representation. Figure adapted from (*43*).

Each caspase tetramer has two cavity-shaped active sites formed by amino acids from both the p17 and p12 subunits and these two active sites function independently (*44*). The catalytic cysteine and histidine residues of caspases are typically located at the ends of β-strands in a unique caspase hemoglobinase fold (*45*). The side chains of Arg_{179} (p17) and Arg_{341} (p12) in the S_1 site participate in a direct charge-charge interaction with the aspartic acid of a substrate,

contributing to the selective recognition of Asp at the P_1 position of a substrate (Fig. 3). The amino acids from the small subunit form the S_2 and S_3 sites. The side chains of P_2 and P_3 residues are mainly exposed to solvent, consistent with the less stringent requirement at these two positions in caspase substrates. The atomic resolution structure of caspase-3 in complex with Z-DEVD-cmk and its implication in catalysis and substrate recognition are discussed in detail in **Chapter 2**.

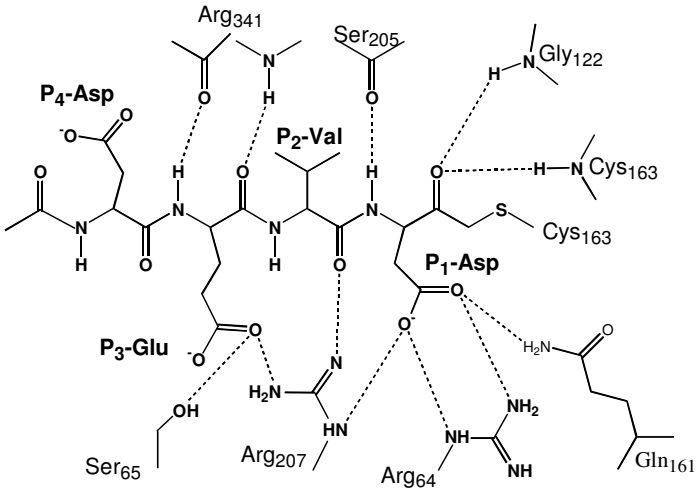

Figure 3. Polar interactions at the active site of caspase-3: Ac-DVAD-cmk complex. (pdb code: 1CP3)

1.2.3 Specificity

Caspases are among the most specific endopeptidases reported so far. An aspartic acid residue is absolutely required at the P_1 position. For example, any substitution in this position in the caspase-1 substrates leads to a >100-fold decrease in cleavage activity (*46, 47*). The P_2 to P_4 positions also show high preference for certain amino acids. Based on the substrate specificity, caspases are divided into three groups (Fig. 1) (*17*). The optimal recognition motif for the first group is WEHD. This group includes the inflammatory caspase-1 and its close homologues caspase-4 and -5. The second group prefers the sequence DEXD (where X is V, T, or H), with a high preference for Asp at the P_4 position. This second group consists of apoptotic effector caspases with either long or short domains (caspase-2, -3 and -7). The inclusion of caspase-2, which contains a long prodomain, may imply that it can function as both an initiator and an effector caspase. In caspase-2, the amino acid at the P_5 position also affects the cleavage

efficiency (*38, 48*). Members of the third group (caspase-6, -8, -9 and -10) preferentially recognize (L/V)EXD.

The major discriminating feature among caspases is the specificity at the S_4 subsite. In caspase-3, the preference for a P_4-Asp is of the order of 100 fold higher when compared to Asn or Glu in P_4. There are two crystal structures for caspase-3 in complex with peptidyl inhibitors having a P_4-Asp. The P_4-Asp forms weak hydrogen bonds with Phe_{250}, Trp_{214} and Asn_{208} (Fig. 4), which only partially accounts for the preference of P_4-Asp. Apart from the S_4 subsite, caspases show a considerable degree of discrimination at the prime sites. Limited structural information is available with regard to the specificity at the prime sites. Using internally quenched fluorescent peptide substrates, Stennicke HR et al (*49*) have found that there is a general preference for small amino acids at the P_1` site preferences for human caspases-1, -3, -6, -7 and -8.

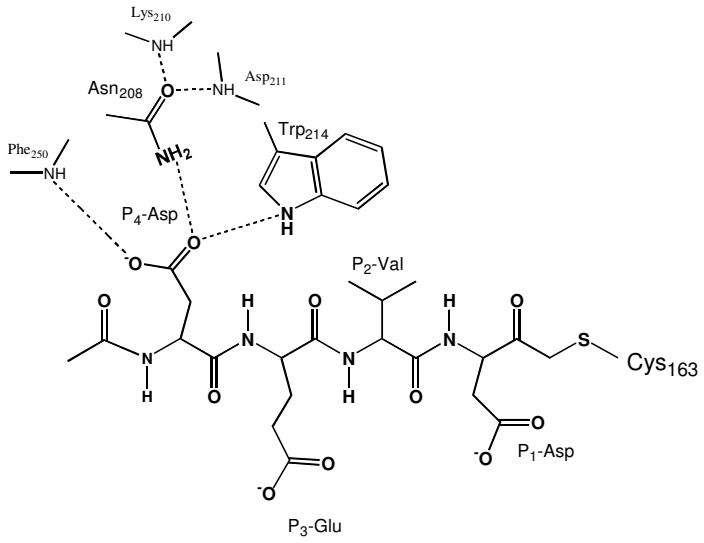

Figure 4. Polar interactions of P_4-Asp based on previously determined crystal structures of caspase-3: DXXD inhibitor complexes (pdb code: 1PAU and 1CP3).

1.2.4 Activation of procaspases

Most biochemical and structural work on caspase activation has been performed with human caspases-3, -7, -8, and -9. A reasonably clear picture has emerged demonstrating the variation and conservation with respect to the caspase activation mechanisms (*10*). The zymogens of the initiator caspases exist within the cell as inactive monomers. These monomeric zymogens require dimerization in order to adopt an active conformation, and this activation is independent of cleavage (*50-52*). The dimerization event occurs in multi-protein activating

complexes to which the caspase zymogens are recruited to by virtue of their N-terminal recruitment domain. The activating complex involved depends on the origin of the death stimulus: in the intrinsic pathway activation occurs on a molecular platform called apoptosome (*53*) and in the extrinsic pathway activation occurs within the death inducing signaling complex (DISC) (*7*). The apoptosome is composed of Apaf-1, caspase-9, caspase-3 and XIAP (X-linked inhibitor of apoptosis protein), while DISC is composed of Fas receptor, FADD (Fas-associating protein with death domain) and caspase-8. In contrast to the initiators, the executioner caspase-3 and -7 zymogens exist within the cytosol as inactive dimers. They are activated by specific proteolytic cleavage in the inter-domain linker region carried out by an initiator caspase, and occasionally by other proteases under specific circumstances (*54-56*). The crystal structures of procaspase-7, active caspase-7, and inhibitor-bound caspase-7 provided a basis to derive a mechanism for the executioner caspase activation, and the dimerization mechanism for initiator caspase activation (*26, 27, 57*). Inflamatory caspases are activated through a multi-protein complex called the inflammasome. The inflammasome is composed of caspase-1, caspase-5, the adapter protein PYCARD and the infectious agent, multidomain protein NALP1(*58*).

1.3 Regulation of caspase activity

1.3.1 Active site inhibitors

A typical caspase inhibitor can be divided into three structural components: the warhead, the P_1 aspartic acid and the P_2-P_4 peptidomimetic.

Warhead

The warhead consists of an electrophile that reacts with the nucleophilic cysteine residue of the active site. Depending on the nature of the groups flanking the warhead, an inhibitor can either be reversible or irreversible. Reversible inhibitors are generally advantageous as they are often more selective towards the target protein compared to irreversible inhibitors. Despite the lack of specificity, a significant advantage associated with irreversible inhibitors is their greater potency in cellular assays of apoptosis. Commonly used warhead groups for the inhibition of caspases along with their chemical structure are given in Fig.5.

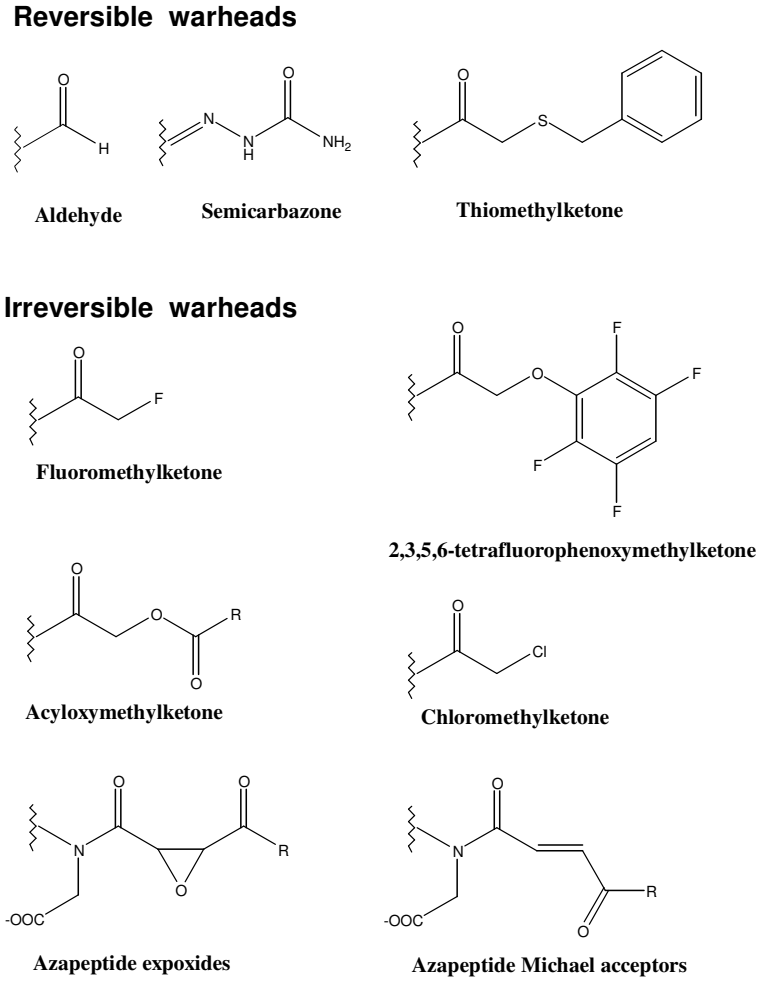

Figure 5: Commonly used "warheads" (electrophilic groups) for the inhibition of caspases.

P_1 Asp

Caspases have a strong preference for an aspartic acid as the P_1 residue (*17, 46, 47*). Therefore this feature has been incorporated into almost all lead compounds (Fig. 6). There are however two examples of compounds lacking the P_1 aspartic acid sub-structure while retaining binding affinity for caspases. In one case, compound-**A** (Fig. 6) was initially identified by high-throughput screening. It was subsequently optimized to a potent and selective low nanomolar inhibitor of caspases-3 and -7 (*59, 60*). The warhead is a cyclic ketoamide and the crystal structure of this compound bound to caspase-3 revealed a tetrahedral intermediate formed between the active site thiolate and the ketone carbonyl group. Despite the lack of significant binding in the S_1 subsite, this series of compounds displays potent inhibitory activity and higher

selectivity for caspases than for other cysteine proteases and inhibition of apoptosis in cell-based assays.

An acyl-sulfonamide (a classic carboxylic acid replacement) was substituted for the aspartic acid residue (compound-**B**) (*61*). In this case the crystal structure revealed that the methane-sulfonamino-carbonyl group in the P_1 position is buried in the S_1 pocket and engages in hydrogen bonding interactions with Arg179 and Arg341 (residues that typically form hydrogen bonds to the P_1 Asp residue). The additional steric bulk of the methane-sulfonyl group is accommodated by rearrangement of the surrounding amino acids.

P_2-P_4 Peptidomimetic

This is the part of caspase inhibitors for which the greatest variety has been generated. In most cases, inhibitor design relies on a substrate analog approach in which a tetrapeptide substrate sequence is the starting point. After incorporation of a suitable warhead, non-peptide substitutions for the P_2-P_4 regions are identified that improve the pharmacokinetic properties of the molecule. With the structural information of different caspases, structure-based design plays a major role in the lead optimization process. Several novel peptidomimetic inhibitors (e.g. Compounds-**C-H**) have been identified. Some of these compounds were shown to rescue mice from lethal experimental hepatitis, decreased circulating levels of plasma markers associated with fulminant hepatic failure (*62*), and neuroprotective effects in a rat model of transient focal ischemia (*63*). However, these inhibitors are irreversible broad spectrum inhibitors, which raise questions regarding their *in vivo* specificity and potential toxicity. Recently, two caspase inhibitors have entered clinical trials. Vertex Pharmaceuticals announced the completion of Phase-IIa clinical trials with Pralnacasan (VX-740; compound-**C**, a caspase-1 specific inhibitor, for the treatment of Rheumatoid Arthritis (RA). This compound is administered orally as an acetal pro-drug which undergoes *in vivo* hydrolysis to the active species possessing an aldehyde warhead (Compound **D**). The aldehyde version of the compound has a K_i of ~1 nM for caspase-1 and inhibits IL-1β secretion from human peripheral blood mononuclear cells (PBMCs) with an EC_{50} of ~0.6 μM. Pralnacasan was found to significantly reduce joint inflammatory symptoms in patients (*64, 65*). The Phase I clinical trials of the second caspase inhibitor, IDN-6556 have been successfully completed for acute alcoholic hepatitis (IDUN pharmaceuticals, now acquired by Pfizer, www.idun.com).

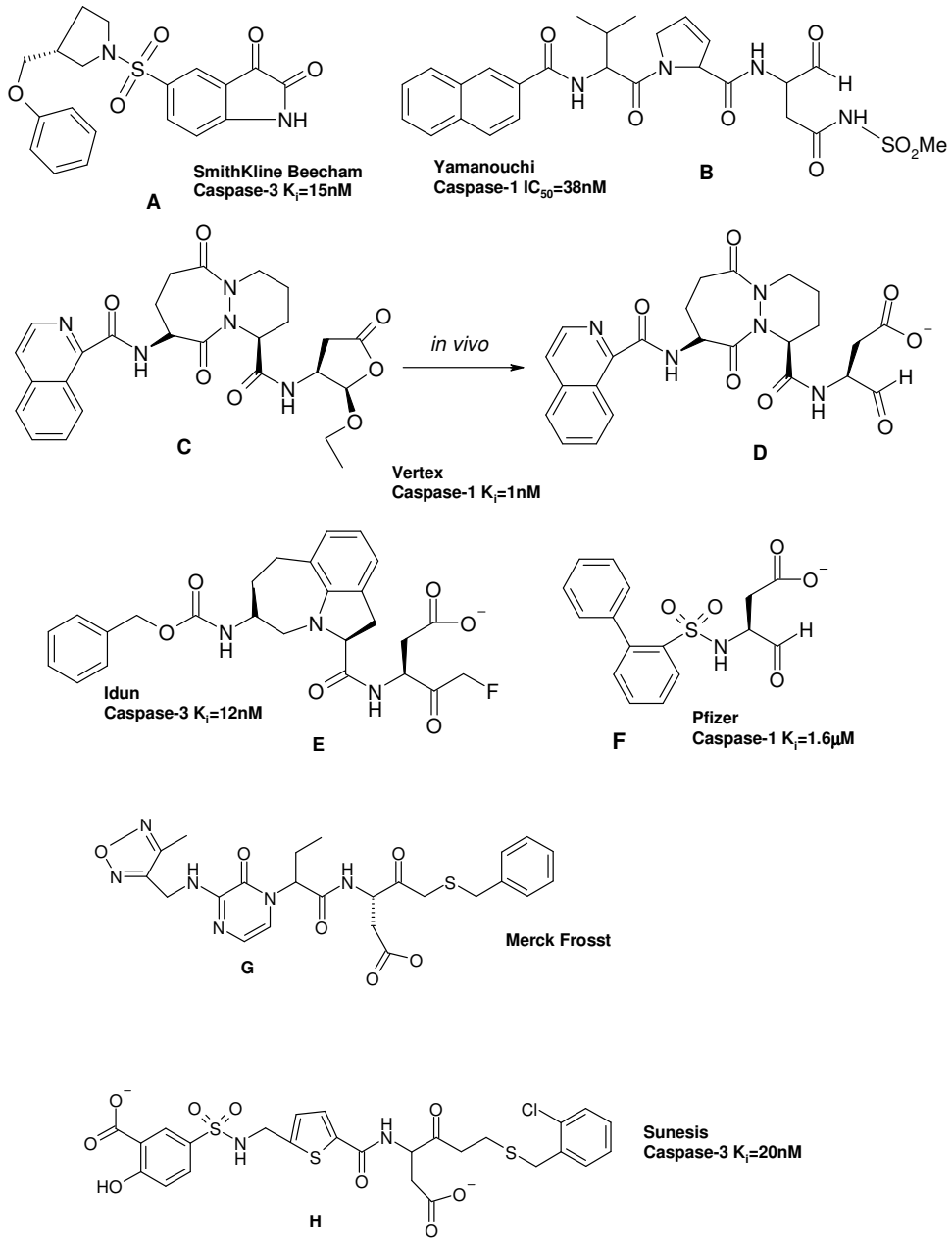

Figure 6: Examples of synthetic inhibitors of the inhibition of caspase activity described in the literature. Figure adapted from (*66*).

The structure of this compound has not been disclosed, but it does possess an irreversible warhead (*67*). However, the structures of earlier compounds developed by IDUN have been

disclosed (e.g. compound-**E**) (*68, 69*). One of these compound (IDN-1965) was shown to dramatically increase survival in rats following Fas-induced liver damage (*70*).

Apoptosis and inflammatory responses are the major host defense mechanisms against viruses. Viruses produce inhibitors of caspases, to prolong the life of host cells for maximal viral replication. These viral inhibitors either directly inhibit caspases (cowpox virus protein CrmA (cytokine response modifier A), baculovirus proteins p35 and IAPs) or inhibit caspase-adapter interactions (v-FLIP (viral FLICE-inhibitory protein)). CrmA is a serpin that directly targets the active site of mature caspases (*71*). After being cleaved by a caspase, however, CrmA stays bound to the caspase and blocks the active site (*72*). p35 is a broad-spectrum caspase-specific inhibitor; it inhibits human caspase-1, -3, -6, -7, -8 and -10 with K_is ranging from 0.1 nM to 9 nM (*73*). In contrast to CrmA and p35, cellular IAPs (inhibitors of apoptosis) are not active-site-specific inhibitors and their inhibition of apoptosis does not require cleavage by caspases. The IAPs, originally identified in the genome of baculovirus based on their ability to suppress apoptosis in infected host cells, antagonize cell death by interacting with and inhibiting the enzymatic activity of mature caspases.

1.3.2 Allosteric site inhibitors

An allosteric site is a remote site where a molecule that is not a substrate may bind and influence the ability of the enzyme to be active. The discovery of allosteric sites generates opportunities for the identification of novel pharmaceuticals and increases the understanding of biological processes. In caspases it has proven difficult to find drug-like caspase inhibitors possessing favorable pharmacokinetic properties, because of a strong preference for an acidic side chain and an electrophilic functionality to bind at the active site (*17*). Allosteric sites provide appealing alternatives for drug discovery because the chemical properties for binding are different from active site-directed compounds (*74-77*).

Active caspases are homo-dimers of hetero-dimers and their oligomeric state is directly linked with the enzymatic activity (*78*). Initiator caspase-1, -8, and -9 shift from the monomeric to the dimeric state when active site inhibitors bind (*51, 79, 80*). An allosteric cavity exists at the dimer interface of active caspases and it was shown previously that this allosteric site can be utilized to modulate the caspase activity (*81*). The amino acids forming the interface are not conserved between different caspases. For example, the interface is hydrophobic in case of

caspase-3, -6 and -7. In contrast, hydrophilic residues are commonly found in caspase-1, 4, -5 and -11. The interfaces of caspase-2, -8, -9 and -11 include both hydrophobic and hydrophilic residues. In addition the size and shape of the dimer interface cavity is differ considerably among the caspase family members. Caspase-8 has the largest cavity, with an approximate volume of 17×15×11 $Å^3$, while the interface cavity in caspase-2 and -3 are slightly smaller. In two of the crystal structures of caspase-8, an oxidised DTT molecule occupies this site (*40, 82*). Caspase-2 has a distinct feature for the dimer formation, as illustrated by the structural study, a disulphide bond between Cys419 and Cys419' from each monomer promotes the dimerization and stabilizes the active caspase-2 (*38*). One of the aims in this thesis was the identification of specific caspase inhibitors that bind to this allosteric site using a structure based design approach **Chapter 5**.

1.3.3 Caspase activators

Selective activation of caspases might be a valuable strategy, especially for the therapy of human cancers. Several strategies to trigger caspase activation specifically in tumor cells are currently being designed. Inducible caspases that can be activated "on demand" have been engineered by fusing them to chemical dimerization domains. After delivery of these chimeric "death switches" by adenoviral gene transfer, caspases can be activated to trigger apoptosis in tumor cells by cell-permeable dimerization drugs (*78, 83*). Inducible caspase-9 (iCasp9) under the control of a prostate-specific, androgen-responsive promoter was targeted to prostate cancer cells (*84*). Another apoptosis-triggering approach is based on fusion proteins that contain effector caspases (*85, 86*).

Activation of caspases *in vivo,* using small molecules might be an effective approach to kill cancer cells or at least to reverse the resistance against anticancer drugs. Caspase-3 is kept in an inactive state by an intramolecular electrostatic interaction facilitated by a triplet of aspartic acid molecules termed the "safety-catch" (*87*). Removal of the safety catch loop resulted in increased autocatalytic maturation and susceptibility to caspase-9. Thus, the release of the caspase-3 "safety catch" may be an important feature for apoptotic competence Attempts have been made to design small pharmacologically active molecules capable of inducing auto-activation in caspases. Maxim Pharmaceutical Inc. has developed a pharmacologically-active caspase activator MX-2060 (*88*).

Arginine-glycine-aspartate (RGD) tripeptides are recognized by integrins in extracellular matrix proteins and can block integrin-mediated signalling and cell adhesion (*89-91*). The RGD motif exhibit marked proapoptotic properties and can directly induce auto-processing (auto-activation) of procaspase-3 (*92*). A strategy to selectively activate caspase-3 using synthetic small molecules which mimic RGD peptides is followed by Merck Frosst (http://www.merckfrosst.ca).

1.3.4 Compartmentalization, phosphorylation and nitrosylation

Different procaspases may be present at different intracellular compartments and their localizations may change during apoptosis (*33*). One of the best examples is that, during Fas-mediated apoptosis, procaspase-8 is recruited from the cytosol to the Fas receptor complex and becomes activated (*7*). This translocation is mediated by the homotypic interaction between the DEDs in the prodomain region of procaspase-8 and that in a Fas-associated adapter protein named FADD. Procaspase-2 is also present in the nucleus as well as the cytoplasm (*93*). In mouse liver, procaspase-3 is present in both cytosol and mitochondria, while procaspase-7 is found only in the cytosol (*94, 95*). Procaspases may normally be compartmentalized away from their substrates to prevent accidental apoptosis; during apoptosis, the activation and coordinate translocation of caspases allow them to move close to their targets (*33*).

As a major form of posttranslational modification, phosphorylation is also employed to modulate caspase activity. One example is the phosphorylation of caspase-9 by Akt (*96*), a serine-threonine protein kinase downstream of phosphatidylinositol 3-kinase, which is implicated in apoptosis suppression mediated by growth factor receptors. Another way to modify caspases post-translationally is by *S*-nitrosylation. Nitric oxide (NO) and related molecules have been found to inhibit apoptosis. A study showed that in unstimulated human cells, the active site of endogenous procaspase-3 is *S*-nitrosylated, but during Fas-mediated apoptosis, it becomes denitrosylated (*97*). The denitrosylation enhances mature caspase-3 activity, although it does not affect procaspase-3 processing.

1.3.5 Caspase substrates

To date, more than 60 proteins have been shown to be substrates of one or more caspases in mammalian cells and the list is still growing (*98*). These substrate proteins contain caspase

cleavage sites in inter-domain linker sequences. Substrate proteins are thus not degraded by caspase processing; instead, caspase cleavage may activate or inactivate the substrate protein's function. Because of the strict requirement for an aspartic acid residue in P_1 and distinct preferences for P_2 to P_4 residues, it is relatively straightforward to identify the likely caspase cleavage sites within a given substrate protein and the likely group of caspases that may recognize them. The substrates identified so far fall into two general groups: a large group of proteins thought to be involved in regulation and execution of apoptosis and a small group of pro-inflammatory cytokine precursors. For many of the identified substrates, the functional consequences of their cleavage have only been inferred from their normal functions. In other cases, the role of caspase cleavage has been experimentally assessed by expressing mutant substrate proteins that have altered caspase cleavage sites or by expressing protein fragments that represent caspase cleavage products. The evolutionary conservation of caspase substrate proteins, in particular their caspase cleavage sites, suggests that caspases were first employed for apoptosis and later co-opted for cytokine processing in mammals (*33*).

Representative list of substrates are the following:

Cell death proteins	Bcl-2, Bid, CrmA, IAP, p28 Bap31, p35 and Procaspases
Cell cycle regulation	Cdc27, Cyclin A, MDM2, p21 (Cip1/Waf1), p27 (Kip1), PITSLRE kinases, Retinoblastoma protein, Wee1 phosphatase
Cytoskeleton	Actin, β-Catenin, Fodrin, Gas2, Gelsolin, Keratin-18 and -19, Lamins, Plakoglobin
Cytokine precursors	Pro-IL-1β, Pro-IL-16, Pro-IL-18
DNA metabolism	Acinus, DNA-dependent protein kinase (DNA-PK), ICAD, PARP
Neurodegenerative disease proteins	APP, Huntingtin, Presenilins
RNA metabolism	Eukaryotic initiation factor 2α, 70-kDa U1-snRNP
Signal transduction	MEKK1, Protein kinase C delta, TCR-ζ chain
Transcription factors	Heat shock factor, GATA-1, Sp1, STAT1, NRF-2
Others	Hsp90, Nedd4, Calpastatin, Rabaptin-5, Transglutaminase

Abbreviations

Bcl-2	B-cell CLL (chronic lymphocytic leukemia)/ lymphoma 2	ICAD	Inhibitor of caspase-3-activated DNase

Bid	BH3 domain-containing pro-apoptotic Bcl-2 family	CrmA	Cow pox cytokine response modifier protein
PARP	POLY (ADP-ribose) polymerase	APP	Amyloid precursor protein
Nedd	Neural precursor cell expressed, developmentally down-regulated	snRNP	Small nuclear ribonucleoprotein particle
Bap	Benzo(a)pyrene	MAP	Mitogen-activated protein kinase
Cdc	cell division cycle	MEKK	murine MAP kinase kinase kinase
Mdm	Murine Double Minute	GATA	Globin transcription factor
Cip	Cyclin B1-interacting protein	STAT	Signal transducer and activator of transcription
Kip	Kinase interacting protein	NRF	Nuclear respiratory factor
Gas	Growth arrest-specific	Hsp	Heat shock protein
IAP	Inhibitor of apoptosis	IL	Interleukin

1.3.6 Physiological functions of caspases

The physiological functions of caspases have been assessed by both pharmacological inhibition and gene knockout experiments (*99*). Because of the overlapping substrate specificities of caspase family members, both pharmacological and genetic approaches have been fruitful in elucidating the redundant and specific roles of caspases. To date, the genes for caspase-1,-2, -3, -8, -9, -11 and -12 have been deleted in mice; human cell lines deficient in caspase-3, -8 and -10 have also been described (*33, 100, 101*). The results from these genetic experiments reveal that mammalian caspases have overlapping and tissue-specific roles in controlling apoptosis in response to specific stimuli.

1.3.7 Pathological consequences of caspases dysregulation

Caspases have a pivotal role in the progression of a variety of neurological disorders. Despite the various causes of such disorders, the mechanism of cell death is similar in a broad spectrum of neurological diseases (*102*). However, the trigger of aberrant caspase activation in most of these diseases is not well understood. In acute neurological diseases, both necrosis and caspase-mediated apoptotic cell death occur (*103*). In contrast, in chronic neurodegenerative diseases, caspase-mediated apoptotic pathways have the dominant role in mediating cell dysfunction and cell death (*104*). A primary difference between acute and chronic neurological

diseases is the magnitude of the stimulus causing cell death. The greater stimulus in acute diseases results in both necrotic and apoptotic cell death, whereas the milder stimulus results in chronic diseases initiate apoptotic cell death.

The amyloid-beta precursor protein (APP) is directly and efficiently cleaved by caspases during apoptosis, resulting in elevated amyloid-beta (A-β) peptide formation (*105*). The predominant site of caspase-mediated proteolysis is within the cytoplasmic tail of APP and cleavage at this site occurs in hippocampal neurons *in vivo* following acute excitotoxic or ischemic brain injury. Caspase-3 is the predominant caspase involved in APP cleavage, consistent with its marked elevation in dying neurons of Alzheimer's disease brains and co-localization of its APP cleavage product with A-β in senile plaques (*106*). Caspases thus appear to play a dual role in proteolytic processing of APP and the resulting propensity for A-β peptide formation, as well as in the ultimate apoptotic death of neurons in Alzheimer's disease (*107*).

Cell and animal models of ALS (Amyotropic lateral sclerosis), along with the finding of a greater than 80% increase in caspase-1 activity in spinal cord samples from humans with ALS indicate that caspases may play an essential role in the pathology of this disease (*108*). A role of caspases in the pathogenesis of Huntington's disease was suggested by the finding that the protein huntingtin is a substrate for caspases. In brains of patients with Huntington's disease increased levels of DNA strand breaks are found, a process typical of apoptotic cells. Tetrapeptide aldehyde inhibitors Ac-DEVD-CHO and Ac-YVAD-CHO were used to demonstrate that caspases cleave other polyglutamine-containing proteins involved in neurodegenerative diseases such as spinal bulbar muscular atrophy (SBMA)(*109*).

Several experimental models of Parkinson's disease have supported a role of caspases in apoptotic dopaminergic cell death (*110-112*). Peptide caspase inhibitors have been shown to protect against 1-methyl-4-phenylpyridinium (MPP+)-induced apoptosis of cultural cerebrellar granular neurons and increase the rate of survival (*113*). Additionally, administration of Z-VAD-FMK prevented the loss of nigral dopaminergic neurons following intrastriatal administration of the neurotoxin 6- hydroxydopamine (6-ODHA). This prevention of dopaminergic neuron loss by Z-VAD-FMK suggests a role for caspases in 6-OHDA-mediated cell death (*114*).

1.3.8 Therapeutic intervention for regulation of caspase activities

Abnormal cell survival is a hallmark of cancer cells, both oncogenes and tumor suppressor genes have been shown to regulate apoptosis. p53, the most frequently mutated human tumor suppressor gene, functions in critical pathways to connect DNA damage to cell cycle arrest and apoptosis (*115*). Reduced apoptosis gives cancer cells a selective advantage in many steps of tumorigenesis. Initially, it allows cancer cells to survive dysregulated growth signals from oncogenes, which would normally induce apoptosis. p53 appears to be a common effector pathway in oncogene and DNA damage-induced apoptosis, but the exact molecular mechanisms connecting p53 activation to caspase activity remains poorly understood (*116*).

The critical role of caspase-mediated cell death in controlling viral infection is reflected by the number of virally encoded genes that interfere with caspase activation or inhibit caspase activity (*8*). Apoptosis of infected cells, either induced autonomously or instructed by CTL (cytotoxic T lymphocytes), can decrease viral replication or spread by limiting the pool of host cells for productive infection, but excessive apoptosis may also lead to tissue dysfunction. The rapid decline in $CD4^+$ T cells by apoptosis in human immunodeficiency virus (HIV) infection has been viewed as a promising target for caspase inhibition (*2*). Apoptosis plays a critical role in the deletion of unnecessary and dangerous lymphocytes. Because the antigen receptors arise from random DNA recombination, autoimmune lymphocytes that recognize self-antigens are constantly produced. Selective depletion of auto-reactive lymphocytes by caspase activation and apoptosis may be a valid therapeutic strategy (*117*).

Excessive apoptosis has been blamed for several serious pathologies for which there are currently limited therapeutic options, including neurodegenerative diseases, ischemia-reperfusion injury, graft-versus-host disease and autoimmune disorders (*33*). Thus caspases are attractive and potential targets for the therapeutic treatment of these disease states (*66*). This thesis adopted a structure based design approach for the identification and X-ray crystallographic structure determination for the validation of the inhibitors that might be specific towards caspases.

1.4 Structure based design of inhibitors for caspases

In the past new drugs have been discovered using a conventional screening approach, which is a very tedious process. However, if the three dimensional structure of the target protein is known, a structure-based drug design strategy can be very successful. Currently, structure/activity relationship for a ligand/receptor interaction can be analyzed by a variety of techniques, like high throughput screening (HTS), NMR, X-Ray, Mass Spectrometry (MS), Surface plasmon resonance etc. The combination of structure-based drug design involving X-ray crystallography has become increasingly popular in drug discovery since it offers the means to identify and optimize lead compounds in terms of their binding affinities and specificities. When combined with *in silico* methods, it can speed-up drug discovery as it provides a faster and cheaper alternative to *in vivo* testing (Fig. 7). Additionally, it allows to screen a large chemical diversity without actually synthesizing the compounds. The process has the potential to discover compounds with acceptable ADME (Absorption, Distribution, Metabolism, and Elimination) and toxicology properties. These properties are poor for substrate based peptide inhibitors which prevent their widespread use in medicinal chemistry. An application of this procedure for the identification of new lead compounds that inhibit caspase-2, -3 and -8 is described in **Chapter 5** of this thesis.

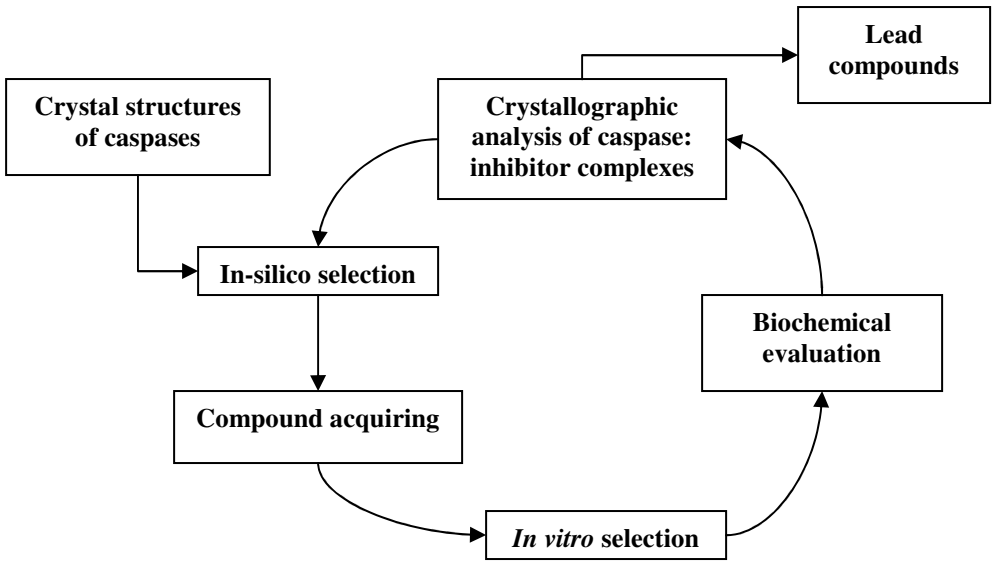

Figure 7. An iterative cycle for the discovery and re-design of lead compounds

1.4.1 Azapeptide Michael acceptors and epoxides as caspase inhibitors

Most of the caspase inhibitors reported so far possess either an aldehyde or halogen methylketone moiety as warhead (*66*). Such inhibitors are very unspecific, since they also inhibit related proteases (*55, 118*). Therefore the search for other potential warheads with a high selectivity for caspases was undertaken. Recently, azapeptide epoxides (Fig. 8a) and Michael acceptors (Fig. 8b) as a new class of irreversible caspase inhibitors that are highly specific for caspases have been identified (*119-121*). Several azapeptide epoxide and Michael acceptor inhibitors with varying prime site constituents were synthesized and their potencies for the inhibition of caspases were determined in an *in vitro* assay in the group of James C. Powers (Georgia institute of technology, Atlanta, USA). **Chapters 3** and **4** describe the structural studies with caspase-3 and -8, using some of these inhibitors. These studies led to the elucidation of the structure based mechanism of the inhibition. In addition, the study revealed the factors determining the prime site specificity.

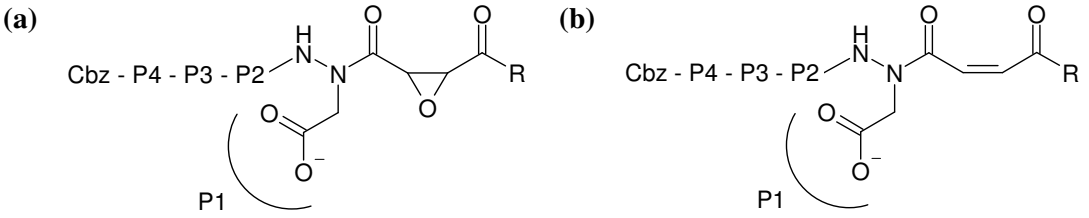

Figure 8. Chemical structure of a typical azapeptide epoxide **(a)** and Michael acceptor **(b)** inhibitor.

The motivation for the design of epoxides was primarily based on the observation that the naturally occurring E-64 (an epoxysuccinyl peptide, L-trans-epoxysuccinyl-leucylamide-(4-guanidino)-butane) is a potent, selective and irreversible inhibitor for cysteine proteases (Fig. 9a) (*122*). E-64 was isolated from *Aspergillus japonicus* (*122, 123*) and it does not inhibit serine proteases, aspartic proteases, or metalloproteases (*124-126*). The synthetic derivatives of E-64, (e.g. E-64c, Fig. 9b) are also potent cysteine protease inhibitors. The design of Michael acceptor inhibitors for caspases was based on the finding, that the fumarate analog of E-64c (Fig.9c) was an inhibitor of Cathepsin-B and -L (*126*).

(a)

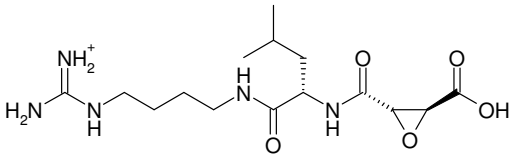

(b)

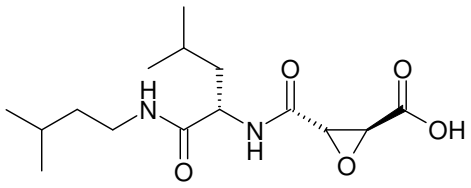

(c)

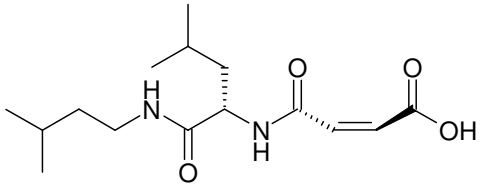

Figure 9. Chemical structure of E-64 **(a)**, E-64c **(b)** and the fumarate analog of E-64c, which are potent and selective inhibitors for cysteine proteases.

1.4.2 Azapeptides

Azapeptides are peptidomimetic compounds in which the C^{α} atom of an amino acid residue is replaced by a nitrogen atom (*127-129*) (Fig. 10). This modification renders certain unique conformational properties to the peptide structure and dynamics because of the loss of chirality and reduction in the flexibility of the parent peptide by restricting the rotation around C^{α}-C bond or the Ψ angle.

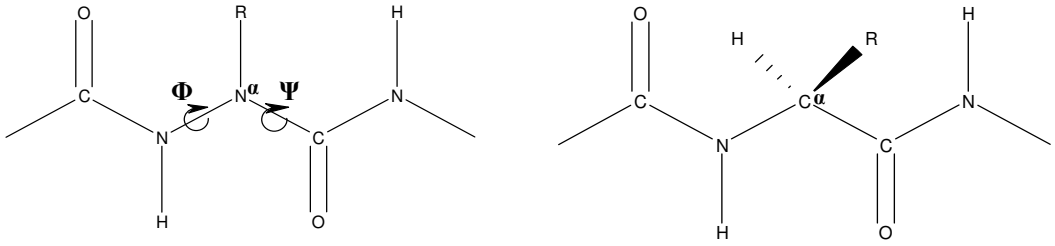

Figure 10. (a) Aza-amino acid and (b) L-amino acid

Azapeptides possess several advantageous features compared to the natural peptides. They are resistant to proteolysis and they offer enhanced stability to acyl-enzyme complex against nucleophilic attack by water molecules during the deacylation step. The increase in acidity of the NH group attached to the N^{α} atom improves the tendency towards the formation of hydrogen bond. Azapeptides therefore possess improved pharmacokinetic properties like

absorption, distribution, metabolism and excretion apart from the metabolic stability, and are widely used as an attractive peptidomimetic in drug design (*130, 131*).

The biological activity of peptides is strongly dependent on their three dimensional structure, because bioactive peptides must adopt a specific conformation in order to bind to an acceptor molecule. Exploration of a binding conformation is one of the most important aspects in designing a potent and selective inhibitor. Stabilisation of a particular conformation can be achieved by incorporating geometric constraints. The most obvious changes can be made by replacing a tetrahedral carbon atom with a planar nitrogen atom (*122*). This leads to the loss of an easily rotatable C^{α}-C bond. Due to this change, azapeptides are more rigid than their conventional peptide counterparts. The rotational barrier is high for N^{α}-N bond because of the repulsive interaction between the nitrogen lone pair which forces the lone pair and the substituents on both nitrogen atoms to be eclipsed in the planar geometry. Substitution of an N^{α} atom generates two structural elements: hydrazine and urea whose conformational properties are described by ϕ and Ψ angles respectively (*129*).

1.4.3 Epoxysuccinyl inhibitors of caspases

An initial attempt to obtain epoxysuccinyl inhibitors for caspase-1 was made by selecting the residues of its precursor, proIL-1β (pro-Interleukin-1β) and replacing the P1-Asp with an epoxysuccinyl moiety. A few compounds were synthesised and tested for their inhibitory activity towards caspase-1, but none of the compounds were found to inhibit caspase-1 (*132*) possibly because, they all lack the critical aspartic acid residue in P1. Alternatively, the group of James C. Powers designed some epoxide peptide inhibitors for caspases (*133*) (Fig. 11). Their design strategy included the placement of an epoxide moiety at the N-terminus of an aspartic acid residue assuming a retro-substrate like binding as commonly witnessed for clan CA cysteine proteases. They have synthesized both D and L amino acid derivatives of this series of compounds. The compounds were tested in an *in vitro* assay, but they failed to inhibit caspase-3, -6 and -8, yet they had some inhibitory activity against papain and cathepsin B.

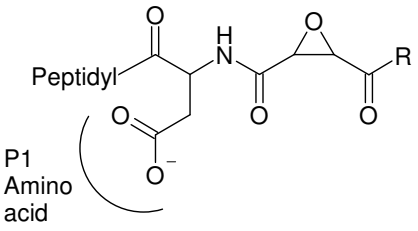

R = OH, OEt, NH-iBu

Figure 11. Design strategy to design α-aminoacyl epoxides for caspases, which failed to inhibit caspases. Figure adapted from (*133*).

The study led to the following hypotheses regarding the binding mechanism of epoxide inhibitors:

i. the binding mode of azapeptide epoxide inhibitors would be opposite to that of E-64 and E-64 derivatives. E-64 like compounds bind to papain and cathepsin B in a manner which is reverse to substrate binding, while azapeptide epoxide might bind in a manner similar to substrate binding.

ii. the epoxysuccinate derivative of azapeptides would be more reactive than simple α-aminoacyl epoxides

1.4.4 Binding mode of epoxysuccinyl inhibitors

More than a dozen x-ray structures of epoxysuccinate derivatives bound to cysteine proteases have been reported (*122*). Three general binding modes have been observed or proposed (Fig. 12). In the most often observed binding mode, the epoxysuccinate binds in the S subsites. However, in contrast to the substrate binding mode (N-terminal to C-terminal, Fig. 12a), the peptide chain of the inhibitor is oriented in the reverse direction (C-terminal to N-terminal, Fig. 12b). In the second binding mode, the inhibitor is located only in the S` subsites (Fig. 12c). Newly developed inhibitors, which extend in both directions, are proposed to bind with both the S and S` subsites (Fig.12d). One crystal structure is available so far for a P and P` extended inhibitor (papain-CLIK148, 1CVZ) (*134*). Nucleophilic attack by the active site cysteine residue is dictated by the binding mode of the peptide portion of the inhibitor. Binding in the S subsites leads to C-2 attack (Fig.12b), whereas binding in the S` subsites leads to C-3 attack (Fig. 12c). So far, the latter binding mode has been observed only with cathepsin B. As a general rule, the covalent bond with the cysteine residue will be formed at the oxirane carbon that possesses the prime site substituent.

Table 2. PDB codes for X-ray crystal structures of cysteine proteases and epoxysuccinyl-based inhibitors. Table adapted from (*122*).

Enzyme	Inhibitor	PDB code
actinidin	E-64	1AEC
cathepsin B	CA-030	1CSB
cathepsin B	CA-074	1QDQ
cathepsin B	E-64c	1ITO
cathepsin K	E-64	1ATK
papain	E-64c	1PE6
papain	E-64c	1PPP
papain	CLIK 148	1CVZ
staphopain	E-64	1CV8

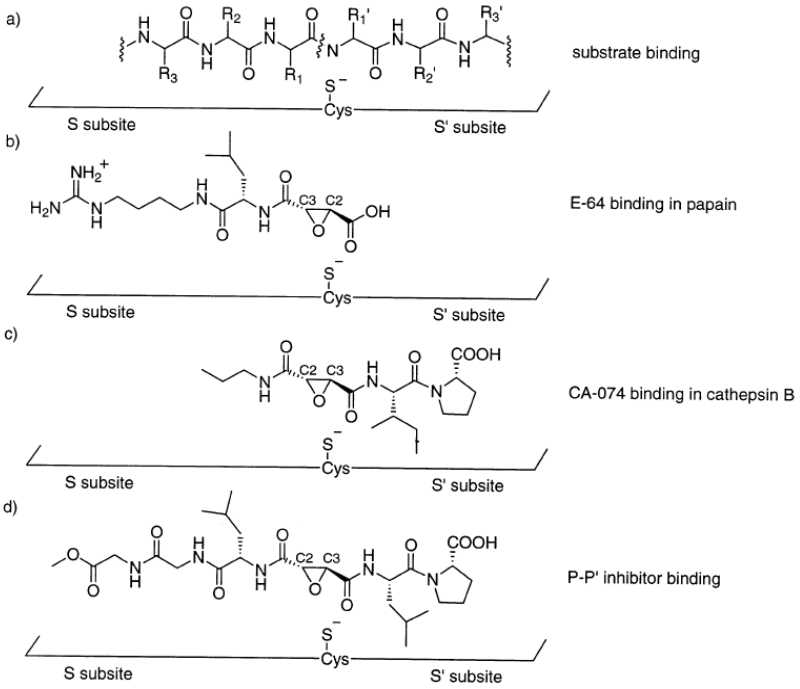

Figure 12. Schematic representation of the binding modes of peptidyl epoxysuccinates: (a) normal binding mode with a peptide substrate; (b) binding mode of E-64 to papain; (c) binding mode of CA-074 to cathepsin B; (d) binding mode of MeO-GlyrGlyrLeur(2*S*,3*S*)-Eps-Leu-Pro-OH to cathepsin B. Arrow indicates the reversed peptide chain. Cys-S^- represents the side-chain thiolate of the active site cysteine residue. Figure adapted from (*122*).

1.5 Low barrier hydrogen bond

The atomic resolution structure of caspase-3 in complex with Z-DEVD-cmk inhibitor (**Chapter 2**) has revealed the formation of a low-barrier hydrogen bond (LBHB) between the P_4-aspartic acid of the inhibitor (Z-DEVD-cmk) and Asp-179 of the N-terminal loop of the β-subunit of caspase-3. A hydrogen bond occurs when two electronegative atoms, such as nitrogen and oxygen, interact with the same hydrogen. The hydrogen is normally covalently attached to one atom, the *donor*, but interacts electrostatically with the other, the *acceptor*. This interaction is due to the dipole between the electronegative atoms and the proton. An enzyme may stabilize the transition state by forming a strong hydrogen bond or it may force the donor atoms into proximity and relieve the resulting destabilization of the enzyme: substrate complex by forming a hydrogen bond (*135*). In either case, this may be a LBHB with possible covalent nature. Hydrogen bond strength in an aprotic solvent is sensitive to change in acidity or basicity (*136*). The hydrogen bond will be strengthened when going from the enzyme: substrate complex to the transition state relative to aqueous solvent. This strengthening arises from the relief of destabilization associated with a poor solvation of the anions in aprotic solvents but this relief can then increase k_{cat}.

The binding energy of a hydrogen bond ranges from very weak ($\Delta G_{formation}$ ~ -2 kcal/mol) to very strong ($\Delta G_{formation}$ < -25 kcal/mol) approaching in some cases, the energy values of covalent bonds (*136*). In weak hydrogen bonds, the proton is covalently bound to one electronegative atom at a distance of ~1.0Å , and electrostatically attracted to another electronegative atom at approximately twice the distance (1.7 to 2.0 Å) (Fig. 13). The overall hydrogen bond length, given by the distance between the two electronegative or heavy atoms, is 2.7 to 3.0Å. The proton has two alternative locations or free energy wells as it can be covalently bound to either A or B (Eq. 1)

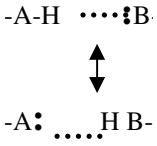

Equation 1. Hydrogen bond between two electronegative atoms A and B.

As the electronegative atoms A and B approach each other, the hydrogen bond is shortened to values between 2.60 and 2.50Å. The length of covalent A-H moiety increases and the noncovalent moiety H…B decreases. The hydrogen bond energy increases (-7 kcal/mol ≥ $\Delta G_{formation}$ ≥ -25 kcal/mol) and the energy barrier between two proton wells decreases (Fig. 13). When the barrier approaches the zero point vibrational energy of the hydrogen, the proton is delocalized between the two wells while a deuterium would remain localized. This state is referred to as LBHB (*137*).

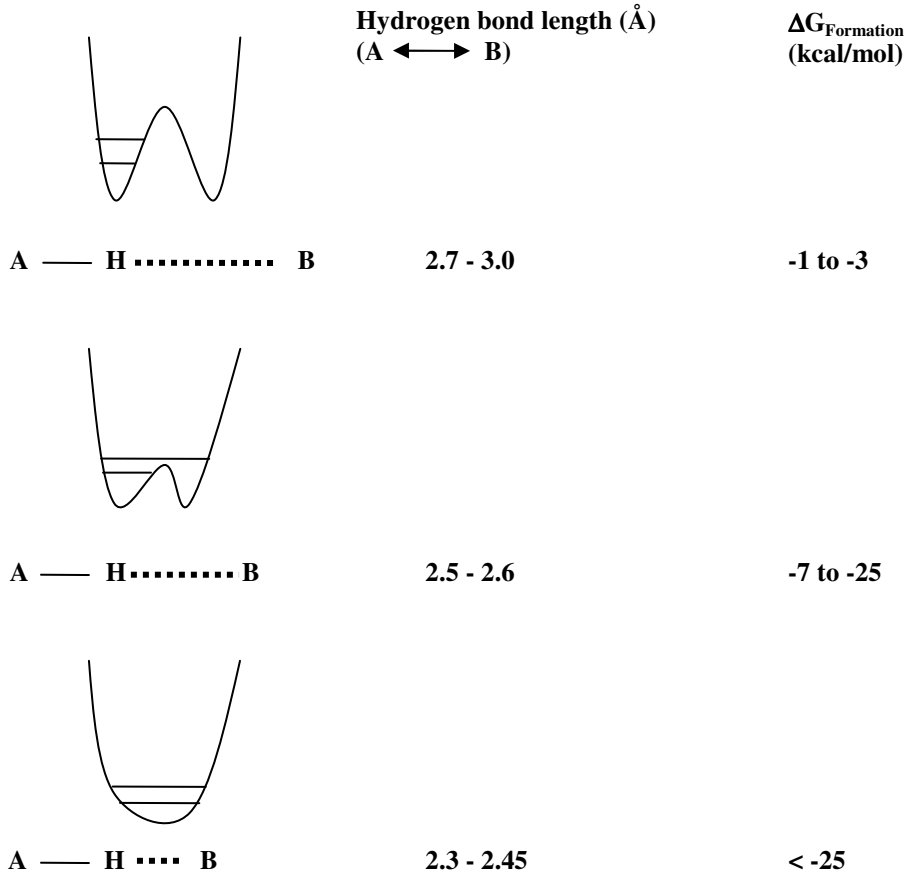

Figure 13. Strengths of hydrogen bonds. Potential functions for weak, double-well (upper), strong-low-barrier (middle), and very-strong-single-well hydrogen bonds (lower) in which the pK_a values of A-H and B-H are equal. Horizontal lines give the zero-point vibrational energy levels of a proton and deuterium. Also indicated are the bond lengths and strengths of such hydrogen bonds. Figure adapted from (*137*).

Specifically, as the O-H…O hydrogen bond length decreases from 2.54 to 2.45Å its free energy increases rapidly from -7.8 to 32 kcal/mol, presumably due to an overlap of the proton and oxygen wave functions. As the heavy atoms continue to approach each other, further shortening the hydrogen bond 2.45-2.3 Å, the barrier between two wells disappears, and the proton is (or deuterium) in a single well. Single well hydrogen bonds are very strong. The proton is at equal distances from the two electronegative atoms.While the strength of the hydrogen bonds correlates with its bond length, little or no correlation is found experimentally and theoretically between strength and bond angle, A - H…B, over a range of 180 ± 30° (*137*). LBHBs are best studied in enzymes and have been proposed to participate in the mechanism of action of hydrolase's, lyases, ligases and several isomerase's (*135*). It is noteworthy that all LBHBs detected so far in enzymes involve carboxyl groups (*138*).

1.6 REFERENCES

(1) Raff, M. (1998) Cell suicide for beginners. *Nature 396*, 119.

(2) Thompson, C. B. (1995) Apoptosis in the pathogenesis and treatment of disease. *Science 267*, 1456-62.

(3) Kerr, J. F., Wyllie, A. H., and Currie, A. R. (1972) Apoptosis: a basic biological phenomenon with wide-ranging implications in tissue kinetics. *Br J Cancer 26*, 239-57.

(4) Grutter, M. G. (2000) Caspases: key players in programmed cell death. *Curr Opin Struct Biol 10*, 649-55.

(5) Alnemri, E. S., Livingston, D. J., Nicholson, D. W., Salvesen, G., Thornberry, N. A., Wong, W. W., and Yuan, J. (1996) Human ICE/CED-3 protease nomenclature. *Cell 87*, 171.

(6) Donepudi, M., and Grutter, M. G. (2002) Structure and zymogen activation of caspases. *Biophys Chem 101-102*, 145-53.

(7) Budihardjo, I., Oliver, H., Lutter, M., Luo, X., and Wang, X. (1999) Biochemical pathways of caspase activation during apoptosis. *Annu Rev Cell Dev Biol 15*, 269-90.

(8) Best, S. M., and Bloom, M. E. (2004) Caspase activation during virus infection: more than just the kiss of death? *Virology 320*, 191.

(9) Shi, Y. (2004) Caspase activation, inhibition, and reactivation: a mechanistic view. *Protein Sci 13*, 1979-87.

(10) Salvesen, G. S., and Abrams, J. M. (2004) Caspase activation - stepping on the gas or releasing the brakes? Lessons from humans and flies. *Oncogene 23*, 2774-84.

(11) Boatright, K. M., and Salvesen, G. S. (2003) Mechanisms of caspase activation. *Curr Opin Cell Biol 15*, 725-31.

(12) Boatright, K. M., and Salvesen, G. S. (2003) Caspase activation. *Biochem Soc Symp*, 233-42.

(13) Salvesen, G. S., and Dixit, V. M. (1999) Caspase activation: the induced-proximity model. *Proc Natl Acad Sci U S A 96*, 10964-7.

(14) Kumar, S., and Colussi, P. A. (1999) Prodomains--adaptors--oligomerization: the pursuit of caspase activation in apoptosis. *Trends Biochem Sci 24*, 1-4.

(15) Thornberry, N. A., Bull, H. G., Calaycay, J. R., Chapman, K. T., Howard, A. D., Kostura, M. J., Miller, D. K., Molineaux, S. M., Weidner, J. R., Aunins, J., and et al. (1992) A novel heterodimeric cysteine protease is required for interleukin-1 beta processing in monocytes. *Nature 356*, 768-74.

(16) Yuan, J., Shaham, S., Ledoux, S., Ellis, H. M., and Horvitz, H. R. (1993) The C. elegans cell death gene ced-3 encodes a protein similar to mammalian interleukin-1 beta-converting enzyme. *Cell 75*, 641-52.

(17) Thornberry, N. A., Rano, T. A., Peterson, E. P., Rasper, D. M., Timkey, T., Garcia-Calvo, M., Houtzager, V. M., Nordstrom, P. A., Roy, S., Vaillancourt, J. P., Chapman, K. T., and Nicholson, D. W. (1997) A combinatorial approach defines specificities of members of the caspase family and granzyme B. Functional relationships established for key mediators of apoptosis. *J Biol Chem 272*, 17907-11.

(18) Hu, S., and Yang, X. (2000) dFADD, a novel death domain-containing adapter protein for the Drosophila caspase DREDD. *J Biol Chem 275*, 30761-4.

(19) Muzio, M., Chinnaiyan, A. M., Kischkel, F. C., O'Rourke, K., Shevchenko, A., Ni, J., Scaffidi, C., Bretz, J. D., Zhang, M., Gentz, R., Mann, M., Krammer, P. H., Peter, M. E., and Dixit, V. M. (1996) FLICE, a novel FADD-homologous ICE/CED-3-like protease, is recruited to the CD95 (Fas/APO-1) death--inducing signaling complex. *Cell 85*, 817-27.

(20) Fernandes-Alnemri, T., Armstrong, R. C., Krebs, J., Srinivasula, S. M., Wang, L., Bullrich, F., Fritz, L. C., Trapani, J. A., Tomaselli, K. J., Litwack, G., and Alnemri, E. S. (1996) In vitro activation of CPP32 and Mch3 by Mch4, a novel human apoptotic cysteine protease containing two FADD-like domains. *Proc Natl Acad Sci U S A 93*, 7464-9.

(21) Boldin, M. P., Goncharov, T. M., Goltsev, Y. V., and Wallach, D. (1996) Involvement of MACH, a novel MORT1/FADD-interacting protease, in Fas/APO-1- and TNF receptor-induced cell death. *Cell 85*, 803-15.
(22) Hofmann, K., Bucher, P., and Tschopp, J. (1997) The CARD domain: a new apoptotic signalling motif. *Trends Biochem Sci 22*, 155-6.
(23) Denault, J. B., and Salvesen, G. S. (2003) Human caspase-7 activity and regulation by its N-terminal peptide. *J Biol Chem 278*, 34042-50.
(24) Yaoita, Y. (2002) Inhibition of nuclear transport of caspase-7 by its prodomain. *Biochem Biophys Res Commun 291*, 79-84.
(25) Meergans, T., Hildebrandt, A. K., Horak, D., Haenisch, C., and Wendel, A. (2000) The short prodomain influences caspase-3 activation in HeLa cells. *Biochem J 349*, 135-40.
(26) Riedl, S. J., Fuentes-Prior, P., Renatus, M., Kairies, N., Krapp, S., Huber, R., Salvesen, G. S., and Bode, W. (2001) Structural basis for the activation of human procaspase-7. *Proc Natl Acad Sci U S A 98*, 14790-5.
(27) Chai, J., Wu, Q., Shiozaki, E., Srinivasula, S. M., Alnemri, E. S., and Shi, Y. (2001) Crystal structure of a procaspase-7 zymogen: mechanisms of activation and substrate binding. *Cell 107*, 399-407.
(28) Qin, H., Srinivasula, S. M., Wu, G., Fernandes-Alnemri, T., Alnemri, E. S., and Shi, Y. (1999) Structural basis of procaspase-9 recruitment by the apoptotic protease-activating factor 1. *Nature 399*, 549-57.
(29) Eberstadt, M., Huang, B., Chen, Z., Meadows, R. P., Ng, S. C., Zheng, L., Lenardo, M. J., and Fesik, S. W. (1998) NMR structure and mutagenesis of the FADD (Mort1) death-effector domain. *Nature 392*, 941-5.
(30) Chou, J. J., Matsuo, H., Duan, H., and Wagner, G. (1998) Solution structure of the RAIDD CARD and model for CARD/CARD interaction in caspase-2 and caspase-9 recruitment. *Cell 94*, 171-80.
(31) Lahm, A., Paradisi, A., Green, D. R., and Melino, G. (2003) Death fold domain interaction in apoptosis. *Cell Death Differ 10*, 10-2.
(32) Barnhart, B. C., Lee, J. C., Alappat, E. C., and Peter, M. E. (2003) The death effector domain protein family. *Oncogene 22*, 8634-44.
(33) Chang, H. Y., and Yang, X. (2000) Proteases for cell suicide: functions and regulation of caspases. *Microbiol Mol Biol Rev 64*, 821-46.
(34) Blanchard, H., Donepudi, M., Tschopp, M., Kodandapani, L., Wu, J. C., and Grutter, M. G. (2000) Caspase-8 specificity probed at subsite S(4): crystal structure of the caspase-8-Z-DEVD-cho complex. *J Mol Biol 302*, 9-16.
(35) Blanchard, H., Kodandapani, L., Mittl, P. R., Marco, S. D., Krebs, J. F., Wu, J. C., Tomaselli, K. J., and Grutter, M. G. (1999) The three-dimensional structure of caspase-8: an initiator enzyme in apoptosis. *Structure Fold Des 7*, 1125-33.
(36) Mittl, P. R., Di Marco, S., Krebs, J. F., Bai, X., Karanewsky, D. S., Priestle, J. P., Tomaselli, K. J., and Grutter, M. G. (1997) Structure of recombinant human CPP32 in complex with the tetrapeptide acetyl-Asp-Val-Ala-Asp fluoromethyl ketone. *J Biol Chem 272*, 6539-47.
(37) Rotonda, J., Nicholson, D. W., Fazil, K. M., Gallant, M., Gareau, Y., Labelle, M., Peterson, E. P., Rasper, D. M., Ruel, R., Vaillancourt, J. P., Thornberry, N. A., and Becker, J. W. (1996) The three-dimensional structure of apopain/CPP32, a key mediator of apoptosis. *Nat Struct Biol 3*, 619-25.
(38) Schweizer, A., Briand, C., and Grutter, M. G. (2003) Crystal structure of caspase-2, apical initiator of the intrinsic apoptotic pathway. *J Biol Chem 278*, 42441-7.
(39) Walker, N. P., Talanian, R. V., Brady, K. D., Dang, L. C., Bump, N. J., Ferenz, C. R., Franklin, S., Ghayur, T., Hackett, M. C., Hammill, L. D., and et al. (1994) Crystal structure of the cysteine protease interleukin-1 beta-converting enzyme: a (p20/p10)2 homodimer. *Cell 78*, 343-52.

(40) Watt, W., Koeplinger, K. A., Mildner, A. M., Heinrikson, R. L., Tomasselli, A. G., and Watenpaugh, K. D. (1999) The atomic-resolution structure of human caspase-8, a key activator of apoptosis. *Structure Fold Des 7*, 1135-43.

(41) Wilson, K. P., Black, J. A., Thomson, J. A., Kim, E. E., Griffith, J. P., Navia, M. A., Murcko, M. A., Chambers, S. P., Aldape, R. A., Raybuck, S. A., and et al. (1994) Structure and mechanism of interleukin-1 beta converting enzyme. *Nature 370*, 270-5.

(42) Nicholson, D. W., Ali, A., Thornberry, N. A., Vaillancourt, J. P., Ding, C. K., Gallant, M., Gareau, Y., Griffin, P. R., Labelle, M., Lazebnik, Y. A., and et al. (1995) Identification and inhibition of the ICE/CED-3 protease necessary for mammalian apoptosis. *Nature 376*, 37-43.

(43) Rajkumar Ganesan, P. R. E. M., Stjepan Jelakovic, Markus G. Grütter. (2005) Crystal structure of caspase-3/DEVD-chloromethyl ketone complex: implications for substrate recognition and catalysis. *to be submitted*.

(44) Esther D. Lenherr, B., A., and Grutter, MG. (2004) Kinetic characterization of caspase-8. *Diploma thesis, Department of Biochemistry, University of Zurich*.

(45) L. Aravind, E. V. K. (2002) Classification of the caspase-hemoglobinase fold: Detection of new families and implications for the origin of the eukaryotic separins. *Proteins: Structure, Function, and Genetics 46*, 355-367.

(46) Sleath, P. R., Hendrickson, R. C., Kronheim, S. R., March, C. J., and Black, R. A. (1990) Substrate specificity of the protease that processes human interleukin-1 beta. *J Biol Chem 265*, 14526-8.

(47) Howard, A. D., Kostura, M. J., Thornberry, N., Ding, G. J., Limjuco, G., Weidner, J., Salley, J. P., Hogquist, K. A., Chaplin, D. D., Mumford, R. A., and et al. (1991) IL-1-converting enzyme requires aspartic acid residues for processing of the IL-1 beta precursor at two distinct sites and does not cleave 31-kDa IL-1 alpha. *J Immunol 147*, 2964-9.

(48) Talanian, R. V., Quinlan, C., Trautz, S., Hackett, M. C., Mankovich, J. A., Banach, D., Ghayur, T., Brady, K. D., and Wong, W. W. (1997) Substrate specificities of caspase family proteases. *J Biol Chem 272*, 9677-82.

(49) Stennicke, H. R., Renatus, M., Meldal, M., and Salvesen, G. S. (2000) Internally quenched fluorescent peptide substrates disclose the subsite preferences of human caspases 1, 3, 6, 7 and 8. *Biochem J 350 Pt 2*, 563-8.

(50) Boatright, K. M., Renatus, M., Scott, F. L., Sperandio, S., Shin, H., Pedersen, I. M., Ricci, J. E., Edris, W. A., Sutherlin, D. P., Green, D. R., and Salvesen, G. S. (2003) A unified model for apical caspase activation. *Mol Cell 11*, 529-41.

(51) Donepudi, M., Mac Sweeney, A., Briand, C., and Grutter, M. G. (2003) Insights into the regulatory mechanism for caspase-8 activation. *Mol Cell 11*, 543-9.

(52) Deveraux, Q. L., Stennicke, H. R., Salvesen, G. S., and Reed, J. C. (1999) Endogenous inhibitors of caspases. *J Clin Immunol 19*, 388-98.

(53) Adams, J. M., and Cory, S. (2002) Apoptosomes: engines for caspase activation. *Curr Opin Cell Biol 14*, 715-20.

(54) Adrain, C., Murphy, B. M., and Martin, S. J. (2005) Molecular Ordering of the Caspase Activation Cascade Initiated by the Cytotoxic T Lymphocyte/Natural Killer (CTL/NK) Protease Granzyme B. *J. Biol. Chem. 280*, 4663-4673.

(55) Schotte, P., Van Criekinge, W., Van de Craen, M., Van Loo, G., Desmedt, M., Grooten, J., Cornelissen, M., De Ridder, L., Vandekerckhove, J., and Fiers, W. (1998) Cathepsin B-Mediated Activation of the Proinflammatory Caspase-11. *Biochemical and Biophysical Research Communications 251*, 379.

(56) Yang, X., Stennicke, H. R., Wang, B., Green, D. R., Janicke, R. U., Srinivasan, A., Seth, P., Salvesen, G. S., and Froelich, C. J. (1998) Granzyme B Mimics Apical Caspases. DESCRIPTION OF A UNIFIED PATHWAY FOR TRANS-ACTIVATION OF EXECUTIONER CASPASE-3 AND -7. *J. Biol. Chem. 273*, 34278-34283.

(57) Wei, Y., Fox, T., Chambers, S. P., Sintchak, J., Coll, J. T., Golec, J. M. C., Swenson, L., Wilson, K. P., and Charifson, P. S. (2000) The structures of caspases-1, -3, -7 and -8 reveal the basis for substrate and inhibitor selectivity. *Chemistry & Biology 7*, 423.

(58) Martinon, F., Burns, K., and Tschopp, J. (2002) The Inflammasome: A Molecular Platform Triggering Activation of Inflammatory Caspases and Processing of proIL-[beta]. *Molecular Cell 10*, 417.

(59) Lee, D., Long, S. A., Adams, J. L., Chan, G., Vaidya, K. S., Francis, T. A., Kikly, K., Winkler, J. D., Sung, C. M., Debouck, C., Richardson, S., Levy, M. A., DeWolf, W. E., Jr., Keller, P. M., Tomaszek, T., Head, M. S., Ryan, M. D., Haltiwanger, R. C., Liang, P. H., Janson, C. A., McDevitt, P. J., Johanson, K., Concha, N. O., Chan, W., Abdel-Meguid, S. S., Badger, A. M., Lark, M. W., Nadeau, D. P., Suva, L. J., Gowen, M., and Nuttall, M. E. (2000) Potent and selective nonpeptide inhibitors of caspases 3 and 7 inhibit apoptosis and maintain cell functionality. *J Biol Chem 275*, 16007-14.

(60) Lee, D., Long, S. A., Murray, J. H., Adams, J. L., Nuttall, M. E., Nadeau, D. P., Kikly, K., Winkler, J. D., Sung, C. M., Ryan, M. D., Levy, M. A., Keller, P. M., and DeWolf, W. E., Jr. (2001) Potent and selective nonpeptide inhibitors of caspases 3 and 7. *J Med Chem 44*, 2015-26.

(61) Okamoto, Y., Anan, H., Nakai, E., Morihira, K., Yonetoku, Y., Kurihara, H., Sakashita, H., Terai, Y., Takeuchi, M., Shibanuma, T., and Isomura, Y. (1999) Peptide based interleukin-1 beta converting enzyme (ICE) inhibitors: synthesis, structure activity relationships and crystallographic study of the ICE-inhibitor complex. *Chem Pharm Bull (Tokyo) 47*, 11-21.

(62) Kim, K. M., Kim, Y. M., Park, M., Park, K., Chang, H. K., Park, T. K., Chung, H. H., and Kang, C. Y. (2000) A broad-spectrum caspase inhibitor blocks concanavalin A-induced hepatitis in mice. *Clin Immunol 97*, 221-33.

(63) Jaeschke, H., Farhood, A., Cai, S. X., Tseng, B. Y., and Bajt, M. L. (2000) Protection against TNF-induced liver parenchymal cell apoptosis during endotoxemia by a novel caspase inhibitor in mice. *Toxicol Appl Pharmacol 169*, 77-83.

(64) Siegmund, B., and Zeitz, M. (2003) Pralnacasan (vertex pharmaceuticals). *IDrugs 6*, 154-8.

(65) Rudolphi, K., Gerwin, N., Verzijl, N., van der Kraan, P., and van den Berg, W. (2003) Pralnacasan, an inhibitor of interleukin-1beta converting enzyme, reduces joint damage in two murine models of osteoarthritis. *Osteoarthritis Cartilage 11*, 738-46.

(66) O'Brien, T. (2004) Prospects for caspase inhibitors. *Mini Rev Med Chem 4*, 153-65.

(67) Reed, J. C. (2001) Apoptosis-regulating proteins as targets for drug discovery. *Trends Mol Med 7*, 314-9.

(68) Grobmyer, S. R., Armstrong, R. C., Nicholson, S. C., Gabay, C., Arend, W. P., Potter, S. H., Melchior, M., Fritz, L. C., and Nathan, C. F. (1999) Peptidomimetic fluoromethylketone rescues mice from lethal endotoxic shock. *Mol Med 5*, 585-94.

(69) Wu, J. C., and Fritz, L. C. (1999) Irreversible caspase inhibitors: tools for studying apoptosis. *Methods 17*, 320-8.

(70) Hoglen, N. C., Hirakawa, B. P., Fisher, C. D., Weeks, S., Srinivasan, A., Wong, A. M., Valentino, K. L., Tomaselli, K. J., Bai, X., Karanewsky, D. S., and Contreras, P. C. (2001) Characterization of the caspase inhibitor IDN-1965 in a model of apoptosis-associated liver injury. *J Pharmacol Exp Ther 297*, 811-8.

(71) Ray, C. A., Black, R. A., Kronheim, S. R., Greenstreet, T. A., Sleath, P. R., Salvesen, G. S., and Pickup, D. J. (1992) Viral inhibition of inflammation: cowpox virus encodes an inhibitor of the interleukin-1 beta converting enzyme. *Cell 69*, 597-604.

(72) Bertin, J., Mendrysa, S. M., LaCount, D. J., Gaur, S., Krebs, J. F., Armstrong, R. C., Tomaselli, K. J., and Friesen, P. D. (1996) Apoptotic suppression by baculovirus P35 involves cleavage by and inhibition of a virus-induced CED-3/ICE-like protease. *J Virol 70*, 6251-9.

(73) Zhou, Q., Krebs, J. F., Snipas, S. J., Price, A., Alnemri, E. S., Tomaselli, K. J., and Salvesen, G. S. (1998) Interaction of the baculovirus anti-apoptotic protein p35 with caspases. Specificity, kinetics, and characterization of the caspase/p35 complex. *Biochemistry 37*, 10757-65.

(74) Birktoft, J. J., Kraut, J., and Freer, S. T. (1976) A detailed structural comparison between the charge relay system in chymotrypsinogen and in alpha-chymotrypsin. *Biochemistry 15*, 4481-5.
(75) Rath, V. L., Ammirati, M., Danley, D. E., Ekstrom, J. L., Gibbs, E. M., Hynes, T. R., Mathiowetz, A. M., McPherson, R. K., Olson, T. V., Treadway, J. L., and Hoover, D. J. (2000) Human liver glycogen phosphorylase inhibitors bind at a new allosteric site. *Chem Biol 7*, 677-82.
(76) Traxler, P., Bold, G., Buchdunger, E., Caravatti, G., Furet, P., Manley, P., O'Reilly, T., Wood, J., and Zimmermann, J. (2001) Tyrosine kinase inhibitors: from rational design to clinical trials. *Med Res Rev 21*, 499-512.
(77) Wiesmann, C., Barr, K. J., Kung, J., Zhu, J., Erlanson, D. A., Shen, W., Fahr, B. J., Zhong, M., Taylor, L., Randal, M., McDowell, R. S., and Hansen, S. K. (2004) Allosteric inhibition of protein tyrosine phosphatase 1B. *Nat Struct Mol Biol 11*, 730-7.
(78) MacCorkle, R. A., Freeman, K. W., and Spencer, D. M. (1998) Synthetic activation of caspases: artificial death switches. *Proc Natl Acad Sci U S A 95*, 3655-60.
(79) Katoh, I., Tomimori, Y., Ikawa, Y., and Kurata, S. (2004) Dimerization and processing of procaspase-9 by redox stress in mitochondria. *J Biol Chem 279*, 15515-23.
(80) Renatus, M., Stennicke, H. R., Scott, F. L., Liddington, R. C., and Salvesen, G. S. (2001) Dimer formation drives the activation of the cell death protease caspase 9. *Proc Natl Acad Sci U S A 98*, 14250-5.
(81) Hardy, J. A., Lam, J., Nguyen, J. T., O'Brien, T., and Wells, J. A. (2004) Discovery of an allosteric site in the caspases. *PNAS 101*, 12461-12466.
(82) Özlem Dogan Ekici, Z. Z. L., Rajkumar Ganesan, Stjepan Jelakovic, Karen Ellis James, Juliana L. Asgian, Jowita Mikolajczyk, Guy S. Salvesen, Markus G Grutter and James C. Powers. (2005) Design, Synthesis, and Evaluation of Aza-Peptide Michael Acceptors as Selective and Potent Inhibitors of Caspases-2, -3, -6, -7, -8, -9, and -10. *to be published*.
(83) Shariat, S. F., Desai, S., Song, W., Khan, T., Zhao, J., Nguyen, C., Foster, B. A., Greenberg, N., Spencer, D. M., and Slawin, K. M. (2001) Adenovirus-mediated transfer of inducible caspases: a novel "death switch" gene therapeutic approach to prostate cancer. *Cancer Res 61*, 2562-71.
(84) Xie, X., Zhao, X., Liu, Y., Zhang, J., Matusik, R. J., Slawin, K. M., and Spencer, D. M. (2001) Adenovirus-mediated tissue-targeted expression of a caspase-9-based artificial death switch for the treatment of prostate cancer. *Cancer Res 61*, 6795-804.
(85) Jia, L. T., Zhang, L. H., Yu, C. J., Zhao, J., Xu, Y. M., Gui, J. H., Jin, M., Ji, Z. L., Wen, W. H., Wang, C. J., Chen, S. Y., and Yang, A. G. (2003) Specific tumoricidal activity of a secreted proapoptotic protein consisting of HER2 antibody and constitutively active caspase-3. *Cancer Res 63*, 3257-62.
(86) Xu, Y. M., Wang, L. F., Jia, L. T., Qiu, X. C., Zhao, J., Yu, C. J., Zhang, R., Zhu, F., Wang, C. J., Jin, B. Q., Chen, S. Y., and Yang, A. G. (2004) A caspase-6 and anti-human epidermal growth factor receptor-2 (HER2) antibody chimeric molecule suppresses the growth of HER2-overexpressing tumors. *J Immunol 173*, 61-7.
(87) Roy, S., Bayly, C. I., Gareau, Y., Houtzager, V. M., Kargman, S., Keen, S. L., Rowland, K., Seiden, I. M., Thornberry, N. A., and Nicholson, D. W. (2001) Maintenance of caspase-3 proenzyme dormancy by an intrinsic "safety catch" regulatory tripeptide. *Proc Natl Acad Sci U S A 98*, 6132-7.
(88) Kasibhatla, S. R., P. Sanjeeva; Drewe, John A. (2002) Methods of identifying potentially therapeutically selective and effective anti-cancer agents that are inducers of apoptosis. *PCT Int. Appl. WO 2002099378*, 45 pp.
(89) Meredith, J. J. E., and Schwartz, M. A. (1997) Integrins, adhesion and apoptosis. *Trends in Cell Biology 7*, 146.
(90) Ruoslahti, E. (1996) RGD and other recognition sequences for integrins. *Annu Rev Cell Dev Biol 12*, 697-715.
(91) Ruoslahti, E., and Pierschbacher, M. D. (1987) New perspectives in cell adhesion: RGD and integrins. *Science 238*, 491-7.

(92) Buckley, C. D., Pilling, D., Henriquez, N. V., Parsonage, G., Threlfall, K., Scheel-Toellner, D., Simmons, D. L., Akbar, A. N., Lord, J. M., and Salmon, M. (1999) RGD peptides induce apoptosis by direct caspase-3 activation. *Nature 397*, 534-9.

(93) Colussi, P. A., Harvey, N. L., and Kumar, S. (1998) Prodomain-dependent nuclear localization of the caspase-2 (Nedd2) precursor. A novel function for a caspase prodomain. *J Biol Chem 273*, 24535-42.

(94) Krajewska, M., Wang, H. G., Krajewski, S., Zapata, J. M., Shabaik, A., Gascoyne, R., and Reed, J. C. (1997) Immunohistochemical analysis of in vivo patterns of expression of CPP32 (Caspase-3), a cell death protease. *Cancer Res 57*, 1605-13.

(95) Zhou, Z., Sun, X., and Kang, Y. J. (2001) Ethanol-induced apoptosis in mouse liver: Fas- and cytochrome c-mediated caspase-3 activation pathway. *Am J Pathol 159*, 329-38.

(96) Cardone, M. H., Roy, N., Stennicke, H. R., Salvesen, G. S., Franke, T. F., Stanbridge, E., Frisch, S., and Reed, J. C. (1998) Regulation of cell death protease caspase-9 by phosphorylation. *Science 282*, 1318-21.

(97) Mannick, J. B., Hausladen, A., Liu, L., Hess, D. T., Zeng, M., Miao, Q. X., Kane, L. S., Gow, A. J., and Stamler, J. S. (1999) Fas-induced caspase denitrosylation. *Science 284*, 651-4.

(98) Stroh, C., and Schulze-Osthoff, K. (1998) Death by a thousand cuts: an ever increasing list of caspase substrates. *Cell Death Differ 5*, 997-1000.

(99) Matikainen, T., Perez, G. I., Zheng, T. S., Kluzak, T. R., Rueda, B. R., Flavell, R. A., and Tilly, J. L. (2001) Caspase-3 Gene Knockout Defines Cell Lineage Specificity for Programmed Cell Death Signaling in the Ovary. *Endocrinology 142*, 2468-2480.

(100) Bergeron, L., Perez, G. I., Macdonald, G., Shi, L., Sun, Y., Jurisicova, A., Varmuza, S., Latham, K. E., Flaws, J. A., Salter, J. C., Hara, H., Moskowitz, M. A., Li, E., Greenberg, A., Tilly, J. L., and Yuan, J. (1998) Defects in regulation of apoptosis in caspase-2-deficient mice. *Genes Dev 12*, 1304-14.

(101) Kuida, K., Zheng, T. S., Na, S., Kuan, C.-Y., Yang, D., Karasuyama, H., Rakic, P., and Flavell, R. A. (1996) Decreased apoptosis in the brain and premature lethality in CPP32-deficient mice. *Nature 384*, 368.

(102) Yuan, J., and Yankner, B. A. (2000) Apoptosis in the nervous system. *Nature 407*, 802-9.

(103) Troy, C. M., and Salvesen, G. S. (2002) Caspases on the brain. *J Neurosci Res 69*, 145-50.

(104) Friedlander, R. M., and Yuan, J. (1998) ICE, neuronal apoptosis and neurodegeneration. *Cell Death Differ 5*, 823-31.

(105) Gervais, F. G., Xu, D., Robertson, G. S., Vaillancourt, J. P., Zhu, Y., Huang, J., LeBlanc, A., Smith, D., Rigby, M., Shearman, M. S., Clarke, E. E., Zheng, H., Van Der Ploeg, L. H., Ruffolo, S. C., Thornberry, N. A., Xanthoudakis, S., Zamboni, R. J., Roy, S., and Nicholson, D. W. (1999) Involvement of caspases in proteolytic cleavage of Alzheimer's amyloid-beta precursor protein and amyloidogenic A beta peptide formation. *Cell 97*, 395-406.

(106) Stone, J. R., Okonkwo, D. O., Singleton, R. H., Mutlu, L. K., Helm, G. A., and Povlishock, J. T. (2002) Caspase-3-Mediated Cleavage of Amyloid Precursor Protein and Formation of Amyloid β Peptide in Traumatic Axonal Injury. *Journal of Neurotrauma 19*, 601-614.

(107) Weidemann, A., Paliga, K., Durrwang, U., Reinhard, F. B. M., Schuckert, O., Evin, G., and Masters, C. L. (1999) Proteolytic Processing of the Alzheimer's Disease Amyloid Precursor Protein within Its Cytoplasmic Domain by Caspase-like Proteases. *J. Biol. Chem. 274*, 5823-5829.

(108) Li, M., Ona, V. O., Gu, eacute, gan, C., Chen, M., Jackson-Lewis, V., Andrews, L. J., Olszewski, A. J., Stieg, P. E., Lee, J.-P., Przedborski, S., and Friedlander, R. M. (2000) Functional Role of Caspase-1 and Caspase-3 in an ALS Transgenic Mouse Model. *Science 288*, 335-339.

(109) Wellington, C. L., Ellerby, L. M., Hackam, A. S., Margolis, R. L., Trifiro, M. A., Singaraja, R., McCutcheon, K., Salvesen, G. S., Propp, S. S., Bromm, M., Rowland, K. J., Zhang, T., Rasper, D., Roy, S., Thornberry, N., Pinsky, L., Kakizuka, A., Ross, C. A., Nicholson, D. W., Bredesen, D. E., and Hayden, M. R. (1998) Caspase Cleavage of Gene Products Associated with Triplet Expansion

Disorders Generates Truncated Fragments Containing the Polyglutamine Tract. *J. Biol. Chem. 273*, 9158-9167.

(110) Coelln, R. v., Kugler, S., Bahr, M., Weller, M., Dichgans, J., and Schulz, J. B. (2001) Rescue from death but not from functional impairment: caspase inhibition protects dopaminergic cells against 6-hydroxydopamine-induced apoptosis but not against the loss of their terminals. *Journal of Neurochemistry 77*, 263-273.

(111) Holtz, W. A., and O'Malley, K. L. (2003) Parkinsonian Mimetics Induce Aspects of Unfolded Protein Response in Death of Dopaminergic Neurons. *J. Biol. Chem. 278*, 19367-19377.

(112) Hurelbrink, C. B., Armstrong, R. J. E., Luheshi, L. M., Dunnett, S. B., Rosser, A. E., and Barker, R. A. (2001) Death of Dopaminergic Neurons in Vitro and in Nigral Grafts: Reevaluating the Role of Caspase Activation. *Experimental Neurology 171*, 46.

(113) Fiskum, G., Starkov, A., Polster, B. M., and Chinopoulos, C. (2003) Mitochondrial Mechanisms of Neural Cell Death and Neuroprotective Interventions in Parkinson's Disease. *Ann NY Acad Sci 991*, 111-119.

(114) Cutillas B, E. M., Gil J, Ferrer I, Ambrosio S. (1999) Caspase inhibition protects nigral neurons against 6-OHDA-induced retrograde degeneration. *Neuroreport. Aug 20;10*, 2605-8.

(115) Evan, G., and Littlewood, T. (1998) A matter of life and cell death. *Science 281*, 1317-22.

(116) Haupt, S., Berger, M., Goldberg, Z., and Haupt, Y. (2003) Apoptosis - the p53 network. *J Cell Sci 116*, 4077-4085.

(117) Zhou, T., Song, L., Yang, P., Wang, Z., Lui, D., and Jope, R. S. (1999) Bisindolylmaleimide VIII facilitates Fas-mediated apoptosis and inhibits T cell-mediated autoimmune diseases. *Nat Med 5*, 42.

(118) Schotte, P., Declercq, W., Van Huffel, S., Vandenabeele, P., and Beyaert, R. (1999) Non-specific effects of methyl ketone peptide inhibitors of caspases. *FEBS Letters 442*, 117.

(119) Asgian, J. L., James, K. E., Li, Z. Z., Carter, W., Barrett, A. J., Mikolajczyk, J., Salvesen, G. S., and Powers, J. C. (2002) Aza-peptide epoxides: a new class of inhibitors selective for clan CD cysteine proteases. *J Med Chem 45*, 4958-60.

(120) Ekici, O. D., Gotz, M. G., James, K. E., Li, Z. Z., Rukamp, B. J., Asgian, J. L., Caffrey, C. R., Hansell, E., Dvorak, J., McKerrow, J. H., Potempa, J., Travis, J., Mikolajczyk, J., Salvesen, G. S., and Powers, J. C. (2004) Aza-peptide Michael acceptors: a new class of inhibitors specific for caspases and other clan CD cysteine proteases. *J Med Chem 47*, 1889-92.

(121) James, K. E., Asgian, J. L., Li, Z. Z., Ekici, O. D., Rubin, J. R., Mikolajczyk, J., Salvesen, G. S., and Powers, J. C. (2004) Design, synthesis, and evaluation of aza-peptide epoxides as selective and potent inhibitors of caspases-1, -3, -6, and -8. *J Med Chem 47*, 1553-74.

(122) Powers, J. C., Asgian, J. L., Ekici, O. D., and James, K. E. (2002) Irreversible Inhibitors of Serine, Cysteine, and Threonine Proteases. *Chem. Rev. 102*, 4639-4750.

(123) Hanada, K. T., Masaharu; Yamagishi, Michio; Ohmura, Sadafumi; Sawada, Jiro; Tanaka, Ichiro. (1978) Studies on thiol protease inhibitors. Part I. Isolation and characterization of E-64, a new thiol protease inhibitor. *Agric. Biol. Chem. 42*, 523-8.

(124) Barrett, A. J. K., Asha A.; Brown, Molly A.; Kirschke, Heidrun; Knight, C. Graham; Tamai, Masaharu; Hanada, Kazunori. (1982) L-trans-Epoxysuccinyl-leucylamido(4-guanidino)butane (E-64) and its analogs as inhibitors of cysteine proteinases including cathepsins B, H, and L. *Biochemical Journal 201*, 189-98.

(125) Hanada, K. T., Masaharu; Morimoto, Shigeo; Adachi, Takashi; Ohmura, Sadafumi; Sawada, Jiro; Tanaka, Ichiro. (1978) Studies on thiol protease inhibitors. Part III. Inhibitory activities of E-64 derivatives on papain. *Agric. Biol. Chem. 42*, 537-41.

(126) Barrett, A. J., Kembhavi, Asha A, Brown, Molly A, Kirschke, Heidrun, Knight, C. Graham, Tamai, Masaharu, Hanada, Kazunori. (1982) L-trans-Epoxysuccinyl-leucylamido(4-guanidino)butane (E-64) and its analogs as inhibitors of cysteine proteinases including cathepsins B, H, and L. *Biochemical Journal 201*, 189-98.

(127) Anamarija Zega, U. U. (2002) AZAPEPTIDES. *Acta Chim. Slov. 49*, 649-662.

(128) Gante, J. (1989) Azapeptides. *Synthesis*, 405-413.
(129) Thormann, M., and Hofmann, H.-J. (1999) Conformational properties of azapeptides. *Journal of Molecular Structure: THEOCHEM 469*, 63-76.
(130) Xing, R., and Hanzlik, R. P. (1998) Azapeptides as inhibitors and active site titrants for cysteine proteinases. *J Med Chem 41*, 1344-51.
(131) Magrath, J., and Abeles, R. H. (1992) Cysteine protease inhibition by azapeptide esters. *J Med Chem 35*, 4279-83.
(132) Bajusz, S., Fauszt, I., Nemeth, K., Barabas, E., Juhasz, A., Patthy, M., and Bauer, P. I. (1999) Peptidyl beta-homo-aspartals (3-amino-4-carboxybutyraldehydes): new specific inhibitors of caspases. *Biopolymers 51*, 109-18.
(133) Ekici, O. D. (2003) in *School of Chemistry and Biochemistry* pp 173, Georgia Institute of Technology, Atlanta.
(134) Tsuge, H., Nishimura, T., Tada, Y., Asao, T., Turk, D., Turk, V., and Katunuma, N. (1999) Inhibition Mechanism of Cathepsin L-Specific Inhibitors Based on the Crystal Structure of Papain-CLIK148 Complex. *Biochemical and Biophysical Research Communications 266*, 411.
(135) Cleland, W. W., Frey, P. A., and Gerlt, J. A. (1998) The Low Barrier Hydrogen Bond in Enzymatic Catalysis. *J. Biol. Chem. 273*, 25529-25532.
(136) Perrin, C. L., and Nielson, J. B. (1997) "STRONG" HYDROGEN BONDS IN CHEMISTRY AND BIOLOGY. *Annual Review of Physical Chemistry 48*, 511-544.
(137) Mildvan, A. S., Harris, T. K., and Abeygunawardana, C. (1999) Nuclear magnetic resonance methods for the detection and study of low-barrier hydrogen bonds on enzymes, in *Methods in Enzymology* pp 219, Academic Press.
(138) Gerd, W. (2005) Analysis of pH-dependent elements in proteins: Geometry and properties of pairs of hydrogen-bonded carboxylic acid side-chains. *Proteins: Structure, Function, and Bioinformatics 58*, 396-406.

2. Extended substrate recognition in caspase-3 revealed by high resolution X-ray structure analysis

Rajkumar Ganesan, Peer R.E. Mittl, Stjepan Jelakovic and Markus G. Grütter

[J. Mol. Biol. *In press*]

Subject area	Protein and nucleic acid structure, function and interaction
Running title	Structural analysis of caspase-3 specificity
Title	**Extended substrate recognition in caspase-3 revealed by high resolution X-ray structure analysis.**
Authors	Rajkumar Ganesan, Peer R.E. Mittl, Stjepan Jelakovic and Markus G. Grütter*
Affiliation	Biochemisches Institut, Universität Zürich
***Corresponding author**	Markus G. Grütter, Biochemisches Institut, Universität Zürich, Winterthurer Strasse 190, CH-8057 Zürich, Switzerland Tel. +41-44-6355580, Fax. +41-44-6356834, e-mail. gruetter@bioc.unizh.ch
Document	Text pages-26; figures-6; tables-2. Words in abstract, 146; characters (including space), 42503
Coordinates	Coordinates and structure factors have been be deposited at the PDB under accession codes 2DKO, 2CJX and 2CJY.
Keywords	Caspase; substrate specificity; safety catch; low-barrier hydrogen bond; radiation damage
Abbreviations	Ac: Acetyl, AMC: 7-amino-4-methyl coumarin, BIR: Baculovirus IAP repeat, cmk: Chloromethyl ketone, LBHB: Low-barrier hydrogen bond, p12: Small subunit of caspase-3, p17: Large subunit of caspase-3, SMAC: Second mitochondrial activator of caspases, XIAP: X-linked inhibitor of apoptosis, Z/Cbz: Benzyloxycarbonyl

Abstract

Caspases are cysteine proteases involved in the signalling cascades of programmed cell death in which caspase-3 plays a central role, since it propagates death signals from intrinsic and extrinsic stimuli to downstream targets. The atomic resolution (1.06 Å) crystal structure of the caspase-3 DEVD-cmk complex reveals the structural basis for substrate selectivity in the S4 pocket. A low-barrier hydrogen bond is observed between the side chains of the P4 inhibitor aspartic acid and Asp179 of the N-terminal tail of the symmetry related p12 subunit. Site directed mutagenesis of Asp179 confirmed the significance of this residue in substrate recognition. In the 1.06 Å crystal structure, a radiation damage induced rearrangement of the inhibitor methylketone moiety was observed. The carbon atom that in a substrate would represent the scissile peptide bond carbonyl carbon clearly shows a tetrahedral coordination and resembles the postulated tetrahedral intermediate of the acylation reaction.

Introduction

Programmed cell death (apoptosis) is a central process in all multi-cellular organisms. This process is highly regulated and involves several different classes of proteins. Apoptosis is triggered by external- and internal stimuli, which are propagated by either extrinsic- or intrinsic cell death pathways. Cysteine Asp-specific proteases (caspases) are common to both pathways.(1-3) In the pre-apoptotic cell caspases are synthesized as inactive proenzymes. Upon triggering of the cell death pathway caspases are activated by proteolytic cleavage on the C-terminal side of well-conserved aspartic acids, cleaving the polypeptide chain into p12- and p17 subunits (4), which are in intimate contact and form one catalytic domain. Active caspases are dimers of two catalytic domains. So far 11 human caspases are known, they are classified into initiator and executioner caspases, depending on their role in the cell death process.(5) Caspase-3 is a key executioner caspase. It occupies a prominent position in the apoptotic cascade where death signals from both the intrinsic and extrinsic stimuli converge to activate downstream death events.

Since apoptosis is a dangerous process for the cell, caspases are highly regulated and selective towards substrates. All caspases recognize tetrapeptide sequence and have an absolute requirement for an aspartic acid in the P1 position. Caspases are subdivided into three specificity families(6), depending on their preference for P4 amino acid. The prototype caspases are caspase-1, -3 and -8 requiring tryptophan, aspartatic acid and leucine residues in the P4 positions, respectively. The specificity of caspase-3 for a P4 aspartic acid is at least 100-fold higher than for a glutamate or an asparagine.(7) Thus the P4 selectivity is nearly as stringent as the P1 selectivity. The P4 selectivity was attributed to different

interactions with residues in loops flanking the P4 binding pocket.(8, 9) Several crystal structures of caspase-3 in complex with substrate analogues are known, which do not sufficiently explain the reason for the high selectivity in the P4 position.(8, 9) The caspase-3 heterotetramer contains two active sites, each of them is formed by residues belonging to one subunit. However, the existence of inhibitors, such as 2-(2,4-Dichlorophenoxy)-*N*-(2-mercapto-ethyl)-acetamide, that bind outside the active site at the subunit interface of caspase mutants supports the hypothesis of an allosteric regulation of caspases.(10)

Caspases are very attractive drug targets as they are implicated in various diseases and precise structural data is of great interest to facilitate the design of selective inhibitors.(11) The reaction mechanism of caspases has not been studied in detail.(4) Site directed mutagenesis studies in caspase-1 emphasized the importance of residues Cys285 and His237.(12) In contrast to the classical catalytic triad described for many serine- and cysteine proteases, where the imidazole group of the active site histidine is involved in the deprotonation of the nucleophile(13-17), His237 in caspase-1 seems to be responsible for the protonation of the leaving group.(18) In papain-like cysteine proteases the interaction between the cysteine and histidine side chains is maintained throughout the catalytic cycle, whereas in caspases this interaction is disrupted by the binding of the substrate or inhibitor. Quantum mechanical and molecular dynamics studies of the deacylation reaction suggested that the active site histidine might also be responsible for the activation of a water molecule that hydrolyzes the thioester bond of the acylated caspase.(19)

Here, we report the crystal structure of the wild-type executioner caspase-3 at atomic resolution 1.06 Å and an Asp179Ala mutant at 1.7 Å resolution, respectively,

both in complex with Z-DEVD-cmk. The high resolution crystal structure of the wildtype caspase-3/Z-DEVD-cmk complex revealed that Asp179 of the symmetry related subunit forms a low-barrier hydrogen bond with the P4 aspartate of the inhibitor, providing experimental evidence that residues from both subunits are responsible for inhibitor recognition nurturing the idea of on an allosteric regulation of caspase-3 activity.(10) In addition, we observed a radiation damage induced rearrangement of the active site that is similar to the tetrahedral intermediate of the acylation reaction.

Results

Overall structure

The 1.06 Å resolution crystal structure of caspase-3/Z-DEVD-cmk provides well defined electron density for residues Ser29 to Thr174 and Ser176 to His277 of the p17- and p12 subunits, respectively. Only electron density for Asp175 at the C-terminus, which is disordered, and for residues 1 to 29 at the N-terminus of the p17 subunit, which were excluded from the expression construct, is missing in the crystal structure of human caspase-3 (SwissProt accession number P42574). The p12- and p17 subunits fold into a central six-stranded mixed β-sheet that is flanked on both sides by 5 α-helices (Fig. 1). This architecture, which is designated as the caspase hemoglobinase fold is conserved throughout all caspase structures.(20) Superposition of the caspase-3/Z-DEVD-cmk structure with known caspase-3 structures reveal rmsd's in the range of 0.32 Å (1gfw)(21) and 0.40 Å (1cp3)(8) for Cα-atoms.

The subunit interface

The active caspase-3 heterotetramer is generated by applying the symmetry operator (1-x, y, 1-z) to all atoms in the asymmetric unit. A total area of 2788 $Å^2$ is

buried upon dimerization of the catalytic domains. In previously published caspase-3 crystal structures, a buried surface area of only 2000 $Å^2$ was reported.(8) The increase in buried surface area in the caspase-3/Z-DEVD-cmk structure is attributed to residues 176 to 184 that wind around the loop formed by residues 246* to 258* (* refers to the symmetry related subunit). In most caspase-3 structures determined so far, the p12 N-terminal tail was disordered explaining the lower value for interface area. Although the interactions between subunits are more intense in the caspase-3/DEVD-cmk complex, the angle between subunits remains unchanged compared to previous caspase-3 structures.[8, 9]

Besides main chain hydrogen bonds between residues in the anti-parallel beta-strands f and f* that were already visible in the other caspase-3 structures, several novel interactions are observed involving the p12 N-terminal tail (Fig. 2a and 2c.). The side chain of Asp179 forms a short hydrogen bond (2.35 Å) with the P4 aspartate side chain of the inhibitor in the symmetry related subunit. The main chain of residues 178 to 179 forms a short parallel β-sheet with main chain of residues 247* to 248* including a hydrogen bond between Asp179-O and Glu248*-N (2.90 Å). The side chains of Asp180 and Asp181 are pointing towards the solvent. The side chain of Val178 stacks onto the side chain of Phe250* in the loop that restricts the S4 pocket and the side chain of Met182 is at Van der Waals distance to the side chain of Glu248. Isotropic temperature factors of the p12 N-terminal tail (for residues 176 to 184 is 29.4 $Å^2$) are similar to the overall average temperature factor (for all residues is 21.3 $Å^2$) with a pronounced minimum for Asp179. Asp179 belongs to a group of three aspartatic acid residues designated as "safety catch", because the mutations within this motif resulted in increased autocatalytic activation and susceptibility to caspase-9 activation.(22)

To investigate the impact of the interaction between Asp179 and AspP4*, the crystal structure of the caspase-3 Asp179-Ala mutant in complex with Z-DEVD-cmk was determined at 1.7 Å resolution. In the Asp179-Ala mutant structure, several well-defined water molecules populate the space around AspP4* (Fig. 2b). The mutation causes a disordering of the p12 N-terminal tail confirming that the rigidity of the tail is a consequence of the interaction between Asp179 and AspP4*. Crystal packing effects can be excluded since wild type and mutant crystals are isomorphic. The lower resolution of the Asp179-Ala mutant also does not seem to be responsible for the lack of interpretable electron density since the conformation of the tail is clearly visible in the 1.7 Å crystal structure of the wild type.

The active site

The P4-site

The conformation of the Z-DEVD-cmk inhibitor is almost identical compared to the conformations seen in previous caspase/inhibitor complex structures. Although the structure was refined at 1.06 Å resolution, the N-terminal Cbz protection group is absent from the final electron density map. Some positive difference electron density at AspP4-N suggests the presence of a carbonyl group, but the bulky phenyl ring is completely disordered (lower number of ligand atoms in Table-2). Similiarly, the N-terminal Cbz protection group is disordered in the structure of the Asp179Ala mutant. The AspP4-Oδ1 atom interacts with Asp179*-Oδ2 (2.35 Å) and both carboxylate groups are approximately coplanar. Distances between AspP4-Oδ1 and the side chain atoms of residues Asn208 and Trp214 are longer than 3.5 Å (Fig. 2a). Moreover, the angles between these side chains are not ideal for the formation of stable hydrogen bonds. AspP4-Oδ2 forms a hydrogen bond with Phe250-N (2.98 Å) as observed

previously.(8, 9) The caspase-3/DEVD-cmk complex was crystallized at pH 4.75, suggesting that Asp179* or AspP4 might be protonated. Therefore, bond lengths and angles between Cγ- and Oδ-atoms in Asp179* and AspP4 were not restrained during the final refinement cycle. Bond lengths between AspP4-Cγ and Oδ1 and Oδ2 are 1.234 Å and 1.243 Å, respectively, whereas in Asp179* the equivalent bond lengths are 1.253 Å and 1.230 Å (Fig. 2c). Because the bond lengths of Cγ-Oδ1 in AspP4 and Cγ-Oδ2 in Asp179* are almost identical, it is assumed that this interaction involves a proton that is shared by both carboxylate groups. Hydrogen bonds between carboxylate groups, where the proton is located at approximately the same distance between oxygen atoms, are defined as low-barrier hydrogen bonds (LBHB), and it is assumed that they contribute a significant amount of binding energy, which is typically in the range between -20 and -30 kcal.mol^{-1}.(23) The distance between Asp179*-Oδ2 and AspP4-Oδ1 is extremely short (2.35 Å), which is in agreement with the LBHB definition.(24) The hydrogen bonding pattern in the S4 pocket is shown in Fig. 2c.

To investigate the contribution of the interaction between Asp179 and AspP4, the kinetic parameters of the Z-DEVD-AMC and Ac-DEVD-AMC hydrolysis by caspase-3 wild type were compared with that of the Asp179-Ala and $\Delta_{176\text{-}181}$ caspase-3 mutants, at different pH values (Table 1). The replacement of Asp179 to alanine has a significant effect on K_m and k_{cat} at acidic and neutral pH values, indicating that this interaction plays a role also at a physiological pH. At neutral pH, the K_m and k_{cat} values are increased approximately 2.5-fold leaving the k_{cat}/K_m-ratio unchanged, whereas at acidic pH the k_{cat}/K_m-ratio of the Asp179-Ala mutant is three to four times larger compared to the wild type. Although the interactions between Asp179 and AspP4 are lost in the Asp179-Ala and $\Delta_{176\text{-}181}$ mutants, the kinetic values of these

mutants are different, suggesting a more complex interaction pattern. In contrast to the Asp179-Ala mutant the K_m and k_{cat} values of the $\Delta_{176-181}$ mutant are decreased two to five fold compared to the wild type. The k_{cat}/K_m-ratio is decreased at neutral pH whereas it is approximately the same at acidic pH. Although the absolute numbers are not identical for the Z-DEVD-AMC and Ac-DEVD-AMC substrates, the changes on the kinetic parameters are independent of the N-terminal protection groups.

The P1-site

The interactions seen for the side chains in the S3, S2 and S1 pockets are similar compared to previous caspase-3 complex crystal structures.(8, 9) The conformation of the covalent interaction between the methylketone and the active site Cys163 are similar in the 1.7 Å crystal structures. However, after extending the resolution to 1.06 Å significant movements of the methylene group and the Cys163-Sγ atom have been observed. This movement is probably caused by radiation damage. The $F_{obs}^{(1.06\ Å)} - F_{obs}^{(1.7\ Å)} \cdot \varphi_{calc}^{(1.06\ Å)}$ map reveals that major differences between the 1.7 Å and the 1.06 Å resolution crystal structures exist in the neighborhood of the active site cysteine (Fig. 3). In the 1.7 Å resolution structure, the methylene group bridges the gap between the keto group and the sulfur atom as it has already been described for many caspase and cysteine protease structures in complex with halogen methylketone inhibitors.(8, 25) In the 1.06 Å resolution structure, the methylene group has moved 1.29 Å away from the active site cysteine and the Cys163-Sγ atom moved 0.41 Å towards AspP1-C. This conformation is closer to the conformation seen in caspase/aldehyde complexes(9, 12, 26) with a tetrahedral coordination of AspP1-C and a short distance between AspP1-C and Cys163-Sγ (2.027 Å) than to the 1.7 Å resolution caspase-3/Z-DEVD-cmk structure with a planar keto group. With a distance of 1.588 Å the bond length between AspP1-C and the methylene group

(AspP1-CM) is significantly longer than normal carbon-carbon single bonds (1.525-1.530 Å) and the distance between AspP1-C and AspP1-O is longer than normal carbon-oxygen double bonds (1.265 Å compared to 1.231-1.249 Å). The AspP1-C atom is clearly tetrahedrally coordinated with all bond angles between 104° and 117°. To investigate the impact of radiation damage a second high resolution data set was collected and the diffraction quality was investigated using program XDSSTAT.(27) This analysis showed a constant decay of diffraction quality (Fig. 4). The R_d-values between subsequent frames were well below 10 % at the beginning of data collection and increased to more than 30 % after 220 frames. A difference Fourier map that was calculated between the 1.7 Å in-house data and the first 40 frames from the first synchrotron run (76 % completeness) gave no indication for a rearrangement of Cys163, whereas a difference Fourier map based on the combined last 50 frames of the first run and the first 40 frames of the third run showed elevated radiation damage.

Discussion

The 1.06 Å crystal structure of caspase-3 in complex with Z-DEVD-cmk reveals novel details concerning the interactions in the P4 site and at the active site cysteine, both of which are important to understand substrate recognition and catalysis. It has been previously shown that caspase-3 has an absolute requirement for an aspartate in the P4 position. However previous structural data of caspase-3 inhibitor complexes failed to explain this pronounced selectivity. The interactions seen in the present 1.06 Å resolution crystal structure confirm that AspP4 is recognized by Asp179, located at the N-terminal part of the small subunit. The extremely short distance and the equal distribution of Cγ-Oδ bond lengths suggest that this interaction resembles a low-barrier hydrogen bond (LBHB), which is

characterized by a low energy barrier for the exchange of the hydrogen atom between interacting dipoles. It is preferentially formed between groups with similar pK_a values. Therefore, the observation of a LBHB between aspartate side chains at acidic pH perfectly agrees with this definition. The energy of a hydrogen bond depends very much on the bond distance ranging from -1 kcal·mol^{-1} to better than -25 kcal·mol^{-1} for distances between 3.0 Å and 2.3 Å, respectively.(24) Therefore, LBHBs with typical bond distances below 2.45 Å are considered to contribute a significant amount of binding energy.

Although the caspase-3 was crystallized at acidic pH, the kinetic data suggests that the observed LBHB contributes binding energy at acidic and physiological pH values. Lowering the pH causes a significant reduction of caspase-3 activity, which is attributed to dissociation of active caspase-3 dimers into inactive monomers and protonation of the active site Cys163. (28) All kinetic values given in Table 1 support this trend. At both pH values the K_m values of the Asp179-Ala mutant are higher compared to the values of the wild type, suggesting that the LBHB increases the affinity of caspase-3 for peptides with an aspartate in P4. Due to the increased affinity, the product of the hydrolysis is released slower from the active site of the wild type, which correlates with the decreased k_{cat} value of the wild type, compared to the Asp179-Ala mutant. At neutral pH, the effects on K_m and k_{cat} are equivalent whereas at acidic pH, the effect on k_{cat} overcompensates the effect on K_m, rendering the Asp179-Ala mutant more active than the wild type.

Interestingly the kinetic constants for the $\Delta_{176\text{-}181}$ mutant differ from the values obtained for the Asp179-Ala mutant. At neutral pH, the deletion of six amino acids at the p12 N-terminal tail decreases the k_{cat}/K_m ratio suggesting that the p12 N-terminal tail has additional functions besides the recognition of the AspP4 side chain. The p12

N-terminal tail could for example be responsible for a transient stabilization of the P4 pocket including the loop formed by residues 246 to 258. The main chain hydrogen bond between Asp179*-O and Glu248-N would be present in the Asp179-Ala mutant but not in the $\Delta_{176\text{-}181}$ mutant structure. Another possible explanation for the different kinetic behaviors of the Asp179-Ala and the $\Delta_{176\text{-}181}$ mutants relies on the assumption that either Asp179, Asp180 or Asp181 occupy the position of the AspP4 in a caspase-3 structure with an empty P4 pocket. Although the p12 N-terminal tail possesses a rigid conformation in the present structure, it can adopt different conformations depending on the nature of the bound ligand. In the structures of caspase-3 in complex with two low-molecular weight inhibitors(29) (pdb-id 1nmq and 1nms), residues Asp179 to Asp181 are bridging the P4 pocket but do not contribute to inhibitor recognition. In the caspase-3/XIAP-BIR2 complex(30) (pdb-id 1I3O) the N-terminal tail is involved in the recognition of the BIR2 domain but it is pointing away from the P4 pocket and occupies the SMAC binding pocket.

Another interesting detail revealed by this high resolution caspase-3 structure concerns the geometry of the active site cysteine. The $F_{obs}^{(1.06\ Å)} - F_{obs}^{(1.7\ Å)} \cdot \varphi_{calc}^{(1.06\ Å)}$ map confirm the rearrangement of the methylene group of the inhibitor. This rearrangement is a clear consequence of radiation damage since the first part of the high resolution data set resembles the conformation seen in the 1.7 Å structure. Unfortunately the transition between both conformations is a continuous process. Therefore it is nearly impossible to record a high resolution data set with reasonable merging statistics that resembles only the rearranged active site. In the high resolution structure the methylene group has moved 1.29 Å away from the active site cysteine and its sulfur atom moves 0.41 Å towards the keto group. Unfortunately the chemical nature of the observed rearrangement product is uncertain. Most likely the observed

structure resembles a zwitterionic intermediate with a methylene cation and a carbonylate anion. The stretching of bond lengths supports the suggested dissipation of charges.

Different mechanisms for the inhibition of cysteine proteases by halomethyl ketones have been postulated. The simplest mechanism relies on a direct displacement of the halide by the thiolate anion (mechanism I in Fig. 5a). In the alternative mechanism the thiolate anion would attack directly the keto group (intermediate *II*) and the halide is released in a second step upon the formation of the zwitterionic sulfonium intermediate *IV.(15)* The present data supports mechanism II. The zwitterionic intermediate postulated for the present structure (*V*) could be a reaction product of the cyclic three-membered sulfonium intermediate (*IV*). In contrast to the proposed mechanism the bond between the sulfonium cation and the methylene group is broken yielding a zwitterionic intermediate similar to *II* but lacking the chloride atom. The interpretation that the present structure resembles a zwitterionic intermediate also agrees with the proposed reaction pathway. During hydrolysis of the peptide bond the N-terminal part of the polypeptide chain forms a thioester adduct with the active site cysteine (*VIII* in Fig. 5b). The formation of this acyl-enzyme travels through a tetrahedral intermediate (*VII*) that is expected to possess a similar conformation as the observed zwitterionic intermediate. In this case the methylene cation resembles the amino group that is released upon the formation of the acyl-enzyme.

It has been reported that the inhibition of caspases by halomethyl ketones is reversible under certain conditions, such as high DTT (1,4-Dithio-threitol) concentrations(31), although this inhibitor class was regarded to inhibit caspases irreversibly. The observed rearrangement helps to explain this behavior. Provided that

the rearrangement from *III* to *V* is also possible in solution in the absence of radiation, the zwitterionic intermediate (*V*) would be hydrolyzed yielding the α-hydroxy methyl ketone peptide and the protonated active site cysteine.

The rearrangement in the active site also affects the surrounding water molecules Wat93 and Wat215 (Fig. 6a). These water molecules are well conserved in other structures of caspases inhibited by halo methylketones, (such as 1cp3)(8) and form hydrogen bonds with His121-ND1 and Gly122-N. After the rearrangement one water molecule has been squeezed out of the active site and the second water molecule moves into the proper position to form short hydrogen bonds with His121-ND1 and Gly122-N (Fig. 6b). Wat238 would therefore be well positioned to stabilize either a negative charge at the oxygen of the keto group or a positive charge at the methylene cation using its lone electron pairs.

Methods

Protein purification

Human recombinant caspase-3 was produced in *E.coli* as inclusion bodies, refolded and purified as described.(32) Briefly, the cloned genes for the large p17-(Met-Ser29-Asp175) and the p12 subunit (Met-Ala-Ser176-His277) of caspase-3 were inserted in the *Nco*I/*Bam*HI sites of pET11d plasmids (Novagen). Site-directed and deletion mutagenesis was performed using the QuikChange method (Stratagene). Mutants were completely sequenced to ensure that only the desired mutations were introduced. For separate expression of both subunits, *E. coli* BL21-CodonPlus (DE3)-RIL cells (Stratagene), containing one of the two plasmids were grown to a density of A_{600} = 0.5 at 37 °C in a 0.5-liter LB medium. Expression was induced by the addition of IPTG (1 mM), and the culture was shaken at 37 °C for 4 hours post induction. Cells were harvested, washed in PBS buffer and lyzed using French press. Owing to over

expression the protein was localized in inclusion body portion. Refolding was achieved by rapid mixing of equimolar amounts of each subunit to a final concentration of about 100 µg of subunit/mL in the refolding buffer (100 mM HEPES (N-2-Hydroxyethyl)piperazine-N'-2-ethane sulfonic acid), pH 7.5, 10% sucrose, 1% CHAPS (3-(3-cholamidopropyl)diethyl-ammonio-1 propanesulfonate), 100 mM NaCl and 10 mM DTT) and was incubated overnight at room temperature with continuous stirring. Misfolded and aggregated protein was removed by centrifugation (5,000*g*, 30 min), and the supernatant was concentrated using an Amicon-stirred cell. To reduce the salt concentration and to facilitate binding to an anion exchange column (Resource-Q, GE Healthcare), the protein solution was dialyzed against the anion exchange buffer (20 mM Tris pH 8.0, 30 mM NaCl and 10 mM DTT) prior to chromatography. The protein was eluted using a 300mM NaCl gradient. The protein was further purified by size exclusion chromatography (Superdex S200, GE Healthcare) with buffer containing 20 mM Tris pH 8.0, 50 mM NaCl and 10 mM DTT. Fractions containing pure and active caspase were pooled and concentrated by ultrafiltration to a final concentration of 10 mg/mL and the final yield was about 5-7 mg/L culture. Eventually, the purified caspase was subsequently inhibited with a 3-fold molar excess of the inhibitor.

Caspase activity assay

The activities of wild type caspase-3 and Asp179-Ala and Δ176-181 mutants were determined as described previously(33) using the fluorescent substrate Z-DEVD-AMC and Ac-DEVD-AMC assays were performed in a buffer containing 40 mM Pipes pH 7.2, 100 mM NaCl, 0.1% CHAPS, 10% sucrose, and 10 mM DTT, at 37°C and in a buffer containing 40 mM sodium acetate pH 4.75, 100 mM NaCl, 0.1% CHAPS, 10% sucrose, and 10 mM DTT, at 37°C. The total reaction volume was 100

µL, and the final concentration of the enzymes was either 10 nM (for assays at pH 7.2) or 100 nM (for assays at pH 4.75). The concentration was determined by active site titration using the Z-DEVD-cmk inhibitor at the desired pH value. Upon dialysis of caspase-3 against the pH 4.75 buffer, approximately 90 % of protein precipitated. The active site titration at pH 4.75 allowed to compensate for this loss of protein in the activity assay. Samples were excited at 360 nm, and the fluorescence emission was monitored at 465 nm. All fluorescence measurements were acquired using a HTS 7000 plus Bio Assay Reader (PerkinElmer Life Sciences). The steady-state parameters, K_m and k_{cat}, were determined from plots of initial velocity versus substrate concentration (Table 1).

Crystallization and data collection

Crystals of the recombinant human caspase-3 and Z-DEVD-cmk inhibitor (Bachem) complex were grown in 2µL hanging drops formed by mixing equal volumes of protein (10 mg/mL in 20 mM Tris/HCl pH 8.0, 10 mM DTT) and reservoir solution (5% (w/v) polyethylene glycol 6000, 100 mM Sodium citrate, pH 4.75). Crystals (~ 300 · 300 · 100 µm) grew within 2-3 days. For data collection, crystals were frozen in the nitrogen stream after a short soak in reservoir solution containing 20% glycerol. The crystal space group was I222 and with unit cell dimensions, a = 67.2 Å, b = 83.3 Å, c = 96.0 Å. Diffraction data were collected at the rotating anode generator (Bruker-Nonius, FR591) at 100 K. Images were integrated with MOSFLM(34) and scaled with SCALA(35) (CCP4 suite of programs). Diffraction data for the caspase-3: Z-DEVD-cmk complex at atomic resolution were collected at the Swiss Light Source synchrotron (Paul Scherrer Institute, Villigen, Switzerland). Three data sets were collected from one crystal with maximum

resolutions of 1.06 Å, 2.5 Å and 1.06 Å and exposure times of 1, 0.5 and 3 seconds, respectively. The data were processed using the programs XDS(36) and XSCALE.(37) Radiation damage was analysed using the program XDSSTAT.(27)

Structure solution and refinement

The structure was solved by the difference Fourier technique. Structure refinement and automated water addition was performed initially using the program CNS(38) at 1.5 Å, model building and manual adjustments with the program O(39) and the atomic resolution refinement (1.06 Å) with SHELXL.(40) The final crystallographic *R* and free *R* factors for caspase-3 complexes are 10.6% and 14.0%, respectively. The model is nearly complete, 249 of a total of 250 residues were modelled into the density map. Asp175 located at the C-terminus of the p17-subunit is the only disordered residue. The final model for caspase-3 complexes consisted of residues 29-174 (p17-fragment) and 176-277 (p12 subunit) along with 353 water molecules and 33 atoms of the inhibitor molecule. In case of the Asp179-Ala mutant, residues 176-185 (p12 subunit) were disordered and have therefore been omitted from the structure. Detailed data collection statistics and parameters are summarized in Table 2. The final models were validated using PROCHECK.(41) Figures were prepared using PyMOL (http://www.pymol.org) and ISIS Draw (MDL, San Leandro, USA).

Acknowledgement

We gratefully acknowledge the Swiss Light Source, Paul Scherrer Institute, Villigen, Switzerland, for providing synchrotron beam time and T. Tomizaki, A. Wagner, and C. Schulze-Briese for their excellent support during data collection. J.

Tschopp from the University of Lausanne is acknowledged for providing the caspase-3 cDNA. Christophe Briand, Daniel Frey and Gaby Sennhauser for help during data collection. Kay Diederichs for providing the XDSSTAT program. The financial support from the Swiss National Science Foundation and the Baugartenstiftung (Zurich, Switzerland) is gratefully acknowledged.

Reference

1. Earnshaw, W. C., Martins, L. M. & Kaufmann, S. H. (1999) *Annual Review of Biochemistry* **68,** 383-424.
2. Grutter, M. G. (2000) *Current Opinion in Structural Biology* **10,** 649.
3. Riedl, S. J. & Shi, Y. (2004) *Nat Rev Mol Cell Biol* **5,** 897-907.
4. Fuentes-Prior, P. & Salvesen, G. S. (2004) *Biochem J* **384,** 201-32.
5. Nicholson, D. W. (1999) *Cell Death Differ* **6,** 1028-42.
6. Thornberry, N. A., Rano, T. A., Peterson, E. P., Rasper, D. M., Timkey, T., Garcia-Calvo, M., Houtzager, V. M., Nordstrom, P. A., Roy, S., Vaillancourt, J. P., Chapman, K. T. & Nicholson, D. W. (1997) *J Biol Chem* **272,** 17907-11.
7. Stennicke, H. R., Renatus, M., Meldal, M. & Salvesen, G. S. (2000) *Biochem J* **350 Pt 2,** 563-8.
8. Mittl, P. R. E., Di Marco, S., Krebs, J. F., Bai, X., Karanewsky, D. S., Priestle, J. P., Tomaselli, K. J. & Grutter, M. G. (1997) *J. Biol. Chem.* **272,** 6539-6547.
9. Rotonda, J., Nicholson, D. W., Fazil, K. M., Gallant, M., Gareau, Y., Labelle, M., Peterson, E. P., Rasper, D. M., Ruel, R., Vaillancourt, J. P., Thornberry, N. A. & Becker, J. W. (1996) *Nat Struct Biol* **3,** 619-25.
10. Hardy, J. A., Lam, J., Nguyen, J. T., O'Brien, T. & Wells, J. A. (2004) *PNAS* **101,** 12461-12466.
11. O'Brien, T. & Lee, D. (2004) *Mini Rev Med Chem* **4,** 153-65.

12. Wilson, K. P., Black, J. A., Thomson, J. A., Kim, E. E., Griffith, J. P., Navia, M. A., Murcko, M. A., Chambers, S. P., Aldape, R. A., Raybuck, S. A. & et al. (1994) *Nature* **370,** 270-5.

13. Carter, P. & Wells, J. A. (1988) *Nature* **332,** 564.

14. Polgar, L. & Asboth, B. (1986) *J Theor Biol* **121,** 323-6.

15. Powers, J. C., Asgian, J. L., Ekici, O. D. & James, K. E. (2002) *Chem Rev* **102,** 4639-750.

16. Schirmeister, T. & Klockow, A. (2003) *Mini Rev Med Chem* **3,** 585-96.

17. Storer, A. C. & Menard, R. (1994) *Methods Enzymol* **244,** 486-500.

18. Brady, K. D., Giegel, D. A., Grinnell, C., Lunney, E., Talanian, R. V., Wong, W. & Walker, N. (1999) *Bioorg Med Chem* **7,** 621-31.

19. Sulpizi, M., Laio, A., VandeVondele, J., Cattaneo, A., Rothlisberger, U. & Carloni, P. (2003) *Proteins* **52,** 212-24.

20. L. Aravind, E. V. K. (2002) *Proteins: Structure, Function, and Genetics* **46,** 355-367.

21. Lee, D., Long, S. A., Adams, J. L., Chan, G., Vaidya, K. S., Francis, T. A., Kikly, K., Winkler, J. D., Sung, C.-M., Debouck, C., Richardson, S., Levy, M. A., DeWolf, W. E., Jr., Keller, P. M., Tomaszek, T., Head, M. S., Ryan, M. D., Haltiwanger, R. C., Liang, P.-H., Janson, C. A., McDevitt, P. J., Johanson, K., Concha, N. O., Chan, W., Abdel-Meguid, S. S., Badger, A. M., Lark, M. W., Nadeau, D. P., Suva, L. J., Gowen, M. & Nuttall, M. E. (2000) *J. Biol. Chem.* **275,** 16007-16014.

22. Roy, S., Bayly, C. I., Gareau, Y., Houtzager, V. M., Kargman, S., Keen, S. L., Rowland, K., Seiden, I. M., Thornberry, N. A. & Nicholson, D. W. (2001) *Proc Natl Acad Sci U S A* **98,** 6132-7.

23. Gerd, W. (2005) *Proteins: Structure, Function, and Bioinformatics* **58,** 396-406.

24. Perrin, C. L. & Nielson, J. B. (1997) *Annual Review of Physical Chemistry* **48,** 511-544.

25. Blanchard, H., Kodandapani, L., Mittl, P. R., Marco, S. D., Krebs, J. F., Wu, J. C., Tomaselli, K. J. & Grutter, M. G. (1999) *Structure Fold Des* **7,** 1125-33.

26. Watt, W., Koeplinger, K. A., Mildner, A. M., Heinrikson, R. L., Tomasselli, A. G. & Watenpaugh, K. D. (1999) *Structure Fold Des* **7,** 1135-43.

27. Diederichs, K. (2006) *Acta Crystallogr D Biol Crystallogr* **62,** 96-101.

28. Feeney, B., Pop, C., Tripathy, A. & Clark, A. C. (2004) *Biochem J* **384,** 515-25.

29. Erlanson, D. A., Lam, J. W., Wiesmann, C., Luong, T. N., Simmons, R. L., DeLano, W. L., Choong, I. C., Burdett, M. T., Flanagan, W. M., Lee, D., Gordon, E. M. & O'Brien, T. (2003) *Nat Biotech* **21,** 308.

30. Riedl, S. J., Renatus, M., Schwarzenbacher, R., Zhou, Q., Sun, C., Fesik, S. W., Liddington, R. C. & Salvesen, G. S. (2001) *Cell* **104,** 791-800.

31. Esther D. Lenherr, B., A., and Grutter, MG (2004) *Diploma thesis, Department of Biochemistry, University of Zurich.*

32. Garcia-Calvo, M., Peterson, E. P., Rasper, D. M., Vaillancourt, J. P., Zamboni, R., Nicholson, D. W. & Thornberry, N. A. (1999) *Cell Death Differ* **6,** 362-9.

33. Stennicke, H. R. & Salvesen, G. S. (2000) *Methods Enzymol* **322,** 91-100.

34. Leslie, A. G. W. (1992) *Joint CCP4/ESF-EACMB Newsletter on Protein Crystallography* **26**.

35. Evans, P. R. (1992) *Proceedings of the CCP4 Study Weekend on Data Collection and Processing, pp 114-122, SRC Daresbury Laboratory, Warrington, U.K.*

36. Kabsch, W. (1988) *J. Appl. Cryst.* **21,** 67-72.

37. Kabsch, W. (1988) *J. Appl. Cryst.* **21,** 916-924.

38. Brunger, A. T., Adams, P. D., Clore, G. M., DeLano, W. L., Gros, P., Grosse-Kunstleve, R. W., Jiang, J. S., Kuszewski, J., Nilges, M., Pannu, N. S., Read, R. J., Rice, L. M., Simonson, T. & Warren, G. L. (1998) *Acta Crystallogr D Biol Crystallogr* **54 (Pt 5),** 905-21.

39. Jones, T. A., Zou, J. Y., Cowan, S. W. & Kjeldgaard (1991) *Acta Crystallogr A* **47 (Pt 2),** 110-9.

40. Sheldrick, G. M. S., T. R (1997) *Methods Enzymol.* **277,** 319-343.

41. Laskowski, R. A., MacArthur, M. W., Moss, D. S. & Thornton, J. M. (1993) *Journal of Applied Crystallography* **26,** 283.

Figure legends

Figure 1. Ribbon diagram of caspase-3/Z-DEVD-cmk complex. The p12- and p17 subunits are shown in light and dark colors. The p12 N-terminal tail is shown in red. The β-sheet strands are labeled.

Figure 2. H-bonding network in the P4 pocket. (a) Stereo diagram for the wild type P4 pocket. Polypeptide chains belonging to different subunits are shown in red and green. Hydrogen bonds and general inter-atomic distances are shown in red and grey, respectively. (b) P4 pocket in the Asp179Ala mutant. (c) Bond lengths and hydrogen bonds in the P4 pocket.

Figure 3. Superposition of active sites in the 1.06 Å and 1.7 Å resolution structures with carbon atoms shown in cyan and magenta, respectively. The $F_{obs}^{(1.06\ Å)} - F_{obs}^{(1.7\ Å)} \cdot \varphi_{calc}^{(1.06\ Å)}$ map was contoured at +5σ (green) and -5σ (red) levels. The $2F_{obs}^{(1.06\ Å)} - F_{calc}^{(1.06\ Å)} \cdot \varphi_{calc}^{(1.06\ Å)}$ map contoured at +3σ is shown in grey.

Figure 4. Radiation damage analysis using the program XDSSTAT (27). Black, red and green symbols refer to data collection runs 1, 2 and 3 at the SLS. Runs 1 and 2 were merged to prepare the final data set for structure refinement. Data from run 3 were used to monitor progression of radiation damage but not for refinement purposes.

Figure 5. (a) Mechanisms of caspase inhibition (adapted from(15)). The 1.7 Å and 1.06 Å resolution structures represent complexes *III* and *V*, respectively. (b) Acylation reaction of proteases. Complexes *VII* and *VIII* represent the tetrahedral intermediate and the acyl-enzyme, respectively.

Figure 6. Active site geometry of the 1.7 Å (a) and 1.06 Å (b) resolution structures. Putative hydrogen bonds and general distances are shown in red and grey, respectively.

Tabel 1: Kinetic parameters for caspase-3: wild type, Asp179-Ala and $\Delta_{176-181}$

Z-DEVD-AMC substrate

	pH 7.2			pH 4.75		
	K_m (μM)	k_{cat} (s^{-1})	k_{cat}/K_m x10^6 ($M^{-1}s^{-1}$)	K_m (μM)	k_{cat} (s^{-1})	k_{cat}/K_m x10^6 ($M^{-1}s^{-1}$)
Wild type	9.7 ± 0.4	7.08 ± 0.07	0.72	8.0 ± 0.5	0.16 ± 0.002	0.020
Asp179-Ala	25.5 ± 3.1	19.04 ± 0.2	0.74	13.0 ± 1.8	1.10 ± 0.01	0.084
$\Delta_{176-181}$	6.9 ± 0.3	1.43 ± 0.01	0.21	2.0 ± 0.2	0.06 ± 0.001	0.033

Ac-DEVD-AMC substrate

	pH 7.2			pH 4.75		
	K_m (μM)	k_{cat} (s^{-1})	k_{cat}/K_m x10^6 ($M^{-1}s^{-1}$)	K_m (μM)	k_{cat} (s^{-1})	k_{cat}/K_m x10^6 ($M^{-1}s^{-1}$)
Wild type	13.8 ± 0.9	6.01 ± 0.06	0.44	12.2 ± 0.5	0.33 ± 0.003	0.027
Asp179-Ala	33.5 ± 2.7	19.56 ± 0.2	0.58	16.3 ± 1.1	1.37 ± 0.01	0.083
$\Delta_{176-181}$	8.8 ± 0.8	1.54 ± 0.01	0.18	4.8 ± 0.2	0.08 ± 0.0001	0.016

Table 2: Data collection and refinement statistics

	Caspase-3: Z-DEVD-cmk	Caspase-3 D179A: Z-DEVD-cmk	Caspase-3: Z-DEVD-cmk
Data collection			
Space group	I222	I222	I222
Cell dimensions			
a, *b*, *c* (Å)	67.7, 83.9, 96.2	68.4, 83.6, 95.8	67.6, 83.8, 96.1
α, β, γ (°)	90.0, 90.0, 90.0	90.0, 90.0, 90.0	90.0, 90.0, 90.0
Resolution (Å)	20-1.06 (1.15-1.06)	20-1.7 (1.8-1.7)	20-1.6 (1.75-1.66)
R_{merge}	0.055(0.37)	0.058 (0.36)	0.041 (0.17)
$I / \sigma I$	7.9 (3.06)	16.4 (3.6)	16.6 (5.7)
Completeness (%)	92 (89)	99.5 (100)	89 (80)
Redundancy	3.1 (2.9)	4.0 (3.9)	2.5 (2.3)
Refinement			
Resolution (Å)	20 - 1.06	20-1.7 (1.8-1.7)	20-1.66
No. reflections	111061	30451	28626
R_{work} / R_{free}	0.142 /0.175	0.181 /0.208	0.173/0.203
No. atoms			
Protein	2059	1921	1996
Ligand/ion	33	33	43
Water	335	372	337
B-factors			
Protein	17.18	16.2	14.92
Ligand/ion	19.48	23.34	23.1
Water	35.07	35.92	32.49
r.m.s deviations			
Bond lengths (Å)	0.017	0.0050	0.0051
Bond angles (°)	2.429	1.275	1.268

Values in parenthesis are for the highest-resolution shell.

Figures

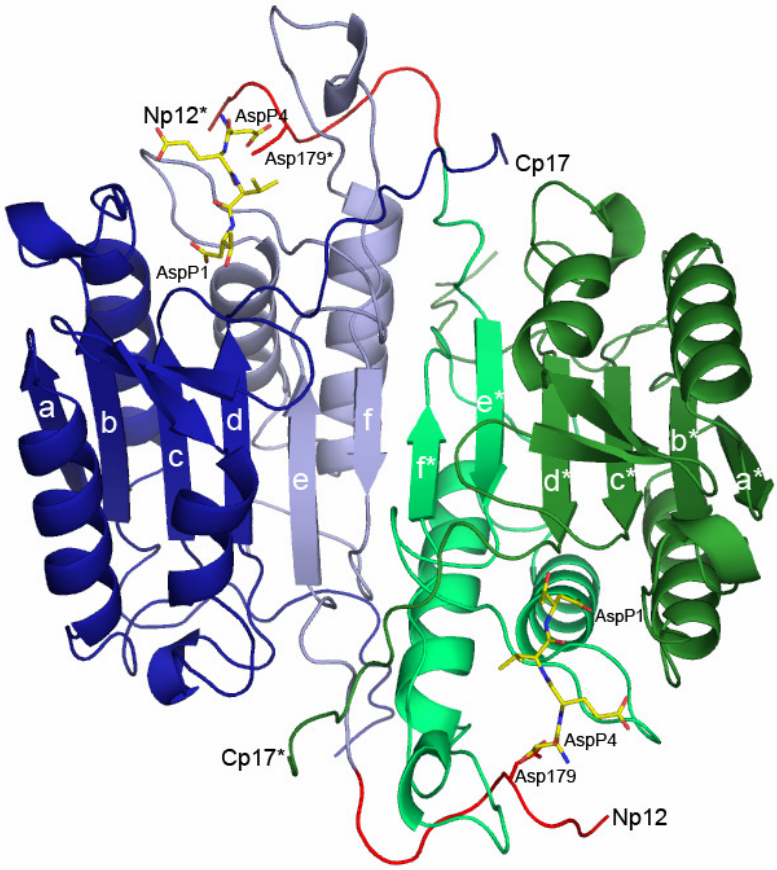

Figure 1.

a.

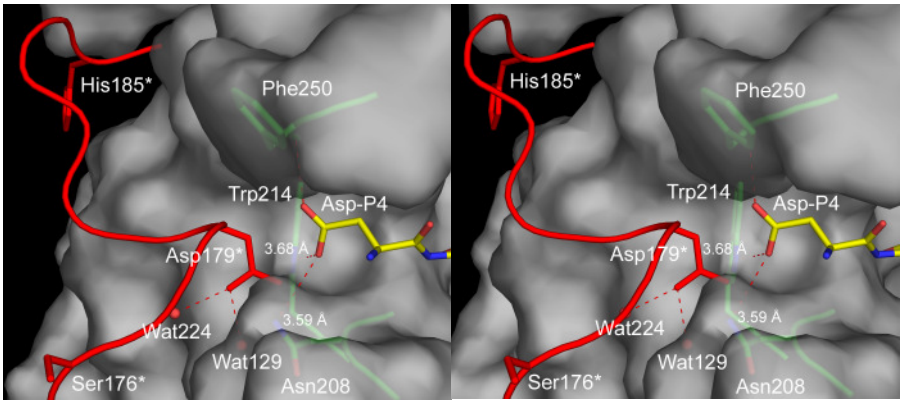
His185*
Phe250
Trp214
Asp-P4
Asp179*
3.68 Å
Wat224
3.59 Å
Wat129
Ser176*
Asn208
His185*
Phe250
Trp214
Asp-P4
Asp179*
3.68 Å
Wat224
3.59 Å
Wat129
Ser176*
Asn208

b.

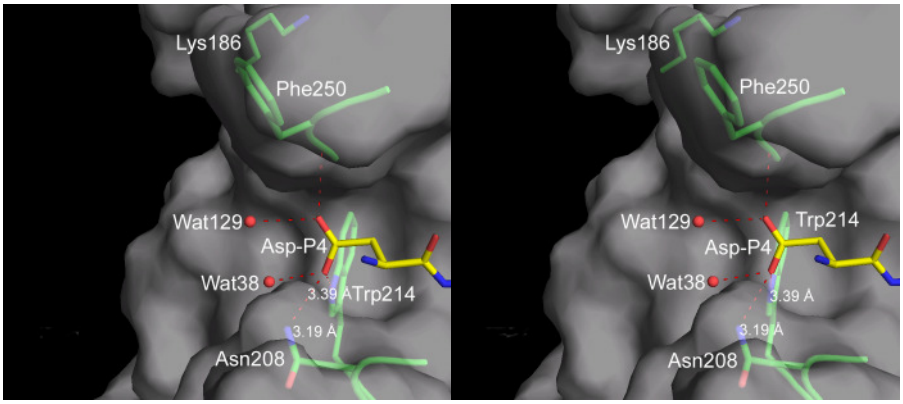
Lys186
Phe250
Wat129
Asp-P4
Wat38
3.39 ÅTrp214
3.19 Å
Asn208
Lys186
Phe250
Wat129
Trp214
Asp-P4
Wat38
3.39 Å
3.19 Å
Asn208

c

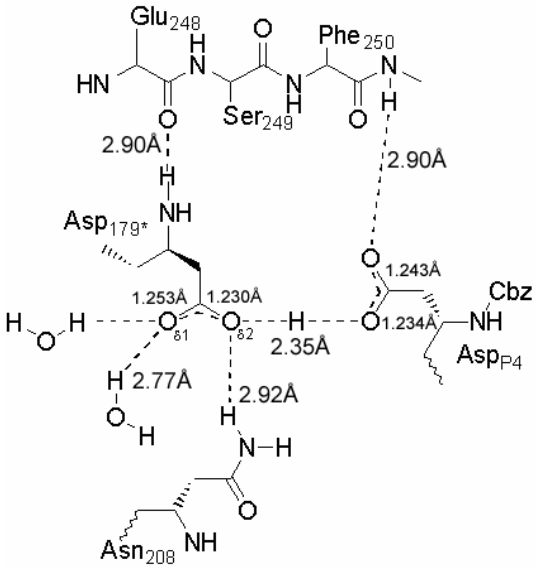
Glu248
Phe250
HN
Ser249
2.90Å
2.90Å
Asp179*
NH
1.243Å
1.253Å
1.230Å
Cbz
H
H
δ1
δ2
2.35Å
1.234Å
NH
AspP4
H 2.77Å
2.92Å
H
N–H
Asn208
NH

Figure 2.

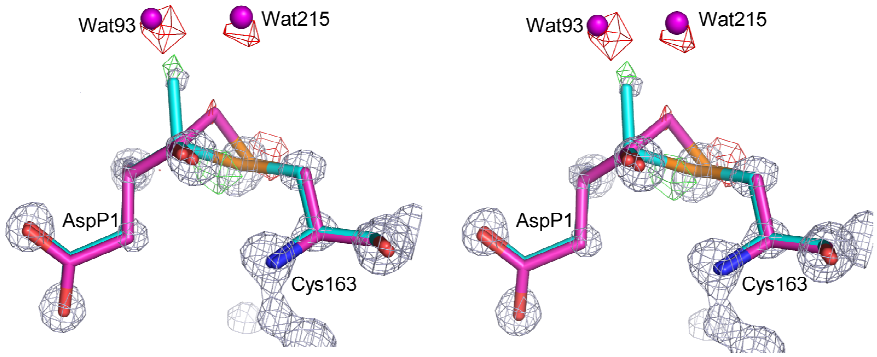

Figure 3.

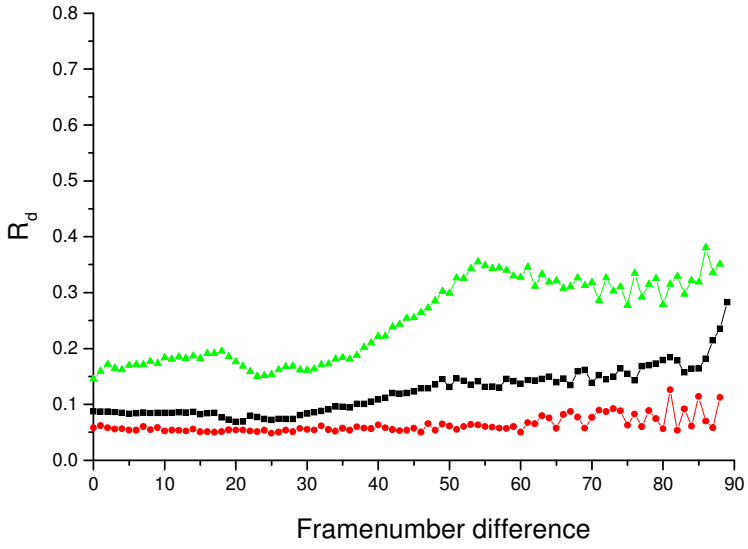

Figure 4.

a.

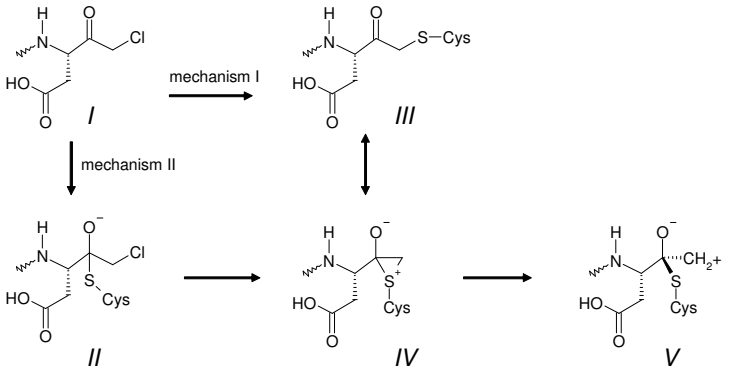

b.

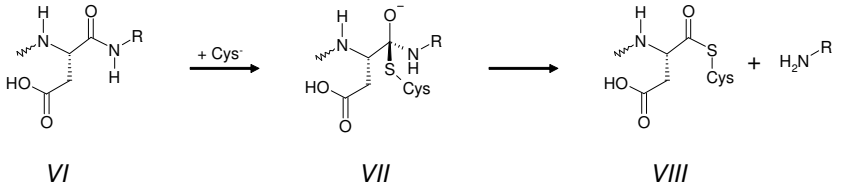

Figure 5.

a.

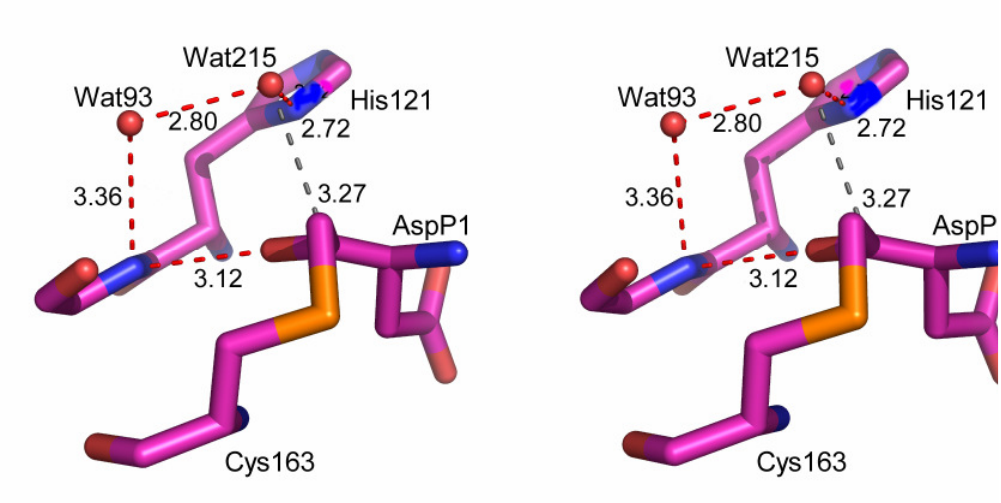
Wat215
Wat93
2.80
His121
2.72
3.36
3.27
AspP1
3.12
Cys163
Wat215
Wat93
2.80
His121
2.72
3.36
3.27
AspP
3.12
Cys163

b.

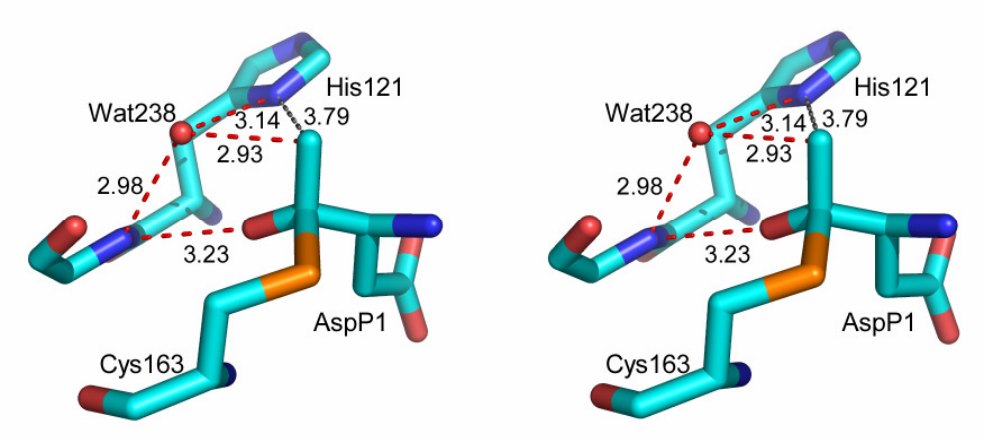
His121
Wat238
3.14
3.79
2.93
2.98
3.23
AspP1
Cys163
His121
Wat238
3.14
3.79
2.93
2.98
3.23
AspP1
Cys163

Figure 6.

3. Design, Synthesis, and Evaluation of Aza-Peptide Michael Acceptors as Selective and Potent Inhibitors of Caspases-2, -3, -6, -7, -8, -9, and -10

Özlem Dogan Ekici, Zhao Zhao Li, Rajkumar Ganesan, Karen Ellis James, Juliana L. Asgian, Jowita Mikolajczyk, Stjepan Jelakovic, Amy J. Campbell, Guy S. Salvesen, Markus G. Grütter and James C. Powers

[J. Med. Chem. *In press*]

Design, Synthesis, and Evaluation of Aza-Peptide Michael Acceptors as Selective and Potent Inhibitors of Caspases-2, -3, -6, -7, -8, -9, and -10

Özlem Dogan Ekici[†], Zhao Zhao Li[†], , Karen Ellis James[†], Juliana L. Asgian[†], Amy J. Campbell[†], Jowita Mikolajczyk[‡], Guy S. Salvesen[‡], Rajkumar Ganesan[§], Stjepan Jelakovic[§], Markus G. Grütter[§] and James C. Powers[†]*

[†]*School of Chemistry and Biochemistry and the Parker H. Petit Institute for Bioengineering and Bioscience, Georgia Institute of Technology, Atlanta, Georgia 30332-0400,* [‡]*Program in Apoptosis and Cell Death Research, The Burnham Institute, 10901 North Torrey Pines Road, La Jolla, California 92037,* [§]*Department of Biochemistry, University of Zurich, 8057-Zurich, Switzerland*

*Correspondence Author: James C. Powers, School of Chemistry and Biochemistry, Georgia Institute of Technology, Atlanta, Georgia, 30332-0400

Tel: (404) 894-4038, Fax: (404) 894-2295

Email: james.powers@chemistry.gatech.edu

ABSTRACT

Aza-peptide Michael acceptors are a novel class of inhibitors that are potent and specific for caspases-2, -3, -6, -7, -8, -9 and -10. The second order rate constants are in the order of 10^6 $M^{-1}s^{-1}$. The aza-peptide Michael acceptor inhibitor **18t** (Cbz-Asp-Glu-Val-AAsp-*trans*-CH=CH-CON(CH_2-1-Napth)$_2$ is the most potent compound and it inhibits caspase-3 with a k_2 value of 5,620,000 $M^{-1}s^{-1}$. **18t** is 13707, 189.2, 6.4, 594, 37470, and 172.9 fold more selective for caspase-3 over caspases-2, -6, -7, -8, -9, and -10, respectively. Aza-peptide Michael acceptors designed with caspase specific sequences do not show any cross reactivity with clan CA cysteine proteases such as papain, cathepsin B, and calpains, demonstrating the selectivity of the inhibitors for clan CD proteases. There is also little to no reactivity toward other clan CD cysteine proteases including legumain, gingipain K, and clostripain. High resolution crystal structures of caspase-3 and caspase-8 in complex with aza-peptide Michael acceptor inhibitors demonstrate the nucleophilic attack on C3 and provide insight into the selectivity and potency of the inhibitors with respect to the P1' moiety.

TOC-Graphic

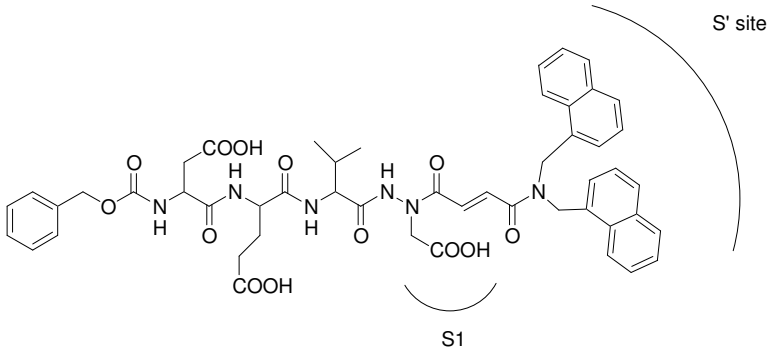

Aza-peptide Michael acceptor inhibitor
Cbz-Asp-Glu-Val-AAsp-*trans*-CH=CH-CON(CH_2-1-Napth)$_2$
18t

INTRODUCTION

Cysteine proteases, also known as thiol proteases have been identified in the biological systems of bacteria, protozoa, fungi, plant viruses, and mammals. Cysteine proteases acylate the peptide bond via a nucleophilic thiol and are involved in numerous physiologically important processes. Cysteine proteases have been grouped into evolutionary families and clans by Rawlings and Barrett.[1,2] The majority of structurally relevant cysteine proteases belong to the well known clan CA, which includes papain, cathepsins, and calpains. Several important cysteine proteases such as caspases, legumain, gingipain, clostripain, and separase belong to a new but smaller clan of cysteine proteases, which is termed as clan CD. The tertiary structure of clan CD proteases shows a unique α/β fold unlike any other protein, with the catalytic residues in the order His, Cys in the sequence. Clan CD cysteine proteases differ from the clan CA proteases also by their substrate specificity requirements. The substrate specificity of clan CD proteases is determined by the S1 pocket, whereas the S2 pocket is the major determinant of substrate specificity with the clan CA cysteine proteases.

Caspases, also known as *c*ysteinyl *asp*artate-specific prote*ases*, are found in worms to flies to humans. Currently, > 15 members are identified, with 11 members in humans.[3] One distinctive feature of this family of enzymes is their near absolute specificity for Asp residue at P1. The only other known mammalian protease with the same specificity requirement is the lymphocyte serine protease granzyme B, which acts as a caspase activator. Caspases have been the focus of both industrial and academic research since their discovery. Over the past decade, the exact roles and functions of individual caspases in cellular systems have been intensely investigated. Some caspases are important mediators of inflammation, whereas others are involved in apoptosis (programmed cell death). Excessive neuronal apoptosis leads to a variety of diseases such as stroke, Alzheimer's disease, Huntington's disease, Parkinson's disease, amyotropic lateral sclerosis (ALS), multiple sclerosis (MS), and spinal muscular atrophy.[4] Caspases are recognized as novel therapeutic targets for central nervous diseases in which cell death occurs mainly by an apoptosis mechanism.[5-8] Hence, potent and specific inhibitors of caspases could lead to the development of potential drugs, which can modulate the apoptotic process.

A number of different classes of inhibitors have been developed for cysteine proteases including reversible transition state inhibitors and a variety of irreversible inhibitors.[9] Relatively few classes have been applied to clan CD cysteine proteases, particulary caspases. Several substrate based caspase inhibitors have been extensively used to address the roles of caspases in cellular systems over the past few years.[10] These include reversible inhibitors such as peptide aldeyhdes (Ac-YVAD-CHO, Ac-DEVD-CHO, Ac-WEHD-CHO) and irreversible inhibitors such as fluoro- or chloromethyl ketones (Z-VAD-FMK, Z-YVAD-FMK/CMK, Z-DEVD-FMK/CMK). A few of these inhibitors have even entered preclinical studies with animal models of human diseases. However, the major disadvantage of these inhibitors is their lack of selectivity. Several of these caspase inhibitors have been recently shown to efficiently inactivate other cysteine proteases, such as cathepsins B, L, and S.[11] Cathepsin B inhibition by Ac-YVAD-CMK rescued neuronal cells against glucose/oxygen deprivation-induced apoptosis, suggesting that other proteases may be involved in the processes previously designated only to caspases. Furthermore, several lysosomal cysteine proteases were shown to be involved in various apoptosis models, although the mechanisms are not yet clear.[12,13] Thus, there is a considerable need for potent and selective caspase inhibitors to elucidate the roles of individual caspases in apoptosis and as potential therapeutics.

A variety of other inhibitors with electrophilic warheads have been reported as irreversible inhibitors effective for clan CA cysteine proteases.[9] One of the first Michael acceptors described in the literature is the fumarate derivative of E-64c (**3**, Figure 1).[14] This inhibitor contains an α,β-unsaturated carbonyl moiety and was found to be an irreversible inhibitor of cathepsin B, cathepsin H, and cathepsin L. Vinyl sulfones and α,β-unsaturated carbonyl derivatives (**4**, Figure 1) have been developed as highly potent inhibitors for exopeptidases such as DPPI and many clan CA cysteine endopeptidases including papain, cathepsins B, L, S, and K, calpains, and cruzain.[15,16] Michael acceptor inhibitors have great potential for use as drugs. One Michael acceptor CRA-3316 developed by Celera as a cruzain inhibitor to treat Chagas' disease is also in clinical trials.[17] Another Michael acceptor AG7088 (Ruprintrivir®) has entered phase II clinical studies with humans as a potential nasally delivered antirhinoviral agent.[18-21] Recently, Michael acceptor inhibitors based on the AG7088 structure drew considerable attention in

the treatment of SARS (Severe Acute Respiratory Syndrome) due to their potential as antiviral agents against the SARS coronavirus.[22]

Our laboratory has recently reported aza-peptide Michael acceptor inhibitors (**2**, Figure 1) that are highly specific for clan CD cysteine proteases.[23] The aza-peptide Michael acceptor structure resembles the substrate peptide sequence (**1**, Figure 1), where the carbonyl group of the double bond moiety replaces the carbonyl group of the scissile bond. Replacement of the α-carbon of the P1 amino acid with a nitrogen results in the formation of the aza-peptide, which allows the ready synthesis of a variety of derivatives. In the fumarate derivative **3**, the Michael acceptor is on the N-terminus of the amino acid residue, while in our aza-peptide design, the warhead is at the C-terminal end of the inhibitor. On the other hand, the design of vinyl sulfones and α,β-unsaturated carbonyl derivatives was based on the optimal peptide sequence of the target enzyme, where the carbonyl of the scissile bond was replaced by the double bond moiety.

In an effort to obtain greater potency and selectivity, we elaborated our aza-peptide Michael acceptor design in the P' portion. Although considerable effort has been devoted to the optimization of interactions of caspase inhibitors at the S1-S4 sites[24,25], interactions of substrates or inhibitors at the S1´ site in the past were analyzed in only very few studies.[26,27] Recently, a few peptidomimetic compounds binding to the groove located near the S1` site of caspase-3 were identified and characterized structurally.[26] We were particularly interested in designing inhibitors for the key executioner caspases-3, -6, and -7 and initiator caspases-2, -8, -9, and -10. Here we also report crystal structures of caspase-3 and caspase-8 in complex with aza-peptide Michael acceptors with different P1' substitutions to elucidate the structural determinants for the preference and discrimination at this site. The analysis of the crystal structures of the caspase: Michael acceptor inhibitor complexes also provide insights into the difference in reactivity of *cis* (**18g**) and *trans* (**18h**) isomers.

CHEMISTRY

We synthesized a variety of aza-peptide Michael acceptors with P1 Asp residue as potential inhibitors for caspases. We previously reported the general method to prepare aza-peptide Michael acceptors in our preliminary communication.[23] Aza-peptide Michael

acceptors for caspases were synthesized by coupling the appropriate substituted peptidyl hydrazides with P1 Asp side chain with the desired fumarate derivative.

A variety of fumarate esters and fumarate mono- and diamides have been synthesized in order to couple to the substituted peptidyl hydrazides (Figure 2). The monobenzyl fumarate **7** was obtained by the addition of 1 eq of benzyl alcohol to monoethyl fumarate **5** using EDC and NMM as coupling reagents followed by the hydrolysis of the ethyl ester **6** in methanol by aqueous NaOH. Mono- and disubstituted amide derivatives **10** and **11** were obtained by coupling the desired primary or secondary amine to monoethyl fumarate **5** and subsequent hydrolysis of the ethyl ester **8** or **9** with 1.2 eq of KOH in ethanol. Monoethyl maleate **13** was synthesized by the alcoholysis reaction of maleic anhydride **12** with ethanol.

Peptidyl hydrazides **14** were obtained by reacting mono-, di-, or tripeptidyl methyl esters with excess hydrazine in methanol. The aza-Asp side chain was introduced by alkylation of the peptidyl hydrazide with *t*-butyl bromoacetate to form the substituted peptidyl hydrazide **15**.

The final aza-peptide Michael acceptors (**16-21 (a-u),** Figure 3) were synthesized primarily by the EDC/HOBt coupling method with the peptide sequences Cbz-Val-NH-NH-CH_2COO-*t*Bu, Cbz-Asp(O-*t*Bu)-Glu(O-*t*Bu)-Val-NH-NH-CH_2COO-*t*Bu, Cbz-Val-Glu(O-*t*Bu)-Val-NH-NH-CH_2COO-*t*Bu, Cbz-Ile-Glu(O-*t*Bu)-Thr-NH-NH-CH_2COO-*t*Bu, and Cbz-Leu-Glu(O-*t*Bu)-Thr-NH-NH-CH_2COO-*t*Bu using an excess of the desired fumarate derivative. To simplify the purification process and maximize the yield various aza-peptide Michael acceptors were synthesized by the mixed anhydride method using the peptide sequences Cbz-Glu(O-*t*Bu)-Val-NH-NH-CH_2COO-*t*Bu, Cbz-Ile-Glu(O-*t*Bu)-Thr-NH-NH-CH_2COO-*t*Bu, and Cbz-Leu-Glu(O-*t*Bu)-Thr-NH-NH-CH_2COO-*t*Bu. In the final step of the aza-peptide Michael acceptor synthesis, the *t*-butyl protecting groups on the aza-Asp, Glu, and Asp residues were deprotected using TFA in CH_2Cl_2 at 0 ºC.

RESULTS AND DISCUSSION

The optimal peptide sequences of the target caspases were utilized in the design of the aza-peptide Michael acceptors. The optimal sequences were derived either from natural caspase cleavage sites or from peptide mapping of caspases with libraries of AMC

substrates.[28] Based on S4 subsite preferences, Thornberry and co-workers divided the caspases into three groups: group I caspases (1, 4, and 5) prefer aromatic amino acid residues at P4; group II caspases (6, 8, 9, and 10) have a preference for branched apolar residues, and group III caspases (2, 3, and 7) prefer an aspartic acid residue. The DEVD and LETD sequences are optimal sequences for caspase-3 and caspase-8, respectively, as determined by positional scanning synthetic combinatorial library.[29,30] The IETD sequence for caspases-6 and -8 is the cleavage sequence of a natural caspase-8 substrate, the caspase-3 proenzyme.[28] The VEVD sequence was chosen as the optimal substrate for caspase-6 in accordance with the branched amino acid preference of this enzyme. The EVD sequence was selected to obtain a truncated caspase-3 inhibitor. Similarly, the VD sequence was chosen to represent a general inhibitor for all the caspases (caspases-2, -3, -6, -7, -8, -9, and -10).

The aza-peptide Michael acceptors with an aza-Asp residue at P1 position and designed with the appropriate target sequences were tested against various caspases for kinetic activity. The aza-peptide Michael acceptors exhibit excellent inhibitory potency against caspases-2, -3, -6, -7, -8, -9, and -10 (Table 1). The second order inhibition rates are as high as 10^6 $M^{-1}s^{-1}$. Generally, the DEVD sequence is the most reactive with caspases-2, -3 and -7. The IETD and LETD sequences are more reactive with the caspases-6, -8, and -9. The VEVD sequence is equally potent as IETD for caspases-6 and -8. Interestingly, the DEVD sequence is the best sequence for caspase-10 although this enzyme was originally included into group II along with caspases-6,-8, and -9. Also the most potent caspase-8 inhibitor has the DEVD sequence. Its favourable interaction with caspase-8 has been demonstgrated in a crystal structure[47]. Similarly, the most potent caspase-9 inhibitor is the one with the EVD tripeptide sequence. This result seems to be an exception to the requirement of the tetrapeptide sequence of caspases for efficient cleavage.

Aza-peptide Michael acceptors are easily extended at their P' site. To gain more insight about the potency and selectivity of the aza-peptide Michael acceptor inhibitors, we modified the substituents on the fumarate moiety extending into the P' site. We utilized various groups like simple alkyl, alkenyl, and aryl groups, as well as halogens,

esters, and amides in the hopes of obtaining selectivity in the P' site among the various caspases.

Caspase-2. In contrast to the other caspases, caspase-2 requires a P5 residue for efficient substrate cleavage. The optimal sequence of caspase-2 is VDVAD, but the caspase-3 specific DEVD sequence still worked best for caspase-2. Because of the P5 requirement, the second order rates of inhibition with caspase-2 remained in the range of 10^2 $M^{-1}s^{-1}$, except for the inhibitors **18g** and **18h**. The most potent inhibitor of caspase-2 was the *cis* isomer **18g** with a k_2 value of 26,200 $M^{-1}s^{-1}$. **18g** was 10-fold more reactive than the *trans* isomer **18h** (k_2 = 2,640 $M^{-1}s^{-1}$). This result was interesting since for the other caspases (3, 6, 7, 8, 9, and 10) **18g** was less potent when compared to its *trans* isomer **18h**. The order of reactivity of the inhibitors with the DEVD sequence according to the substituent Y is as follows: COOEt (*cis*) > COOEt (*trans*) > $CON(CH_3)CH_2Ph$ > $CON(CH_2\text{-}1\text{-}Napth)_2$ > CON-tetrahydroquinoline > $CON(CH_3)CH_2CH_2Ph$ > COPh > $CONHCH_2Ph$ > $CONHCH_2$-4-F-Ph > $CONHCH_2CH_2Ph$ > $CON(CH_2Ph)_2$. It seems that the esters are the best substitutents and the disubstituted amides are more preferred over the monosubstituted amides.

Caspase-3. Considerably high rates were obtained for the inhibitors with the caspase-3 specific DEVD sequence against caspase-3. The most potent caspase-3 inhibitor was **18t** (Cbz-Asp-Glu-Val-AAsp-*trans*-CH=CH-$CON(CH_2\text{-}1\text{-}Napth)_2$) with a second order inhibition rate of 5,620,000 $M^{-1}s^{-1}$. With caspase-3, the order of reactivity of the inhibitors with various substituents on the double bond moiety is $CON(CH_2\text{-}1\text{-}Napth)_2$ > $CON(CH_2Ph)_2$ > $CON(CH_3)CH_2Ph$ > CON-tetrahydroquinoline > CO_2Et (*trans*) > $CONHCH_2$-4-F-Ph > $CONHCH_2CH_2Ph$ > $CONHCH_2Ph$ > CO_2CH_2Ph > $CON(CH_3)CH_2CH_2Ph$ > CO_2Et (*cis*) > COPh. Generally, the bulky aromatic groups were preferred in the prime site of this enzyme. The disubstituted amide derivatives worked better than the monosubstituted ones and the ester derivatives. Replacement of the amide or the ester group by a carbonyl group caused a decrease in potency by 10-fold. **18f** (Cbz-Asp-Glu-Val-AAsp-*trans*-CH=CH-COPh) inhibits caspase-3 with a k_2 value of 122,000 $M^{-1}s^{-1}$. **18g**, the inhibitor with the *cis* configuration of the double bond moiety is a potent inhibitor of caspase-3 (k_2 = 1,060,000 $M^{-1}s^{-1}$). However, the *trans* ethyl ester derivative **18h** is twice as potent against caspase-3 (k_2 = 2,130,000 $M^{-1}s^{-1}$). Considerable

decrease in potency was observed with the EVD sequence based inhibitor **17h** (k_2 = 38,600 $M^{-1}s^{-1}$) with caspase-3, which emphasizes the importance of an acidic P4 residue for increased potency. In addition, our caspase-3 inhibitors are equally if not more potent than chloromethyl ketone inhibitors such as Cbz-DEVD-CMK which has a k_2/K_I value of 1,000,000 $M^{-1}s^{-1}$.[11] More importantly, the aza-peptide Michael acceptors are much more selective (See the Cross-reactivity Section).

Caspase-7. The DEVD sequence worked also best with caspase-7. The second order rate constants were in the range of 10^5 $M^{-1}s^{-1}$. Cbz-Asp-Glu-Val-AAsp-*trans*-CH=CH-CON(CH_2-1-Napth)$_2$ (**18t**) is the most potent inhibitor with a second order rate constant of 875,000 $M^{-1}s^{-1}$. The order of reactivity with the substituted Y group among the DEVD series is as follows: CON(CH_2-1-Napth)$_2$ > CON(CH_2Ph)$_2$ > CONHCH_2-4-F-Ph > CON(CH_3)CH_2Ph > CONHCH_2CH_2Ph > CONHCH_2Ph > CO_2Et (*trans*) > CON(CH_3)CH_2CH_2Ph > CO_2Et (*cis*) > CON-tetrahydroquinoline > CO_2CH_2Ph > COPh. Similar to caspase-3, bulky aromatic groups such as benzyl or napthyl groups which extend deep into the pocket are preferred at the caspase-7 S' subsite. There is no distinct preference for disubstituted amide group preference like in the case of caspase-3. However, amide substituents still work generally better than the ester ones. **18m** (Cbz-Asp-Glu-Val-AAsp-*trans*-CH=CH-CONHCH_2-4-F-Ph) is still the best monosubstituted amide inhibitor for both caspase-3 and caspase-7. The rate of inhibition is 10 fold lower (**18f** ,k_2 = 10,8000 $M^{-1}s^{-1}$), where only a carbonyl group is present instead of an amide or ester group in the substituent structure. There is also a decrease in potency with the tripeptide inhibitor **17h** (k_2 = 52,400 $M^{-1}s^{-1}$) indicating that the P4 amino acid is an important factor in potency with caspase-7.

Caspases-6 and -8. The IETD sequence works best with caspase-6, whereas the LETD sequence is ideal for caspase-8. Caspase-8 prefers leucine > valine > aspartic acid at its P4 position. This preference offers some room for the selectivity of caspase-8 over caspase-6, where caspase-6 prefers valine > threonine > leucine at the same position (P4).[27] The best caspase-6 inhibitor is **20k** (Cbz-Ile-Glu-Thr-AAsp-CH=CH-CONPh) with a k_2 value of 99,200 $M^{-1}s^{-1}$. Unfortunately, this inhibitor also potently inactivates caspase-8 (k_2 = 245,000 $M^{-1}s^{-1}$). The order of reactivity with differing Y groups for caspase-6 within the IETD sequence is as follows: CONHPh > CO_2Et (*trans*) >

$CON(CH_2Ph)_2$ > $CON(CH_3)CH_2Ph$ > CO_2CH_2Ph > $CONHCH_2CH_2Ph$ > $CONHCH_2Ph$. There is no distinct preference for any substitution pattern at the caspase-6 S' subsite. Monosubstituted amide derivative **20k** is the most preferred, but the disubstituted amide derivatives **20o**, **20p**, and **20r** are also potent inhibitors. The other caspase-6 specific sequence (VEVD) also yielded very potent inhibition. The inhibitor **19h** (Cbz-Val-Glu-Val-AAsp-CH=CH-COOEt) inhibits caspase-6 with a k_2 value of 83,600 $M^{-1}s^{-1}$. However, the VEVD sequence seems to be less selective. Not only it inhibits caspase-8 potently (k_2 = 175,800 $M^{-1}s^{-1}$), it also inhibits caspase-3 with a k_2 of 41,200 $M^{-1}s^{-1}$.

Although the LETD sequence is determined to be the best one for caspase-8, other caspase-specific sequences are also preferred by this enzyme. The most potent caspase-8 inhibitor is the one that is actually designed for caspase-3 with the DEVD sequence. Hence, **18h** (Cbz-Asp-Glu-Val-AAsp-*trans*-CH=CH-COOEt) has a second order rate constant of 272,960 $M^{-1}s^{-1}$ with caspase-8. Also, the inhibitor **20k** with the IETD sequence is a very potent caspase-8 inhibitor (k_2 = 245,000 $M^{-1}s^{-1}$). The same Y group (CONHPh) when attached to a LETD sequence (**21k**) makes a less potent inhibitor with caspase-8 (k_2 = 176,000 $M^{-1}s^{-1}$). For the inhibitors with the LETD sequence the order of reactivity with caspase-8 with differing Y groups is as follows: COOEt (*trans*) > CON-tetrahydroquinoline > $CON(CH_3)CH_2$-1-Napth > $CONHPh$ > $CONHCH_2$-4-F-Ph > $CON(CH_3)CH_2Ph$ > $CON(CH_2Ph)_2$ > $CONHCH_2CH_2Ph$ > $COOCH_2Ph$ > $CON(CH_3)CH_2CH_2Ph$ > $CONHCH_2Ph$. The inhibitor **21h** (Cbz-Leu-Glu-Thr-AAsp-*trans*-CH=CH-COOEt) is the best one among this series with a k_2 value of 237,000 $M^{-1}s^{-1}$. The tetrahydroquinoline derivative **21u** (Cbz-Leu-Glu-Thr-AAsp-*trans*-CH=CH-CON-tetrahydroquinoline) is less potent than the ethyl ester derivative **21h**, but it is more selective over caspase-6. Interestingly, one of the most potent caspase-8 inhibitors is the tripeptide derivative **17h** (Cbz-Glu-Val-AAsp-*trans*-CH=CH-COOEt) with a k_2 value of 244,000 $M^{-1}s^{-1}$. In general, higher rates were obtained with caspase-8 where Y is a small sized group such as ethyl and when Y is not extending deeply into the S' subsite.

Caspase-9. The rates of inhibition of caspase-9 by the aza-peptide Michael acceptors are not as high as the other members of the caspase family we have tested. However, the LETD is still the best sequence with rates in the range of $10\text{-}10^3$ $M^{-1}s^{-1}$. The best inhibitors are **21s** and **21o** with k_2 values of 5,030 $M^{-1}s^{-1}$ and 4,320 $M^{-1}s^{-1}$,

respectively. However, the most potent caspase-9 inhibitor is the tripeptide derivative **17h** (Cbz-Glu-Val-AAsp-*trans*-CH=CH-COOEt) with a k_2 value of 32,900 $M^{-1}s^{-1}$. Surprisingly, a considerable decrease in potency is observed with the same Y group (ethyl) when attached to a tetrapeptide sequence. The inhibitor **21h** (Cbz-Leu-Glu-Thr-AAsp-*trans*-CH=CH-COOEt) inhibits caspase-9 very weakly (k_2 = 37 $M^{-1}s^{-1}$).

Caspase-10. The best inhibitors of caspase-10 have the caspase-3 optimal sequence DEVD. The rates of inhibition are in the range of 10^3-10^4 $M^{-1}s^{-1}$ and the best inhibitor is Cbz-Asp-Glu-Val-AAsp-*trans*-CH=CH-COOEt (**18h**, k_2 = 49,900 $M^{-1}s^{-1}$). The order of reactivity with differing Y groups with the DEVD sequence is as follows: COOEt (*trans*) > $CONHCH_2$-4-F-Ph > $CON(CH_2$-1-Napth$)_2$ > $CONHCH_2CH_2Ph$ > $CON(CH_3)CH_2Ph$ > $COOCH_2Ph$ > $CONHCH_2Ph$ > COOEt (*cis*) > $CON(CH_3)CH_2CH_2Ph$ > CON-tetrahydroquinoline > $CON(CH_2Ph)_2$. The tripeptide inhibitor **17h** works equally well as some of the tetrapeptide inhibitors with caspase-10 (k_2 = 8,940 $M^{-1}s^{-1}$). Once again, this result indicates that with group II caspases (6, 8, 9, 10) the absence of the P4 residue is not as crucial as for group III caspases (2, 3, 7) for potency and selectivity.

Caspase Selectivity. In general, the most potent inhibitors of a target caspase were the ones that were designed with its ideal sequence, although in some cases caspases-8, -9, and -10 exhibited exceptions. Interestingly, the most specific inhibitors were still very potent but they were not the most potent ones. The most specific inhibitor for caspase-3 was Cbz-Asp-Glu-Val-AAsp-*trans*-CH=CH-$CON(CH_2Ph)_2$ (**18r**, k_2 = 3,000,000 $M^{-1}s^{-1}$), which is 27 300, 588, 8.4, 348, 6670, and 476 fold more selective for caspase-3 over caspases-2, -6, -7, -8, -9, and -10, respectively. The most specific caspase-6 inhibitor was Cbz-Ile-Glu-Thr-AAsp-*trans*-CH=CH-COOEt (**20h**, k_2 = 88,700 $M^{-1}s^{-1}$). It is 295.6, 13.2, 167.4, 1.6, and 12.9 fold more selective for caspase-6 over caspases-2, -3, -7, -8, and -10, respectively. The most selective caspase-8 inhibitor was Cbz-Leu-Glu-Thr-AAsp-*trans*-CH=CH-COOEt (**21h**, k_2 = 237,000 $M^{-1}s^{-1}$), which is 42.6, 12.6, and 6405 fold more selective for caspase-8 over caspases-3, -6, and -9, respectively.

The selectivity of the aza-peptide Michael acceptor inhibitors with the DEVD sequence for caspase-3 over caspase-7 is 6.9-16.8 fold. Selectivity between caspase-3

and caspase-7 was hard to achieve, since the DEVD sequence is the ideal one for both enzymes. The selectivity of caspase-3 over caspase-2 is as high as 10^5 fold, because of the P5 requirement of caspase-2. The selectivity for caspase-3 over caspase-6 is usually around 500 fold. However, when one obtained selectivity over caspase-6, it was difficult to obtain selectivity also for caspase-8. The range of selectivity for caspase-3 over caspase-8 was only up to 37-fold, except in the case of the inhibitor **18r**. It has been previously shown that the prime site of caspase-8 differs from that of the other caspases by the presence of a helix-turn-helix insertion ranging from residues 245-253, which is unique to caspase-8.[31] Clearly, we have taken advantage of this structural difference by designing an inhibitor with a dibenzyl amide substituent on the double bond moiety, which resulted in optimal selectivity. Generally, caspase-10 behaved similarly to caspase-8, however it yielded less potent inhibitors. Lastly, the rates of inhibition of caspase-9 were quite low when compared to the other caspases (3, 6, 7, 8, and 10).

In addition to the tri- and tetrapeptidyl aza-peptide Michael acceptors we also made several dipeptidyl derivatives with the VD sequence in the hopes of obtaining a potent and broad spectrum inhibitor for caspases. Due to enhanced aqueous solubility, it has been previously shown that the inhibitor Z-VD-fmk was more active than the tri- and tetrapeptide based inhibitors such as Z-VAD-fmk in certain cell culture models of apoptosis.[32] Unfortunately, our dipeptide inhibitor Cbz-Val-AAsp-*trans*-CH=CH-COOEt (**16h**) weakly inactivated caspase-3 (k_2 = 8,000 $M^{-1}s^{-1}$), caspase-7 (k_2 = 2,680 $M^{-1}s^{-1}$), caspase-9 (k_2 = 5,260 $M^{-1}s^{-1}$) and caspase-10 (k_2 = 389 $M^{-1}s^{-1}$). It did not show any inhibition of caspases-2, -6 or -8. The two amide derivatives **16j** and **16l** showed little potency toward caspase-3 (k_2 values are 184 $M^{-1}s^{-1}$ and 185 $M^{-1}s^{-1}$, respectively), caspase-7 (k_2 values are 55 $M^{-1}s^{-1}$ and 60 $M^{-1}s^{-1}$, respectively), caspase-9 (k_2 values are 32 $M^{-1}s^{-1}$ and 20 $M^{-1}s^{-1}$, respectively), but no activity against caspases-2, -6, -8 or -10. The dipeptide aza-peptide Michael acceptors with simple alkyl, alkenyl or halogen substituents remained unreactive toward all the caspases (2, 3, 6, 7, 8, 9, and 10). The decreased potency of the dipeptide derivatives toward caspases is in accordance with the previous observation of the requirement of at least tripeptides for binding and recognition.

Cross Reactivity with Clan CA and Other Clan CD Proteases. The aza-peptide Michael acceptors designed for caspases show little to no inhibition of the clan CA cysteine proteases papain, cathepsin B, and calpain, where the specificity is determined primarily by the S2 subsite. The inhibitors **18h**, **18i**, **18l**, and **21i** showed essentially no inhibition against papain, cathepsin B, and calpain after an incubation period of one hour (Table 2).

We also tested the cross reactivity of our inhibitors with other members of clan CD proteases such as legumain, clostripain, and gingipain K. Legumain has a strict requirement for Asn at P1, whereas clostripain and gingipain K prefer Orn and Lys at the same position. Aza-peptide Michael acceptors designed for caspases did not show any activity against those enzymes after being incubated for one hour. Likewise, the aza-peptide Michael acceptor inhibitors with legumain, clostripain, and gingipain K specific sequences did not show any cross reactivity with clan CA enzymes or between each other.[23] Clearly, the aza-peptide Michael acceptor design is specific for clan CD enzymes.

Stability Studies. We tested the stability of the aza-peptide Michael acceptors toward simple thiol nucleophiles such as thiol DTT contained in the caspase assay buffer. A representative group of inhibitors (2.5-4 mM) were treated with 10 mM DTT in the caspase assay buffer with a pH of 7.2 at 25 °C. The reactivity of the Michael acceptor double bond was monitored by UV spectrum at 250 nm for a period of 15 hours. The half-lives were obtained from first order rate plots of ln(At/A0) versus time.

We observed that the ester derivative **18h** (Cbz-Asp-Glu-Val-AAsp-CH=CH-COOEt) had a half-life of 10 minutes. The amide substituted Michael acceptors appeared to be less reactive toward DTT under the same conditions. The monosubstituted amide derivative **18l** (Cbz-Asp-Glu-Val-AAsp-CH=CH-CONHCH$_2$Ph) had a half life of 58 minutes, where the disubstituted amide derivative **18o** (Cbz-Asp-Glu-Val-AAsp-CH=CH-CON(CH$_3$)CH$_2$Ph) was twice as long stable with a half-life of 116 minutes. The dienyl derivative **16b** (Cbz-Val-AAsp-CH=CH-CH=CH-CH$_3$) was essentially stable over the period of 15 hours of monitoring.

Aza-peptide Michael acceptors designed for other clan CD proteases such as legumain, gingipain and clostripain specific sequences were also tested for stability

against DTT.[23] The half-life of the legumain inhibitor Cbz-Ala-Ala-AAsn-CH=CH-COOEt in the legumain assay buffer (pH = 5.8) with excess DTT was 19 minutes. When tested at a higher pH (6.8) the half-life of the same inhibitor shortened to 3.7 minutes.

It should be noted that the pH of the assay buffer has a considerable effect on the stability of the inhibitors against DTT. The DTT thiol has a pKa value of 9.2. The lower the pH, the lower is the concentration of the deprotonated thiol group of DTT. Hence, a nucleophilic attack on the Michael acceptor double bond is more favored at higher pH values.

We also anticipate that the nature of the P' substituent on the double bond contributes significantly to the overall stability of the inhibitor. In general, the order of stability of our inhibitors is as follows: alkyl > amide > ester. It has been previously demonstrated by Freidig and coworkers that simple acrylates are more reactive than simple acrylamides to thiol nucleophiles such as glutathione.[33] Ethyl acrylate reacts with glutathione 85 times faster than ethyl acrylamide with second order rate constants of 0.66 $M^{-1}s^{-1}$ and 7.8 x 10^{-3} $M^{-1}s^{-1}$, respectively. Our results of the reactivity of the ester and amide substituted inhibitors indicate a strong correlation with the observed reactivity of acrylates and acrylamides with glutathione.

Mechanism of Inhibition. In general, the inactivation of cysteine proteases by Michael acceptor inhibitors proceeds through the nucleophilic attack of the active site cysteine thiol group on the C3-carbon of the Michael acceptor double bond. The mechanism of inhibition of caspases by aza-peptide Michael acceptors could involve irreversible thioalkylation of the active site Cys by the two pathways shown in Figure 4. Theoretically, if the substituent on the double bond is an acyl derivative such as ester or amide, the formation of both thioether adducts **22** and **23** is possible upon a nucleophilic attack taking place either at the C-2 or C-3 carbon on the double bond moiety. If the substituent is a simple alkyl or halogen, only the C-3 carbon is the possible site for the Michael addition reaction.

Based on the results of the NMR study and the stability studies of our inhibitors with DTT, we previously hypothesized that a nucleophilic attack of the active site thiol group at the C-2 would be more favorable.[23] However, to determine conclusively the

point of attack, crystal structures of five caspase-double bond complexes were determined.

X-ray structure analysis of Caspase Inhibitor Complexes. We have determined four crystal structures of caspase-3-inhibitor complexes and the structure of one caspase-8 inhibitor complex. The Michael acceptors used for the structural studies with caspase-3 are two stereo isomers (*cis* and *trans*) of the ethyl ester derivatives **18g** and **18h** respectively, a benzyl ester derivative (**18i**) and a N-methyl-benzyl amide derivative (**18o**). We have determined the structure of caspase-8 complexed with **21t** which is a tetrahydroisoquinoline derivative. These inhibitor complexes are unique since they have inhibitor moieties which interact with S' subsites of enzyme unlike most caspase-inhibitor complex structures published to date.

The overall structures of the polypeptide chain in the complexes are quite similar to the other known crystal structures of the caspase family[34-37]. The superposition of the Cα atoms of the subunits result in a root mean square deviation of 0.2 Å for caspase-8 and 0.35 Å for caspase-3 inhibitor complexes. This indicates that large scale conformational transitions do not occur upon binding of the P` portion of the inhibitor structure, however conformational changes do occur in parts of the enzyme directly interacting with the inhibitor to improve the fit. The interactions of the P1-P4 moieties of the Michael acceptor inhibitors bind to the substrate binding cleft of the caspase active site similarly as already previously observed in the peptidyl aldehyde or halogen methyl ketone inhibitor complexes[34-37] closely mimicking substrate binding from P1 to P4.

The high resolution crystal structures clearly demonstrate that the nucleophilic attack takes place at the C-2 carbon more precisely on the *re* face. This results in a covalent thioether bond between the C-2 carbon and the sulfur atom of the active site Cys residue. As a result of the nucleophilic attack, the hybridization of both the C-2 and C-3 carbons change from sp^2 to sp^3 yielding a tetrahedral C-2 carbon and a chiral tetrahedral C-3 carbon with the R–configuration (Fig 6a-b).

Caspase-3 Inhibitor Complexes. As observed in the crystal structures of caspases complexed with halo methyl ketones[26,36], the P1 azapeptide carbonyl points towards the "oxyanion hole" and it is stabilized by the amide protons of Gly122 and

Cys163. A unique feature of all the crystal structures of caspase-3 Michael acceptor complexes is the rotation of the catalytic His121 about Chi2 by approximately 20 degrees. In this new orientation the imidazole ring is ideally placed to form a hydrogen bond to the carboxylate of P1-Asp (Fig 6c). The distance of this hydrogen bond ranges from 3.3-3.6 Å in our complexes. This interaction between the catalytic His121 and P1-Asp is not observed in any other caspase crystal structure reported so far. Apart from this interaction, His121 also forms a hydrogen bond to the azapeptide P1` carbonyl. The interactions of the P2 and P3 residues are similar to those reported in other caspase-3 structures[34,36].

The P1` site in caspase-3 is predominantly hydrophobic and it is defined by four loop regions. The 179-loop (between strand β1 and helix α2), the 240-loop (between strand β3 and helix α3) and the C-terminal loop belong to the alpha subunit, whereas the fourth loop (between strand β4 and helix α3) is from the β subunit. The approximate solvent accessible volume of the prime site cavity is 900 $Å^3$. In the Michael acceptor **18o**, the P1` moiety is a N-methyl-benzyl amide derivative. The phenyl ring points towards the one side of the S1` pocket and stabilized by hydrophobic contacts with Thr166 and Tyr204 while the N-methyl group is stabilized by Phe128 (Fig. 7b). This is most reactive caspase-3 inhibitor of those studied crystallographically. In the case of the benzyl derivative **18i**, the electron density for the phenyl ring is not well defined as indicated by high B values. In the ethyl ester derivative formed from **18h** and **18g**, the ethyl group interacts with the side chains of Phe128 and His121. To avoid steric hindrance and in tandem to maintain the hydrophobic contact with the ethyl group of the inhibitor, the side chain of Met61 of the 179-loop adopts a different conformation. This conformation is quite different from that observed in all other known caspase-3 structures. As expected, the atoms of the products formed from the two stereoisomers (**18g** and **18h)** of the ethyl ester overlay well on superposition. Additionally, in both structures , the C-3 carbon adopts a R-configuration indicating the attack is on the *re* face of the inhibitor (Fig 7a).

Caspase-8. Unlike in caspase-3: Michael acceptor inhibitor complexes, in the caspase-8 complex the P1` carbonyl is stabilized by the side chain of P2-Thr instead of

the catalytic His317. The P4-Leu is stabilized in the manner similar to the P4-Ile as exemplified in the crystal structure of caspase-8:Ac-IETD-CHO complex[35]. The phenyl ring of the capping residue Cbz in **21t** stacks favorably on top of Pro415, subsequently the puckering of this Pro is different from the one which is observed in other caspase-8 inhibitor complex structures[35,37,38].

The S1` site of caspase-8 is different from all other caspases due to the helix-turn-helix insertion in the 179-loop[37]. We have determined the structure of caspase-8 in complex with **21t**. This compound is a tetrahydroisoquinoline derivative in which the tetrahydroisoquinoline occupies the hydrophobic S1' pocket defined by the residues Leu254, Ile257 and Tyr324 (Fig. 8). As a consequence this bulky hydrophobic moiety displaces the 179-loop by about 1.0 Å when compared to other caspase-8 inhibitor complexes. More importantly, significant changes in the side chain conformation of Arg258 are observed. Arg258 recognizes P3-Glu and its backbone carbonyl is critical for maintaining a hydrogen bond with Nε1 of the catalytic His317. In the complex with **21t** the side chain of Arg258 is pointing towards Ser175 and in addition is involved in a hydrogen bond with the backbone carbonyl of Ser175. Such conformational changes might cost binding energy, which in turn is compensated by the formation of favourable hydrogen bonds or by hydrophobic interactions. Such differences are particularly observed in caspase-8 as it has a unique helix-turn-helix insertion loop at that site[37].

Stereochemistry. In our design of the aza-peptide Michael acceptors the double bond moiety has two different substitutents. One is the peptide chain and the other is the differing Y group, which consists of various groups such as alkyl, alkenyl, aryl, halogen, ester or amide. Therefore, the double bond in aza-peptide Michael acceptors has two isomers: the *cis* isomer and the *trans* isomer. We focused our attention of making mainly fumarate analogs. However, we made one inhibitor with the *cis* configuration on the double bond moiety (**18g**). This inhibitor turned out to be the most potent inhibitor of caspase-2 (k_2 = 26,200 $M^{-1}s^{-1}$), when compared to the fumarate analogs. **18g** was also quite potent with the other caspases as well (Table 1). It was less potent than the *trans* isomer **18h**, but overall it was more reactive than some of the fumarate analogs. The weaker inhibition by the *cis* isomer (**18g**) compared to the *trans* isomer (**18h**) could be

due to an inherent difference in chemical reactivity of the two isomers and/or to weaker binding of the *cis* isomer to the enzyme. In an attempt to search for some structural reasons for this behavior, we have co-crystallized both the isomers with caspase-3. The crystal structure of the *cis* and *trans* isomer complexes were determined at 1.76 Å and 1.86 Å resolution, respectively. In the *cis* complex the B-factor values of the inhibitor in general and P1' atoms in particular are higher than the *trans* complex, indicating higher mobility and/or lower occupancy in the active site. Consequently, the difference electron density for the bound inhibitor in the active sites of the caspase-3 *cis* complex is weaker than for the *trans* isomer. Nonetheless the electron density maps were good enough to fit the inhibitor model into the active site. The superposition of the *cis* and the *trans* complexes reveals that the bound covalent adducts overlap well with similar side chain rearrangements in the two complex structures. From structural considerations alone one would argue that both compounds bind with equal potency which is confirmed by kinetic data (give here precise values).

CONCLUSION

Aza-peptide Michael acceptors with the Asp residue at P1 are a novel class of inhibitors for caspases-2, -3, -6, -7, -8, -9, and -10. The inhibitors have excellent inhibitory potency and selectivity for clan CD cysteine proteases, where the second order rate constants are as high as 5,620,000 $M^{-1}s^{-1}$. Aza-peptide Michael acceptors designed for caspases have been tested with a variety of other cysteine proteases for cross reactivity. They do not show cross reactivity with the clan CA proteases such as papain, cathepsin B and calpain. Aza-peptide Michael acceptors designed for caspases show little to no cross reactivity with legumain which has a specifity for Asn at P1. They do not react with other clan CD proteases gingipain K and clostripain with specificities Lys and Orn at P1, respectively.

Analysis of our crystal structures reveals that the nucleophilic attack takes place on the C3-carbon of the double bond, thus additional substitution might be tolerated in the C2-carbon. In an effort to obtain greater selectivity among caspases-2, -3, -6, -7, -8, -9, and -10, we modified the P' substituent on the double bond for each appropriate

caspase sequence. Our results indicate that caspases-3 and -7 can tolerate bulky and aromatic residues in the prime site. Caspases-6 and -10 can accommodate a variety of different substituents at the same position, whereas caspase-8 prefers smaller P' substituents such as the ethyl group. Currently, we are continuing to refine our design on the P' site, where we would like exploit the further possibilities for some polar interactions in the prime site. By introducing substituents on the double bond with a variety of different electron-withdrawing characters, we are also hoping to improve the stability of aza-peptide Michael acceptors toward thiol nucleophiles such as the thiol DTT.Aza-peptide Michael acceptors' potency and selectivity for caspases make them great candidates for potential use as probes in cellular function studies and as drugs. Due to the strict requirement of the negatively charged Asp residue at P1 and the peptide chain itself, the hydrophobic character of our inhibitors is significantly low. By introducing non-peptide moieties to replace the peptide backbone and shielding the side chain carboxylic acid group with certain isosteres, one can increase the hydrophobicity and hence the bioavailability of our caspase inhibitors.

EXPERIMENTAL SECTION

Enzyme Assays

Caspase-2, -3, -6, -7, -8, -9 and -10. Caspases-2, -3, -6, -7, -8, -9 and -10 were expressed in *E. coli* and purified in Guy Salvesen's laboratory at the Burnham Institute, La Jolla, CA, according to the methods previously described by Stennicke and Salvesen. [40] Inhibition rates were determined by the progress curve method described by Tian and Tsou. [41] This method is suitable for measuring irreversible inhibition rates with fast inhibitors, where the inhibitor, the substrate and the enzyme are incubated together and the rate of substrate hydrolysis is measured continuously. The rate of substrate hydrolysis in the presence of the inhibitor was monitored for 20 minutes. The progress curve of inhibition, where the product formation approaches an asymptote is described in the equation

$$\ln ([P_\infty]-[P]) = \ln [P_\infty] - A[I]t$$

where [P] and $[P_\infty]$ are the product concentrations at t and $t = \infty$ respectively, A is the apparent rate constant in the presence of the substrate. The apparent rate constants

were determined from the slopes of plots of ln ($[P_\infty]$-[P]) versus time (t) in seconds as previously described, where A = slope / [I].

For competitive and irreversible inhibition, the apparent rate constant is converted to the second order rate constant k_2 by taking into consideration the effect of the substrate concentration on the apparent rate constant. The second order rate constant is described as in the equation:

$k_2 = A * (1 + [S] / K_M)$

Assays using the fluorogenic substrates Ac-DEVD-AMC (λ_{ex} = 360 nm, λ_{em} = 465 nm), Z-VDVAD-AFC (λ_{ex} = 430 nm, λ_{em} = 535 nm), and Ac-LEHD-AFC were carried out on a Tecan Spectra Fluor microplate reader at 37 ^oC. The K_M values for Ac-DEVD-AMC with caspase-3 (K_M = 9.7 μM), caspase-6 (K_M = 236.35 μM), caspase-7 (K_M = 23.0 μM), caspase-8 (K_M = 6.79 μM), and caspase-10 (K_M = 20.2 μM) were determined in the laboratory of Guy Salvesen. The K_M value for Ac-LEHD-AFC with caspase-9 (K_M = 114 μM) was also determined in the laboratory of Guy Salvesen. The K_M value for Z-VDVAD-AFC with caspase-2 was found to be 80.5 μM. The k_2 values are 2.24-fold higher than the apparent rate for caspase-2 because of the 100 mM [S] and K_M = 80.5 μM. The k_2 values are 11.31-fold higher than the apparent rate for caspase-3 because of the 100 mM [S] and K_M = 9.7 μM. The k_2 values are 1.42-fold higher than the apparent rate for caspase-6 because of the 100 mM [S] and K_M = 236.35 μM. The k_2 values are 5.35-fold higher than the apparent rate for caspase-7 because of the 100 mM [S] and K_M = 23.0 μM. The k_2 values are 15.73-fold higher than the apparent rate for caspase-8 because of the 100 mM [S] and K_M = 6.79 μM. The k_2 values are 2.32-fold higher than the apparent rate for caspase-9 because of the 150 mM [S] and K_M = 114 μM. The k_2 values are 8.43-fold higher than the apparent rate for caspase-10 because of the 150 mM [S] and K_M = 20.2 μM.

The concentration of the caspase-3 stock solution was 2 nM in the assay buffer. Assay buffer is a 1:1 mixture of caspase buffer (40 mM Pipes, 200 mM NaCl, 0.2% (w/v) CHAPS, sucrose 20% (w/v)) and 20 mM DTT solution in H_2O at pH 7.2. The concentration of the substrate stock solution was 2 mM in DMSO. The enzyme was pre-activated for 10 min at 37 ^oC in the assay buffer. The standard 100 μL reaction was

started by adding 40 μL of assay buffer, 5 μL of various amounts of inhibitor (stock solution concentrations varied from 5 x 10^{-3} M to 4.84 x 10^{-7} M in DMSO), and 5 μL of substrate in DMSO (100 μM final concentration) at 37 ^{o}C. 50 μL of 2 nM enzyme stock solution (final concentration: 1 nM) was added to the mixture after 1 min and reading started immediately for 20 min at 37 ^{o}C. Inhibition experiments were repeated in duplicate and standard deviations determined.

Caspase-2 kinetic assays were performed using Z-VDVAD-AFC as the substrate (2 mM stock solution in DMSO) and with the same conditions as caspase-3. The concentration of the caspase-2 stock solution was 86.7 nM in the assay buffer (final concentration in the well: 43.3 nM). The inhibitor stock solution concentrations varied from 5 x 10^{-3} M to 1 x 10^{-4} M in DMSO. Caspase-6 kinetic assays were performed using the same conditions and the same substrate (Ac-DEVD-AMC, 2 mM stock solution in DMSO). The enzyme stock solution was 10 nM (final concentration in the well: 5 nM) in the assay buffer. The inhibitor stock solution concentrations varied from 5 x 10^{-3} M to 2.42 x 10^{-6} M in DMSO. Caspase-7 kinetic assays were performed using the same conditions and the same substrate (Ac-DEVD-AMC, 2 mM stock solution in DMSO). The enzyme stock solution was 10 nM (final concentration in the well: 5 nM) in the assay buffer. The inhibitor stock solution concentrations varied from 5 x 10^{-3} M to 2.5 x 10^{-6} M in DMSO.

Caspase-8 kinetic assays were performed using the same conditions and the same substrate (Ac-DEVD-AMC, 2mM stock solution in DMSO). The enzyme stock solution was 100 nM (final concentration in the well: 50 nM) in the assay buffer. The inhibitor stock solution concentrations varied from 5 x 10^{-3} M to 2.42 x 10^{-6} M in DMSO.

Caspase-9 kinetic assays were performed using Ac-LEHD-AFC as the substrate (3 mM stock solution in DMSO) and with the following conditions. The concentration of the caspase-9 stock solution was 150 nM in the assay buffer (final concentration in the well: 75 nM). Assay buffer is a 1:1 mixture of buffer (200 mM Hepes, 100 mM NaCl, 0.01% (w/v) CHAPS, sucrose 20% (w/v)) and 20 mM DTT solution in H_2O at pH 7.0. The assay buffer was supplemented with 0.7 M sodium citrate. The enzyme was pre-activated for 10 min at 37 ^{o}C in the assay buffer. The inhibitor stock solution concentrations varied from 5 x 10^{-3} M to 2.5 x 10^{-5} M in DMSO.

Caspase-10 kinetic assays were performed using the same substrate as caspase-3 (Ac-DEVD-AMC, 3 mM stock solution in DMSO) and with the following conditions. The concentration of the caspase-10 stock solution was 50 nM in the assay buffer (final concentration in the well: 25 nM). Assay buffer is a 1:1 mixture of buffer (200 mM Hepes, 0.2% (w/v) CHAPS, PEG 20% (w/v)) and 20 mM DTT solution in H_2O at pH 7.0. The enzyme was pre-activated for 10 min at 25 ^oC in the assay buffer. The inhibitor stock solution concentrations varied from 5 x 10^{-3} M to 2.5 x 10^{-5} M in DMSO.

***S. mansoni* Legumain**. Conor R. Caffrey in James McKerrow's laboratory performed the *S. mansoni* legumain kinetic assays at the Sandler Center for Basic Research in Parasitic Diseases, University of California at San Francisco, San Francisco, CA. The zymogen form of schistosome legumain SmAE was expressed in *Pichia*. The lyophilized enzyme (50-100 mg) was reconstituted in 1.5 mL 0.5 M sodium acetate, pH 4.5 containing 4 mM DTT, and left to stand at 37 °C for 3-4 hours to allow for auto-activation of the zymogen. In a black 96-well microtiter plate, 50 µL of activated enzyme was added to an equal volume of 0.1 M citrate-phosphate buffer pH 6.8 containing 4 mM DTT. The inhibitors, added as 1 µL aliquots (serial water dilutions of DMSO stock solutions, 2 to 0.00002 µM [final]), were preincubated with the protease at room temperature for 20 min. After incubation, 100 uL of the same buffer containing 20 µM substrate (Cbz-Ala-Ala-Asn-AMC) was added to the wells and the reaction monitored for 20 minutes. A plot of the RFU/min versus the inhibitor concentration [µM] permitted calculation of an IC_{50} value.

Pichia cell culture medium containing recombinant *S. mansoni* pro-legumain was incubated overnight at room temperature in 0.3 M sodium acetate, pH 4.5, 2 mM DTT to allow autoactivation of the endogenous zymogen. Inhibitor (1 µl) at 6 concentrations (to yield 0 to 1 µM [final]) was spotted into a 96-well black microtiter plate. To this was added 180 µl 0.1 M citrate-phosphate buffer, pH 6.8, containing 2 mM DTT and 20 µM Cbz-AAN-AMC substrate. Activated legumain (20 µl) was added to the mix and the progress of inhibition followed every 2 seconds for 30 minutes at 25 °C (Molecular Devices Flex Station fluorometer in the injection mode; ex 355/em 460).

Clostripain. Clostripain was purchased from Sigma Chemical Co. (St. Louis, MO) as a solid which was dissolved in an activation solution of 8 mM DTT at a

concentration of 5.962 μM and stored at -20 °C prior to use. The inhibition of clostripain began with the addition of 25 μl of stock inhibitor solution (concentration varies by inhibitor) in DMSO to a solution of 250 μl of 20 mM Tris/HCl, 10 mM $CaCl_2$, 0.005% Brij 35, 2 mM DTT buffer at pH 7.6 (clostripain buffer) and 5 μl of the stock enzyme solution. Aliquots (25 μl) of this incubation mixture were taken at various time points and added to a solution containing 100 μl of the clostripain buffer and 5 μl of Z-Phe-Arg-AMC substrate solution (0.139 mM) in DMSO. The enzymatic activity was monitored by following the change in fluorescence at 465 nm. All data obtained was processed by pseudo-first order kinetics.

Gingipain K. Gingipain K stock solution was obtained from Jan Potempa's lab (University of Georgia, Athens, GA) in a buffer containing 20 mM Bis-Tris, 150 mM NaCl, 5 mM $CaCl_2$, 0.02% NaN_3, at pH 8.0 at a concentration of 9 μM, which was stored at -20 °C prior to use. Before using the enzyme, an aliquot (1 μl) of the stock enzyme was diluted to a concentration of 4.61 nM in 1.951 ml of a solution of 0.2 M Tris/HCl, 0.1 M NaCl, 5 mM $CaCl_2$, 2 mM DTT at pH 8.0 (gingipain K buffer) and kept at 0 °C. This solution was used only for one day, as freezing the enzyme at this concentration destroyed all activity. The inhibition of gingipain K began with the addition of 25 μl of stock inhibitor solution (concentration varies by inhibitor) in DMSO to 244 μl of the diluted enzyme solution (4.61 nM) in gingipain K buffer warmed to rt. Aliquots (20 μl) of this were taken at various time points and added to a solution containing 100 μl of the gingipain K buffer and 5 μl of Suc-Ala-Phe-Lys-AMC • TFA as the substrate (0.910 mM stock) in DMSO. The enzymatic activity was monitored by following the change in fluorescence at 465 nm. The data for gingipain K was processed by pseudo-first order kinetics.

Cathepsin B. Irreversible kinetic assays were performed by the incubation method with human liver cathepsin B. Enzymatic activities of cathepsin B were measured in 0.1 M $KHPO_4$, 1.25 mM EDTA, 0.01% Brij, pH 6.0 buffer and at 23 °C using Cbz-Arg-Arg-AMC as the substrate. To a freshly prepared enzyme stock solution of cathepsin B (approximately 6.98 x 10-3 μg/μL) in enzyme buffer containing DTT (0.1 mM) was added an additional 300 μL of enzyme buffer and 30 μL of a stock inhibitor

solution in DMSO. At various time intervals 50 μL aliquots were withdrawn from the incubation mixture and added to 200 μL enzyme buffer containing Cbz-Arg-Arg-AMC (500 μM). Substrate hydrolysis was monitored using a Tecan Spectra Fluor microplate reader (λ_{ex} = 360 nm, λ_{em} = 465 nm). Pseudo first-order rate constants (k_{obs}) were obtained from plots of ln v_t/v_0 versus time.

Papain. Irreversible kinetic assays were performed by the incubation method with papaya latex papain. An enzyme stock solution for the papain assays was freshly prepared from 330 μL of enzyme storage solution (1.19 mg/ml) diluted with 645 μL papain buffer (50 mM Hepes, and 2.5 mM EDTA at pH 7.5) and 25 μL of DTT (0.1 M). The incubation mixture was prepared from 300 μL buffer, 30 μL of inhibitor stock solution (DMSO), and 30 μL of enzyme stock solution. At various times aliquots (50 μL) were withdrawn and added to 200 μL of Cbz-Phe-Arg-pNA substrate in buffer (53.7 μM). The absorbance of released *p*-nitroaniline was monitored at 405 nm on a Molecular Devices Thermomax plate reader.

Calpain I. Irreversible kinetic assays were performed by the incubation method with calpain I from porcine erythrocytes. Enzymatic activities of calpain I were measured at 23 °C in 50 mM Hepes buffer (pH 7.5) containing 10 mM cysteine and 5 mM $CaCl_2$, using Suc-Leu-Tyr-AMC as the substrate. To 30 μL of an enzyme stock solution (1 mg/ml) of calpain I was added 300 μL of incubation buffer and 30 μL of a stock inhibitor solution in DMSO. At various time intervals 50 μL aliquots were withdrawn from the incubation mixture and added to 200 μL enzyme buffer containing Suc-Leu-Tyr-AMC (1.6 mM). Substrate hydrolysis was monitored using a Tecan Spectra Fluor microplate reader (λ_{ex} = 360 nm, λ_{em} = 465 nm). Pseudo first-order rate constants (k_{obs}) were obtained from plots of ln v_t/v_0 versus time.

Determination of the Stability of the Inhibitors in Buffer and in the Presence of DTT. The stability of a representative group of inhibitors was studied by monitoring the UV spectrum of solutions at 250 nm, at 25 ºC. The concentrations of the inhibitors were 2.5-4.0 mM and of DTT was 10 mM. The pH of the buffer solution was 7.2 and it contained about 50 % (v/v) DTT. The half-lives ($t_{1/2}$) were obtained from first-order rate plots of ln(A_t/A_0) versus time (15 hours) and the correlation coefficients were greater than 0.99.

An aliquot (50 μL) of 4 mM Cbz-Asp-Glu-Val-AAsp-CH=CH-COOEt was added to 450 μL of assay buffer, and the stability of the inhibitor was monitored spectrophotometrically at 250 nm for every 30 minutes for 4 hours. A half-life of 10 min was obtained from the first order rate plot from absorbance (250 nm) versus time (15 hours).

An aliquot (50 μL) of 2.5 mM Cbz-Asp-Glu-Val-AAsp-CH=CH-CONHCH$_2$Ph was added to 450 μL of assay buffer, and the stability of the inhibitor was monitored spectrophotometrically at 250 nm for every 30 minutes for 4 hours. A half-life of 58 min was obtained from the first order rate plot from absorbance (250 nm) versus time (15 hours).

An aliquot (50 μL) of 2.5 mM Cbz-Asp-Glu-Val-AAsp-CH=CH-CON(CH$_3$) CH$_2$Ph was added to 450 μL of assay buffer, and the stability of the inhibitor was monitored spectrophotometrically at 250 nm for every 30 minutes for 4 hours. A half-life of 116 min was obtained from the first order rate plot from absorbance (250 nm) versus time (15 hours).

An aliquot (50 μL) of 2.5 mM Cbz-Val-AAsp-CH=CH-CH=CH-CH$_3$ was added to 450 μL of assay buffer, and the stability of the inhibitor was monitored spectrophotometrically at 250 nm for every 30 minutes for 4 hours. The inhibitor was essentially stable over the course of the study.

Crystal Structures-Caspase purification. Human recombinant caspase-3 and caspase-8 were produced in *E.coli* as inclusion bodies, refolded and purified. Briefly, for caspase-3, the cloned genes for the large p17 subunit (Met-Ser^{29}-Asp^{175}) and the small p12 subunit (Met-Ala-Ser^{176}-His^{277}) were inserted in the *Nco*I/*Bam*HI sites of pET11d plasmids (Novagen). For caspase-8, the cloned genes for the large p18 subunit (Met-Gly-Glu^{218}-Asp^{374}) and the small p12 subunit (Met-Ala-Glu^{376}-Asp^{479}) were inserted in the *Nco*I/*Bam*HI sites of pET11d plasmids (Novagen). For separate expression of both subunits, *E. coli* BL21-CodonPlus (DE3)-RIL cells (Stratagene), containing one of the two plasmids were grown to a density of A_{600} = 0.5 at 37 °C in a 0.5-liter LB medium. Expression was induced by the addition of IPTG (1 mM), and the culture was shaken at 37 °C for 4 hours post induction. Cells were harvested, washed in PBS buffer and lyzed using a French press. Owing to over expression the protein was localised in inclusion

body portion. Refolding was achieved by rapid mixing of equimolar amounts of each subunit to a final concentration of about 100 µg of subunit/ml in the refolding buffer (100 mM HEPES, pH 7.5, 10% sucrose, 1% CHAPS, 100 mM NaCl and 10 mM DTT) and was incubated overnight at room temperature with continuous stirring. Misfolded and aggregated protein was removed by centrifugation (5,000 x *g*, 30 min), and the supernatant was concentrated using an Amicon-stirred cell. To reduce the salt concentration and to facilitate binding to an anion exchange column (ResQ 1mL, Amersham Biosciences), the protein solution was dialyzed against the anion exchange buffer (20 mM Tris pH 8.0, 30 mM NaCl and 10 mM DTT) prior to chromatography. The protein was eluted using a 300 mM NaCl gradient. The pure and active caspase-3 and caspase-8 were further purified by size exclusion chromatography on an analytical S200 column with buffer containing 20 mM Tris pH 8.0, 50 mM NaCl and 10mM DTT. Fractions containing pure and active caspase were pooled and concentrated by ultrafiltration (centricon, NMWL 10,000 Da) to a final concentration of 10 mg/ml and the final yield was about 5-7 mg/litre culture. Eventually, the purified caspases were subsequently inhibited with a 3-fold molar excess of the inhibitor in a buffer containing 20 mM Tris pH 8.0 and 10mM DTT.

Crystallization and Data Collection. Co-crystals of the complex between recombinant human caspase and the Michael acceptor inhibitors were grown from 2µl hanging drops formed by mixing equal volumes of protein (10 mg/ml in 20 mM Tris/HCl pH 8.0, 10 mM DTT) and reservoir solution. The reservoir solution consists of 15% (w/v) polyethylene glycol 6000, 100 mM sodium citrate, pH 5.0 in case of caspase-3 and 1.4 M sodium citrate, 100 mM HEPES/NaOH pH 8.0 in case of caspase-8. Crystals (~ 100 x 100 x 50 µm) grew within 2-3 days. For data collection, crystals were frozen in the nitrogen stream after a short soak in reservoir solution containing 20% glycerol for caspase-3. The crystals of caspase-3 complexes belong to the space group I222 and the typical unit cell dimensions were, $a = 67.2$ Å, $b = 83.3$ Å, $c = 96.0$ Å. Diffraction data were collected at the rotating anode generator (Bruker-Nonius, FR591) at 100 K. Images were integrated with MOSFLM [42] and scaled with SCALA [43] from the CCP4 suite of programs.

Diffraction data for caspase-8:inhibitor complex was collected at the Swiss Light Source synchrotron (Paul Sherrer Institute, Villigen, Switzerland). The x-ray data was collected without utilising any cryo protectant. The crystals of caspase-8 complex belongs to $P3_121$ space group and the unit cell dimensions are $a = 67.2$ Å, $b = 83.3$ Å, $c = 96.0$ Å. The data reduction were done with program XDS[44] and scaled with XSCALE[45].

Structure Solution and Refinement. The structure was solved by the difference Fourier technique. Structure refinement and automated water addition were performed using the program CNS[46] and the model building was done with program O. Iterative cycles of refinement and model building was performed. Manual adjustments were done with program O. The final crystallographic *R* and free *R* factors for caspase-3 complexes are in the range of 16-19 % and 19-22% respectively. The final model for caspase-3 complexes consisted of residues 29-174 of α subunit and 176-277 of β subunit. For the caspase-8 complex the final *R* and free *R* factors are 16.8% and 20.1%, respectively. The final model shows residues 223-371 of α subunit and 390-479 of β subunit, 326 water molecules and 1 DTT molecule.

Coordinates. The atomic coordinates for caspase inhibitor complexes have been deposited with the Protein Data Bank. The accession codes are listed under Table 4.

Acknowledgements. The work was supported by a grant from the National Institute of General Medical Sciences (GM61964). K. J. acknowledges a fellowship from the Center for the Study of Women, Science, and Technology (WST) at Georgia Tech, and J. A. acknowledges a fellowship from the Molecular Design Institute under prime contract from the Office of Naval Research. We gratefully acknowledge the Swiss Light Source, Paul Scherrer Institute, Villigen, Switzerland, for providing synchrotron beam time and T. Tomizaki, A. Wagner, and C. Schulze-Briese for their excellent support during data collection. J. Tschopp from the University of Lausanne is acknowledged for providing the caspase-3 cDNA. The financial support from the Swiss National Science Foundation and the Baugartenstiftung (Zurich, Switzerland) is gratefully acknowledged.

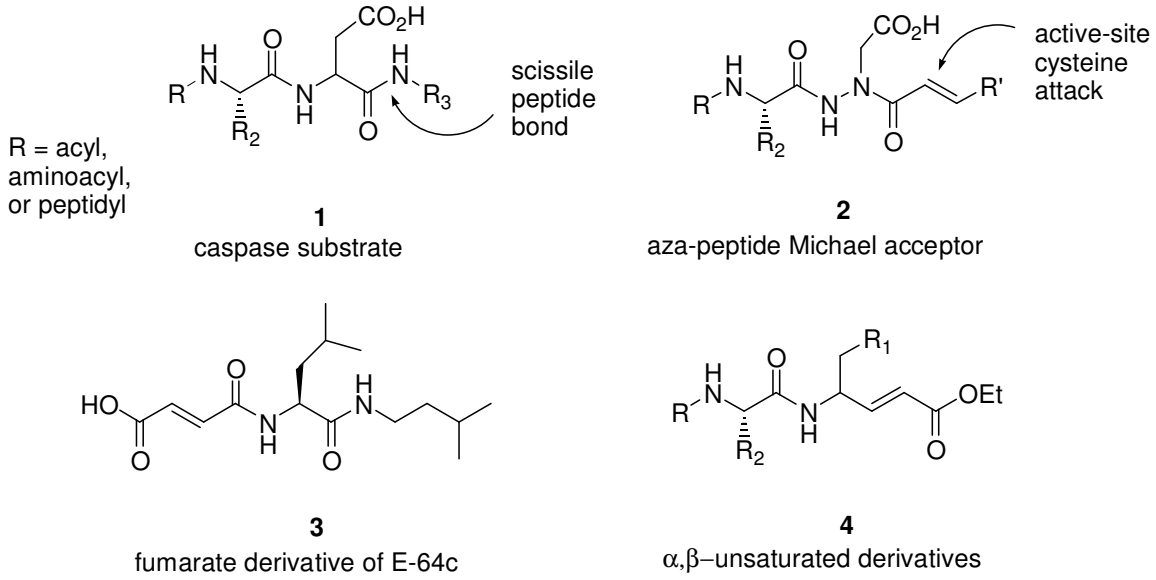

Figure 1. Aza-peptide Michael Acceptor Design

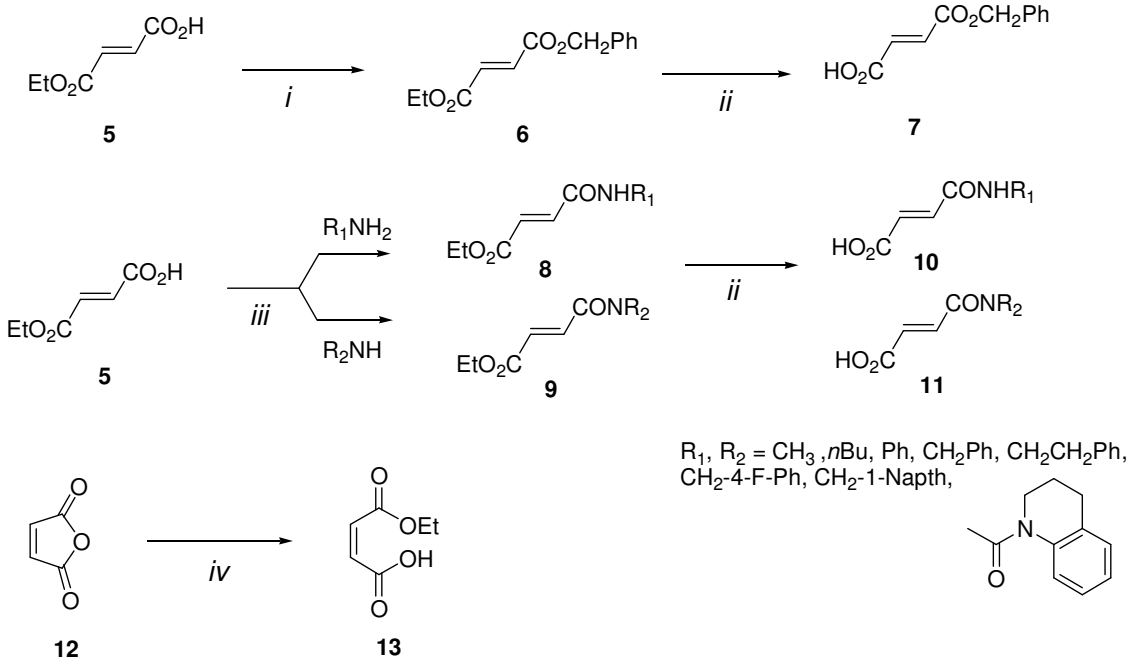

Figure 2. Synthesis of Fumarate and Maleate Derivatives. (i) NMM, EDC, BzlOH, DMF; (ii) KOH, EtOH, r.t.; (iii) NMM, iBCF, CH_2Cl_2; (iv) EtOH, r.t.

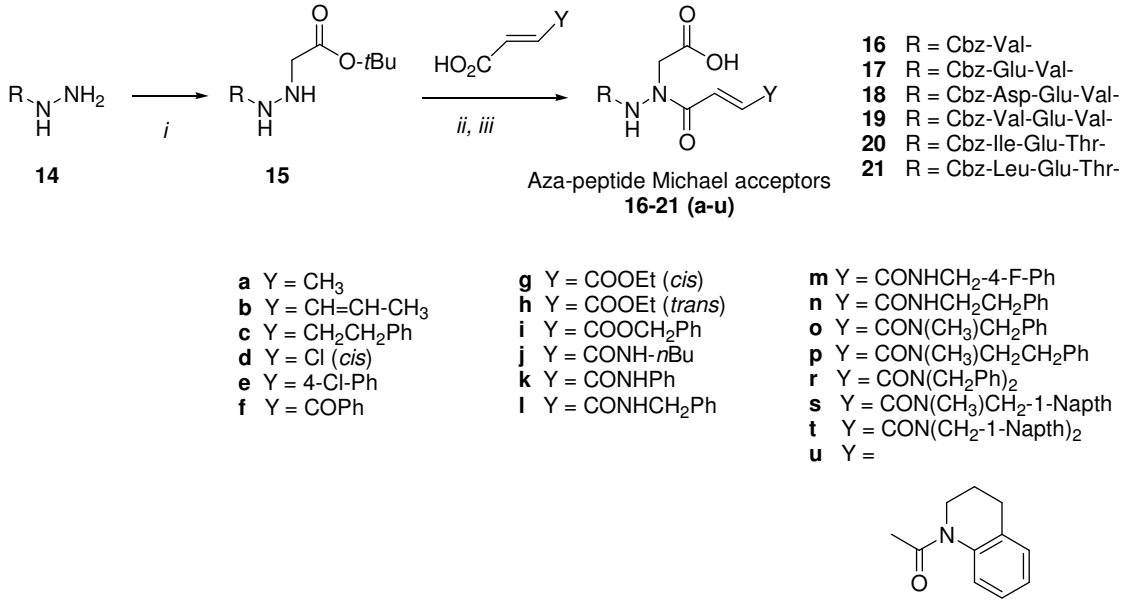

Figure 3. Synthesis of Aza-Asp Michael acceptors. Reagents are the following: (i) $BrCH_2COO$-*t*Bu, NMM, DMF; (ii) EDC, HOBt, DMF or NMM, iBCF, DMF; (iii) TFA, CH_2Cl_2

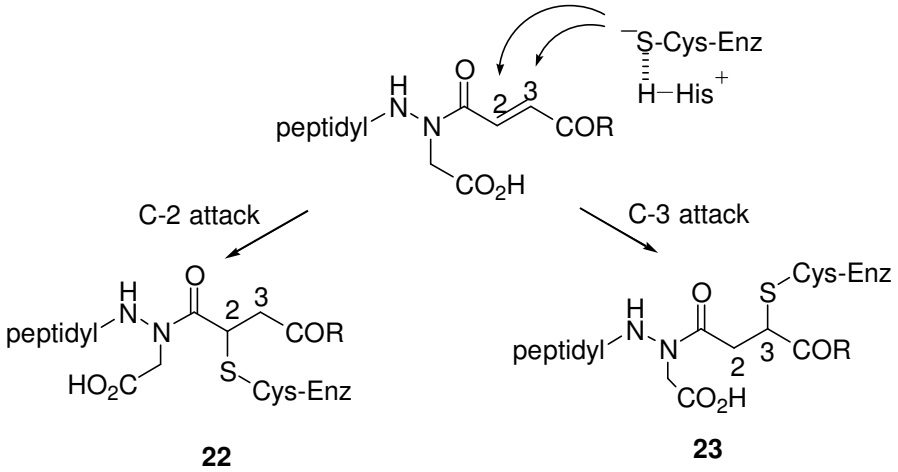

Figure 4. Proposed Mechanism of Inhibition of Caspases by Aza-Peptide Michael Acceptors

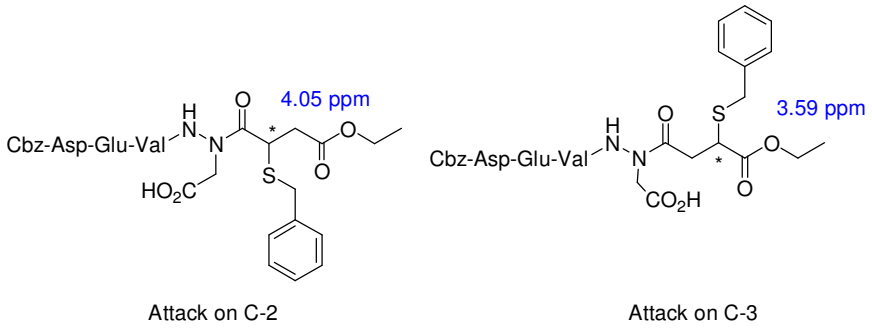

Attack on C-2 Attack on C-3

Figure 5. Chemical Shifts of the Reaction Products with Benzylmercaptan

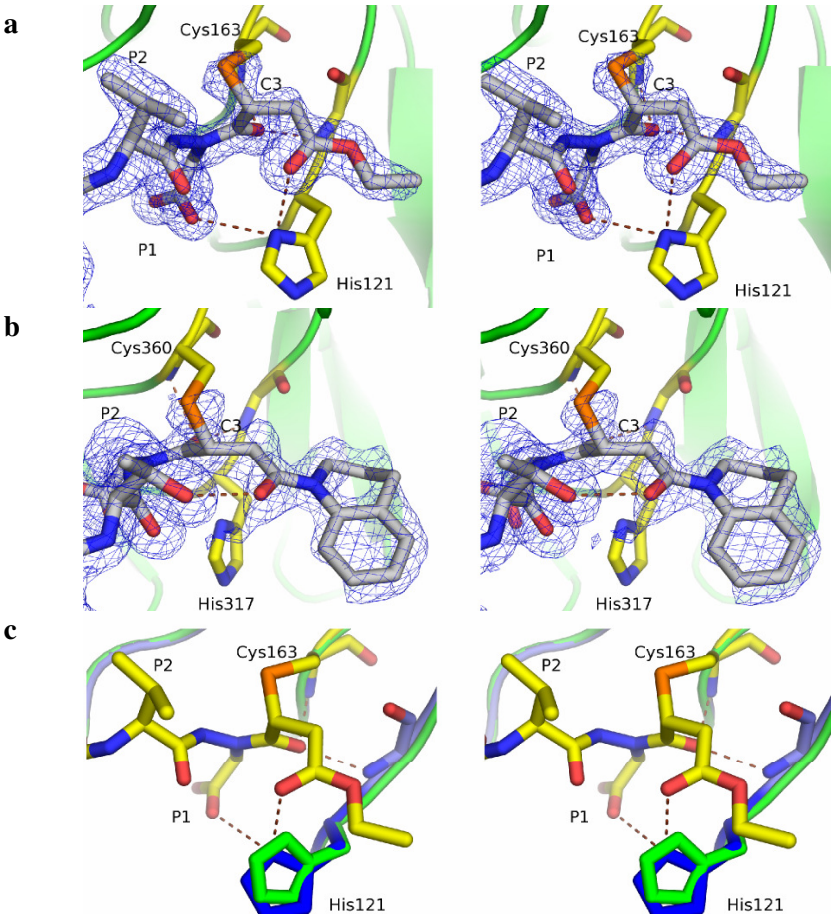

Fig 6: Stereo view of the atomic model of **(a)** Caspase-3 in complex with 18h and **(b)** Caspase-8 in complex with 21t overlaid with an electron density map contoured at 1.0 σ. Potential hyrdogen bond interactions are drawn in brown dashed lines. The residues involved in interaction with the inhibitor and catalytic dyad Cys163/His121 are highlighted.
(c) Stereo view of the active site residues of caspase-3 in complex with **18h** (blue) overlaid on top of structure of caspase-3:Ac-DEVD-CHO complex (green pdb code : 1PAU). The atoms of the inhibitor **(18h)** are highlighted in yellow. The catalytic His121 of **18h** complex is rotated approximately 20° about its Chi2 angle, which enables it to form a hydrogen bond with P1-Asp and P1` carbonyl groups.

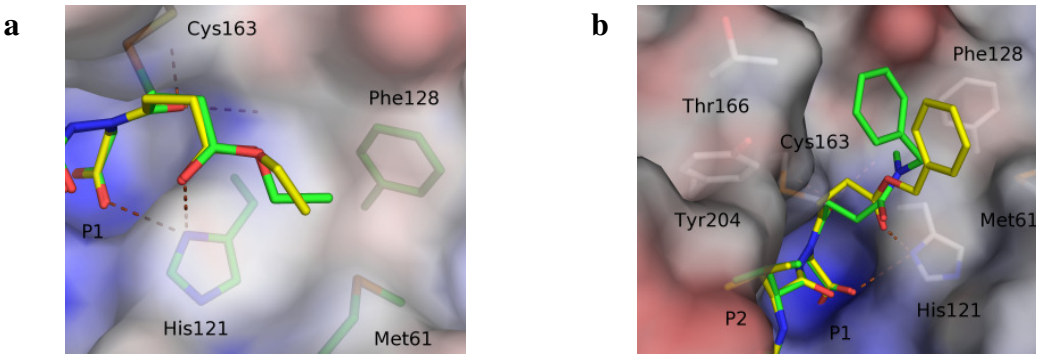

Fig. 7 Surface representation of the active site of caspase-3 with the active site and prime site residues are highlighted **(a)** Superposition of atoms of the inhibitor **18g** (cis isomer in yellow) and **18h** (trans isomer is green). **(b)** Superposition of atoms of the inhibitor **18i** (Benzyl ester derivative in yellow) and **18o** (N-methyl, benzyl amide derivative is green). The **18i** inhibitor is able to form a hydrogen bond with the catalytic His121 while **18o** is not involved in such an interaction.

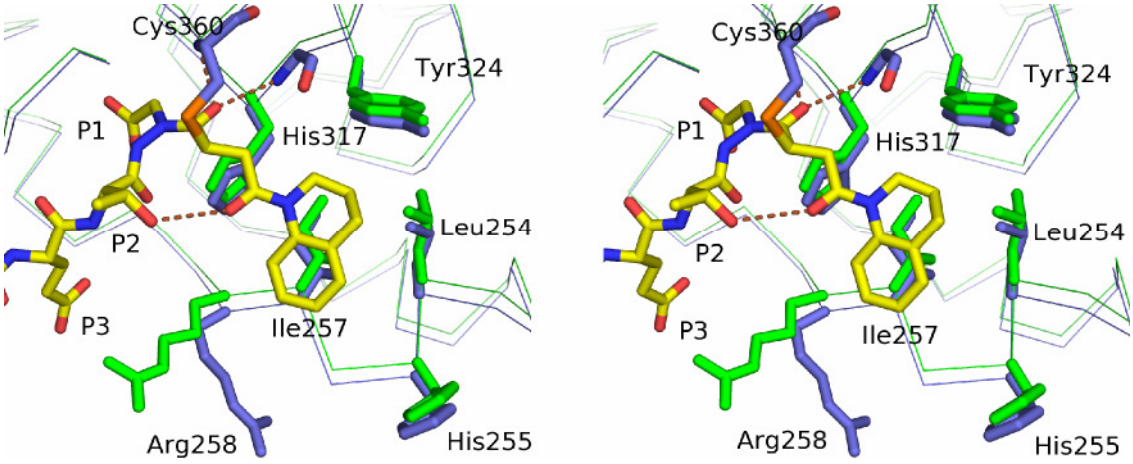

Fig. 8. Superposition of the crystal structure of caspase-8:**21t** complex (in blue) with the crystal structure of caspase-8: Ac-IETD-CHO (in green, pdb code 1QTN). Large scale movement of the 179-loop apart from the different conformation of Arg258 are depicted. The hydrogen bond between the P1` carbonyl and the side chain of P2-Thr are given in brown dashed line.

Table 1. Inhibition of Caspases by Aza-Peptide Michael Acceptors

Inhibitor	k2 a(M-1s-1)						
	Caspase-2	Caspase-3	Caspase-6	Caspase-7	Caspase-8	Caspase-9	Caspase-10
16a Cbz-Val-AAsp-CH=CH-CH3	ND	NI	NI	ND	NI	ND	ND
16b Cbz-Val-AAsp-CH=CH-CH=CH-CH3	NI	NI	NI	NI	NI	NI	NI
16c Cbz-Val-AAsp-CH=CH-CH2CH2Ph	ND	NI	NI	ND	NI	ND	ND
16d Cbz-Val-AAsp-CH=CH-Cl	NI	NI	NI	NI	NI	NI	NI
16e Cbz-Val-AAsp-CH=CH-4-Cl-Ph	NI	NI	NI	NI	NI	NI	NI
16h Cbz-Val-AAsp-CH=CH-COOEt	NI	8,000	NI	2,680 ± 60	NI	5,240 ± 380	389 ± 87
16j Cbz-Val-AAsp-CH=CH-CONH-nBu	NI	184 ± 9	NI	55 ± 5	NI	32 ± 13	NI
16l Cbz-Val-AAsp-CH=CH-CONHCH2Ph	NI	185	NI	60 ± 1	NI	20 ± 2	NI
17h Cbz-Glu-Val-AAsp-CH=CH-COOEt	90 ± 10	38,600 ± 4,200	3,540 ± 4,200	52,400 ± 10,600	244,000 ± 30,000	32,900 ± 10,250	8,940 ± 5,250
18f Cbz-Asp-Glu-Val-AAsp-CH=CH-COPh	165 ± 85	122,000	1,800 ± 13	10,800 ± 2,000	9,720 ± 500	ND	930 ± 80
18g Cbz-Asp-Glu-Val-AAsp-CH=CH-COOEt (cis)	26,200 ± 6,000	1,060,000 ± 92,500	11,000 ± 515	139,000 ± 4,500	181,000 ± 13,700	ND	13,500 ± 2,300
18h Cbz-Asp-Glu-Val-AAsp-CH=CH-COOEt (trans)	2,640 ± 10	2,130,000 ± 99,130	35,575 ± 0	239,000 ± 55,600	272,960 ± 18,370	ND	49,900 ± 7,000
18i Cbz-Asp-Glu-Val-AAsp-CH=CH-COOCH2Ph	ND	1,700,000 ± 106,000	8,470	114,000 ± 15,900	121,000 ± 13,700	ND	28,300 ± 7,700
18l Cbz-Asp-Glu-Val-AAsp-CH=CH-CONHCH2Ph	130 ± 20	1,750,000 ± 18,500	3,210 ± 105	249,000 ± 52,500	78,235 ± 8,000	2,010 ± 150	19,400 ± 400
18m Cbz-Asp-Glu-Val-AAsp-CH=CH-CONHCH2-4-F-Ph	130 ± 20	2,100,000 ± 26,400	4,400 ± 361	329,000 ± 53,300	85,100 ± 9,700	900 ± 70	37,700 ± 2,550
18n Cbz-Asp-Glu-Val-AAsp-CH=CH-CONHCH2CH2Ph	120 ± 10	1,950,000 ± 53,000	3,470 ± 52	267,000 ± 15,000	129,000 ± 27,400	655 ± 50	31,400 ± 3,600
18o Cbz-Asp-Glu-Val-AAsp-CH=CH-CON(CH3)CH2Ph	660 ± 240	2,640,000 ± 397,000	9,500 ± 210	275,000 ± 11,300	90,300 ± 18,250	820 ± 215	29,400 ± 830
18p Cbz-Asp-Glu-Val-AAsp-CH=CH-CON(CH3)CH2CH2Ph	320 ± 25	1,180,000 ± 264,000	4,000 ± 413	172,000 ± 72,000	31,900 ± 2,800	425 ± 10	9,570 ± 5,240
18r Cbz-Asp-Glu-Val-AAsp-CH=CH-CON(CH2Ph)2	110 ± 25	3,000,000 ± 80,000	5,100 ± 0	359,000 ± 8,400	8,600 ± 1,600	450 ± 30	6,300 ± 50
18t Cbz-Asp-Glu-Val-AAsp-CH=CH-CON(CH2-	410 ± 60	5,620,000 ±	29,700 ±	875,000 ±	9,460 ± 880	150 ±	32,500 ±

1-Napth)2		1,120,000	540	106,000		10	5,250
18u Cbz-Asp-Glu-Val-AAsp-CH=CH-CON-tetrahydroquinoline	390 ± 90	2,300,000 ± 26,500	5,700 ± 0	137,000 ± 25,000	118,000 ± 14,800	340 ± 120	8,330 ± 1,400
19h Cbz-Val-Glu-Val-AAsp-CH=CH-COOEt	115 ± 20	41,200 ± 8,600	83,600 ± 8,400	3,650 ± 1,330	175,800 ± 6,800	340 ± 120	6,600 ± 690
20h Cbz-Ile-Glu-Thr-AAsp-CH=CH-COOEt	300 ± 160	6,740 ± 1,650	88,700 ± 33,700	530 ± 10	56,500 ± 3,800	ND	6,900 ± 250
20i Cbz-Ile-Glu-Thr-AAsp-CH=CH-COOCH2Ph	110 ± 40	2,300 ± 77	23,350 ± 1,650	660 ± 210	148,400	ND	15,200 ± 2,500
20k Cbz-Ile-Glu-Thr-AAsp-CH=CH-CONHPh	365 ± 20	7,030 ± 720	99,200 ± 10,800	920 ± 60	245,000 ± 22,800	940 ± 275	9,210 ± 377
20l Cbz-Ile-Glu-Thr-AAsp-CH=CH-CONHCH2Ph	15 ± 3	2,250 ± 560	16,800 ± 1,030	100 ± 20	61,300 ± 2,300	440 ± 160	503 ± 209
20n Cbz-Ile-Glu-Thr-AAsp-CH=CH-CONHCH2CH2Ph	30 ± 0	4,750 ± 565	18,700 ± 1,250	440 ± 95	71,000 ± 13,700	615 ± 160	8,290 ± 1,560
20o Cbz-Ile-Glu-Thr-AAsp-CH=CH-CON(CH3)CH2Ph	95 ± 8	6,000 ± 100	45,900 ± 5,000	390 ± 90	59,700 ± 4,500	845 ± 190	8,500 ± 300
20p Cbz-Ile-Glu-Thr-AAsp-CH=CH-CON(CH3)CH2CH2Ph	38 ± 1	5,480 ± 26	ND	1,020 ± 440	60,500 ± 8,000	760 ± 335	8,770 ± 1,780
20r Cbz-Ile-Glu-Thr-AAsp-CH=CH-CON(CH2Ph)2	76 ± 1	9,570 ± 1,230	83,900 ± 29,000	1,140 ± 210	39,500 ± 0	1,930 ± 35	7,930 ± 2,510
21h Cbz-Leu-Glu-Thr-AAsp-CH=CH-COOEt	NI	5,560 ± 290	18,700 ± 1,040	NI	237,000 ± 52,700	37 ± 0	NI
21i Cbz-Leu-Glu-Thr-AAsp-CH=CH-COOCH2Ph	480 ± 170	4,600 ± 330	47,600 ± 2,500	1,570 ± 135	98,400 ± 9,130	ND	18,900 ± 1,580
21k Cbz-Leu-Glu-Thr-AAsp-CH=CH-CONHPh	290 ± 150	4,700 ± 308	11,400 ± 2,060	730 ± 200	176,000 ± 2,280	1,190 ± 230	6,050 ± 1,380
21l Cbz-Leu-Glu-Thr-AAsp-CH=CH-CONHCH2Ph	66 ± 25	1,120	1,550 ± 50	340 ± 15	70,170 ± 13,700	1,400 ± 260	14,400 ± 1,900
21m Cbz-Leu-Glu-Thr-AAsp-CH=CH-CONHCH2-4-F-Ph	70 ± 1	4,490 ± 410	3,100 ± 465	410 ± 60	171,000 ± 36,500	1,695 ± 30	9,380 ± 1,560

21n Cbz-Leu-Glu-Thr-AAsp-CH=CH-CONHCH2CH2Ph	110 ± 40	5,400 ± 51	2,150 ± 52	440 ± 60	121,000 ± 2,300	1,760 ± 190	17,900 ± 2,300
21o Cbz-Leu-Glu-Thr-AAsp-CH=CH-CON(CH3)CH2Ph	140 ± 25	6,000 ± 100	10,800 ± 410	520 ± 60	169,000	4,320 ± 930	8,430 ± 710
21p Cbz-Leu-Glu-Thr-AAsp-CH=CH-CON(CH3)CH2CH2Ph	50 ± 10	2,620 ± 26	2,550 ± 413	290 ± 170	65,300 ± 5,700	960 ± 30	6,190 ± 820
21r Cbz-Leu-Glu-Thr-AAsp-CH=CH-CON(CH2Ph)2	110 ± 10	8,630 ± 1,330	14,100 ± 1,440	760 ± 100	129,000 ± 13,700	1,105 ± 460	8,080 ± 1,660
21t Cbz-Leu-Glu-Thr-AAsp-CH=CH-CON-tetrahydroquinoline	92 ± 51	12,100 ± 720	13,000 ± 1,850	540 ± 30	216,000 ± 4,600	1,660 ± 710	9,000 ± 500
21s Cbz-Leu-Glu-Thr-AAsp-CH=CH-CON(CH3)CH2-1-Napth	290 ± 110	11,200 ± 1,130	21,700 ± 206	1,100 ± 35	179,000 ± 38,800	5,030 ± 555	13,600 ± 970

NI = no inhibition, ND = not determined, Cbz = $PhCH_2$-OCO-; [a] Assay buffer was 40 mM Pipes, 200 mM NaCl, 0.2% (w/v) CHAPS, sucrose 20% (w/v) and 10 mM DTT, at pH 7.2, with Ac-DEVD-AMC as the substrate.

Table 2. Cros Reactivity of Caspase Inhibitors with Clan CA and Other Clan CD Enzymes

					k_2 ($M^{-1}s^{-1}$)		
	Inhibitor	**Cathepsin B**	**Papain**	**Calpain**	**Legumain**	**Clostripain**	**Gingipain K**
18h	Cbz-Asp-Glu-Val-AAsp-CH=CH-COOEt	NI	NI	NI	NI	NI	NI
18i	Cbz-Asp-Glu-Val-AAsp-CH=CH-$COOCH_2Ph$	NI	ND	ND	ND	NI	NI
18l	Cbz-Asp-Glu-Val-AAsp-CH=CH-$CONHCH_2Ph$	NI	ND	ND	ND	NI	NI
21i	Cbz-Leu-Glu-Thr-AAsp-CH=CH-$COOCH_2Ph$	<10	NI	<10	NI	NI	NI

NI = No inhibition, ND = not determined.

Table 3. X-ray data collection statistics of caspase: Michael acceptor complex crystals

	Caspase-3 : Cbz-DEVaD-CH=CH - CO_2Et (*trans*) **18h**	Caspase-3 : Cbz-DEVaD-CH=CH - CO_2Et (*cis*) **18g**	Caspase-3 : Cbz-DEVaD-CH=CH - CO_2Bzl **18i**	Caspase-3 : Cbz-DEVaD-CH=CH-CON(CH_3)Bzl **18o**	Caspase-8 : Cbz-LETaD-CH=CH-CO tetrahydro-quinoline **21t**
Resolution range (Å) (last shell)	20 - 1.76 (1.86 - 1.76)	20 - 1.86 (1.96 - 1.86)	20 - 1.93 (2.03 - 1.93)	20 - 2.45 (2.58 - 2.45)	10 - 1.95 (2.05 – 1.95)
Unique reflections	25781 (3441)	22830 (2606)	19537 (2531)	10094 (1402)	21841 (1561)
Redundancy	4.3 (4.0)	5.0 (4.7)	3.3 (3.1)	5.8 (5.4)	12 (13)
R_{merge} (%)	5.4 (20.8)	7.6 (43.9)	7.8 (26.2)	7.9 (24.3)	5.2 (9.0)
Completeness (%)	95.3 (87.8)	97.8 (84.1)	94.3 (85)	99.2 (95.8)	98.5 (99.5)
Average I/σ	19.1 (6.6)	17.3 (4.5)	12.8 (4.2)	19.6 (7.0)	36.4 (24.7)

Table 4. Refinement statistics of caspase: Michael acceptor crystal structures

	Caspase-3 : Cbz-DEVaD-CH=CH - CO_2Et (*trans*) **18h**	Caspase-3 : Cbz-DEVaD-CH=CH - CO_2Et (*cis*) **18g**	Caspase-3 : Cbz-DEVaD-CH=CH - CO_2Bzl **18i**	Caspase-3 : Cbz-DEVaD-CH=CH-CON(CH_3)Bzl **18o**	Caspase-8 : Cbz-LETaD-CH=CH-CO tetrahydro-quinoline **21t**
Resolution (Å)	20 - 1.76	20 - 1.86	20 - 1.93	20 - 2.45	10 - 1.95
R_{cryst}	15.9	18.4	16.1	16.8	16.8
R_{free}	18.4	21.5	19.7	21.0	20.1
Number of atoms					
Protein	1996	1996	1996	1996	1912
Ligand	49	49	54	55	56
Water	419	303	363	303	411
Average B-factors					
Protein (Å^2)	11.94	15.47	13.4	19.73	17.3
Ligand (Å^2)	18.98	30.7	29.5	42.5	23.1
Water (Å^2)	33.61	31.8	33.3	27.0	37.0
PDB accession code	**2C1E**	**2C2K**	**2C2M**	**2C2O**	**2C2Z**

REFERENCE:

(1) Barrett, A. J.; Rawlings, N. D. Evolutionary lines of cysteine peptidases. *Biol Chem* **2001**, *382*, 727-733.

(2) Barrett, A. J.; Rawlings, N. D.; O'Brien, E. A. The MEROPS database as a protease information system. *J Struct Biol* **2001**, *134*, 95-102.

(3) Denault, J. B.; Salvesen, G. S. Caspases: keys in the ignition of cell death. *Chem Rev* **2002**, *102*, 4489-4500.

(4) Yuan, J.; Yankner, B. A. Apoptosis in the nervous system. *Nature* **2000**, *407*, 802-809.

(5) Talanian, R. V.; Brady, K. D.; Cryns, V. L. Caspases as targets for anti-inflammatory and anti-apoptotic drug discovery. *J. Med. Chem.* **2000**, *43*, 3351-3371.

(6) Los, M.; Burek, C. J.; Stroh, C.; Benedyk, K.; Hug, H.; Mackiewicz, A. Anticancer drugs of tomorrow: apoptotic pathways as targets for drug design. *Drug Discov Today* **2003**, *8*, 67-77.

(7) Salgado, J.; Garcia-Saez, A. J.; Malet, G.; Mingarro, I.; Perez-Paya, E. Peptides in apoptosis research. *J Pept Sci* **2002**, *8*, 543-560.

(8) Friedlander, R. M. Apoptosis and caspases in neurodegenerative diseases. *N Engl J Med* **2003**, *348*, 1365-1375.

(9) Powers, J. C.; Asgian, J. L.; Ekici, O. D.; James, K. E. Irreversible Inhibitors of Serine, Cysteine, and Threonine Proteases. *Chemical Reviews* **2002**, *102*, 4693-4750.

(10) Nicholson, D. W. Caspase structure, proteolytic substrates, and function during apoptotic cell death. *Cell Death Differ* **1999**, *6*, 1028-1042.

(11) Rozman-Pungercar, J.; Kopitar-Jerala, N.; Bogyo, M.; Turk, D.; Vasiljeva, O.; Stefe, I.; Vandenabeele, P.; Bromme, D.; Puizdar, V.; Fonovic, M.; Trstenjak-Prebanda, M.; Dolenc, I.; Turk, V.; Turk, B. Inhibition of papain-like cysteine proteases and legumain by caspase-specific inhibitors: when reaction mechanism is more important than specificity. *Cell Death Differ* **2003**, *10*, 881-888.

(12) Leist, M.; Jaattela, M. Triggering of apoptosis by cathepsins. *Cell Death Differ* **2001**, *8*, 324-326.

(13) Turk, B.; Stoka, V.; Rozman-Pungercar, J.; Cirman, T.; Droga-Mazovec, G.; Oreic, K.; Turk, V. Apoptotic pathways: involvement of lysosomal proteases. *Biol Chem* **2002**, *383*, 1035-1044.

(14) Barrett, A. J.; Kembhavi, A. A.; Brown, M. A.; Kirschke, H.; Knight, C. G.; Tama, M.; Hanada, K. L-*trans*-Epoxysuccinyl-leucylamido(4-guanidino)butane (E-64) and Its Analogues as Inhibitors of Cysteine Proteinases Including Cathepsin B, H, and L. *Biochem. J.* **1982**, *201*, 189-198.

(15) Hanzlik, R. P.; Thompson, S. A. Vinylogous amino acid esters: a new class of inactivators for thiol proteases. *J Med Chem* **1984**, *27*, 711-712.

(16) Thompson, S. A.; Andrews, P. R.; Hanzlik, R. P. Carboxyl-Modified Amino Acids and Peptides as Protease Inhibitors. *J. Med. Chem.* **1986**, *29*, 104-111.

(17) Lee, P. J. T. R. D. K. J. Irreversible cysteine protease inhibitors containing vinyl groups conjugated to electron withdrawing groups; Axys Pharmaceuticals, Inc. (South San Francisco, CA): US, 2001.

(18) Matthews, D. A.; Dragovich, P. S.; Webber, S. E.; Fuhrman, S. A.; Patick, A. K.; Zalman, L. S.; Hendrickson, T. F.; Love, R. A.; Prins, T. J.; Marakovits, J. T.; Zhou, R.; Tikhe, J.; Ford, C. E.; Meador, J. W.; Ferre, R. A.; Brown, E. L.; Binford, S. L.; Brothers, M. A.; DeLisle, D. M.; Worland, S. T. Structure-assisted design of mechanism-based irreversible inhibitors of human rhinovirus 3C protease with potent antiviral activity against multiple rhinovirus serotypes. *Proc Natl Acad Sci U S A* **1999**, *96*, 11000-11007.

(19) Patick, A. K.; Binford, S. L.; Brothers, M. A.; Jackson, R. L.; Ford, C. E.; Diem, M. D.; Maldonado, F.; Dragovich, P. S.; Zhou, R.; Prins, T. J.; Fuhrman, S. A.; Meador, J. W.;

Zalman, L. S.; Matthews, D. A.; Worland, S. T. In vitro antiviral activity of AG7088, a potent inhibitor of human rhinovirus 3C protease. *Antimicrob Agents Chemother* **1999**, *43*, 2444-2450.

(20) Zhang, K. E.; Hee, B.; Lee, C. A.; Liang, B.; Potts, B. C. Liquid chromatography-mass spectrometry and liquid chromatography-NMR characterization of in vitro metabolites of a potent and irreversible peptidomimetic inhibitor of rhinovirus 3C protease. *Drug Metab Dispos* **2001**, *29*, 729-734.

(21) Dragovich, P. S.; Prins, T. J.; Zhou, R.; Brown, E. L.; Maldonado, F. C.; Fuhrman, S. A.; Zalman, L. S.; Tuntland, T.; Lee, C. A.; Patick, A. K.; Matthews, D. A.; Hendrickson, T. F.; Kosa, M. B.; Liu, B.; Batugo, M. R.; Gleeson, J. P.; Sakata, S. K.; Chen, L.; Guzman, M. C.; Meador, J. W., 3rd; Ferre, R. A.; Worland, S. T. Structure-based design, synthesis, and biological evaluation of irreversible human rhinovirus 3C protease inhibitors. 6. Structure-activity studies of orally bioavailable, 2-pyridone-containing peptidomimetics. *J Med Chem* **2002**, *45*, 1607-1623.

(22) Sirois, S.; Wei, D. Q.; Du, Q.; Chou, K. C. Virtual screening for SARS-CoV protease based on KZ7088 pharmacophore points. *J Chem Inf Comput Sci* **2004**, *44*, 1111-1122.

(23) Ekici, O. D.; Gotz, M. G.; James, K. E.; Li, Z. Z.; Rukamp, B. J.; Asgian, J. L.; Caffrey, C. R.; Hansell, E.; Dvorak, J.; McKerrow, J. H.; Potempa, J.; Travis, J.; Mikolajczyk, J.; Salvesen, G. S.; Powers, J. C. Aza-peptide Michael acceptors: a new class of inhibitors specific for caspases and other clan CD cysteine proteases. *J Med Chem* **2004**, *47*, 1889-1892.

(24) Choong, I. C.; Lew, W.; Lee, D.; Pham, P.; Burdett, M. T.; Lam, J. W.; Wiesmann, C.; Luong, T. N.; Fahr, B.; DeLano, W. L.; McDowell, R. S.; Allen, D. A.; Erlanson, D. A.; Gordon, E. M.; O'Brien, T. Identification of potent and selective small-molecule inhibitors of caspase-3 through the use of extended tethering and structure-based drug design. *J Med Chem* **2002**, *45*, 5005-5022.

(25) O'Brien, T., Lee, D. Prospects for caspase inhibitors. *Mini Rev Med Chem* **2004**, *4*, 153-165.

(26) Becker, J. W.; Rotonda, J.; Soisson, S. M.; Aspiotis, R.; Bayly, C.; Francoeur, S.; Gallant, M.; Garcia-Calvo, M.; Giroux, A.; Grimm, E.; Han, Y.; McKay, D.; Nicholson, D. W.; Peterson, E.; Renaud, J.; Roy, S.; Thornberry, N.; Zamboni, R. Reducing the peptidyl features of caspase-3 inhibitors: a structural analysis. *J Med Chem* **2004**, *47*, 2466-2474.

(27) Stennicke, H. R.; Renatus, M.; Meldal, M.; Salvesen, G. S. Internally quenched fluorescent peptide substrates disclose the subsite preferences of human caspases 1, 3, 6, 7 and 8. *Biochem J* **2000**, *350 Pt 2*, 563-568.

(28) Thornberry, N. A. Caspases: key mediators of apoptosis. *Chemistry & Biology* **1998**, *5*, R97-R103.

(29) Thornberry, N. A.; Rano, T. A.; Peterson, E. P.; Rasper, D. M.; Timkey, T.; Garcia-Calvo, M.; Houtzager, V. M.; Nordstrom, P. A.; Roy, S.; Vaillancourt, J. P.; Chapman, K. T.; Nicholson, D. W. A combinatorial approach defines specificities of members of the caspase family and granzyme B. Functional relationships established for key mediators of apoptosis. *J. Biol. Chem.* **1997**, *272*, 17907-17911.

(30) Talanian, R. V.; Quinlan, C.; Trautz, S.; Hackett, M. C.; Mankovitich, J. A.; Banach, D.; Ghayur, T.; Brady, K. D.; Wong, W. W. Substrate specificities of caspase family proteases. *J. Biol. Chem.* **1997**, *272*, 9677-9682.

(31) Wei, Y.; Fox, T.; Chambers, S. P.; Sintchak, J.; Coll, J. T.; Golec, J. M.; Swenson, L.; Wilson, K. P.; Charifson, P. S. The structures of caspases-1, -3, -7 and -8 reveal the basis for substrate and inhibitor selectivity. *Chem Biol* **2000**, *7*, 423-432.

(32) Yang, W.; Guastella, J.; Huang, J. C.; Wang, Y.; Zhang, L.; Xue, D.; Tran, M.; Woodward, R.; Kasibhatla, S.; Tseng, B.; Drewe, J.; Cai, S. X. MX1013, a dipeptide

caspase inhibitor with potent in vivo antiapoptotic activity. *Br J Pharmacol* **2003***, 140*, 402-412.

(33) Freidig, A. P.; Verhaar, H. J. M.; Hermens, J. L. M. Comparing the potency of chemicals with multiple modes of action in aquatic toxicology: Acute toxicity due to narcosis versus reactive toxicity of acrylic compounds. *Environmental Science & Technology* **1999***, 33*, 3038-3043.

(34) Rotonda, J.; Nicholson, D. W.; Fazil, K. M.; Gallant, M.; Gareau, Y.; Labelle, M.; Peterson, E. P.; Rasper, D. M.; Ruel, R.; Vaillancourt, J. P.; Thornberry, N. A.; Becker, J. W. The three-dimensional structure of apopain/CPP32, a key mediator of apoptosis. *Nature Struct. Biol.* **1996***, 3*, 619-625.

(35) Watt, W.; Koeplinger, K. A.; Mildner, A. M.; Heinrikson, R. L.; Tomasselli, A. G.; Watenpaugh, K. D. The atomic-resolution structure of human caspase-8, a key activator of apoptosis. *Structure Fold Des* **1999***, 7*, 1135-1143.

(36) Mittl, P. R.; Marco, S. D.; Krebs, J. F.; Bai, X.; Karanewsky, D. S.; Priestle, J. P.; Tomaselli, K. J.; Grütter, M. G. Structure of recombinant human CPP32 in complex with the tetrapeptide Acetyl-Asp-Val-Ala-Asp fluoromethyl ketone. *J. Biol. Chem.* **1997***, 272*, 6539-3547.

(37) Blanchard, H.; Kodandapani, L.; Mittl, P. R.; Marco, S. D.; Krebs, J. F.; Wu, J. C.; Tomaselli, K. J.; Grutter, M. G. The three-dimensional structure of caspase-8: an initiator enzyme in apoptosis. *Structure Fold Des* **1999***, 7*, 1125-1133.

(38) Xu, G.; Cirilli, M.; Huang, Y.; Rich, R. L.; Myszka, D. G.; Wu, H. Covalent inhibition revealed by the crystal structure of the caspase-8/p35 complex. *Nature* **2001***, 410*, 494-497.

(39) Batchelor, M. J.; Mellor, J. M. The Use of Dichloromaleic and Bromomaleic Anhydrides in the Synthesis of Lactones by the Intramolecular Diels-Alder Reaction. *Journal of the Chemical Society-Perkin Transactions 1* **1989**, 985-995.

(40) Stennicke, H. R.; Salvesen, G. S. Caspases: preparation and characterization. *Methods* **1999***, 17*, 313-319.

(41) Tian, W.-X.; Tsou, C.-L. Determination of the rate constant of enzyme modification by measuring the substrate reaction in the presence of the modifier. *Biochemistry* **1992***, 21*, 1028-1032.

(42) Leslie, A. G. W. *MOSFLM User Guide Version 6.2.3*; Medical Research Council (MRC) Laboratory of Molecular Biology: Cambridge, U.K., 1994.

(43) - The CCP4 suite: programs for protein crystallography Collaborative Computational Project, Number 4. *Acta Crystallogr D Biol Crystallogr* **1994***, 50*, 760-763.

(44) Kabsch, W. Automatic indexing of rotation diffraction patterns. *J Appl Cryst* **1988***, 21*, 67-72.

(45) Kabsch, W. Evaluation of single-crystal X-ray diffraction data from a position-sensitive detector. *J Appl Cryst* **1988***, 21*, 916-924.

(46) Brunger, A. T.; Adams, P. D.; Clore, G. M.; DeLano, W. L.; Gros, P.; Grosse-Kunstleve, R. W.; Jiang, J. S.; Kuszewski, J.; Nilges, M.; Pannu, N. S.; Read, R. J.; Rice, L. M.; Simonson, T.; Warren, G. L. Crystallography & NMR system: A new software suite for macromolecular structure determination. *Acta Crystallogr D Biol Crystallogr* **1998***, 54 (Pt 5)*, 905-921.

(47) Blanchard, H., M. Donepudi, Tschopp, M., Kodandapani, L., Wu, J. C., Grutter, M. G. "Caspase-8 specificity probed at subsite S(4): crystal structure of the caspase-8-Z-DEVD-cho complex." *J. Mol. Biol.* **2000**, *302(1),* 9-16.

4.0 Exploring the S4 and S1 prime subsite specificities in caspase-3 with aza-peptide epoxide inhibitors

Rajkumar Ganesan, Stjepan Jelakovic, Amy J. Campbell, Zhao Zhao Li, Juliana L. Asgian, James C. Powers and Markus G. Grütter

[Biochemistry *In press***]**

Exploring the S4 and S1 prime subsite specificities in caspase-3 with aza-peptide epoxide inhibitors[†]

Rajkumar Ganesan[‡], Stjepan Jelakovic[‡], Amy, J. Campbell[§], Zhao Zhao Li[§], Juliana L. Asgian[§], James C. Powers[§] and Markus G. Grütter[‡]*

[‡]Department of Biochemistry, University of Zurich, Switzerland

[§]School of Chemistry and Biochemistry, Georgia Institute of Technology, Atlanta, Georgia 30332-0400

*Correspondence to: Markus G. Grütter, Department of Biochemistry, University of Zurich, Winterthurerstrasse 190, CH−8057, Zurich, Switzerland, Tel: +41 (44) 635 5580, Fax: +41 (44) 635 6834, Email: gruetter@bioc.unizh.ch

[†] The financial support from the Swiss National Science Foundation (6M3100A-1022181) and Baugartenstiftung (Zürich, Switzerland) and from the National Institute of General Medical Sciences (GM61964) is gratefully acknowledged.

RECEIVED DATE

Running title: Specificity of caspase−3 analyzed using aza−peptide epoxides

Keywords: Caspase, aza−peptides, epoxysuccinyl inhibitors, substrate specificity, safety catch, low−barrier hydrogen bond.

Footnotes

Abbreviation: AAsp: Aza-aspartic acid, AMC: 7−amino−4−methyl coumarin, LBHB: Low−barrier hydrogen bond, Z/Cbz: Benzyloxycarbonyl, E−64: L−trans−epoxysuccinyl−leucylamide−(4−guanidino)−butane

Coordinates

The atomic coordinates and structure factures for caspase−3 aza−peptide epoxide inhibitor complexes have been deposited with the Protein Data Bank and the accession codes are 2CDR, 2CNK, 2CNL, 2CNO and 2CNN.

ABSTRACT

Caspase−3 is a prototypic executioner caspase which plays a central role in apoptosis. Aza−peptide epoxides are a novel class of irreversible inhibitors that are highly specific for clan CD cysteine proteases. The five crystal structures of caspase−3: aza−peptide epoxide inhibitor complexes reported here reveal the structural basis for the mechanism of inhibition and the specificities at the S1' and the S4 subsites. Unlike the clan CA cysteine proteases, the catalytic histidine in caspase−3 plays a critical role during protonation and subsequent ring opening of the epoxide moiety and facilitates nucleophilic attack by the active site cysteine. The nucleophilic attack takes place on the C−3 carbon atom of the epoxide and results in an irreversible alkylation of the active site cysteine residue. A favorable network of hydrogen bonds involving the oxyanion hole, catalytic histidine and the atoms in the prime site of the inhibitor enhance the binding affinity and specificity of the aza−peptide epoxide inhibitors towards caspase−3. The studies also reveal that subtle movements of the N−terminal loop of the β−subunit occur, when the P4 Asp is replaced by a P4 Ile, whereas the N−terminal loop and the "safety catch" Asp179 are completely disordered when the P4 Asp is replaced by P4 Cbz group.

Introduction

Caspases are a family of cysteine aspartate specific proteases which have essential functions in apoptosis and cytokine activation (*1, 2*). Based on their biological functions, they are classified as initiators (caspase−8, -9 and -2) and executioners (caspase−3, -6 and -7). Caspase−3 is the most abundant caspase *in vivo* (*3-5*) and it is the best characterized family member. Apart from its established role as a prototypic executioner caspase, several non−apoptotic roles of caspase−3 are emerging (*6-8*). Currently, many industrial and academic laboratories are engaged in the design of specific inhibitors for caspase−3 to regulate its activity for therapeutic intervention of diseases like myocardial infarction, Alzheimer's, stroke, Parkinson's, sepsis and Huntington's disease (*9*). Even though the executioner caspases-3 and -7 share high sequence similarity and substrate specificity, they have distinct roles in apoptosis (*10*). Thus specific inhibitors for caspases would assist in deciphering the precise role of each caspase in the execution phase of apoptosis. Caspases demonstrate stringent specificity for an aspartic acid residue in P_1 position of a substrate. Within the caspase family the substrate selectivity is highest for the P_4 residue (*11*). Apart from P_4, the prime site could also be utilized to gain specificity among caspases. Although considerable effort has been devoted to the optimization of interactions of caspase inhibitors in the S_1−S_4 subsites (*9, 12*), only a few studies exist that analyze the interactions of substrates or inhibitors at the prime site (*13-16*).

Initial studies using fluorescent peptidyl substrates indicated a preference for small residues (Gly, Ala, Ser) at position P_1' for caspase−1, −3, −6 and −8. A few peptido−mimetic compounds that bind to the prime site were identified for caspase−3 and were characterized structurally (*13*). The halogen methyl ketones and aldehydes are the most commonly used electrophilic groups (warheads) which were coupled with the preferred tetra/penta peptide recognition sequence of caspases (*9*). Since these warheads are highly reactive and tend to inhibit other clan CA cysteine proteases (*17-20*), the search for potential warheads which are highly selective for caspases becomes increasingly important. To overcome the

problem of lack of selectivity, we have recently reported the identification and characterization of aza−peptide epoxide and Michael acceptors as a new class of irreversible caspase inhibitors that are highly specific for clan CD cysteine proteases (*21-23*). In this paper, we report the crystal structures of caspase−3 in complex with five of the aza−peptide epoxides inhibitors, containing modifications at the P_1' and P_4 positions, to understand the specificity, binding mode and the mechanism of inhibition in these regions of the active site. The modifications at the prime site were intended to gain selectivity for caspase−3, while the study with a tripeptide (−EVD−) derivative and a tetrapeptide (−IETD−) derivative, was aimed at understanding the influence of the P_4−residue interaction and ordering of the N−terminal loop of the β−subunit. The C-3 carbon atom of the epoxide moiety binds covalently to the thiol group of the active site cysteine of caspase-3. This observation is in contrast to the previous proposal where the covalent bond was reported to occur between the C-2 carbon atom of the epoxide inhibitor and thiol group of active site cysteine in caspase-1 (*23*).

Experimental procedures

Materials and methods:

Caspase purification. Human recombinant caspase−3 was produced in *Escherichia coli* as inclusion bodies, refolded and purified. Briefly, the cloned genes for the α−subunit (Met−Ser_{29}−Asp_{175}) and the β−subunit (Met−Ala−Ser_{176}−His_{277}) were inserted in the *Nco*I/*Bam*HI sites of pET11d plasmids (Novagen). For separate expression of both subunits, *Escherichia coli* BL21−CodonPlus (DE3)−RIL cells (Stratagene), containing one of the two plasmids were grown to a density of A_{600} = 0.5 at 37°C in 0.5−liter Luria−Bertani medium. Expression was induced by the addition of IPTG (1 mM), and the culture was shaken at 37°C for 4 hours post induction. Cells were harvested, washed in PBS buffer and lyzed using a French press. Owing to overexpression the protein was localized in the inclusion body portion. Refolding was achieved by rapid mixing of equimolar amounts of each subunit to a final

concentration of about 100 µg of subunit/L in the refolding buffer (100 mM HEPES, pH 7.5, 10% sucrose, 1% CHAPS, 100 mM NaCl and 10 mM DTT) and was incubated overnight at room temperature with continuous stirring. Misfolded and aggregated protein was removed by centrifugation (5,000 x *g*, 30 min), and the supernatant was concentrated using an Amicon−stirred cell. To reduce the salt concentration and to facilitate binding to an anion exchange column (Resource−Q, GE Healthcare), the protein solution was dialyzed against the anion exchange buffer (20 mM Tris pH 8.0, 30 mM NaCl and 10 mM DTT) prior to chromatography. The protein was eluted using a 300 mM NaCl gradient. The pure and active caspase−3 was further purified by size exclusion chromatography (Superdex S200, GE Healthcare) with buffer containing 20 mM Tris pH 8.0, 50 mM NaCl and 10 mM DTT. Fractions containing pure and active caspase were pooled and concentrated by ultrafiltration to a final concentration of 10 mg/mL and the final yield was about 5−7 mg/L culture. The purified caspase was subsequently inhibited with a 3−fold molar excess of the inhibitor.

Crystallization and Data Collection. Co−crystals of the complex between recombinant human caspase−3 and aza−peptide epoxide inhibitors were grown from 2−4 µL hanging drops formed by mixing equal volumes of protein (10 mg/mL in 20 mM Tris/HCl pH 8.0, 10 mM DTT) and reservoir solution. The reservoir solution consisted of 15% (w/v) polyethylene glycol 6000, 100 mM Sodium citrate, pH 5.0. Crystals (~300 x 200 x 100 µm) grew within 2−3 days. For data collection, crystals were frozen in the nitrogen stream after a short soak in reservoir solution containing 20% glycerol. The crystals belong to the space group I222 and the typical unit cell dimensions were a = 67.2 Å, b = 83.3 Å and c = 96.0 Å. Diffraction data for the inhibitors **(1)**, **(2)**, **(3)**, and **(5)** were collected using a rotating anode generator (Bruker−Nonius, FR591) at 100 K. Images were integrated with MOSFLM (*24*) and scaled with SCALA (*25*) from the CCP4 suite of programs. Diffraction data for the inhibitor **(4)** were collected at the Swiss Light Source synchrotron (Paul Scherrer Institute, Villigen, Switzerland). The data processing was done with the program XDS (*26*).

Structure Solution and Refinement. The structure was solved by the difference Fourier technique. Structure refinement and automated water addition were performed using the program CNS (*27*) and model building was done with the program O (*28*). Iterative cycles of refinement and model building were performed. To simplify the dictionary of restraints for aza−peptide epoxide inhibitors, the molecule was treated as three parts, the N−terminal blocking group (Cbz), tripeptide portion (DEV) and the P_1−AAsp along with P_1' peptidomimetic. The final crystallographic *R* and free *R* factors were in the range of 16−19% and 19−22%, respectively. The final model consisted of residues 29−174 of α−subunit and 176−277 of β−subunit in case of **(1)**, **(2)**, **(3)** and **(5)** and the residues 176−185 of the β−subunit were disordered in case **(4)**. A summary of the crystallographic data processing and refinement statistics for the caspase−3: aza−peptide epoxide inhibitor complexes are given in Table 1 and 2 respectively.

RESULTS

Inhibitor design. The inhibitor potency critically depends on the structure of the peptide moiety and the chemical reactivity of the warheads. Inhibitors like E−64 and their synthetic analogs containing an epoxysuccinyl moiety as the warhead, are specific inhibitors for clan CA cysteine proteases (*29*). Epoxysuccinyl dipeptides without an aspartic acid residue do not inhibit caspase-1 (*30*) and a variety of epoxysuccinyl peptides containing aspartate do not inhibit other caspases (J. C. Powers and Özlem Dogan Ekici, unpublished results). The reason for the inertness of E−64 derivatives against caspases might be the unparalleled selectivity for an aspartic acid residue in the S_1 subsite or the location of the warhead. The design strategy for the inhibitors presented here was to place an epoxide group at the C−terminus of a P_1 aza aspartate and also to retain an additional carbonyl group at the prime site by using the epoxysuccinyl moiety (Fig. 1).

Structure based mechanism of inhibition. Epoxides are weak electrophiles but they tend to become highly electrophilic upon protonation. Protonation is critical for the ring opening and subsequent alkylation of the active site thiol group of Cys_{163}. When the epoxides are flanked by carbonyl groups on either side, they are pre−activated and referred to as epoxysuccinyl inhibitors. This strategy has led to the identification of compounds that are potent inhibitors of caspases (*21, 23*). These inhibitors possess a dual advantage as a result of the combination of the high reactivity of the activated epoxides coupled with enhanced binding properties of regular substrate like peptides.

In general, the inactivation of cysteine proteases by epoxide inhibitors proceeds through the nucleophilic attack of the active site thiol group on either the C−2 or C−3 carbon atom of the oxirane ring. This irreversible thioalkylation could follow two different pathways (Fig. 2). In a previously study, it was proposed that the nucleophilic active site thiol group of caspase−1 reacts on the C−2 carbon atom of an aza−peptide epoxide inhibitor (*23*). In contrast, the high resolution crystal structures of caspase−3 complexes presented here clearly demonstrate that the nucleophilic attack is on the *re* face of the C−3 carbon atom, creating a covalent thioether bond (typically $C–S^{\gamma} = 1.8Å$) between the C−3−carbon and the sulfur atom of the active site cysteine (Cys_{163}) (Fig. 3a). Aza-peptides with good leaving groups will inhibit both serine and cysteine proteases with formation of stable acyl enzyme derivatives (*30, 31*). The acyl enzyme complexes formed by reaction of aza−peptides with cysteine proteases are thiocarbamates and are generally more stable when compared to the thioesters formed from normal peptide substrates. The reason is the inability of a water molecule to nucleophilically attack the thiocarbamyl group of the acyl enyzme complex (*32*). The increased stability of thiocarbamates is a consequence of the unique conformational and electronic properties of the aza-amino acid residue containing an α−nitrogen atom.

As a consequence of the nucleophilic attack by the active site thiolate following a S_N2 reaction mechanism, the stereochemistry of the enzyme inhibitor adduct undergoes an inversion in configuration.

The configuration changes from *2S,3S to 2R,3R* (Fig. 3a). The change at the C−2 carbon atom is due to the nucleophilic attack, while the change at the C−3 carbon atom is due to the alteration in the ranking order of the substituents. The high resolution and well defined electron density map allowed us to make an unambiguous interpretation of the chiralities at the C−2 and C−3 atoms. The stereochemical changes observed in our structural studies are similar to those observed in other cysteine protease:epoxysuccinyl inhibitor complexes (*29, 31, 33*).

In the case of clan CA cysteine proteases, the critical protonation event of the epoxide ring is driven by water molecules (*34*). The enzyme−inhibitor structures with compounds **(1–5)** show that the nascent hydroxyl group formed as a result of the epoxide ring opening, is oriented towards the active site His_{121} forming a hydrogen bond (hydrogen bond distance ranging from 2.7−2.9Å) (Fig. 4). This indicates strongly that in caspases (or at least caspase−3), unlike in clan CA cysteine proteases, the catalytic His_{121} plays a key role in the protonation and subsequent ring opening of the epoxide ring.

Structure and binding mode of caspase−3: aza−peptide epoxide inhibitors. We have determined five crystal structures of caspase−3: aza−peptide epoxide inhibitor complexes. The interactions of the P_1−P_4 moieties of the aza−peptide epoxide inhibitors in the substrate binding cleft of caspase−3 are similar to those observed for peptidyl aldehyde or halogen methyl ketone inhibitors (*35, 36*), thus closely mimicking substrate−like binding. The inhibitors used for the structural studies were all trans *(2S,3S)* stereoisomers. The tetrapeptide (−DEVD−) based inhibitors are: the N,N−dibenzyl amide derivative **(1)**, the N−benzyl amide derivative **(2)** and the benzyl ester derivative **(3)**. The tripeptide (−EVD−) based inhibitor is a N−phenethyl amide derivative **(4)** and compound **(5)** is a tetrapeptide (−IETD−) based inhibitor containing an alanine residue blocked by an N−benzyloxycarbonyl group at the C−terminus. The chemical structures along with the key hydrogen bond interactions in the prime site of the

caspase−3: aza−peptide epoxide inhibitor complexes are illustrated in Fig. 4a−e. A hydrogen bond between the prime site carbonyl group and a water molecule is conserved in all the complexes (Fig. 4).

The overall structure of the enzyme in the complexes analyzed here is similar to other known crystal structures of caspase−3 (*35, 36*). The α− and β−subunits fold into a central six−stranded mixed β−sheet that is flanked on both sides by 5 α−helices. This architecture, which is designated as the caspase hemoglobinase fold is conserved throughout all caspase structures. Superposition of the C^{α} atoms of different caspase−3 inhibitor complexes resulted in a root mean square deviation of 0.3Å (*35, 36*). This indicates that large scale conformational changes do not occur upon binding of the prime site substituents. However rearrangements occur in residues that directly interact with the inhibitor. The geometries of the epoxide inhibitors bound to caspase−3 were well−defined in the electron density maps, allowing an unambiguous interpretation of the atoms of the inhibitor located in the prime site (Fig. 3a).

Influence of inhibitor structure on binding and rate of inactivation. Aza−peptides are analogs of peptides in which the α−CH group is exchanged by a nitrogen atom (*37-39*). This substitution has a profound effect on the reactivity and results in the loss of the chiral centre. The presence of the free electron pair on the aza−nitrogen atom leads to an extension of the area of planarity in comparison to a normal peptide linkage (*40*). The additional limitation of free rotation seems to allow the side chains to adopt a configuration which is in−between the D− and L−configuration (*37, 38*). As a consequence, there is an increase in acidity of the NH group attached to the aza−nitrogen atom, which strengthens the P_1−amide hydrogen bond to the backbone carbonyl group of Ser_{205} (Fig 3c). The importance of the backbone intermolecular hydrogen bond interaction was studied previously (*41*). A dramatic decrease in potency was observed for caspase−1 when the P_1−amide proton was replaced by a methyl group underscoring the significance of this interaction for binding and potency. In the current structures, the

inhibitor moiety extends along the primed and non−primed subsites of the enzyme and it is stabilized by a series of hydrogen bonds and hydrophobic interactions (Fig. 4).

Interactions at the prime site of caspase−3. The structural and chemical properties of the prime site region of caspase−3 indicate a preference to bind hydrophobic moieties of an inhibitor. Inhibitors containing such prime site residues might bind with higher affinity and would offer higher selectivity for caspase−3. The prime site in caspase−3 is predominantly hydrophobic and is delineated by four loop regions: the 179−loop (between strand β1 and helix α2), the 240−loop (between strand β3 and helix α3), the C−terminal loop from the α subunit, and by a loop (between helix α3 and strand β4) from the β subunit. The interactions of the P_2 and P_3 residues of the inhibitor are similar to the ones reported in other caspase−3 structures (*35, 36*). In all crystal structures reported here, the P_1 carbonyl group which is a part of the aza−aspartic acid, is extending towards the oxyanion hole and is stabilized by hydrogen bonds to the backbone amide nitrogen's of Gly_{122} and Cys_{163} (Fig. 4). These interactions are similar to those observed in the crystal structures of caspases in complex with halo methyl ketones (*35, 42*). These interactions contribute to the stabilization of the enzyme inhibitor complex and also help to orient the inhibitor ideally for the subsequent nucleophilic attack by the active site Cys_{163} S^{γ} atom.

A unique feature of all crystal structures of caspase−3 aza−peptide epoxide complexes is the rotation of the catalytic His_{121} around χ1 and χ2 by approximately 15°. During this rotation, the hydrogen bond between the His_{121} N^{ε} atom and the backbone carbonyl of Thr_{62} (putative third residue of the catalytic triad) stays intact because the geometry of this hydrogen bond is nearly collinear with the C^{α}–C^{β} bond (Fig. 3c). The movement of His_{121} is required because otherwise a steric clash with the newly formed hydroxyl group at the C−2 carbon atom would occur. This movement results in the formation of a hydrogen bond with P_1 AAsp residue in case of the structure of caspase−3 in complex with **(5)**. The

interaction between the catalytic His_{121} and P_1 AAsp would implies that His_{121}, apart from its implications in catalysis, plays a role in substrate binding.

Inhibitor **(1)** is the most potent inhibitor used in this structural study. It possesses a bulky dibenzyl moiety which best fits the large cavity in the prime site and effectively buries altogether about 740 $Å^2$ of the enzyme accessible surface on binding. The order of reactivity correlates well with the calculated buried surface area upon the binding of the inhibitor (Table 3). While one of the phenyl rings is involved in hydrophobic interaction with Tyr_{204}, Thr_{166} and Glu_{123}, the other phenyl ring fits the hydrophobic pocket formed by Met_{61} and Phe_{128} of the prime site (Fig. 5a). The monobenzyl derivative **(3)**, unlike its dibenzyl counterpart, has a proton donating amide group and forms a hydrogen bond with the backbone carbonyl group of Gly_{122}. Despite this additional hydrogen bond, the absence of the second phenyl ring resulted in a 50% decrease in the observed k_2 value (Table 3). Moreover, the phenyl ring is not placed ideally in the hydrophobic pocket, rather it is oriented in an unfavorable position towards the carboxyl group of Glu_{123} (Fig. 5a). A superposition of the benzyl ester derivative **(2)** with **(1)** shows, that its phenyl ring occupies the same pocket as one of the phenyl rings of compound **(1)**. Compound **(2)** is as potent as compound **(1)** as it effectively buries the residues Tyr_{204}, Thr_{166} and Glu_{123} delineating this pocket (Fig. 5a). The decreased affinity for compounds **(4)** and **(5)** is predominantly due to the non−optimal residues in P_4 position. In addition, the extension of the aliphatic chain by one carbon in compound **(4)** does not seem to improve the affinity in the prime site. The terminal phenyl ring is very flexible as it is destabilized due to the presence of a charged side chain of Glu123. On the other hand, the presence of an alanine residue in the prime site in case of compound **(5)** appears to be favorable as its methyl group is stabilized by the side chain of P_2 threonine residue (Fig. 5b).

Specificity of caspase−3 in the S_4 pocket. Caspase−3 and caspase−7 are highly selective for an aspartic acid as the P_4 residue (*11*). In case of caspase−3, the affinity for an Asp in P_4 is 100−fold higher

than for a Glu/Asn at this position (*16*). The structural basis for this observation was revealed recently (*43*). The N−terminal loop consisting of residues 176−185 of the β−subunit plays a vital role in the substrate recognition, particularly at the subsites S_4 and S_5. The predominant factors contributing to binding affinity of an inhibitor are (i) a "Low−barrier hydrogen bond" (LBHB) between the P_4 Asp (in the case of **(1)**, **(2)** and **(3)**) and the "safety catch" Asp_{179}, and (ii) a cluster of hydrophobic interactions between the Val_{178}, Phe_{250}, Phe_{248} and P_5−Cbz group. In contrast to the former observation (*43*), the P_5−Cbz group is well ordered in all the crystal structures reported here (Fig. 3b). The electron density map is well defined and the B−factor values for the atoms of P_5−Cbz are comparable to the rest of the inhibitor moiety. The P_5−Cbz group is stabilized by the hydrophobic cluster formed by Val_{178}, Phe_{250}, Phe_{252} and Lys_{229}.

In order to study the influence of the P_4 residue on the ordering of the N−terminal loop and in particular the interaction which prevailed between the P_4 aspartate and the "safety catch" Asp_{179}, we have determined two crystal structures of caspase−3 with suboptimal inhibitors containing an isoleucine residue in P_4 (IETD) and a tripeptide (EVD) based inhibitor. Procaspase−3 exists as an inactive zymogen and it is activated through proteolytic cleavage by the initiator caspase−8/−9 during apoptosis to separate the α− and the β−subunits. The subunits then rearrange to produce an active caspase−3 molecule. Autocatalytic activation of procaspase−3 by an active caspase−3 is a way to amplify the apoptotic signal and the cleavage occurs at Asp_{175} located at the inter−subunit linker region. The cleavage sequence (^{172}–IETD–^{175}) matches the peptide sequence of the compound **(5),** thus the structure is a representation of the interactions of a substrate and the enzyme during the autocatalytic activation. In case of compound **(5)**, the lower value for the second order inactivation rate constant (k_2) emphasizes the importance of the P_4 Asp in comparison to the sub−optimal P_4 Ile residue (*23*). The P_4 Ile in compound **(5)** topologically occupies the same place as a P_4 Asp. It is stabilized through hydrophobic contacts to Trp_{206}, Trp_{214} and Phe_{250} (Fig. 6b). Large scale movements of the residues shaping the

substrate binding site are observed. The most dramatic change occurs with Trp_{206}, which rotates 15° around χ1 and is thus displaced by about 1.3 Å. The movement of Trp_{206} is necessary to prevent steric clashes with the P_4 Ile residue. This also influences the neighboring hydrophobic residues like Leu_{168}, Phe_{256}, Tyr_{204} and Trp_{214}, all of which adapt to the needs of accommodating the sub−optimal P_4 Ile. These structural observations are in good agreement with the initial hypothesis concerning the reorganization of tryptophan residues during caspase−3 activation. The placement of an isoleucine residue in the S_4 subsite, results in drastic decrease in the affinity, due to non−productive binding. As a consequence, the main chain atoms of the N−terminal loop of the β−subunit (residues 176−185) are displaced by about 0.5 Å in comparison to the other crystal structures in complex with compounds **(1)**, **(2)** and **(3)**. No change in the side chain conformations of residues 176−185 in the N−terminal loop is observed. In case of the tripeptidic inhibitor **(4)**, the blocking group Cbz occupies the S_4 pocket and it is stabilized by hydrophobic contacts with residues Trp_{206}, Trp_{214} and Phe_{250} (Fig 6a). An interesting feature of the structure in complex with compound **(4)** is that the N−terminal loop of the β−subunit, in particular residues 176−185, is completely disordered. No interpretable electron density for the N−terminal loop residues was observed. This is a consequence of the removal of both the anchor points which prevailed in the crystal structure complexes of compounds **(1)**, **(2)** and **(3)**.

DISCUSSION

Strategies to specifically target caspase−3 for therapeutic intervention could be fruitful in the treatment of variety of diseases. A large number of caspase:inhibitor complexes have been studied by X−ray crystallography (*12, 35, 36, 42, 44, 45*). The caspase structures increased the understanding of their important role in apoptosis and have revealed a wide variety of binding modes and geometries. Most of the inhibitors bind to the S_1−S_4 subsites of the active site, while less is known about the binding

at the S_1' subsite. In this paper, we describe the structural basis for the mechanism of inhibition and the binding mode of aza−peptide epoxides by caspase−3. Analysis of the crystal structures reveals that the nucleophilic attack takes place on the C−3 carbon of the epoxide ring, thus additional substitution might be tolerated at the C−2 carbon. The binding of the aza−peptides mimics substrate like binding in the S_1−S_4 subsites. In sharp contrast to clan CA cysteine proteases, the epoxide ring is protonated by the catalytic His_{121} in caspases. Our aza−peptide epoxide inhibitors demonstrate very high selectivity towards caspases. The prominent reasons for this is the design strategy of placing the epoxide moiety at the C−terminus of an aza aspartic acid residue resulting in the overall stabilization of the charged groups like the oxyanion hole, catalytic histidine and P_1 AAsp of the inhibitor. The other plausible reasons for selectivity might arise from the mechanistic differences between clan CA and CD cysteine proteases. The capability to recognize both D− and L−configurations of the substrates with similar reactivity is a unique feature of caspases (*46*). The P_1 aza manipulation to form aza−peptide results in the change in the configuration of the P_1 residue from L to intermediate planar D/L geometry. The difference in geometry prevents the nucleophilic attack on the warhead group by other proteases while caspases recognize compounds with this geometry as normal peptidic substrates with similar efficiency. Serine protease like granzyme B, having a preference for aspartic acid at the P_1 position, might lack the nucleophilicity required for the epoxide ring opening in a S_N2−like displacement.

Selective inhibition of a particular caspase can be achieved by exploiting the specificity at the prime site. The highly homologous executioner caspases−3 and −7 possess slightly different size and shape of the prime site. While the prime site in caspase−7 is a deep and narrow pocket, the prime site in caspase−3 is more open and broad. We wanted to capitalize on the affinity of hydrophobic residues at the prime site to design some potent and specific inhibitors. Our inhibitors show reasonable selectivity towards caspase−3 due to the presence of the prime site constituent. The structural studies with non-

ideal P_4 substituents revealed that the ordering of the N−terminal loop of the β-subunit is dictated by two key interactions: (i) the LBHB and (ii) the hydrophobic cluster discussed above. A dramatic shift occurs in the observed k2 value, if a P_4 Asp is replaced by a P_4 Ile which can be explained by the large scale movements of the residues shaping the substrate binding site. The N−terminal loop of the β-subunit is completely disordered in the crystal structure if both key interactions are missing. This leads to insufficient charge compensation and a conformational change that decreases the binding surface, implying a drop in the binding affinity. Therefore, the S_4 subsite in capsase−3 has a strong preference for an aspartic acid. In conclusion, we have highlighted the structural basis for achieving selective inhibition of caspase−3 by utilizing the variations and subtle differences, particularly in the S_4 and S_1' subsites.

ACKNOWLEDGEMENT

We gratefully acknowledge Dr. Peer R.E. Mittl for fruitful discussions. We thank the Swiss Light Source, Paul Scherrer Institute, Villigen, Switzerland, for providing synchrotron beam time and C. Schulze−Briese for his excellent support during data collection. J. Tschopp from the University of Lausanne is acknowledged for providing the caspase−3 cDNA.

REFERENCES

(1) Grütter, M. G. (2000) Caspases: key players in programmed cell death. *Curr. Opin. Struct. Biol. 10*, 649-55.

(2) Nicholson, D. W. (1999) Caspase structure, proteolytic substrates, and function during apoptotic cell death. *Cell Death Differ. 6*, 1028-42.

(3) Gervais, F. G., Xu, D., Robertson, G. S., Vaillancourt, J. P., Zhu, Y., Huang, J., LeBlanc, A., Smith, D., Rigby, M., and Shearman, M. S. (1999) Involvement of caspases in proteolytic cleavage of Alzheimer's amyloid-β precursor protein and amyloidogenic A-β peptide formation. *Cell 97*, 395.

(4) Stennicke, H. R., Deveraux, Q. L., Humke, E. W., Reed, J. C., Dixit, V. M., and Salvesen, G. S. (1999) Caspase-9 can be activated without proteolytic processing. *J. Biol. Chem. 274*, 8359-8362.

(5) Stennicke, H. R., Jurgensmeier, J. M., Shin, H., Deveraux, Q., Wolf, B. B., Yang, X., Zhou, Q., Ellerby, H. M., Ellerby, L. M., Bredesen, D., Green, D. R., Reed, J. C., Froelich, C. J., and Salvesen, G. S. (1998) Pro-caspase-3 is a major physiologic target of caspase-8. *J. Biol. Chem. 273*, 27084-27090.

(6) Gulyaeva, N. V. (2003) Non-apoptotic functions of caspase-3 in nervous tissue. *Biochemistry (Mosc.) 68*, 1171-80.

(7) Gulyaeva, N. V., Kudryashov, I. E., and Kudryashova, I. V. (2003) Caspase activity is essential for long-term potentiation. *J. Neurosci. Res. 73*, 853-64.

(8) Schwerk, C., and Schulze-Osthoff, K. (2003) Non-apoptotic functions of caspases in cellular proliferation and differentiation. *Biochem. Pharmacol. 66*, 1453-8.

(9) O'Brien, T. (2004) Prospects for caspase inhibitors. *Mini Rev. Med. Chem. 4*, 153-65.

(10) Slee, E. A., Adrain, C., and Martin, J. S. (2001) Executioner caspase-3, -6, and -7 perform distinct, non-redundant roles during the demolition phase of apoptosis. *J. Biol. Chem. 276*, 7320-7326.

(11) Thornberry, N. A., Rano, T. A., Peterson, E. P., Rasper, D. M., Timkey, T., Garcia-Calvo, M., Houtzager, V. M., Nordstrom, P. A., Roy, S., Vaillancourt, J. P., Chapman, K. T., and Nicholson, D. W. (1997) A combinatorial approach defines specificities of members of the caspase family and granzyme B. Functional relationships established for key mediators of apoptosis. *J. Biol. Chem. 272*, 17907-11.

(12) Fuentes-Prior, P., and Salvesen, G. S. (2004) The protein structures that shape caspase activity, specificity, activation and inhibition. *Biochem. J. 384*, 201-32.

(13) Becker, J. W. (2004) Reducing the peptidyl features of caspase-3 inhibitors:a structural analysis. *J. Med. Chem. 47*, 2466-74.

(14) Goode, D. R., Sharma, A. K., and Hergenrother, P. J. (2005) Using peptidic inhibitors to systematically probe the S1' site of caspase-3 and caspase-7. *Org. Lett. 7*, 3529-3532.

(15) Petrassi, H. M., Williams, J. A., Li, J., Tumanut, C., Ek, J., Nakai, T., Masick, B., Backes, B. J., and Harris, J. L. (2005) A strategy to profile prime and non-prime proteolytic substrate specificity. *Bioorg. Med. Chem. Lett. 15*, 3162.

(16) Stennicke, H. R., Renatus, M., Meldal, M., and Salvesen, G. S. (2000) Internally quenched fluorescent peptide substrates disclose the subsite preferences of human caspases 1, 3, 6, 7 and 8. *Biochem. J. 350 Pt 2*, 563-8.

(17) Gray, J., Haran, M. M., Schneider, K., Vesce, S., Ray, A. M., Owen, D., White, I. R., Cutler, P., and Davis, J. B. (2001) Evidence that inhibition of cathepsin-B contributes to the neuroprotective properties of caspase inhibitor Tyr-Val-Ala-Asp-chloromethyl ketone. *J. Biol. Chem. 276*, 32750-5.

(18) Rozman-Pungercar, J., Kopitar-Jerala, N., Bogyo, M., Turk, D., Vasiljeva, O., Stefe, I., Vandenabeele, P., Bromme, D., Puizdar, V., Fonovic, M., Trstenjak-Prebanda, M., Dolenc, I., Turk, V., and Turk, B. (2003) Inhibition of papain-like cysteine proteases and legumain by caspase-specific inhibitors: when reaction mechanism is more important than specificity. *Cell Death Differ. 10*, 881-8.

(19) Schotte, P., Declercq, W., Van Huffel, S., Vandenabeele, P., and Beyaert, R. (1999) Non-specific effects of methyl ketone peptide inhibitors of caspases. *FEBS Lett. 442*, 117.

(20) Schotte, P., Van Criekinge, W., Van de Craen, M., Van Loo, G., Desmedt, M., Grooten, J., Cornelissen, M., De Ridder, L., Vandekerckhove, J., and Fiers, W. (1998) Cathepsin B-mediated activation of the proinflammatory caspase-11. *Biochem. Biophys. Res. Commun. 251*, 379.

(21) Asgian, J. L., James, K. E., Li, Z. Z., Carter, W., Barrett, A. J., Mikolajczyk, J., Salvesen, G. S., and Powers, J. C. (2002) Aza-peptide epoxides: a new class of inhibitors selective for clan CD cysteine proteases. *J. Med. Chem. 45*, 4958-60.

(22) Ekici, O. D., Gotz, M. G., James, K. E., Li, Z. Z., Rukamp, B. J., Asgian, J. L., Caffrey, C. R., Hansell, E., Dvorak, J., McKerrow, J. H., Potempa, J., Travis, J., Mikolajczyk, J., Salvesen, G. S., and Powers, J. C. (2004) Aza-peptide Michael acceptors: a new class of inhibitors specific for caspases and other clan CD cysteine proteases. *J. Med. Chem. 47*, 1889-92.

(23) James, K. E., Asgian, J. L., Li, Z. Z., Ekici, O. D., Rubin, J. R., Mikolajczyk, J., Salvesen, G. S., and Powers, J. C. (2004) Design, synthesis, and evaluation of aza-peptide epoxides as selective and potent inhibitors of caspases-1, -3, -6, and -8. *J. Med. Chem. 47*, 1553-74.

(24) Evans, P. R. (1992) Data reduction. *Proceedings of the CCP4 study weekend on data collection and processing*.

(25) Leslie, A. G. W. (1992) Scala. *Joint CCP4/ESF-EACMB Newsletter on Protein Crystallography 26*.

(26) Kabsch, W. (1988) Automatic indexing of rotation diffraction patterns. *J. Appl. Cryst. 21*, 67-72.

(27) Brunger, A. T., Adams, P. D., Clore, G. M., DeLano, W. L., Gros, P., Grosse-Kunstleve, R. W., Jiang, J. S., Kuszewski, J., Nilges, M., Pannu, N. S., Read, R. J., Rice, L. M., Simonson, T., and Warren, G. L. (1998) Crystallography & NMR system: A new software suite for macromolecular structure determination. *Acta Crystallogr. D Biol. Crystallogr. 54 (Pt 5)*, 905-21.

(28) Jones, T. A., Zou, J. Y., Cowan, S. W., and Kjeldgaard. (1991) Improved methods for building protein models in electron density maps and the location of errors in these models. *Acta Crystallogr. A 47 (Pt 2)*, 110-9.

(29) Powers, J. C., Asgian, J. L., Ekici, O. D., and James, K. E. (2002) Irreversible inhibitors of serine, cysteine, and threonine proteases. *Chem. Rev. 102*, 4639-4750.

(30) Bajusz, S., Fauszt, I., Nemeth, K., Barabas, E., Juhasz, A., Patthy, M., and Bauer, P. I. (1999) Peptidyl beta-homo-aspartals (3-amino-4-carboxybutyraldehydes): new specific inhibitors of caspases. *Biopolymers 51*, 109-18.

(31) Schirmeister, T., and Klockow, A. (2003) Cysteine protease inhibitors containing small rings. *Mini Rev. Med. Chem. 3*, 589.

(32) Gupton, B. F., Carroll, D. L., Tuhy, P. M., Kam, C. M., and Powers, J. C. (1984) Reaction of azapeptides with chymotrypsin-like enzymes. New inhibitors and active site titrants for chymotrypsin A alpha, subtilisin BPN', subtilisin Carlsberg, and human leukocyte cathepsin G. *J. Biol. Chem. 259*, 4279-4287.

(33) Otto, H. H., and Schirmeister, T. (1997) Cysteine proteases and their inhibitors. *Chem. Rev. 97*, 133-172.

(34) Varughese, K. I., Ahmed, F. R., Carey, P. R., Hasnain, S., Huber, C. P., and Storer, A. C. (1989) Crystal structure of a papain-E-64 complex. *Biochemistry 28*, 1330-2.

(35) Mittl, P. R., Di Marco, S., Krebs, J. F., Bai, X., Karanewsky, D. S., Priestle, J. P., Tomaselli, K. J., and Grütter, M. G. (1997) Structure of recombinant human CPP32 in complex with the tetrapeptide acetyl-Asp-Val-Ala-Asp fluoromethyl ketone. *J. Biol. Chem. 272*, 6539-47.

(36) Rotonda, J., Nicholson, D. W., Fazil, K. M., Gallant, M., Gareau, Y., Labelle, M., Peterson, E. P., Rasper, D. M., Ruel, R., Vaillancourt, J. P., Thornberry, N. A., and Becker, J. W. (1996) The three-dimensional structure of apopain/CPP32, a key mediator of apoptosis. *Nat. Struct. Biol. 3*, 619-25.

(37) Anamarija Zega, U. U. (2002) Azapeptides. *Acta Chim. Slov. 49*, 649-662.

(38) Gante, J. (1989) Azapeptides. *Synthesis*, 405-413.

(39) Thormann, M., and Hofmann, H. J. (1999) Conformational properties of azapeptides. *J. Mol. Struct. (Theochem.) 469*, 63-76.

(40) Hartmut Niedrich, and Christa Oehme. (1972) Hydrazinverbindungen als heterobestandteile in peptiden. XV. Synthese von eledoisin-octapeptiden mit den carbazylresten azaglycin und α-azaasparagin statt glycin und asparagin. *Journal für Praktische Chemie 314*, 759-768.

(41) Mullican, M. D., Lauffer, D. J., Gillespie, R. J., Matharu, S. S., Kay, D., Porritt, G. M., Evans, P. L., Golec, J. M. C., and Murcko, M. A. (1994) The synthesis and evaluation of peptidyl aspartyl aldehydes as inhibitors of ICE. *Bioorg. Med. Chem. Lett. 4*, 2359.

(42) Blanchard, H., Kodandapani, L., Mittl, P. R., Marco, S. D., Krebs, J. F., Wu, J. C., Tomaselli, K. J., and Grütter, M. G. (1999) The three-dimensional structure of caspase-8: an initiator enzyme in apoptosis. *Structure 7*, 1125-33.

(43) Ganesan, R., Mittl, P. R. E., Jelakovic, S., and Grütter, M. G. (2006) Extended substrate recognition in caspase-3 revealed by high resolution X-ray structure analysis. *(J. Mol. Biol. In press)*.

(44) Watt, W., Koeplinger, K. A., Mildner, A. M., Heinrikson, R. L., Tomasselli, A. G., and Watenpaugh, K. D. (1999) The atomic-resolution structure of human caspase-8, a key activator of apoptosis. *Structure 7*, 1135-43.

(45) Wilson, K. P., Black, J. A., Thomson, J. A., Kim, E. E., Griffith, J. P., Navia, M. A., Murcko, M. A., Chambers, S. P., Aldape, R. A., Raybuck, S. A., and et al. (1994) Structure and mechanism of interleukin-1 beta converting enzyme. *Nature 370*, 270-5.

(46) Prasad, C. V. C., Prouty, C. P., Hoyer, D., Ross, T. M., Salvino, J. M., Awad, M., Graybill, T. L., Schmidt, S. J., Kelly Osifo, I., and Dolle, R. E. (1995) Structural and stereochemical requirements of time-dependent inactivators of the interleukin-1[beta] converting enzyme. *Bioorg. Med. Chem. Lett. 5*, 315.

Table 1. X−ray data collection statistics of caspase−3: aza−peptide epoxide complex crystals[a]

	(1)	**(2)**	**(3)**	**(4)**	**(5)**
	Caspase−3: Cbz−**DEVaD**−(S,S) EP−CO−N($CH_2Ph)_2$	Caspase−3 : Cbz−**DEVaD**−(S,S) EP−$COO−CH_2Ph$	Caspase−3 : Cbz−**DEVaD**−(S,S) EP−CO−NH−CH_2Ph	Caspase−3 : Cbz−**EVaD**−(S,S) EP−CO−NH−CH_2CH_2Ph	Caspase−3: Cbz−**LETaD**−(S,S) EP−CO−Ala−$NHCH_2$ Ph
Space group	I222				
Unit cell dimensions (Å)	a = 65.9 b = 83.4 c = 96.4	a = 66.8 b = 83.8 c = 96.5	a = 67.7 b = 84.0 c = 96.2	a = 69.1 b = 83.5 c = 95.8	a = 67.9 b = 83.7 c = 96.2
Resolution range (Å)	20.0−1.70 (1.79−1.70)	20.0−1.75 (1.84−1.75)	20.0−1.67 (1.76−1.67)	20.0−2.05 (2.15−2.05)	20.0−1.69 (1.78−1.69)
Unique reflections	28860 (3974)	27485 (3983)	31449 (4313)	16966 (2257)	30129 (3591)
Redundancy	4.1 (3.8)	3.8 (3.6)	4.4 (4.3)	4.5 (5.9)	4.6 (4.3)
R_{merge} (%)	4.8 (29.9)	5.6 (24.6)	6.4 (32.6)	2.5 (3.6)	6.6 (28.1)
Completeness (%)	97.7 (93.0)	99.7 (100)	98.1(93.4)	95.4 (97.7)	97.8 (85.5)
Average I/σ	18.8 (3.9)	17.0 (5.5)	17.3(3.8)	31.9 (25.3)	19.3 (4.3)

[a]The values in the parentheses refer to that of the highest resolution shell

Table 2. Refinement statistics of caspase−3: aza−peptide epoxide crystal structures

	(1)	**(2)**	**(3)**	**(4)**	**(5)**
	Caspase−3 : Cbz−**DEVaD**−(S,S) EP−CO−N(CH_2Ph)$_2$	Caspase−3 : Cbz−**DEVaD**−(S,S) EP−COO−CH_2Ph	Caspase−3 : Cbz−**DEVaD**−(S,S) EP−CO−NH−CH_2Ph	Caspase−3 : Cbz−**EVaD**−(S,S) EP−CO−NH−CH_2CH_2Ph	Caspase−3: Cbz−**IETaD**−(S,S) EP−CO−Ala−NH−CH_2Ph
Resolution (Å)	20.0 – 1.70	20.0 – 1.75	20.0 – 1.67	20.0 – 2.05	20.0 – 1.69
R	17.4	16.2	18.5	16.4	18.0
R_{free}	20.1	18.9	21.4	19.4	20.4
Number of atoms					
Protein	2004	1996	2004	1931	1996
Ligand	62	55	55	48	60
Water	363	403	361	299	348
Average B−factors					
Protein (Å^2)	18.2	13.1	18.8	14.2	16.9
Ligand (Å^2)	31.6	22.5	30	41.0	35.6
Water (Å^2)	38	34.3	37.7	31.1	36.0

Table 3. The second order inactivation rate constants (k_2) and buried surface area for aza–peptide epoxide inhibitors against caspase–3.

	Aza–peptide epoxide inhibitors[a]	**k_2 ($M^{-1}s^{-1}$)**[b]	**Buried accessible surface area (Å^2)**
(1)	Cbz–**DEVaD**–(S,S) EP–CO–N(CH_2Ph)2	2,170,000	742
(2)	Cbz–**DEVaD**–(S,S) EP–COO–CH_2Ph	1,910,000	682
(3)	Cbz–**DEVaD**–(S,S) EP–CO–NHCH_2Ph	1,090,000	619
(4)	Cbz–**EVaD**–(S,S) EP–CO–NH–CH_2CH_2Ph	27,300	614
(5)	Cbz–**LETaD**–(S,S) EP–CO–Ala–NH–CH_2Ph	1,280	618

[a]aza-aspartic acid residue is represented by aD

[b]k_2 values were compiled from (*23*).

FIGURE LEGENDS

Figure 1: The design of aza−peptide epoxide inhibitors was based on the structure of caspase substrates. Selectivity was achieved by the introduction of an epoxide moiety at the C−terminus of the P_1−aza aspartic acid residue.

Figure 2: Two possible pathways for the mechanism of inhibition caspase by aza−peptide epoxides involving either a C−2 attack or a C−3 attack resulting in the epoxide ring opening and formation of a thio−ether adduct.

Figure 3: Close-up view of the active site of caspase−3. **(a)** The nucleophilic attack resulted in the formation of a covalent bond between S^{γ} and C−3 carbon and the stereochemistry of the enzyme inhibitor **(2)** adduct underwent an inversion in configuration from *2S*,*3S* to *2R*,*3R*. The prominent hydrogen bond interactions include the P_1 carbonyl with the oxyanion hole, and the catalytic His_{121} with the prime site hydroxyl group (C−2 carbon). (see Fig.4a-e) **(b)** A low barrier hydrogen bond (bond length 2.4 Å) is observed between the P_4−Asp of the inhibitor **(2)** and the "safety catch" Asp_{179} from the N−terminal loop of the β−subunit. **(c)** The superposition of the active site residues of caspase−3 in complex with compound **(5)** and Ac−DEVD−CHO complex (green, pdb code: 1PAU). The catalytic His_{121} of compound **(5)** complex is rotated approximately 15° about its χ1 and χ2 angles, resulting in a hydrogen bond formation with P_1-AAsp while retaining its interaction with Thr_{62}. The electron density map was contoured at 1.0 σ and the hydrogen bond interactions are drawn as red dashed lines. The residues belonging to the other monomer are indicated by an asterisk.

Figure 4: Chemical structures and hydrogen bond networks at the prime site for caspase−3 in complex with aza−peptide inhibitors **(1)**−**(5)**. The nascent hydroxyl group at the C2−carbon atom formed as a result of nucleophilic attack is involved in a hydrogen bond formation with the catalytic His_{121}. The P_1−carbonyl group is stabilized with hydrogen bond interaction of the "oxyanion hole" while the P_1 prime carbonyl group is stabilized

with a conserved water molecule. The interaction between the P_1−Asp and His_{121} in case of the structure of caspase−3 in complex with compound **(5)** implies apart, from its implications in catalysis, that His_{121} plays a role in substrate binding.

Figure 5: Surface representation of the active site of caspase−3. The active site and prime site residues are shown in stick representation. **(a)** Superposition of compounds (**1**) (blue), **(2)** (green), and compound **(3)** (yellow). The biphenyl derivative effectively buries the residues Tyr_{204}, Thr_{166}, Glu_{123}, Phe_{128} and Met_{61} in the prime site. **(b)** Superposition of the compound **(4)** (green) and compound **(5)** (yellow). The methyl group of the alanine residue of compound **(5)** in the prime site is stabilized through hydrophobic contacts with the P_2 Thr residue.

Figure 6: **(a)** Superposition of compound **(4)** and compound **(2)**. The Cbz group of compound **(4)** occupies the S_4 binding pocket resulting in the disordering of the N−terminal loop (residues 176-185) of the β−subunit. **(b)** Superposition of compound **(5)** and compound **(2)**. The isoleucine residue in compound **(5)** occupies the S_4 binding pocket resulting in the displacement of the N−terminal loop of the β−subunit by about 0.5 Å. Large scale deviations of main chain atoms as well as side chain conformations of the residues, Trp_{206}, Phe_{256}, Leu_{168}, and Trp_{214} in the selectivity loop are observed in both the crystal structures.

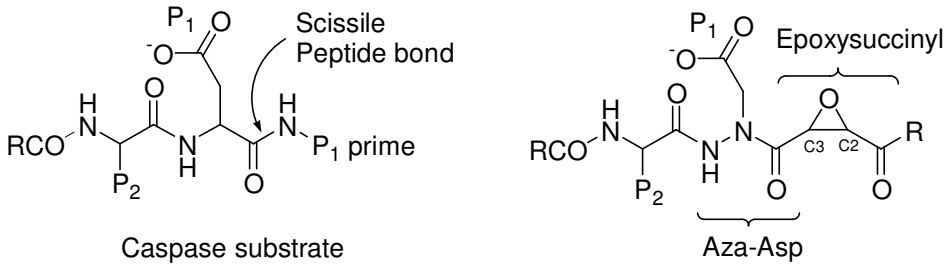

Figure-1

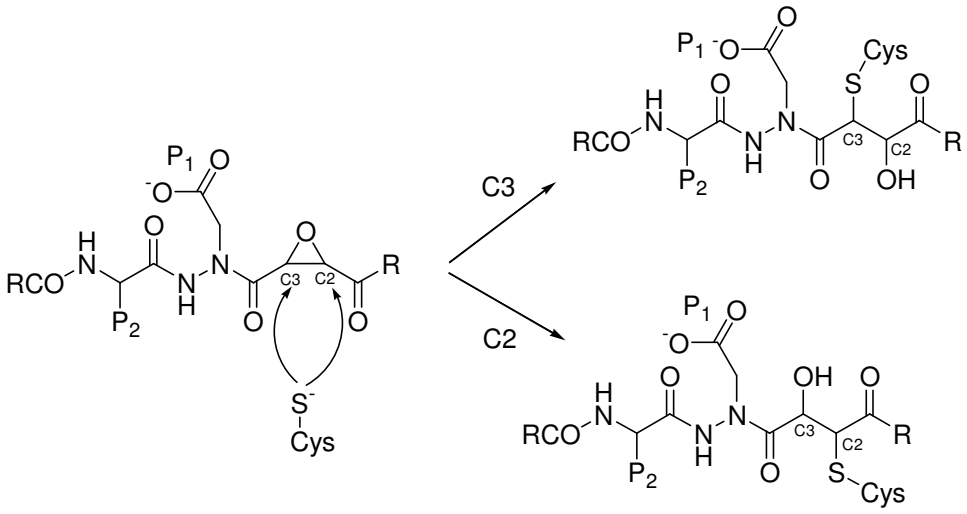

Figure-2

a

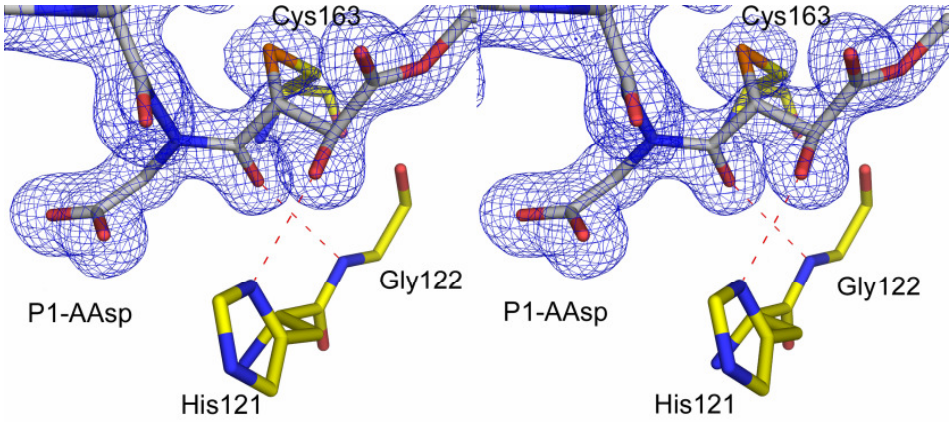

b

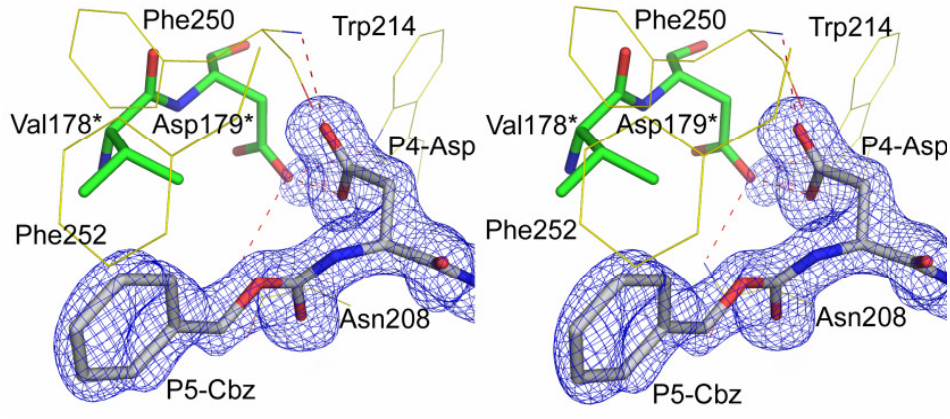
Phe250
Trp214
Val178*
Asp179*
P4-Asp
Phe252
Asn208
P5-Cbz
Phe250
Trp214
Val178*
Asp179*
P4-Asp
Phe252
Asn208
P5-Cbz

c

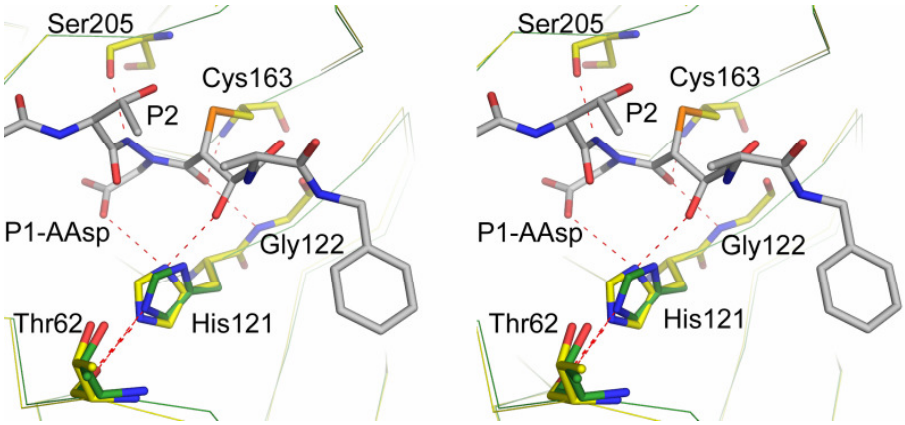
Ser205
Cys163
P2
P1-AAsp
Gly122
Thr62
His121
Ser205
Cys163
P2
P1-AAsp
Gly122
Thr62
His121

Figure-3

a

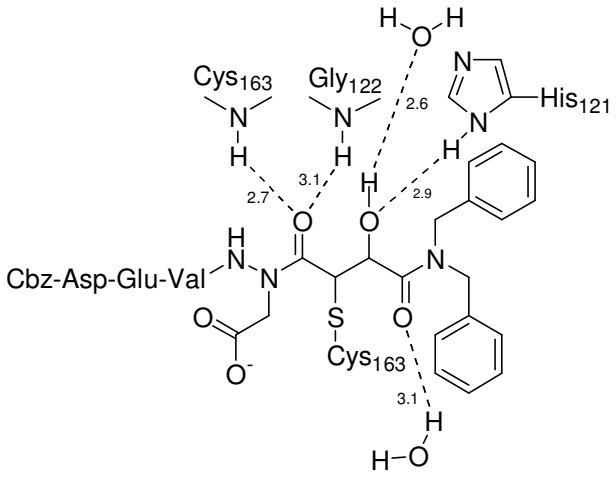
Cys163
Gly122
His121
Cbz-Asp-Glu-Val
Cys163
2.6
3.1
2.7
2.9
3.1

b

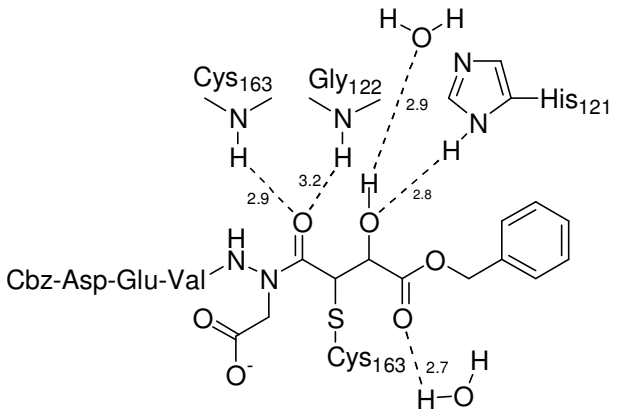
Cys163
Gly122
His121
Cbz-Asp-Glu-Val
Cys163

c

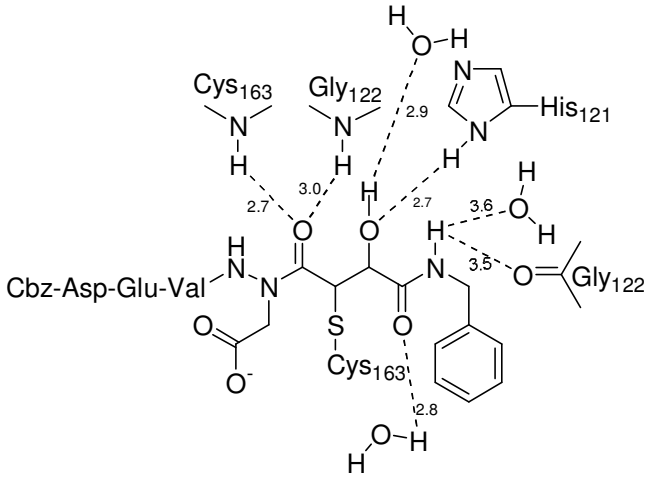
Cys163
Gly122
His121
Cbz-Asp-Glu-Val
Gly122
Cys163

d

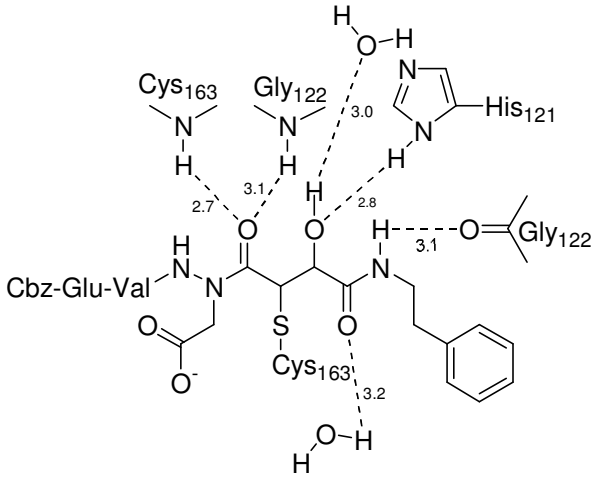
Cys163
Gly122
His121
Cbz-Glu-Val
Gly122
Cys163

e

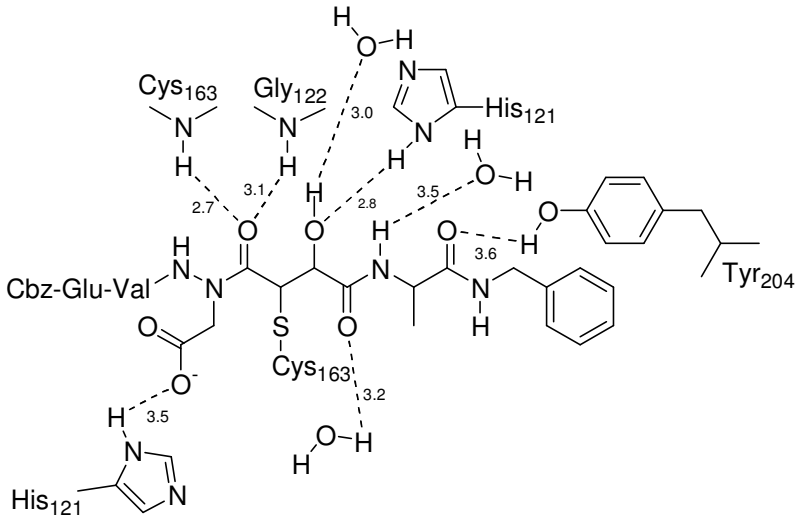

Figure-4

a

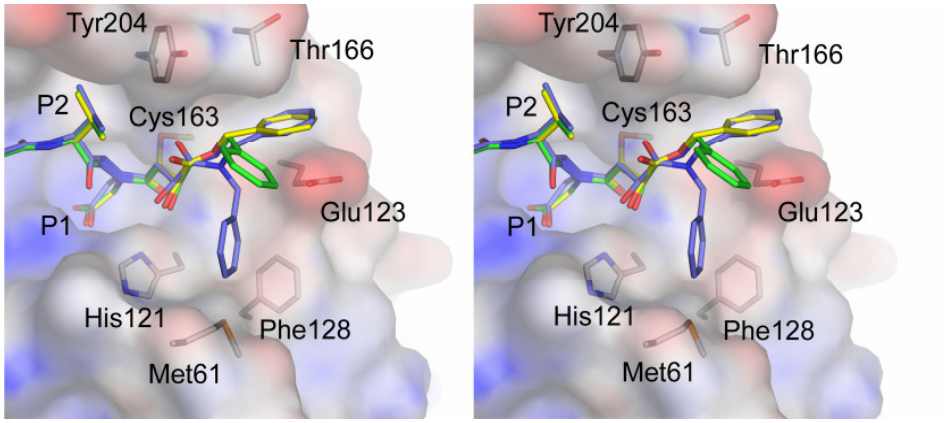

b

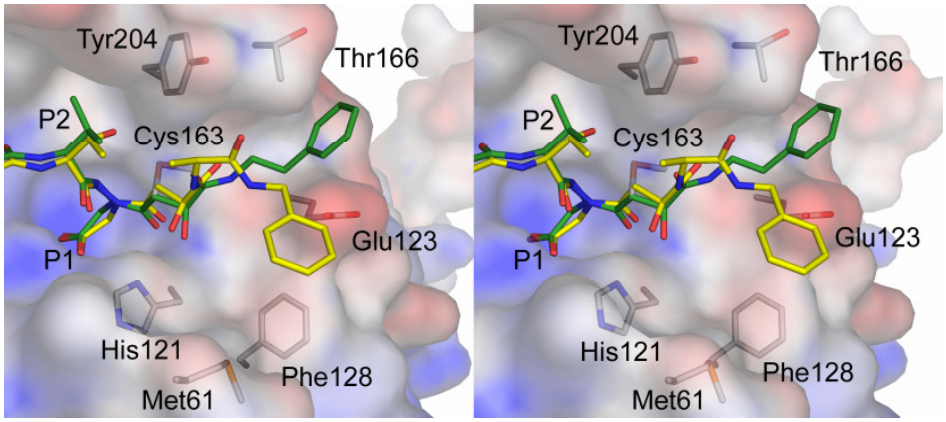

a **Figure-5**

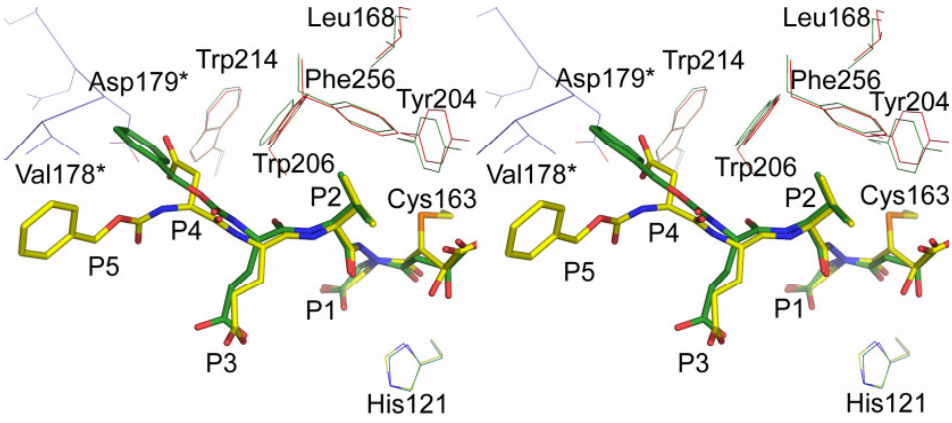
Leu168
Trp214
Asp179*
Phe256
Tyr204
Val178*
Trp206
P2
Cys163
P4
P5
P1
P3
His121
Leu168
Trp214
Asp179*
Phe256
Tyr204
Val178*
Trp206
P2
Cys163
P4
P5
P1
P3
His121

b

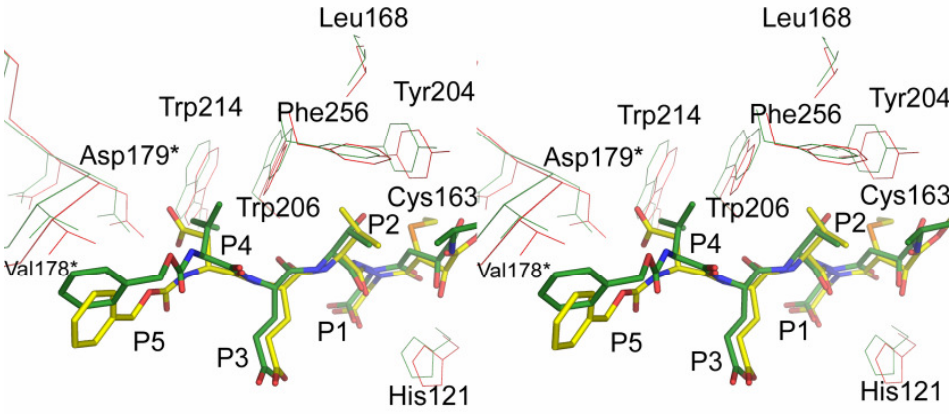
Leu168
Trp214
Phe256
Tyr204
Asp179*
Cys163
Trp206
P2
P4
Val178*
P5
P3
P1
His121
Leu168
Trp214
Phe256
Tyr204
Asp179*
Trp206
Cys163
P2
P4
Val178*
P5
P3
P1
His121

Figure-6

"For Table of Contents Use Only"

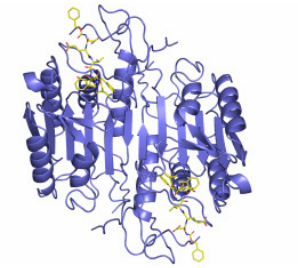

Exploring the S4 and S1 prime subsite specificities in caspase-3 with aza-peptide epoxide inhibitors

Rajkumar Ganesan, Stjepan Jelakovic, Amy J. Campbell, Zhao Zhao Li, Juliana L. Asgian, James C. Powers and Markus G. Grütter

5.0 Structure based design of inhibitors for caspases: Insights from the crystal structures of caspase-3 small molecule inhibitor complexes

Rajkumar Ganesan, Stjepan Jelakovic, Amedeo Caflisch and Markus G. Grütter

[Manuscript in preparation]

GRAPHICAL ABSTRACT

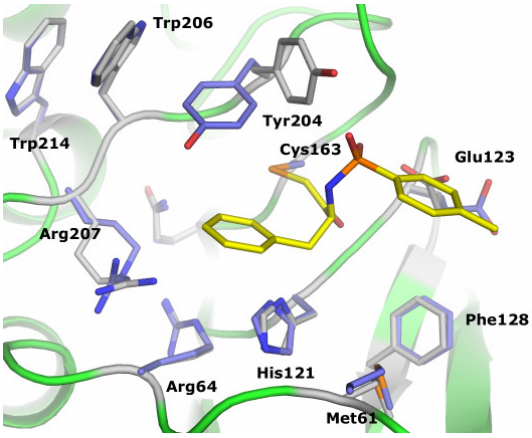

Crystal structure of the caspase-3:NSC-89167 complex revealed that it binds only in the S1 prime subsite leaving the subsites S1-S4 unoccupied leading to significant conformational changes in residues shaping these sites.

Title **Structure based design of inhibitors for caspases: Insights from the crystal structures of caspase-3 small molecule inhibitor complexes.**

Authors Rajkumar Ganesan, Stjepan Jelakovic, Amedeo Caflisch and Markus G. Grütter*

Affiliation Department of Biochemistry, University of Zurich, Switzerland.

***Correspondence** Markus G. Grütter, Department of Biochemistry, University of Zurich, Winterthurerstrasse 190, CH-8057-Zurich, Switzerland, Tel: +41 (44) 635 5580, Fax: +41 (44) 635 6834, Email: gruetter@bioc.unizh.ch

ABSTRACT

A significant interest persists towards the identification of non-peptidic inhibitors for regulating caspase activity leading to the therapeutic intervention of variety of diseases like myocardial infarction, Alzheimer's, stroke, Parkinson's, sepsis and Huntington's disease. We report the identification of several small molecule inhibitors through a structure based design approach involving an *in silico* selection, *in vitro* high throughput screening for the inhibition of caspase activity and further validation by X-ray structure determination of three caspase-3:inhibitor complexes. Inhibitors targeting either the active site of caspase-3 or the allosteric site of caspase-8 were identified. Insights from the crystal structures of caspase-3 in complex with two of the active site inhibitors revealed that these compounds bind only to the prime site of caspase-3 thus leaving the subsites S1-S4 unoccupied. Conformation of residues shaping the S1-S4 subsites support an induced fit mechanism for the binding of the substrates at the active site. Size exclusion chromatographic experiments indicated that the inhibition of caspase-8 activity by two of our allosteric inhibitors was achieved through the modulation of the oligomerization state.

KEYWORDS Caspases, *in silico* screening, X-ray structure, allosteric inhibitors.

INTRODUCTION

Caspases represent a unique class of cysteine aspartate-specific proteases because of their substrate specificity and biological functions [1, 2]. Inhibition of caspase represents a highly promising avenue for intervention in a number of conditions involving apoptosis-mediated cell and tissue damage [3]. Many potent caspase inhibitors have been prepared based on structures of the caspase peptide substrates. However, due to their peptidyl structure, most of these inhibitors do not possess good cell permeability to be considered as candidates for drug development [3]. So far 11 human caspases are known, they are classified into initiator or executioner caspases, depending on their hierarchy in the cell death process. Caspases demonstrate stringent specificity for an aspartic acid residue in P_1 position and they use their active site thiol to cleave peptide/protein targets exclusively at the C–terminus to an aspartic acid residue. Within the caspase family, a certain degree of selectivity for substrates resides in S_4 and S_1 prime subsites. Caspases have been subdivided into three main specificity families, the caspase-1, -3 and -8 family require a tryptophan, aspartic acid and leucine residue respectively in the P_4 positions of a substrate. Caspase inhibitors typically contain an electrophilic group termed 'warhead' which reacts with the nucleophilic active site cysteine residue. The most commonly used warheads are halogen methyl ketones and aldehydes, which were coupled with the preferred tetra/penta peptide recognition sequence of caspases to produce potent inhibitors.

Caspases are homo-dimers of hetero-dimers with the active site in close proximity of the dimer interface [4]. Structure-based thermodynamic analysis indicates that residues from the dimer interface of caspase-3 are critical for stabilizing the active site loops [5]. The dimer interface of caspase-3, a prototypic executioner comprises about 2500 $Å^2$ of hydrophobic surface area, mainly contributed by residues that belong to the small subunit [6]. At the interface between the hetero-dimers, a cavity is formed [1, 6-12] and the

largest cavity is formed by caspase-8 with an approximate volume of 17 × 15 × 11 $Å^3$, while the cavities formed by the caspase-2 and -3 are smaller. Due to the differences in shape and chemical properties of the surface of the cavity in different caspases, specific inhibition by compounds binding in the cavity through this allosteric mode of inhibition can be envisaged [12].

Here we present the identification and structural characterization of small molecule inhibitors either binding to the substrate binding site of caspase-3 or to the interface cavity of caspase-8, using an *in silico* screening approach combined with enzyme assays and structure determination. Initially, an *in silico* docking approach was carried out using the fragment-based docking suite DAIM-SEED-FFLD [13-16] to compounds carrying an aldehyde or halogen methyl ketone warhead binding best to the active site of caspase-3. The same docking approach was also carried out for the identification of compounds that might bind to the dimer interface cavity. Enzyme *in vitro* inhibition assays and structure determination of a selected subset of the newly identified inhibitors showed its potential to find low-molecular weight inhibitors. The combined profile of the compounds analyzed provides a starting point for the optimization of new chemically different caspase-3 inhibitors.

EXPERIMENTAL PROCEDURES

In this work we used *in silico* screening for identifying compounds containing a halogen methyl ketone or aldehyde group, which can form a covalent bond with the catalytic cysteine residue of caspases. Screening the Available Chemical Directory database (ACD about 240'000 compounds), the National Cancer Institute 3D database (NCI-3D 140'000 compounds) and the Cambridge Crystallographic Data Centre database (250'000 compounds) yielded a total of about 7200 molecules containing a halogen methyl ketone or aldehyde group. In order to search for inhibitors which bind to the

cavity at the dimer interface and thereby could influence the activity, we used the NCI diversity set of compounds for screening against three different caspase targets. The NCI diversity set covers a wide range of structural space and is a library of compounds with non-redundant pharmacophore profiles [17].

For docking of the molecules into the active site used a fragment-based docking procedure consisting of the three programs DAIM [13], SEED [14, 15] and FFLD [16, 18]. The used computational approach presumes three fragments for the placement of a flexible ligand in the binding site. DAIM decomposes a larger ligand into fragments and also determines the anchor fragments used in an initial rigid docking procedure [13]. Optimal positions and orientations for the small to medium-sized fragments generated by DAIM are determined by SEED [14, 15]. This program places polar fragments into a predefined binding pocket on condition that at least one hydrogen bond is formed to the protein whereas apolar fragments are docked into hydrophobic regions. The fragments are then being docked exhaustively. Binding energies are calculated as the sum of van der Waals and electrostatic terms taking into account the interaction energies between the fragment and the protein, as well as desolvation energies [16, 18]. In the last step of the docking procedure, the whole molecule is being docked flexibly into the binding pocket by the program FFLD. This program uses a genetic algorithm for the modification of the torsion angles and applies an efficient scoring function [19, 20]. The placement of the ligand in the binding site is defined by the anchor points defined by SEED, therefore only the conformation of the ligand is being altered. For efficiency reasons, the scoring function used in FFLD does not explicitly include solvation and is based solely on van der Waals and hydrogen bond energy terms. Nevertheless, the solvation effects are being indirectly considered by utilizing the best binding modes previously determined by SEED.

The crystal structures of caspase-3 (PDB accession codes 1CP3, 1NME, 1NMQ, 1NMS) of caspase-8 (PDB accession code 1QTN) and caspase-2 (PDB accession code 1PYO) were used as the basis of the docking experiments [6, 8, 9, 21, 22]. For caspase-3 we used multiple structures as templates in order to partially take into account protein flexibility induced by ligand binding. Coordinates of caspase-8 structure in complex with Ac-IETD-CHO was chosen due to the high resolution 1.20 Å (pdb accession code 1QTN). Prior to docking the binding sites were defined by analysis of the residues involved in the formation of the active site pocket or the cavity at the dimer interface, respectively. All crystallographic water molecules were removed from the protein structures. The 2D structures from the NCI diversity set were converted to 3D coordinates by using the program Corina [23]. Hydrogen atoms, considering appropriate ionization states, atom types and partial charges were assigned to the protein targets and the ligands using the programs Babel [24] and WITNOTP [25].

A docking protocol was established by docking of known inhibitors in the active sites of different caspase-3 structures. Different ligand poses obtained from the docking procedure were energy minimized, while keeping protein atoms rigid, using the CHARMM force field [26]. After inspection of the best scored poses in the active sites of the four different protein structures used as templates for the docking, implausible poses were discarded. This selection was based on criteria as eventual clashes with the protein and other unfavorable interactions. The docked binding modes of the energetically most favorable compounds were analyzed by visual inspection. Compounds with plausible poses, including the 1990 compounds of the NCI diversity set, were either obtained from the Drug Synthesis and Chemistry Branch, the Developmental Therapeutics Program, NCI or purchased from external suppliers and tested in an *in vitro* activity assay for their inhibition potency. The "structural diversity set" is a publicly available set of structurally diverse chemical compounds (about 2000) from the National Cancer Institute (NCI). The

compounds are prepared as a 10 mM solution in DMSO and are available in 96-well microtitre plate.

Caspase purification. The human recombinant caspases were produced in *Escherichia coli* as inclusion bodies, refolded and purified as described previously [27]. Briefly, for separate expression of both subunits, *E. coli* BL21−CodonPlus (DE3)−RIL cells (Stratagene), containing one of the two plasmids were grown to a density of A_{600} = 0.5 at 37 °C in 0.5−liter Luria−Bertani medium. Expression was induced by the addition of IPTG (1 mM), and the culture was shaken at 37 °C for 4 hours post induction. Cells were harvested, washed in PBS buffer and lyzed using a French press to retrieve the protein localized in the inclusion body portion. Refolding was achieved by rapid dilution of equimolar amounts of each subunit to a final concentration of about 100 µg of subunit/mL. The protein was purified by anion exchange chromatography (Resource−Q, GE Healthcare). As a last step, the active caspase was further purified by size exclusion chromatography (Superdex S200, GE Healthcare).

***In vitro* caspase assay based screening.** The screening process consisted of measuring the inhibitory activity of the compound under test against a defined concentration of recombinant caspases. Typically, the enzyme (10 nM) was incubated with 100 µM of the compounds for 30 min at 37°C. The remaining caspase activity was assayed fluorometrically using the fluorogenic substrates Ac-DEVD-AMC. The caspase activity was determined from the initial rate of hydrolysis of substrate by measuring the accumulation of the fluorogenic product 7-amino-4-methylcoumarin. The increase in sample fluorescence was measured at an excitation wavelength of 360 nm and an emission wavelength of 460 nm for 15-30 min at 37°C using an HTS 7000 Plus Bio Assay plate reader (Perkin Elmer). Both, the enzymes and the substrates were diluted in the assay buffer consisting of 20 mM piperazine-N,N`-bis (2-ethanesulfonic acid) (PIPES) pH 7.2, 100 mM NaCl, 10 mM 1,4-dithiothreitol (DTT), 1 mM EDTA, 0.1% (w/v) 3-((3-

cholamidopropyl)-dimethyl-ammonio)-1-propane sulfonate (CHAPS) and 10% (w/v) sucrose. The active caspase concentration was determined by active site titration using a covalently binding inhibitor Ac-DEVD-cmk. As a pre-requisite for the assay, the concentration of DMSO was less than 2% and the substrate to enzyme ratio was at least 50. The typical assay volume was 100 μL in a 96-well microtitre plate.

Crystallization and structure determination. For the crystallization studies, the purified caspase-3 was subsequently inhibited with a 3-fold molar excess of the inhibitor. Co-crystals of the complex between caspase-3 and small molecule inhibitors were grown from hanging drops formed by mixing equal volumes of protein (10 mg/mL in 20 mM Tris/HCl pH 8.0, 10 mM DTT) and reservoir solution. The reservoir solution consisted of 0-15% (w/v) polyethylene glycol 6000, 100 mM sodium citrate pH 5.0. Prior to data collection, crystals were frozen in the nitrogen stream after a short soak in reservoir solution containing 20% glycerol. The crystals belong to the space group I222 and the unit cell dimensions are as listed in Table 3. X-ray data for the inhibitor **(1)** was collected at the Swiss Light Source synchrotron (Paul Sherrer Institute, Villigen, Switzerland). The data processing was done with program XDS [28]. Diffraction data for the inhibitors **(5)** and **(8)** were collected with the rotating anode generator (Bruker-Nonius, FR591) at 100 K. Images were integrated with MOSFLM [29] and scaled with SCALA [30] from the CCP4 suite of programs. The structure was solved by the difference Fourier technique. The model building was done with program O [31] and structure refinement was performed using the program CNS [32]. The topology and parameter files for the energy minimized inhibitor were generated using the program XPLO2D [33]. The final crystallographic *R* and free *R* factors were in the range of 18-20% and 19-22% respectively. The final models consisted of residues 29-174 of the α-subunit and residues 186-277 of the β–subunit for the all three caspase-3:inhibitor complexes described here.

RESULTS

The results of the re-docking experiments are shown in Figure 1. The predicted binding modes for the inhibitors **(1)**, **(5)**, and **(8)** were very similar to the experimental binding modes. The observed rmsd values to the crystallographic coordinates were in the range of 0.5-1.1 Å (Table 1). In order to facilitate crystallization and subsequent structure determination, we focused our docking efforts towards the irreversible warhead possessing a halogen methyl ketone moiety rather than the reversible aldehyde group. Visual inspection of the best scored poses of our docking results, led to the subset of 27 compounds which were ordered either at the NCI open chemicals repository or with the commercial suppliers. 21 of these compounds could be obtained and were subsequently assayed for the inhibitory activity against caspase-3. At least 8 of these compounds showed more than 50% inhibition in the caspase activity assay. The relative inhibition data for these compounds along with their chemical structures are given in Table-2. The structure-based design approach as described above was also employed for the identification of allosteric inhibitors for caspases. *In silico* pre-selection followed by an *in vitro* HTS screening yielded a series of compounds, the relative inhibitory activity values for these inhibitors and their chemical structures are summarized in Table 4.

Crystallographic studies for the active site directed inhibitors of caspase-3

All the identified inhibitors listed in Table 2 were screened for co-crystallization with caspase-3. The three compounds **(1)**, **(5)**, and **(8)** yielded suitable crystals for collecting diffraction data. A summary of the crystallographic data processing and refinement statistics is given in Table 3. Additionally, we obtained co-crystals of caspase-3 in complex with the compounds **(3)**, **(4)**, **(6)**, and **(7)**. Unfortunately, these crystals were either too small or were not diffracting to reasonable resolution despite several optimization attempts.

The overall conformation of caspase-3 is similar in all of the three inhibitor complexes reported here and is also similar to the other known crystal structures of caspase-3:inhibitor complexes [6, 7]. The halogen methyl ketone warhead groups are covalently bonded to the thiol group of the active site cysteine through a thio-ether bond.

The compound **(5)** mimics an aspartic acid coupled to a methylene chloride moiety at the C-terminus. The binding mode is very similar to that of the inhibitors possessing a P_1-aspartate moiety [6, 7]. The compound **(5)** occupies the S_1 subsite and is stabilized by ionic interactions with Arg64 and Arg207 apart from the hydrogen bond interaction with Gln161 (Fig. 2b and 4b). In the other known structures, caspases typically form two critical mainchain-mainchain interactions with the peptidic inhibitors. One of the interactions is between the P_1-amide protons of the inhibitor and the backbone carbonyl of the conserved Ser205, the other interaction is between the P_3-carbonyl group with the amide proton of the conserved Arg207. The lack of the amide group in the compound **(5)** and thus the missing hydrogen bond interaction renders methylene carbons very flexible. The carbonyl group of the inhibitor is stabilized by the "oxyanion hole" formed by the amide protons of cysteine Cys163 and Gly122. Being the smallest inhibitor, it just occupies the S_1 subsite thus leaving the subsites S_2-S_4 unoccupied. As a consequence, the residues involved in shaping these sites have different orientations compared to the ones observed in other known structures [6, 7]. One significant change is observed in the case of Tyr204, which rotates about 90° and occupies the P_2-pocket where it is stabilized by hydrophobic contacts with Cys163, Trp206 and Phe256 (Fig. 2b).

In contrast to the mode of binding observed in the caspase-3:compound **(5)** complex, compound **(1)** binds only in the prime site of caspase-3. Due to this unusual binding along the prime site, the substrate binding subsites S_1-S_4 are unoccupied. Apart from some movements of the side chain conformation of residues forming these subsites,

a similar conformational change of Tyr204 as observed in case of caspase-3: compound **(5)** complex was also observed in this structure. Given the lack of the critical P_1-Asp residue, the S_1 subsite is occupied by a cluster of water molecules. As a consequence, the active site Arg207 is displaced by about 0.5 Å in comparison to caspase-3: compound **(5)** complex and it also adopts a different side chain conformation. The inhibitor is covalently bound to the active site cysteine residue and the P_1-carbonyl group of the inhibitor is stabilized partly by the "oxyanion hole" (the amide protons of Gly122) (Fig 2a, 3a and 4a). One of the phenyl rings of the inhibitor covers the S_1 subsite and is involved in hydrophobic contacts with Tyr204 and His121, while the p-toluyl group is stabilized by the side chains of Thr166 and Glu123. Furthermore, it is evident from the crystal structure that the sulfone amide group is not involved in direct interactions to the protein and instead forms water-mediated interactions with the main chain carbonyl groups of Gly122 and Gly165. Therefore, the sulfone amide presumably could be replaced by other groups linking the p-toluyl and the benzyl groups of the inhibitor. Since the amide group is not involved in any contacts, it might be advantageous to replace the sulfone amide group by a sulfone group.

Although the binding of the carbamic acid group in the structure of the caspase-3: compound **(8)** complex is reminiscent of the binding of the sulfone amide group of compound **(1)**, the two aromatic rings of compound **(8)** bind to completely different regions to the active site. One of the phenyl ring is well placed in a deep hydrophobic cavity delineated by cluster of residues Thr166, Leu168, Tyr204 and Phe256, while the other phenyl ring is stabilised by hydrophobic contacts with Met61 and Phe128 (Fig 2c, 3b and 4c). The carbonyl group of the inhibitor is stabilized by hydrogen bond interaction with the amide proton of Gly122. An additional stabilizing interaction is observed between the carbonyl group of the inhibitor and the catalytic His121. As already observed

for the compounds **(1)** and **(5)**, a similar conformational change of Tyr204 is observed here as well. Therefore, the conformation reported for most of the caspase-3 peptidic inhibitor complexes [6, 7] is due to displacement of the Tyr204 by the P_2-Val residue of the inhibitor. Thus the observed conformational changes of the active site residues like Tyr204 and Arg207 provide a glimpse of adaptability and plasticity of the active site residues. Additionally, these observations also support an induced-fit mechanism in a concerted fashion involving both the enzyme and substrate amino acid residues.

Size exclusion chromatography

In an attempt to assess whether the modulation of caspase activity by allosteric inhibitors is due to the altering of the monomer-dimer equilibrium, we have performed size exclusion chromatography experiments for caspase-8 in complex with two of the identified allosteric inhibitors. The uninhibited caspase-8 exists in monomer-dimer equilibrium with 80-85% of the protein in the dimeric form (Fig. 5). This equilibrium can be shifted to higher degree of dimer formation, by the addition of potent inhibitors [34]. Two of the identified allosteric inhibitors showed varying degree of shift in the monomer-dimer equilibrium. This observation indicated that apart from weakening of the dimer interface and subsequently shifting the equilibrium towards the formation of monomers, these inhibitors also seem to induce some conformational changes which propagate from the dimer interface to the active site and thereby results in decreased activity. Accordingly, the results from the size exclusion chromatographic experiments indicate that the inhibition of caspase-8 activity by the allosteric inhibitors **(9)** and **(10)** is achieved through the modulation of the oligomerization state. Nevertheless, the precise mechanism by which they achive this modulation awaits further structural and biochemical characterization.

DISCUSSION

From experimental observations at the atomic level of how inhibitors bind to their macromolecular targets, specific interactions that are important in molecular recognition can be inferred. Apart from the de novo design of novel lead compounds, the structural information obtained in this study could aid in the improvement of existing inhibitors. We have shown that our fragment-based docking procedure is capable of reproducing the binding modes of known caspase-3 inhibitors and that the *in silico* screening approach identifies novel compounds in compound databases exhibiting caspase-3 inhibitory activity. The observed mode of binding was different in all our three caspase-3:inhibitor complexes determined. The high-resolution crystal structures reported here provides insights into the architecture of the active site, which might be useful for the design of more potent caspase-inhibitors by considering not only the S_1-S_4 pockets but also the S_1 prime subsite. Moreover, the replacement of some fragments of the crystallographically determined compounds in complex with caspase-3 by more favorable moieties could eventually be utilized for the optimization of the compounds. Preliminary tests using the NCI diversity set of approximately 2000 compounds also showed that the combination of *in silico* docking and high-throughput screening might be implemented for the identification of allosteric inhibitors for caspases without the need for an electrophilic warhead group. Size exclusion chromatography experiments indicated that the inhibition of caspase-8 activity by two of the found allosteric inhibitors was achieved through the modulation of the oligomerization state shifting the equilibrium towards the formation of monomeric caspases. Thus this strategy capitalizes on the feature that caspases activity would be attenuated when its oligomerization state is perturbed. The detailed investigation of allosteric regulation of caspases which includes the determination of the stoichiometry, affinity and critical residues involved in the interaction with the ligand moiety has to be established in the near future. In conclusion, we have showed that our

fragment-based docking procedure is capable of reproducing the binding modes of known caspase-3 inhibitors and that our *in silico* screening approach could be used for screening of databases for compounds exhibiting caspase inhibition activity.

Coordinates. Crystallographic coordinates and structure factors for the three caspase-3:inhibitor complex structures have been deposited to the Protein Data Bank with accession ID PDB1, PDB2 and PDB3.

ACKNOWLEDGEMENT. We gratefully acknowledge Dr. Peer R.E. Mittl for the fruitful discussion and critical reading of the manuscript. We thank the staff at the Swiss Light Source, Paul Scherrer Institute, Villigen, Switzerland, for synchrotron beam time. The financial support from the Swiss National Science Foundation and the Baugartenstiftung (Zurich, Switzerland) is gratefully acknowledged. The authors acknowledge the National Cancer Institute for providing the chemical samples.

REFERENCES

[1] Fuentes-Prior, P.; Salvesen, G. S. The protein structures that shape caspase activity, specificity, activation and inhibition. *Biochem J* **384:**201-232; 2004.

[2] Grutter, M. G. Caspases: key players in programmed cell death. *Current Opinion in Structural Biology* **10:**649; 2000.

[3] O'Brien, T. Prospects for caspase inhibitors. *Mini Rev Med Chem* **4:**153-165; 2004.

[4] MacCorkle, R. A.; Freeman, K. W.; Spencer, D. M. Synthetic activation of caspases: artificial death switches. *Proc Natl Acad Sci U S A* **95:**3655-3660; 1998.

[5] Piana, S.; Sulpizi, M.; Rothlisberger, U. Structure-based thermodynamic analysis of caspases reveals key residues for dimerization and activity. *Biochemistry* **42:**8720-8728; 2003.

[6] Mittl, P. R. E.; Di Marco, S.; Krebs, J. F.; Bai, X.; Karanewsky, D. S.; Priestle, J. P.; Tomaselli, K. J.; Grutter, M. G. Structure of Recombinant Human CPP32 in Complex with the Tetrapeptide Acetyl-Asp-Val-Ala-Asp Fluoromethyl Ketone. *J. Biol. Chem.* **272:**6539-6547; 1997.

[7] Rotonda, J.; Nicholson, D. W.; Fazil, K. M.; Gallant, M.; Gareau, Y.; Labelle, M.; Peterson, E. P.; Rasper, D. M.; Ruel, R.; Vaillancourt, J. P.; Thornberry, N. A.; Becker, J. W. The three-dimensional structure of apopain/CPP32, a key mediator of apoptosis. *Nat Struct Biol* **3:**619-625; 1996.

[8] Schweizer, A.; Briand, C.; Grutter, M. G. Crystal structure of caspase-2, apical initiator of the intrinsic apoptotic pathway. *J Biol Chem* **278:**42441-42447; 2003.

[9] Watt, W.; Koeplinger, K. A.; Mildner, A. M.; Heinrikson, R. L.; Tomasselli, A. G.; Watenpaugh, K. D. The atomic-resolution structure of human caspase-8, a key activator of apoptosis. *Structure Fold Des* **7:**1135-1143; 1999.

[10] Wei, Y.; Fox, T.; Chambers, S. P.; Sintchak, J.; Coll, J. T.; Golec, J. M.; Swenson, L.; Wilson, K. P.; Charifson, P. S. The structures of caspases-1, -3, -7 and -8 reveal the basis for substrate and inhibitor selectivity. *Chem Biol* **7:**423-432; 2000.

[11] Wilson, K. P.; Black, J. A.; Thomson, J. A.; Kim, E. E.; Griffith, J. P.; Navia, M. A.; Murcko, M. A.; Chambers, S. P.; Aldape, R. A.; Raybuck, S. A.; et al. Structure and mechanism of interleukin-1 beta converting enzyme. *Nature* **370:**270-275; 1994.

[12] Hardy, J. A.; Lam, J.; Nguyen, J. T.; O'Brien, T.; Wells, J. A. Discovery of an allosteric site in the caspases. *PNAS* **101:**12461-12466; 2004.

[13] Caflisch, P. K. a. A. *to be published.*

[14] Majeux, N.; Scarsi, M.; Apostolakis, J.; Ehrhardt, C.; Caflisch, A. Exhaustive docking of molecular fragments with electrostatic solvation. *Proteins* **37:**88-105; 1999.

[15] Majeux, N.; Scarsi, M.; Caflisch, A. Efficient electrostatic solvation model for protein-fragment docking. *Proteins* **42:**256-268; 2001.

[16] Scarsi, M., Apostolakis, J & Caflisch, A. *J. Phys. Chem* **A**; 1997.

[17] Shi, L. M.; Fan, Y.; Lee, J. K.; Waltham, M.; Andrews, D. T.; Scherf, U.; Paull, K. D.; Weinstein, J. N. Mining and visualizing large anticancer drug discovery databases. *J Chem Inf Comput Sci* **40:**367-379; 2000.

[18] Scarsi, M.; Majeux, N.; Caflisch, A. Hydrophobicity at the surface of proteins. *Proteins* **37:**565-575; 1999.

[19] Budin, N.; Majeux, N.; Caflisch, A. Fragment-Based flexible ligand docking by evolutionary optimization. *Biol Chem* **382:**1365-1372; 2001.

[20] Cecchini, M.; Kolb, P.; Majeux, N.; Caflisch, A. Automated docking of highly flexible ligands by genetic algorithms: a critical assessment. *J Comput Chem* **25:**412-422; 2004.

[21] Choong, I. C.; Lew, W.; Lee, D.; Pham, P.; Burdett, M. T.; Lam, J. W.; Wiesmann, C.; Luong, T. N.; Fahr, B.; DeLano, W. L.; McDowell, R. S.; Allen, D. A.; Erlanson, D. A.; Gordon, E. M.; O'Brien, T. Identification of potent and selective small-molecule inhibitors of caspase-3 through the use of extended tethering and structure-based drug design. *J Med Chem* **45:**5005-5022; 2002.

[22] Erlanson, D. A.; Lam, J. W.; Wiesmann, C.; Luong, T. N.; Simmons, R. L.; DeLano, W. L.; Choong, I. C.; Burdett, M. T.; Flanagan, W. M.; Lee, D.; Gordon, E. M.; O'Brien, T. In situ assembly of enzyme inhibitors using extended tethering. *Nat Biotechnol* **21:**308-314; 2003.

[23] Sadowski, J. a. G., J. From atoms and bonds to three-dimensional atomic coordinates: automatic model builder. *Chemical Reviews* **93:**2567-2581; 1993.

[24] BABEL: Modification and conversion program. *http://openbabel.sourceforge.net*.

[25] Widmer, A. WITNOTP: A computer program for molecular modeling. *Novartis AG, Basel, Switzerland*.

[26] Brooks, B. R. B., R.E. *J. Comput. Chem*; 1983.

[27] Garcia-Calvo, M.; Peterson, E. P.; Rasper, D. M.; Vaillancourt, J. P.; Zamboni, R.; Nicholson, D. W.; Thornberry, N. A. Purification and catalytic properties of human caspase family members. *Cell Death Differ* **6:**362-369; 1999.

[28] Kabsch, W. Automatic indexing of rotation diffraction patterns. *J. Appl. Cryst.* **21:**67-72.; 1988.

[29] Leslie, A. G. W. Joint CCP4/ESF-EACMB Newsletter on Protein Crystallography 26.Scala. 1992.

[30] Evans, P. R. Data reduction. *Proceedings of the CCP4 Study Weekend on Data Collection and Processing, pp 114-122, SRC Daresbury Laboratory, Warrington, U.K*; 1992.

[31] Jones, T. A.; Zou, J. Y.; Cowan, S. W.; Kjeldgaard. Improved methods for building protein models in electron density maps and the location of errors in these models. *Acta Crystallogr A* **47 (Pt 2):**110-119; 1991.

[32] Brunger, A. T.; Adams, P. D.; Clore, G. M.; DeLano, W. L.; Gros, P.; Grosse-Kunstleve, R. W.; Jiang, J. S.; Kuszewski, J.; Nilges, M.; Pannu, N. S.; Read, R. J.; Rice, L. M.; Simonson, T.; Warren, G. L. Crystallography & NMR system: A new software suite for macromolecular structure determination. *Acta Crystallogr D Biol Crystallogr* **54 (Pt 5):**905-921; 1998.

[33] Kleywegt, G. J. Dictionaries for Heteros. *CCP4/ESF-EACBM Newsletter on Protein Crystallography* **31:**pp. 45-50.; 1995.

[34] Donepudi, M.; Mac Sweeney, A.; Briand, C.; Grutter, M. G. Insights into the regulatory mechanism for caspase-8 activation. *Mol Cell* **11:**543-549; 2003.

Table 1. Redocking and cross docking of halogen methyl ketone inhibitors

	iCP3	iNME	iNMS
1CP3	0.5	3.8	3.7
1NME	1.0	1.1	1.4
1NMS	4.0	1.5	0.9

Table 2. List of active site directed inhibitors with their relative inhibitory activities for caspase-3[a].

(1)	NSC-89167 CAS: 329-30-6	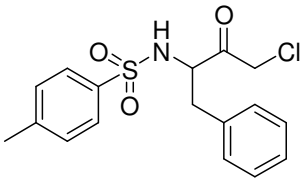 71%
(2)	NSC-24873 CAS:1775-46-8	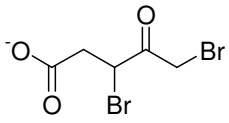 69%
(3)	NSC-107152 CAS:10161-88-3	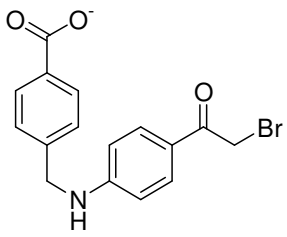 68%

(4)	NSC-211621 CAS:19159-87-6	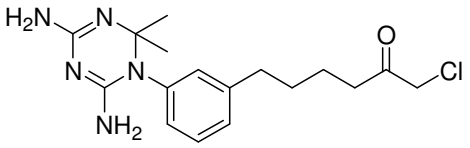 66%
(5)	NSC-18508 CAS: 60254-71-9	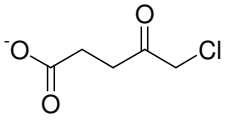 59%
(6)	NSC-106024 CAS: 10161-89-4	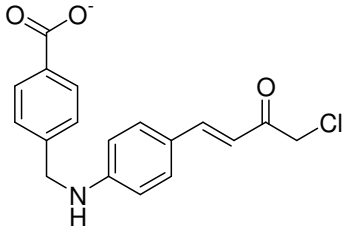 53%
(7)	NSC-107443 CAS:37660-62-1	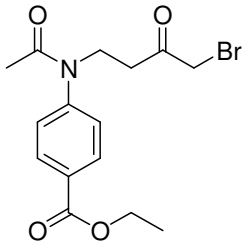 53%
(8)	NSC-251810 CAS: 26049-94-5	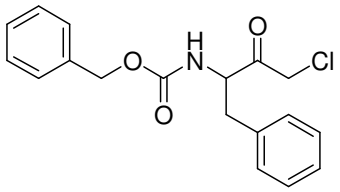 50%

[a] The relative inhibitory activities against caspase-3 are indicated below the chemical structures.

Table 3. X-ray data collection and refinement statistics[a]

	(1) ***NSC 89167***	**(2)** ***NSC 251810***	**(3)** ***NSC 18508***
Space group		I222	
a (Å)	68.7	69.5	68.5
b (Å)	83.5	83.7	83.5
c (Å)	96.1	95.8	95.8
Resolution range (Å)	20 - 1.57 (1.65-1.57)	20 – 1.86 (1.95 - 1.86)	20 – 1.89 (2.0-1.89)
No. of unique reflections	28900 (5491)	23676 (3379)	21385 (3029)
I/σI	30.5 (4.3)	27.8 (13.8)	21.1 (8.2)
R_{merge} (%)	9.8 (22.0)	4.2 (10.6)	5.0 (16.9)
Completeness (%)	96.9 (88.4)	99.3 (98.5)	96.1 (94.5)
R	18.6	19.9	18.5
R_{free}	19.6	22.6	21.9
rmsd bond (Å)	0.0081	0.0068	0.0051
rmsd angles(deg)	1.559	1.4831	1.2441
Average B (Å^2)			
Protein	11.5	11.5	13.3
Ligand atoms	34.6	44.5	32.8
Water molecules	30.5	31.1	28.9
No of atoms			
Protein	1931	1931	1931
Ligand atoms	22	22	8
Water molecules	399	393	289

[a]The values in the parentheses refer to that of the highest resolution shell

Table 4: Influence on the activity and oligomerization state of caspase-8 due to the inhibitor binding

	Relative inhibitory activity (%)	Modulation of oligomerization state		Chemical structure
		% Monomer	% Dimer	
Caspase-8 **(uninhibited)**	0	17	83	
Caspase-8 + **NSC-50352**	90	57	43	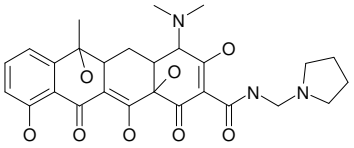 **(9)**
Caspase-8 + **NSC-117274**	85	91	9	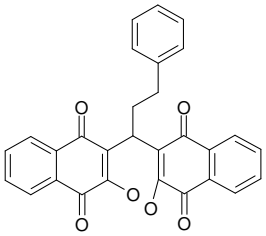 **(10)**

FIGURE LEGENDS

Figure 1: Comparison of the docking poses with the corresponding conformations observed in the known caspase-3:inhibitor structures from PDB entries **(a)** 1CP3, **(b)** 1NME, and **(c)** 1NME. The rmsd between the modeled and the crystallographically observed conformations are in the range 0.5 – 1.1 Å.

Figure 2: Cartoon representation of the crystal structure of caspase-3 in complex with active site directed inhibitors **(a)** compound **(1)** **(b)** compound **(5)** and **(c)** compound **(8)**, superimposed with the structure of caspase-3/DEVD complex (grey). The atoms of the inhibitor are in yellow and the residues of caspase-3 involved in the interaction are in blue. The conformational change of Tyr204 is observed in the all the three caspase-3:inhibitor complexes reported here.

Figure 3: Surface representation illustrating the differences in the binding mode of the structure of caspase-3 in complex with compound **(1)** and **(8), (a)** and **(b)** respectively. Even though both the compounds bind to the S1 prime subsite, the orientations of the aromatic rings are different to one another.

Figure 4: Network of polar interactions in the structure of caspase-3 in complex with compounds **(1)**, **(5)** and **(8), (a-c)** respectively. Compound **(5)** is involved in an extensive network of polar interactions, while compounds **(1)** and **(8)** are stabilized predominantly by hydrophobic contacts.

Figure 5: Size exclusion chromatographic profiles reflecting the modulation of oligomerization state induced by allosteric inhibitor binding to caspase-8. The uninhibited caspase-8 exists predominantly in the dimeric form. The allosteric inhibitors, compounds **(9)** and **(10)**, inactivate caspase-8 by shifting the equilibrium towards the formation of monomer.

(a)

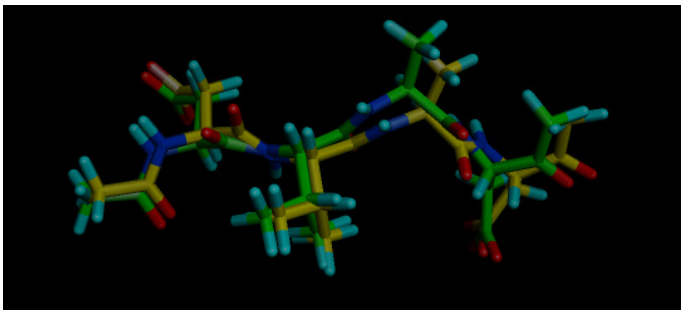

(b)

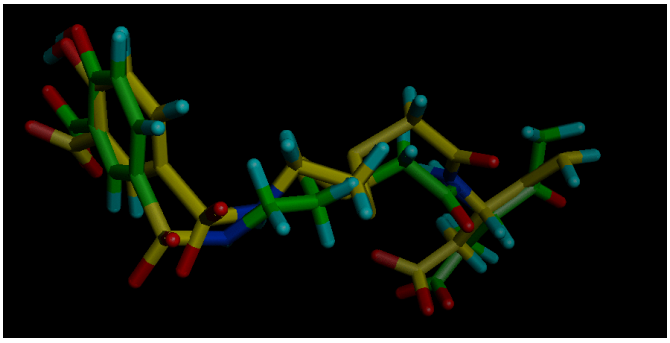

(c)

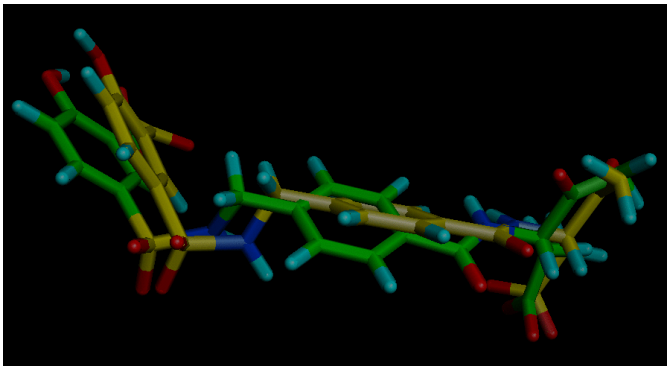

Figure 1

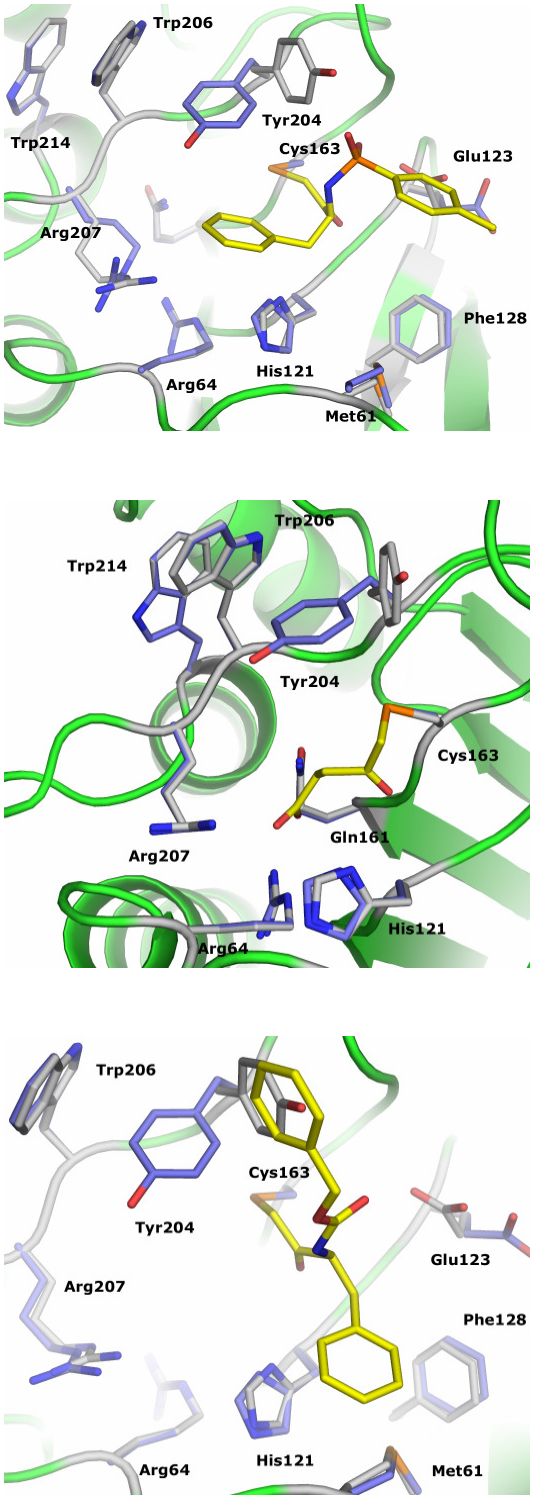
(a)
Trp206
Tyr204
Trp214
Cys163
Glu123
Arg207
Phe128
His121
Arg64
Met61
(b)
Trp206
Trp214
Tyr204
Cys163
Gln161
Arg207
His121
Arg64
(c)
Trp206
Cys163
Tyr204
Glu123
Arg207
Phe128
His121
Met61
Arg64

Figure 2

(a)

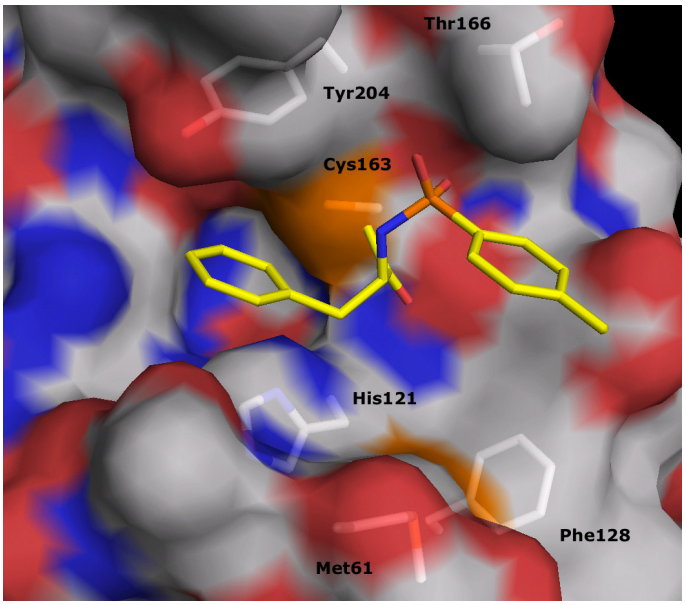
Thr166
Tyr204
Cys163
His121
Phe128
Met61

(b)

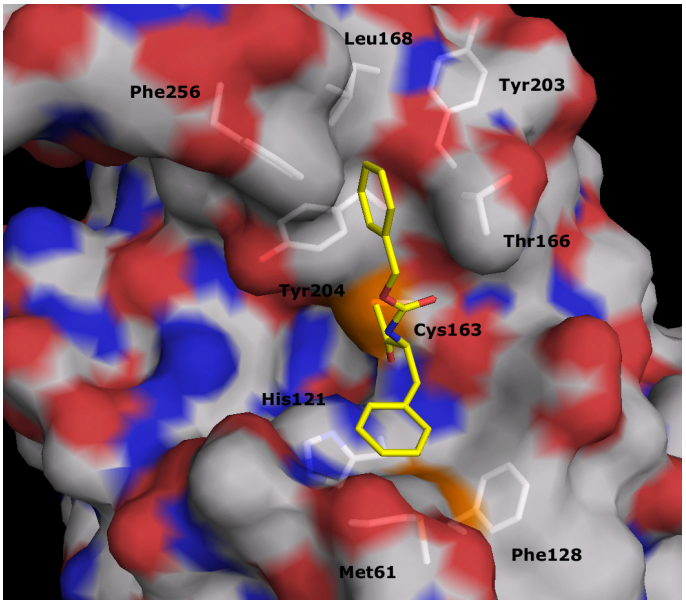
Leu168
Phe256
Tyr203
Thr166
Tyr204
Cys163
His121
Phe128
Met61

Figure 3

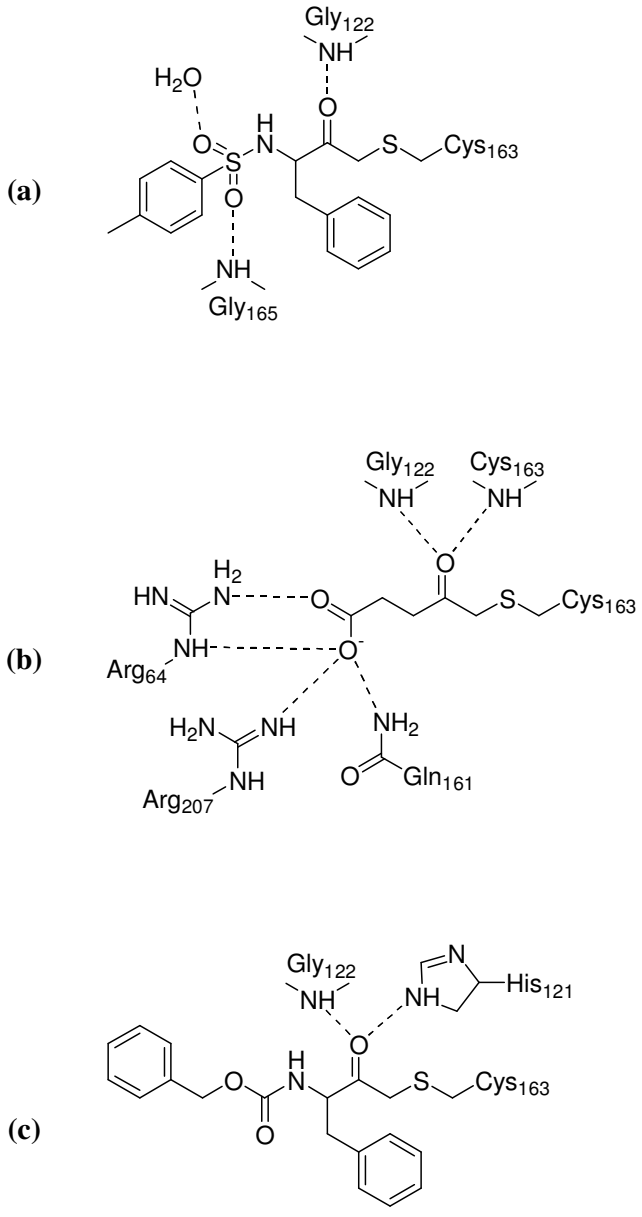
(a)
Gly122
NH
H2O
O
H
N
O
S
Cys163
S
O
NH
Gly165
(b)
Gly122
Cys163
NH
NH
O
H2
HN
N
O
S
Cys163
NH
Arg64
O-
H2N
NH
NH2
NH
O
Gln161
Arg207
(c)
Gly122
NH
N
NH
His121
O
H
N
O
S
Cys163
O
O

Figure 4

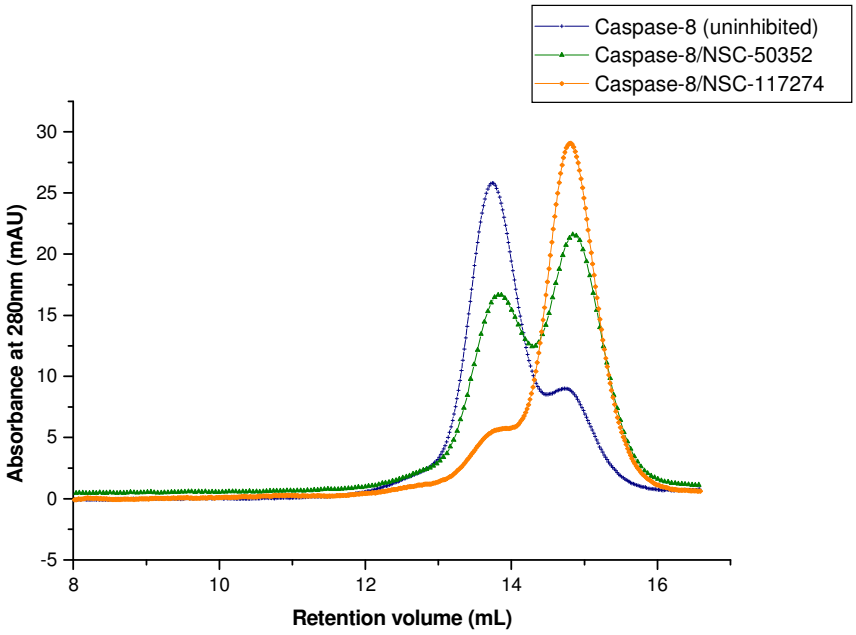
Caspase-8 (uninhibited)
Caspase-8/NSC-50352
Caspase-8/NSC-117274
Absorbance at 280nm (mAU)
Retention volume (mL)
30
25
20
15
10
5
0
-5
8
10
12
14
16

Figure 5

Appendix A An attempt towards the structure determination of procaspase-3

A.1 Introduction

Caspase activation is an important event as it defines a cellular response to the onset of apoptosis [1]. Like the other caspases, caspase-3 exists in normal cells as an inactive zymogen and must be activated by proteolytic processing. Procaspase-3 is organized with an amino-terminal pro-domain followed by the large (p17) subunit and the small (p12) subunit, as shown in Fig. 1. There are two amino acid sequences, ESMD↓S (residues 25-29) and IETD↓S (residues 172-176) in the 32-kDa procaspase-3 that have been found to be the cleavage sites for the production of the p17 and p12 subunits [2]. At both sites, the cleavage occurs between the aspartic and serine residues. The first cleavage event is after Asp175 to produce partly active caspase-3 which subsequently cleaves itself after Asp29 to generate a fully active and functional caspase-3.

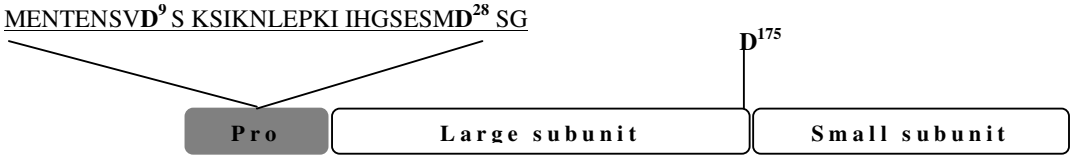

Figure 1. Schematic representation of full-length procaspase-3, showing the pro-domain sequence and the cleavage sites, D9, D28 and D175.

While the longer prodomains of the initiator caspases associate with factors required for enzyme activation through specific folded domains [3], the function of the smaller prodomains of effector caspases is unclear. For all effector caspases studied to date, the N terminus is disordered and not visible in the crystal structures. Even in the crystal structure of procaspase-7, the prodomain (residues 1-23) and adjacent residues (residues 24-55) are disordered [4, 5]. Nonetheless, several studies suggest that the prodomain of effector caspases have specific roles. Proteolytic removal of the prodomain of human effector caspase-6 contributes to cleavage and activation of human caspase-8 [6], and the prodomain of *Xenopus* caspase-7 regulates nuclear transport [7]. The prodomain in human effector caspase-7 regulates both the activation rate and enzyme activity *in vivo* [8]. Finally, the prodomain of human caspase-3 may act as a silencing element by retaining the caspase in an inactive state [9].

A.2 Cloning, expression and purification

The protease domain of procaspase-3 (ΔproC3) consisting of the α subunit and the β subunit along with the N-terminal 6xHis tag were cloned into a pET28 plasmid (Novagen) using the restriction sites BamH I and Xho I. The active site C163A (catalytic cysteine mutated to alanine) mutation was introduced using the Stratagene quick change mutagenesis kit (Strategene). The oligonucleotide primers used for the PCR based cloning strategy are listed in Table-1. Clones having correct sequence directionality were identified through DNA sequencing. The cloned gene (Met-6xHis-GSM-S^{29}-His^{277}) was expressed in *E. coli* BL21 (DE3) Codon plus RIL (Stratagene). The cells were grown to a density of A_{600} = 0.5 at 30°C in a 0.5-litre Luria-Bertani culture. Expression was induced by the addition of IPTG (1 mM), and the culture was shaken at 25 °C for 4 hours post induction. Cells were harvested by centrifugation at 5000 *g* for 30 minutes. Bacterial pellets were resuspended in buffer A (50 mM NaH_2PO_4 pH 8.0, 300 mM NaCl, 2 mM β-mercapto-ethanol and 10 mM Imidazole) and lyzed on ice using a French press. The supernatant was separated from cell debris by centrifugation at 20,000 *g* for 30 min.

Table-1: List of primers for ΔproC3 cloning

#	Primer_name	Oligonucleotide sequence
1	pC3p17_fwd	GCGGGATCCATGAGCGGTATCTCCCTGGACAACA
2	pC3p17_rev	GTCTGTCTCAATGCCACAGTCTGTCTCAATGCCACAGTCCAGT
3	pC3_C163A_fwd	CAAACTTTTCATTATTCAGGCC**GCA**CGTGGTACAGAACTGGACTG
4	pC3_C163A_rev	CAGTCCAGTTCTGTACCACG**TGC**GGCCTGAATAATGAAAAGTTTG

All steps were performed at 4°C unless otherwise noted. The resulting supernatant was then run through a pre-equilibrated (with buffer A) Ni-nitrilo-triacetic acid-agarose column according to the manufacturer's instructions (Qiagen). Unspecifically bound contaminating proteins were washed off using buffer B (50 mM NaH_2PO_4 pH 8.0, 300 mM NaCl, 2 mM β-mercapto-ethanol and 50 mM imidazole). The ΔproC3 was eluted with buffer-C (50 mM NaH_2PO_4 pH 8.0, 300 mM NaCl, 2 mM β-mercapto-ethanol and 250 mM imidazole). The fractions were analyzed by SDS-PAGE. The fractions containing the pure protein were pooled, concentrated (YM10 membrane), and dialyzed first against buffer D (50 mM Tris-HCl, pH 8.0, 50 mM NaCl, 1 mM EDTA and 5 mM β-mercapto-ethanol). The ΔproC3 was further purified by size exclusion chromatography on an analytical Superdex S200 column (Amersham Biosciences) with buffer E (20 mM Tris pH 8.0, 50 mM NaCl and 10 mM DTT). The final yield was about 30 mg/litre culture.

A.3 Biophysical experiments of ΔproC3

A.3.1 Size exclusion chromatography

During the course of the purification of ΔproC3, it was unusual to observe that the protein eluted at about 14.5 mL which is typical for a protein of an approximate size of 30 kDa, but in contrast, it has been previously established that ΔproC3 exists in solution as a dimer with an apparent mass of 59.4 kDa [10]. As we could observe from the size exclusion chromatogram, the elution profile reveals the presence of a single peak with no aggregation. For comparison, the size exclusion chromatography was performed under identical experimental condition for the active caspase-3 and caspase-8. Overlaying the elution profiles, we could clearly observe that ΔproC3 is a more compared in shape to active caspases (Fig.2). The elution volumes of the three proteins analyzed here are given under table 2.

Table-2: Elution volume for ΔproC3, active caspase-3 and active caspase-8

Protein	Elution volume (monomer mL)	Elution volume (dimer mL)
ΔproC3	-	14.6
Caspase-3	-	13.8
Caspase-8	14.6	13.6

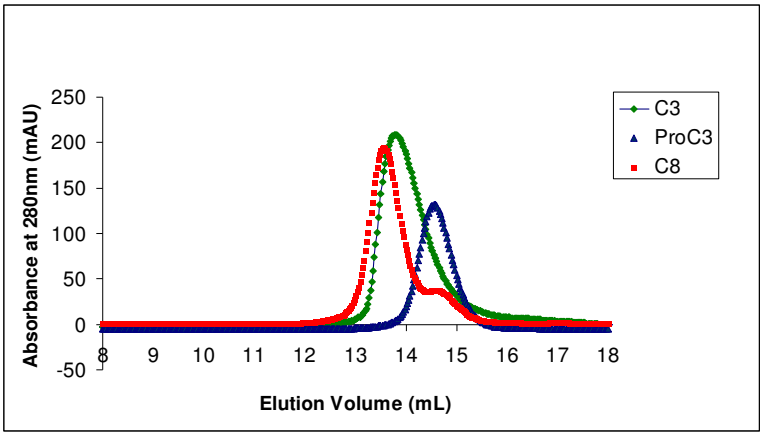

Figure 2: Size exclusion chromatographic profiles for ΔproC3, active caspase-3 and active caspase-8.

The instrument was pre-calibrated with BSA as a standard protein. Its elution profile is included for reference. Table 4 lists the weight-average molecular mass of the proteins obtained from static light scattering.

Size exclusion chromatography coupled to static light scattering and refractive index detector

To further analyze the oligomerization state, ΔproC3 was subjected to a size exclusion chromatographic column (Analytical Superdex S200, Amersham Pharmacia) coupled to static light scattering (Mini-Dawn, Wyatt Technologies) and refractive index detectors (Fig.3).

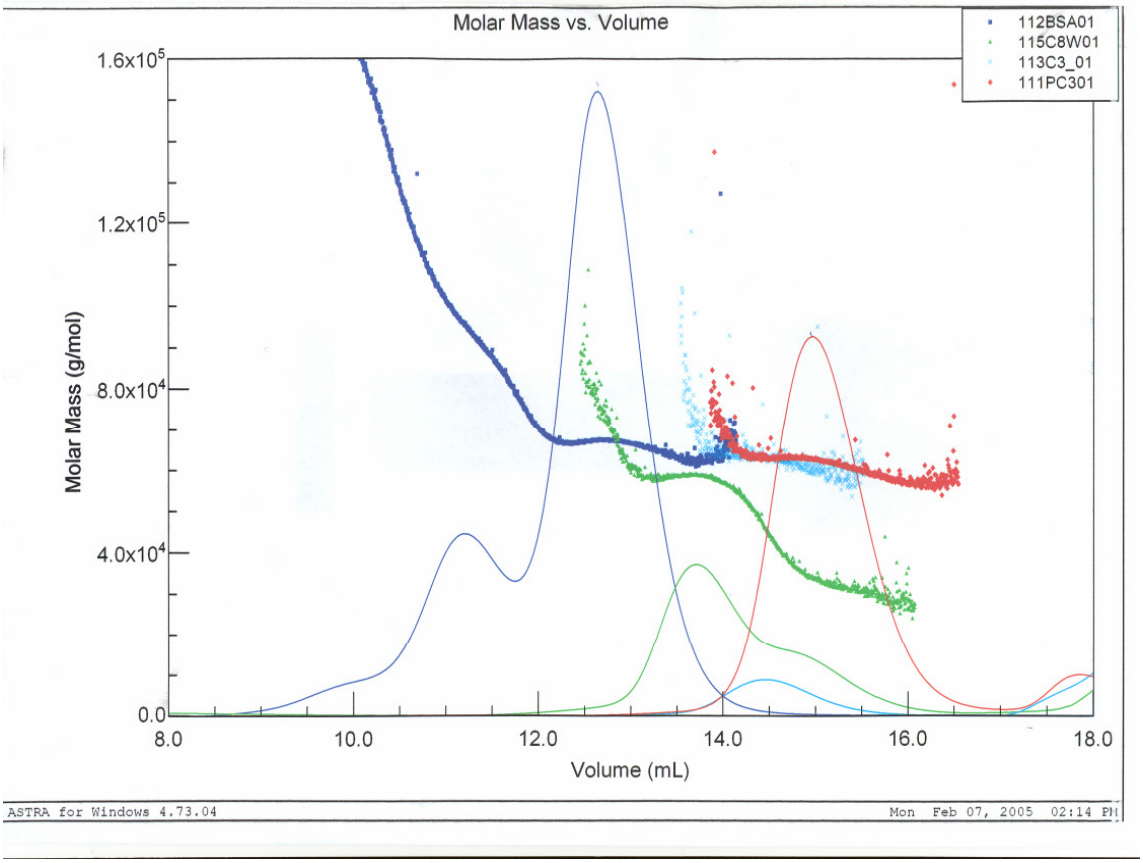

Figure 3: Size exclusion chromatography coupled to a static light scattering and refractive index detectors. Solid lines indicate the absorbance at 280 nm while the fitting (symbols) for the calculated weight-average molecular mass was done based on the scattering of the particles in solution.

Table-3: Calculated weight-average molecular mass of the ΔproC3, active caspase-3 and -8

Protein	Mw (kDa)	
	Monomer	dimer
ΔproC3	-	63
Caspase-3	-	62
Caspase-8	31	59

A.3.2 Circular dichroism spectroscopy

The folding behaviour and thermal stability of ΔproC3 were analysed (Fig.5) at a concentration of 20 μM in a buffer containing 20 mM Tris-HCl pH 8.0, 50 mM NaCl and 10 mM DTT by monitoring both spectrum and thermal denaturation by CD spectroscopy. The measurements were performed on a Jasco-715 spectropolarimeter equipped with a computer-controlled water bath, using thermostated cuvettes with a 1 mm or 10 mm path length. The far-UV CD spectrum was measured continuously from 250 to 200 nm. The buffer scan was subtracted from the protein scan. Thermal unfolding curves were measured by continuously recording the ellipticity at 222 nm and with data collection every 20 s.

Analysis of heat-induced unfolding curves describing a two-state transition between the folded and the unfolded state. The unfolding constant is defined as:

$$K_U = f_U / (1-f_U) \quad (1)$$

where f_U is the fraction of unfolded peptide. At each temperature, the observed molar ellipticity per residue of the folded and the unfolded state is

$$[\theta] = f_U[\theta_U] + (1- f_U)[\theta_F] \quad (2)$$

where $[\theta_U]$ and $[\theta_F]$ are the molar ellipticity per residue of the unfolded and folded protein, respectively. $[\theta_U]$ and $[\theta_F]$ were assumed to be linear functions of temperature of the general form $[\theta_i] = [\theta_{i,0}] + \alpha_i T$ or $[\theta_i] = [\theta_{i,0}] + \alpha_i$[denaturant], with i indicating the U or F state.

Combining 1 and 2,

$$[\theta] = (K_U / (1-K_U) ([\theta_U] - [\theta_F]) + [\theta_F] \quad (3)$$

The slope α_F of the pre-transition baseline was obtained from a fit according to equation 3. The slope α_U of the post-transition baseline of the thermal unfolding curves was very small and was fixed at zero. Using the above equation, the midpoint of protein denaturation was calculated to be 69.5 °C.

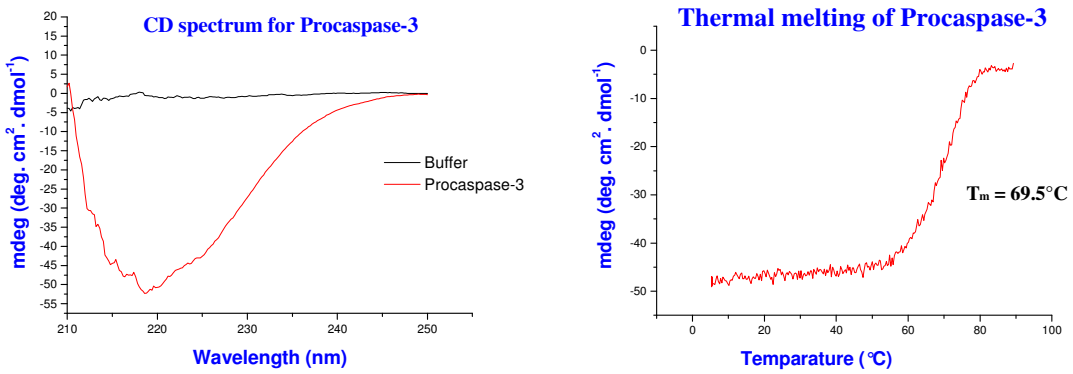

Figure 5. Left panel. Far-UV CD spectrum of ΔproC3 (red) and buffer (black). The spectrum of the protein shows a typical α/β secondary structure. **Right panel.** Thermal melting experimental trace of ΔproC3. The calculated Tm is 69.5 °C according to equation 3.

The CD spectrum resembles a typical spectrum for a globular protein of the α/β fold and thermal denaturation curves showed that ΔproC3 is thermally stable with a melting temperature of 69.5°C.

A.3.3 Isothermal titration calorimetry

Synthetic peptides containing the arginine–glycine–aspartate (RGD) motif have been used extensively as inhibitors of integrin–ligand interactions in studies of cell adhesion, migration, growth and differentiation [11, 12], because the RGD motif is an integrin-recognition motif found in many ligands. A recent report has revealed that RGD-containing peptides are able to directly induce apoptosis without any requirement for integrin-mediated cell clustering or signalling[13]. Additionally RGD-containing peptides enter cells and directly induce auto-processing and enzymatic activity of procaspase-3. Using the breast carcinoma cell line MCF-7, which has a functional deletion of the caspase-3 gene, the study confirmed that caspase-3 is required for RGD-mediated cell death. In addition to an RGD motif, pro-caspase-3 also contains a potential RGD-binding motif, aspartate–aspartate–methionine (DDM), near the site of processing to produce the p12 and p17 subunits. On the basis of the ability of RGD–DDX interactions to trigger integrin activation [14], the study concluded that RGD peptides induce apoptosis by triggering conformational changes that promote procaspase-3 autoprocessing and activation. These findings provided an alternative molecular explanation for the potent pro-apoptotic properties of RGD peptides in models of angiogenesis, inflammation and cancer metastasis[15]. Another recent report suggested that the recombinant caspase-8 and 9 also bind to RGDS peptide [16].

The binding of "RGDS" peptide to ΔproC3 was assessed by isothermal titration calorimetry (ITC). ITC is the most quantitative means available for measuring the thermodynamic properties of a protein-ligand interaction. ITC measures the binding equilibrium directly by determining the heat evolved or absorbed, on association of a ligand with its binding partner. In a single experiment, the values of the binding constant (K_a), the stoichiometry (n), and the enthalpy of binding (ΔH_b) can be determined. The free energy and entropy of binding are determined from the association constant. In combination with structural information, the energetics of binding can provide a complete dissection of the interaction and aid in identifying the most important regions of the interface and the energetic contributions.

The measurements were performed on a VP-ITC instrument (MicroCal Inc., Northampton, MA). The calorimeter was calibrated according to the manufacturer's description. Samples of protein and peptide were thoroughly dialyzed in a buffer containing 20 mM Tris-HCl pH 8.0, 50 mM NaCl and 10 mM β-mercapto-ethanol to minimize artifacts due to minor differences in buffer composition. Concentration was determined after dialysis. The sample cell (1.36 mL) was loaded with 206 μM of ΔproC3 and the peptide solution (4 mM) was used as a titrant. A titration experiment typically consisted of 25-27 injections, each of 8 or 10 μL volume and 10 or 12 s duration, with a 5 min interval between additions (stirring rate 300 rpm). No detectable ΔH of binding was observed indicating either there is no specific binding or if there is binding it is not accompanied by heat change (Fig.6).

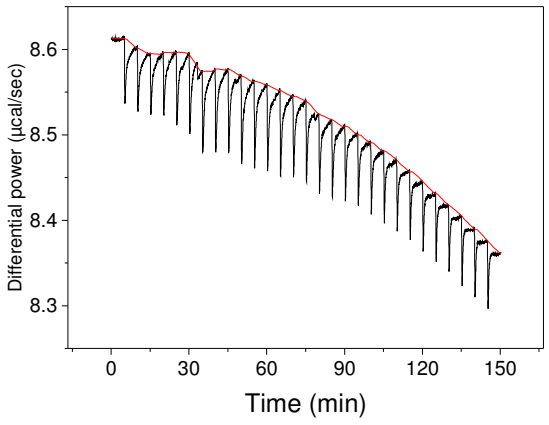

Figure 6: Isothermal titration calorimetric profile of ΔproC3 on titration against "RGDS" peptide. Plot of the differential power (μcal/sec) against the injection time (min).

A.4 Crystallization trials

Attempts to screen for the crystallization condition for ΔproC3 were performed with the help of the high-throughput nano-drop crystallization facility (Department of Biochemistry, University of Zurich, Switzerland). The purity of ΔproC3, as judged by Reversed Phase-HPLC and SDS-PAGE, used for the purpose of crystallization was greater than 98%. The protein was dialyzed against a buffer containing 20 mM Tris-HCl pH 8.0 and 10mM DTT and concentrated to a final protein concentration of 20mg/mL. Several standard screens were used for the screening of ΔproC3 alone or in complex with "RGD" binding peptides like "RGDS" and "cyclic GRGDSP". No promising crystals were identified.

A.5 Discussion and future perspectives

The crystal structure of a procaspase-3 would establish the structural determinants for the above discussed unique feature of procaspase-3 activation involving a change in pH or by the addition of "RGD" peptides. With an aim to determine the structure of procaspase-3, it was successfully cloned and characterized biochemically and biophysically. Procaspase-3 is a dimer in solution as evidenced from the size exclusion chromatography and it seems to be a compact species. The results from the CD experiments demonstrated that the protein is well folded and thermally stable. Unfortunately ITC experiments were unsuccessful under these experimental conditions. Nevertheless, the binding characteristic of RGDS peptide can be analysed in the future at a lower temperature (4°C) or using a different peptide like GRGDNP or RGD. Future experiments could include intrinsic fluorescence and surface plasma resonance experiments.

The close proximity of the C-terminal loop of the large subunit and the N-terminal loop of the small subunit strongly favours for the X-linked (or the interdigitated) model rather than the associative model of procaspase-3 activation. In particular, the conformation of the N-terminal loop which emerged from the current thesis work favors the interdigitated model. In contrast, the crystal structures of the procaspase-7, the closest homolog of procaspase-3, has established that the dimer procaspase-7 is associative in nature [4, 5]. But there were some limitations to the interpretation of the structural study, especially the inter-subunit linker under debate is disordered in one molecule and in the other molecule, the linker occupies the dimer interface. The structures were resolved at nominal resolution (2.7-2.9Å) and B-factor values for the model as a whole and the inter-subunit linker in particular were quite high of the order of 65 and 110 respectively. Even though caspase-3 and -7 share striking similarity in the amino acid sequence and in the three-dimensional structure, they have distinct and non-redundant functional roles [17]. So there might be a remote chance for a different activation model.

A.6 References

1. Earnshaw, W.C., L.M. Martins, and S.H. Kaufmann, *Mammalian caspases: structure, activation, substrates, and functions during apoptosis.* Annu Rev Biochem, 1999. **68**: p. 383-424.
2. Nicholson, D.W., et al., *Identification and inhibition of the ICE/CED-3 protease necessary for mammalian apoptosis.* Nature, 1995. **376**(6535): p. 37-43.
3. Shi, Y., *Mechanisms of caspase activation and inhibition during apoptosis.* Mol Cell, 2002. **9**(3): p. 459-70.
4. Chai, J., et al., *Crystal structure of a procaspase-7 zymogen: mechanisms of activation and substrate binding.* Cell, 2001. **107**(3): p. 399-407.
5. Riedl, S.J., et al., *Structural basis for the activation of human procaspase-7.* Proc Natl Acad Sci U S A, 2001. **98**(26): p. 14790-5.
6. Cowling, V. and J. Downward, *Caspase-6 is the direct activator of caspase-8 in the cytochrome c-induced apoptosis pathway: absolute requirement for removal of caspase-6 prodomain.* Cell Death Differ, 2002. **9**(10): p. 1046-56.
7. Yaoita, Y., *Inhibition of nuclear transport of caspase-7 by its prodomain.* Biochem Biophys Res Commun, 2002. **291**(1): p. 79-84.
8. Denault, J.B. and G.S. Salvesen, *Human caspase-7 activity and regulation by its N-terminal peptide.* J Biol Chem, 2003. **278**(36): p. 34042-50.
9. Meergans, T., et al., *The short prodomain influences caspase-3 activation in HeLa cells.* Biochem J, 2000. **349**(Pt 1): p. 135-40.
10. Pop, C., et al., *Removal of the pro-domain does not affect the conformation of the procaspase-3 dimer.* Biochemistry, 2001. **40**(47): p. 14224-35.
11. Ruoslahti, E., *RGD and other recognition sequences for integrins.* Annu Rev Cell Dev Biol, 1996. **12**: p. 697-715.
12. Werb, Z., *ECM and cell surface proteolysis: regulating cellular ecology.* Cell, 1997. **91**(4): p. 439-42.
13. Buckley, C.D., et al., *RGD peptides induce apoptosis by direct caspase-3 activation.* Nature, 1999. **397**(6719): p. 534-9.
14. Du, X.P., et al., *Ligands "activate" integrin alpha IIb beta 3 (platelet GPIIb-IIIa).* Cell, 1991. **65**(3): p. 409-16.
15. Humphries, M.J., K. Olden, and K.M. Yamada, *A synthetic peptide from fibronectin inhibits experimental metastasis of murine melanoma cells.* Science, 1986. **233**(4762): p. 467-70.
16. Aguzzi, M.S., et al., *RGDS peptide induces caspase 8 and caspase 9 activation in human endothelial cells.* Blood, 2004. **103**(11): p. 4180-7.
17. Slee, E.A., C. Adrain, and S.J. Martin, *Executioner caspase-3, -6, and -7 perform distinct, non-redundant roles during the demolition phase of apoptosis.* J Biol Chem, 2001. **276**(10): p. 7320-6.

Appendix B Cloning, expression, purification and crystallization trials for caspase-5

B.1 Introduction

Caspase-5 is a member of the caspase-1 sub-family consisting of caspase-1, -4 and -5, which are cytokine activators. It shares about 52% and 77% sequence similarity with caspase-1 and -4 respectively. Caspase-5 is expressed at a much lower level than caspase-1 and -4 [1, 2] and it has similar substrate specificity as caspase-1 and -4 and it prefers to cleave the substrates containing a (W/L)EHD motif. It exists as an inactive zymogen like all other caspases and in the zymogen form it contains a CARD (caspase activation and recruitment) domain in the prodomain apart from the protease domain. Limited information is available concerning the precise sites at which procaspase-5 is processed to produce active caspase-5. Maturation of caspase-1 results from cleavage after the aspartate residues at positions 119, 297 and 316, with the latter two residues being conserved in caspase-4 (Asp-270 and Asp-289) and caspase-5 (Asp-311 and Asp-330); by analogy, this probably represents the removal of a linker peptide.

To date the mechanism of caspase-5 activation and its role in cytokine activation are poorly understood. Based on its expression pattern and sequence homology, caspase-5 was proposed to be the human ortholog of mouse caspase-11 [3]. Like caspase-11, protein levels of caspase-5 are increased by LPS (lipopolysaccharide) [3]. Moreover, caspase-5 is involved in IL-1β processing and can interact with caspase-1 [4]. Caspase-1 and caspase-5 are constituents of the NALP1 inflammasome, a complex that can trigger cleavage of proIL1-β. It is likely that caspase-4 and caspase-5 arose from the gene duplication of a caspase-11-like ancestral gene. Frameshift mutations of caspase-5 are frequently found in endometrial carcinoma [5]. Moreover, caspase-5 cleaves Max, a central component of the Myc/Max/Mad network of transcription factors that is frequently deregulated in tumors [6], suggesting a regulatory role of caspase-5 in tumorgenesis. Two specific cleavage sites for caspases in Max were identified, one at IEV**E**^{10}↓S and one at SAFD^{135}↓G, which are cleaved *in vitro* by caspase-5 and caspase-7. Mutational analysis indicates that both sites are also used *in vivo*. Thus Max represents the first caspase-5 substrate.

The unusual cleavage after a glutamic acid residue is observed only with the full-length, DNA-binding competent Max protein but not with corresponding peptides, suggesting that structural determinants might be important for this activity. Furthermore, cleavage by

caspase-5 is inhibited by the protein kinase CK2 (casein kinase II) mediated phosphorylation of Max at Ser-11, a previously mapped phosphorylation site *in vivo*.

B.2 Cloning, expression and purification

The active recombinant caspase-5 was cloned, expressed and purified as described previously [7]. A PCR based strategy was adopted for cloning of active caspase-5 using the primers listed under table 1. Briefly, the cloned genes for the large p20 (Met-Ala^{135}-Asp^{311}) and the small p10 subunit (Met-Ala-Ser^{331}-Asn^{418}) were inserted in the *Nco*I/*Bam*HI sites of pET11d plasmids (Novagen). For separate expression of both subunits, *E. coli* BL21-CodonPlus (DE3)-RIL cells (Stratagene), containing one of the two plasmids were grown to a density of A_{600} = 0.5 at 37 °C in a 0.5-liter LB medium. Expression was induced by the addition of IPTG (1 mM), and the culture was shaken at 37 °C for 4 hours post induction. Cells were harvested, washed in PBS buffer and lyzed using a French press.

Owing to overexpression the protein was localised in the inclusion body portion. Refolding was achieved by rapid mixing of equimolar amounts of each subunit to a final concentration of about 100 µg of subunit/ml in the refolding buffer (100 mM HEPES, pH 7.5, 10% sucrose, 1% CHAPS, 100 mM NaCl and 10 mM DTT) and was incubated overnight at room temperature with continuous stirring. Misfolded and aggregated protein was removed by centrifugation (5,000 x *g*, 30 min), and the supernatant was concentrated using an Amicon-stirred cell. To reduce the salt concentration and to facilitate binding to a cation exchange column (MonoS 1mL, Amersham Biosciences), the protein solution was dialyzed against the cation exchange buffer (50mM HEPES pH 6.5, 1% CHAPS and 10mM DTT) prior to chromatography. The protein was eluted using a 300 mM NaCl gradient. The yield of the purified caspase-5 was only 0.3 mg/L.

Owing to pronounced autocatalytic activity and week dimer stabilization forces prevailing in the caspase-1 subfamily, we had to adopt a different strategy. After refolding and concentration the protein was subjected to for purification by size exclusion chromatography on an analytical superdex S200 column (Amersham Biosciences) using a buffer containing 50 mM Tris pH 7.5, 50 mM NaCl, 1% CHAPS and 10 mM DTT. Fractions containing pure and active caspase were pooled and concentrated by ultrafiltration (centricon, NMWL 10,000 Da) and the final yield was about 1 mg/litre culture. Thus purified caspase-5 had reasonable purity and the crystallization experiments were set-up, but no crystals were obtained.

Table-1: List of primers used for the cloning of caspase-5.

#	Primer_name	Oligonucleotide sequence
1	C5_p20_fwd	5‘-GTCACCATGGCAGGTCCACCTGAGTCAGCAG-3‘
2	C5_p20_ rev	5‘-GCGGATCCGCTTAGTCTCTGACCCAGAG-3’
3	C5_p10_fwd	5‘-GTCACCATGGCTTCTGTTTGCAAGATCCAC-3‘
4	C5_p10_ rev	5‘-GCGGATCCGCTTAATTGCCAGGAAAGAGG-3‘

B.3 Future perspective

The crystal structure of caspase-5 along with the functional characterization would be of broad interest to the research community for understanding its specific role in cytokine activation. In particular, it might shed light onto the very unique and unusual feature of caspase-5 to cleave the Max protein next to a glutamate residue. With an aim for obtaining a more stable and pure protein suitable for crystallization experiments, an alternate procedure, caspase-5 can be re-cloned, expressed and purified as a full length protein instead of the current strategy of separately expressing the α- and β-subunits.

B.4 Reference

1. Faucheu, C., et al., *Identification of a cysteine protease closely related to interleukin-1 beta-converting enzyme.* Eur J Biochem, 1996. **236**(1): p. 207-13.
2. Munday, N.A., et al., *Molecular cloning and pro-apoptotic activity of ICErelII and ICErelIII, members of the ICE/CED-3 family of cysteine proteases.* J Biol Chem, 1995. **270**(26): p. 15870-6.
3. Lin, X.Y., M.S. Choi, and A.G. Porter, *Expression analysis of the human caspase-1 subfamily reveals specific regulation of the CASP5 gene by lipopolysaccharide and interferon-gamma.* The Journal Of Biological Chemistry, 2000. **275**(51): p. 39920.
4. Martinon, F., K. Burns, and J. Tschopp, *The Inflammasome: A Molecular Platform Triggering Activation of Inflammatory Caspases and Processing of proIL-[beta].* Molecular Cell, 2002. **10**(2): p. 417.
5. Schwartz, S., Jr., et al., *Frameshift mutations at mononucleotide repeats in caspase-5 and other target genes in endometrial and gastrointestinal cancer of the microsatellite mutator phenotype.* Cancer Res, 1999. **59**(12): p. 2995-3002.
6. Krippner-Heidenreich, A., et al., *Targeting of the transcription factor Max during apoptosis: phosphorylation-regulated cleavage by caspase-5 at an unusual glutamic acid residue in position P1.* The Biochemical Journal, 2001. **358**(Part 3): p. 705.
7. Garcia-Calvo, M., et al., *Purification and catalytic properties of human caspase family members.* Cell Death Differ, 1999. **6**(4): p. 362-9.

Appendix C Mutational studies to understand the selectivity for P_4 Asp in caspase-8

C.1 Introduction

Caspases demonstrate their specificity in substrate recognition at the S_4 subsite and previous studies established the preferred substrate recognition sequences for each caspases [1-4]. However, caspase-8 was shown to have more plasticity in its S_4 pocket in its ability to bind both an "optimal" IETD inhibitor and a "sub-optimal" DEVD inhibitor [5, 6]. The other group-III caspases like caspase-6, 9 and 10 do not seem to possess a broader specificity as observed in caspase-8. From the crystal structure of caspase-8:Z-DEVD-CHO inhibitor complex it was evident that the P_4 aspartate makes hydrogen bonds with the side chains of Trp348 and Asn342 (Fig.1). Among the interacting partners, the residue Trp348 is conserved in all of the group family members, while the residue Asn342 is unique for caspase-8 (Fig.2) and might be a good candidate for governing specificity.

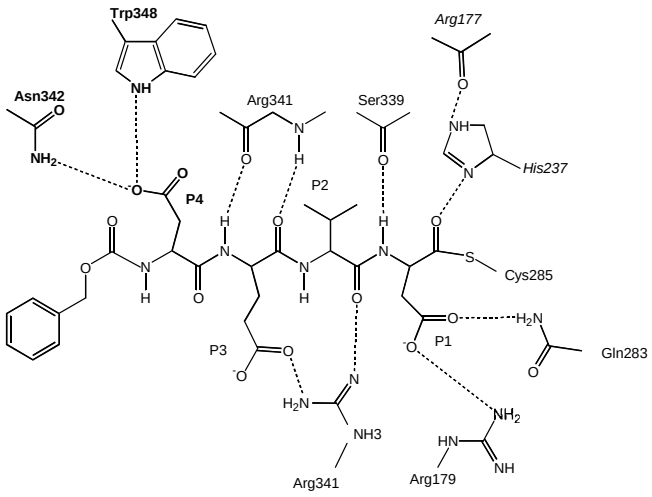

Figure 1: Network of polar interactions in the active site of the caspase-8:Z-DEVD-CHO inhibitor complex. The P_4 Asp in stabilised by hydrogen bond with Trp348 and Asn342.

A more detailed understanding of the molecular determinants of caspase-8 specificity was sought. To pursue such studies, mutations within the active site region were carried out using a point mutation approach. To investigate the specificity of the S_4 pocket in caspase-8 with respect to other Group III caspases, the three p12 point mutants of caspase-8 (N342D), (N342E) and (N342H) were constructed. The chosen Asp, Glu, and His are the equivalent residues found within caspase-9, caspase-6, and

caspase-10, respectively (Table 1 and Fig.2). These three caspases do not favour binding to a P_4 Asp [1].

```
                339         349
C8              SYRNPAEGTWY
C10             SFRHVEEGSWY
C6              SHRETVNGSWY
C9              SWRDPKSGSWY
```

Figure 2: Sequence alignment (selectivity loop region) of group-III caspase sub-family.

Table 1: Caspase-8 S_4 subsite mutants

	Residue 342	**caspase-8 mutants**
Caspase-8	N	wildtype
Caspase-10	H	N342H
Caspase-9	D	N342D
Caspase-6	E	N342E

Enzyme kinetic studies have been performed on the mutants using Ac-DEVD-amc as substrate. The results indicated that the mutant N342H has higher specificity in comparison to the wildtype caspase-8. In contrast the mutants N342D and N342E had drastically lower catalytic efficiency (Table 2) [7]. In an attempt to validate the kinetic observations on a structural level, the three mutants were purified to homogeneity and screened for crystallization in complex with the inhibitor Ac-DEVD-cmk.

Table 2: Kinetic parameters for caspase-8 mutants against Ac-DEVD-amc. Table adapted from [7].

Protein	**K_M (mM)**	**k_{cat} (s^{-1})**	**k_{cat}/K_M ($M^{-1}s^{-1}$)**
wtC8	11 ± 1	1.15 x 10-2 ± 2 x 10-4	1030 ± 17
C8(N342H)	27 ± 4	4.8 x 10-2 ± 2 x 10-3	1820 ± 140
C8(N342D)	96 ± 5	5.7 x 10-3 ± 1 x 10-4	59 ± 1
C8(N342E)	169 ± 22	5.1 x 10-4 ± 2 x 10-5	3.0 ± 0.1

C.2 Experimental procedures

Cloning of wild-type and point mutants of caspase-8

Wild-type caspase-8 was cloned and expressed in E. *coli* as previously described [1, 5]. Briefly, the p18 and p12 cDNA were inserted into the pET11d (Novagen) vector and point mutations were introduced by PCR based cloning strategies. The oligonucleotide primers used for the PCR are listed in Table 3. Clones having correct sequence directionality were identified via DNA sequencing.

Table 3: Oligonucleotide primers for generating the mutants of caspase-8. Table adapted from [7].

Caspase-8 p12 oligonucleotides	Oligonucleotide sequence
N342D sense	TCCTACCGAGACCCTGCAGAG
N342D antisense	CTCTGCAGGGTCTCGGTAGGA
N342E sense	TCCTACCGAGAACCTGCAGAG
N342E antisense	CTCTGCAGGTTCTCGGTAGGA
N342H sense	TCCTACCGACATCCTGCAGAG
N342H antisense	CTCTGCAGGATGTCGGTAGGA

Expression, purification and crystallization of caspase-8 mutants

Clones were expressed in and refolded from inclusion bodies [8]. The caspase-8 mutants were purified using two step anion exchange chromatography, first step using a Sepharose-Q column and the second step with a Resource-Q column (Amersham Pharmacia) as described previously [9]. The purified caspase-8 mutants were subsequently inhibited with a 3-fold molar excess of the inhibitor Ac-DEVD-cmk in a buffer containing 20 mM Tris pH 8.0 and 10 mM DTT. Co-crystals of the complex between the caspase-8 mutants and the inhibitor were grown from 2 µl hanging drops formed by mixing equal volumes of protein (20 mg/mL) and reservoir solution at 20°C. The reservoir solution consists of 1.2 - 1.5 M sodium citrate, 100 mM HEPES pH 8.0. All the three mutants yielded crystals, but the crystals were either multiple or fragile needles (Fig.3a-c). Despite several attempts to optimize the crystallization condition with respect protein concentration, crystallization temperature, pH and sodium citrate concentration, very few crystals of reasonable quality were obtained.

Figure 3a: Crystal of caspase-8 N342D: Ac-DEVD-cmk

Figure 3b: Crystals of caspase-8 N342E: Ac-DEVD-cmk

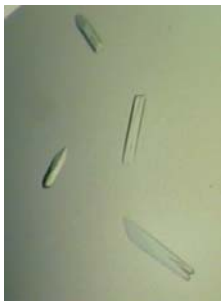

Figure 3c: Crystals of caspase-8 N342H: Ac-DEVD-cmk

Prior to data collection, the crystals were isolated and frozen in the nitrogen stream. Diffraction data were either collected using a rotating anode generator (Bruker-Nonius, FR591) at 100 K or at the Swiss Light Source synchrotron (Paul Sherrer Institute, Villigen, Switzerland). The resolution ranges for the crystals were in the range of 2.9 - 3.8 Å. The diffraction data were not of a good quality and eventually the data processing was not possible.

C.3 Discussion and future perspectives

In this study a classical point mutant approach was pursued in examining the active site specificity of caspase-8. Many studies have investigated the amino acid substrate preferences for caspases. The conclusions were that the P_1 Asp is fundamental for caspase recognition and that additionally the P_4 residue determines specificity among the family members. Very little data has been accrued about the exact specificity determinants for individual caspases, including caspase- 8. The X-ray crystal structure of caspase-8 in complex with a tetrapeptidic inhibitor comprising a “sub-optimal” P_4 Asp residue showed that an Asp in P_4 is instead well tolerated. Based on that, the specificity of the caspase-8 S_4 pocket, in relation to Group III caspases, was examined further by mutation and enzyme kinetics. Unfortunately, attempts to identify the structural determinants were unsuccessful. A future direction to partly accomplish the task might be to crystallize the caspase-8 mutants with the optimal inhibitor Ac-IETD-cmk rather than the sub-optimal Ac-DEVD-cmk. Additionally, future experiments could also include the profiling of other caspase substrates with these mutants for further kinetic characterization of their specificities.

C.4 Reference

1. Rano, T.A., et al., *A combinatorial approach for determining protease specificities: application to interleukin-1beta converting enzyme (ICE).* Chem Biol, 1997. **4**(2): p. 149-55.
2. Stennicke, H.R., et al., *Internally quenched fluorescent peptide substrates disclose the subsite preferences of human caspases 1, 3, 6, 7 and 8.* Biochem J, 2000. **350 Pt 2**: p. 563-8.
3. Talanian, R.V., et al., *Substrate specificities of caspase family proteases.* J Biol Chem, 1997. **272**(15): p. 9677-82.
4. Thornberry, N.A., et al., *A combinatorial approach defines specificities of members of the caspase family and granzyme B. Functional relationships established for key mediators of apoptosis.* J Biol Chem, 1997. **272**(29): p. 17907-11.
5. Blanchard, H., et al., *Caspase-8 specificity probed at subsite S(4): crystal structure of the caspase-8-Z-DEVD-cho complex.* J Mol Biol, 2000. **302**(1): p. 9-16.
6. Blanchard, H., et al., *The three-dimensional structure of caspase-8: an initiator enzyme in apoptosis.* Structure Fold Des, 1999. **7**(9): p. 1125-33.
7. DONEPUDI, M., *Caspase-8: Structure, Specificity and Activation.* PhD thesis, Faculty of mathematics and sciences, 2003. Part 1, Chapter 3.
8. Garcia-Calvo, M., et al., *Purification and catalytic properties of human caspase family members.* Cell Death Differ, 1999. **6**(4): p. 362-9.
9. Ekici, O., Rajkumar, G., Li, ZZ., James, KE., Asgian, JL., Mikolajczyk, J., Jelakovic, S., Salvesen, GS., Grutter, MG., and Powers, JC, *"Design, Synthesis, and Evaluation of Aza-Peptide Michael Acceptors as Selective and Potent Inhibitors of Caspases-2, -3, -6, -7, -8, -9, and -10"*. to be submitted, 2005.

Acknowledgements

A journey is easier when you travel together. Interdependence is certainly more valuable than independence. This thesis is the result of almost four years of work whereby I have been accompanied and supported by many people. It is a pleasant aspect that I have now the opportunity to express my gratitude for all of them. The first person I would like to thank is my supervisor **Prof. Markus Grütter,** for his continuous support right throughout my PhD. I owe him lots of gratitude for being my mentor and for providing me independence to proceed with my projects. I will remain forever grateful for the confidence he bestowed on me and for being accepted into his group. Thanks to **Prof. Raimund Dutzler** for co-refereeing my thesis. I am greatly indebted to **Dr. Stjepan Jelakovic,** for his guidance and help. I have always admired his extensive working enthusiasm. He afforded numerous thought provoking discussions (even on weekends) and taught me much in crystallography. We always had excellent time, in and out of the department along with his family. Thanks to **Dr. Peer Mittl**. He not only shaped my knowledge in apoptosis and caspases, but also assisted me for my manuscripts and thesis preparation. I extend my gratitude to all of my colleagues (both current and former students in Grütter's group). I would like to acknowledge **Prof. Amedeo Caflisch** and **Prof. James C. Powers** for their staunch support for collaborative work. My special thanks to all the colleagues and friends of other labs in our Department and in ETH. Thanks to the administration, workshop and IT department of the Biochemistry Institute, University of Zurich. The chain of my gratitude would be definitely incomplete if I forget to feel a deep sense of gratitude to my family members in particular to my wife Sathyadevi for their endless love, guidance and encouragement.

Publications

Rajkumar Ganesan, Peer R.E. Mittl, Stjepan Jelakovic and Markus Grütter **"Extended substrate recognition in caspase-3 revealed by the high resolution X-ray structure analysis"** (J. Mol. Biol. *In press*)

Özlem Dogan Ekici, Zhao Zhao Li, Karen Ellis James, Juliana L. Asgian, **Rajkumar Ganesan**, Jowita Mikolajczyk, Stjepan Jelakovic, Guy S. Salvesen, Markus Grütter and James C. Powers **"Design, Synthesis and Evaluation of Aza-Peptide Michael Acceptors as Selective and Potent Inhibitors of Caspases-2, -3, -6, -7, -8, -9 and -10"** (J. Med. Chem. *In press*)

Rajkumar Ganesan, Stjepan Jelakovic, Amy J. Campbell, Juliana L. Asgian, Özlem Do an Ekici, Zhao Zhao Li, James C. Powers and Markus Grütter **"Exploring the S4 and S1 prime subsite specificities in caspase-3 with aza-peptide epoxide inhibitors"** (Biochemistry *In press*)

Rajkumar Ganesan, Stjepan Jelakovic, Amedeo Caflisch and Markus Grütter **"Structure based design of inhibitors for caspases: Insights from the crystal structures of caspase-3 small molecule inhibitor complexes"** (Manuscript in preparation)

Poster/Presentations

"**Crystal structure of caspase-3 in complex with 5-Chloro-4-oxo-pentanoic acid**" *Swiss apoptosis meeting*, Bern, September 16th - 17th, 2004

"**Crystal structures of caspase-3 in complex with aza-peptide epoxides inhibitors: Exploring the P1`site preferences**", *22nd Winter School on Proteinases and their inhibitors: recent developments* Tiers, Italy, March 2nd- 6th, 2005

Curriculum vitae

Surname:	GANESAN
First name:	Rajkumar
Date of Birth:	23rd November 1977
Nationality:	Indian

Education

2002-2006	Dissertation, Department of Biochemistry, University of Zürich. Supervisor: Prof. Markus Grütter Title: "Structure, specificity and inhibition of human caspase-3 and -8"
2001	Research associate, Vigyanix (India) Project Manager: Dr. Shantanu Choudhary Title: "Target validation and inhibitor profiling for receptor tyrosine kinases and HIV proteases"
2001	Summer research fellow, National Centre for Biological Sciences (NCBS) Bangalore, India. Supervisor: Dr. R. Sowdhamini. Title: "Computational approach to the study the nature of interactions in non-polar parts of polar residues in proteins"
1999-2001	M.Sc (Applied Chemistry), National Institute of Technology, Tiruchirappalli, India
1996-1999	B.Sc (Chemistry), Loyola College, University of Madras, Chennai, India
1984-1996	Pre-degree studies, Railway Schools, Chennai, India

Erklärung

Diese Dissertation wurde selbständig, ohne unerlaubte Hilfe im Sinne von §3 und §5 der Promotionsordnung vom 8. Juli 2002 angefertigt. Bei der Abfassung der Dissertation wurden keine anderen als die darin angegebenen Hilfsmittel benützt.

Zürich, 18 January 2006

(G. Rajkumar)